

Transverse-momentum-dependent distributions

Charlotte Van Hulse
University of Alcalá

AdT

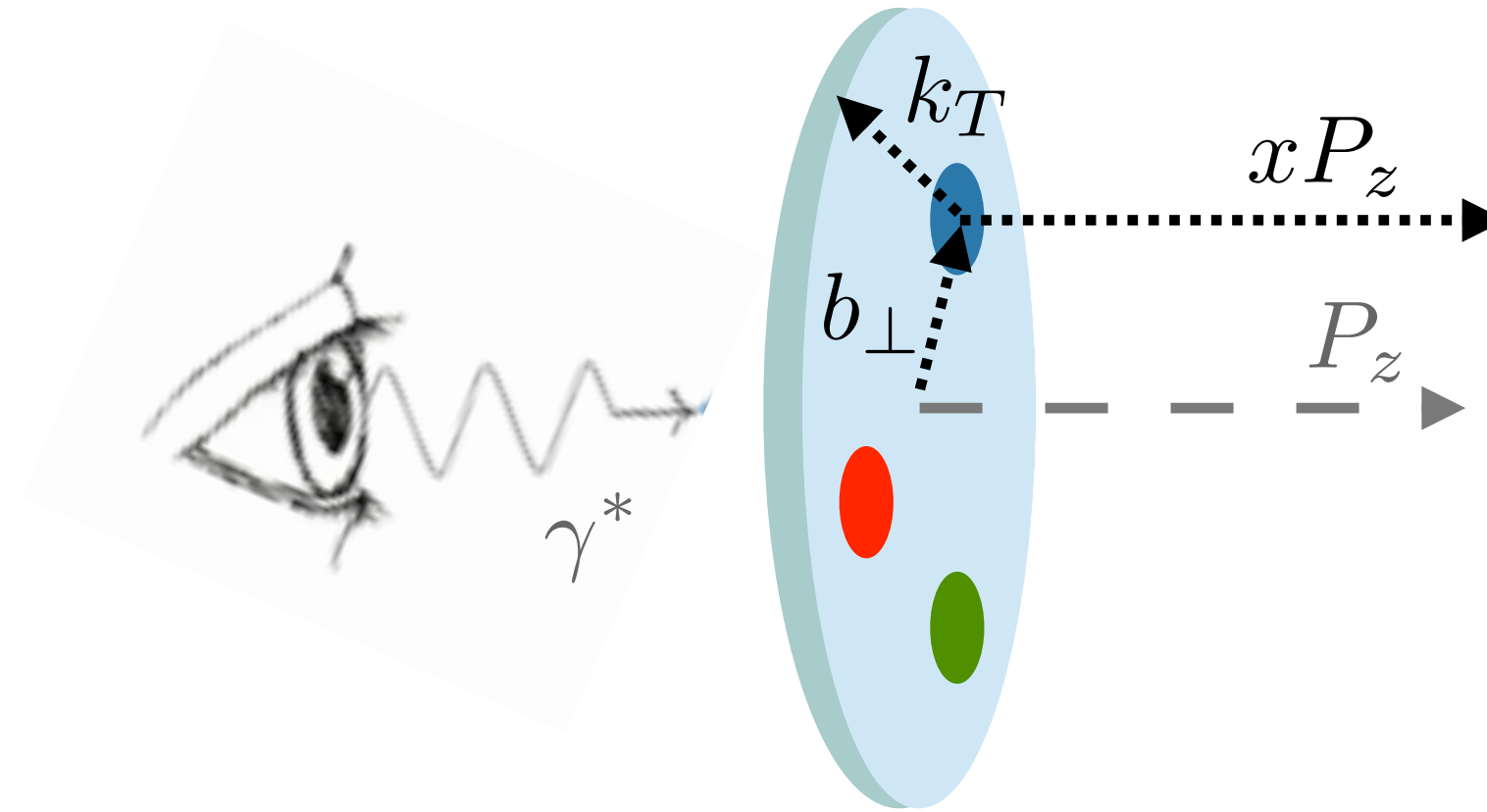


Comunidad
de Madrid

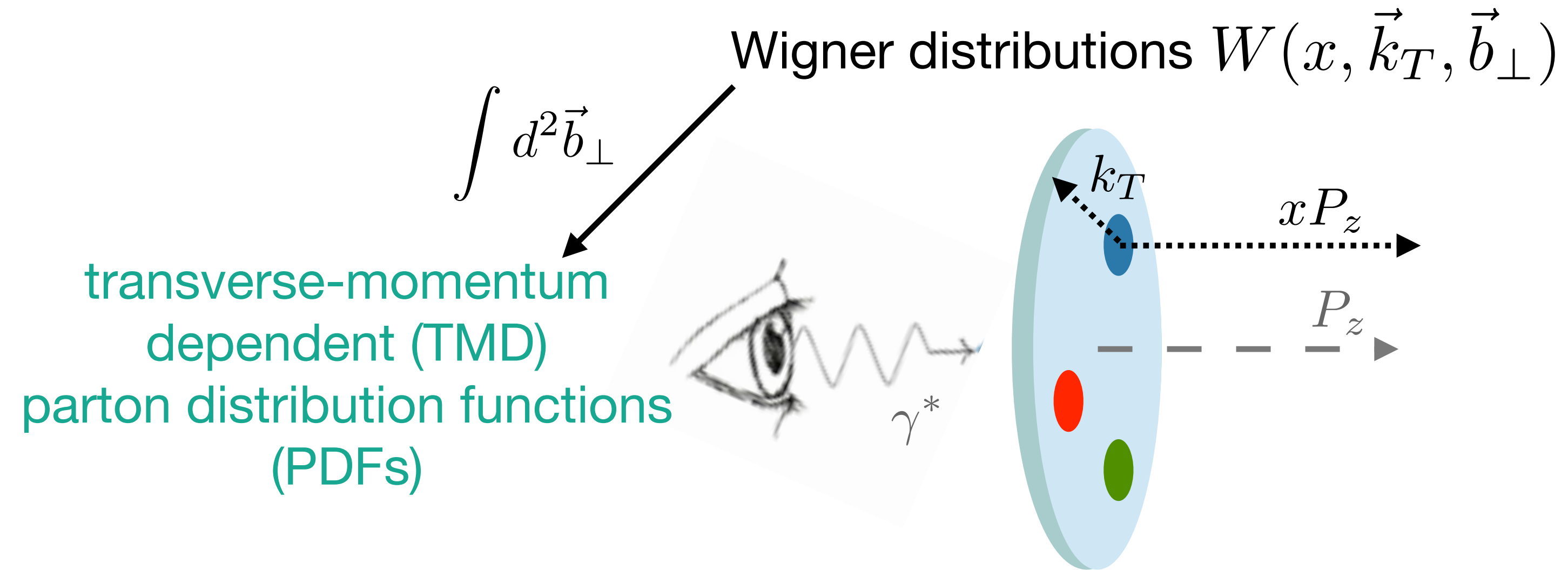
International School of Nuclear Physics
From quarks and gluons to hadrons and nuclei
Erice, Sicily
September 18-24, 2023

The various dimensions of the nucleon structure

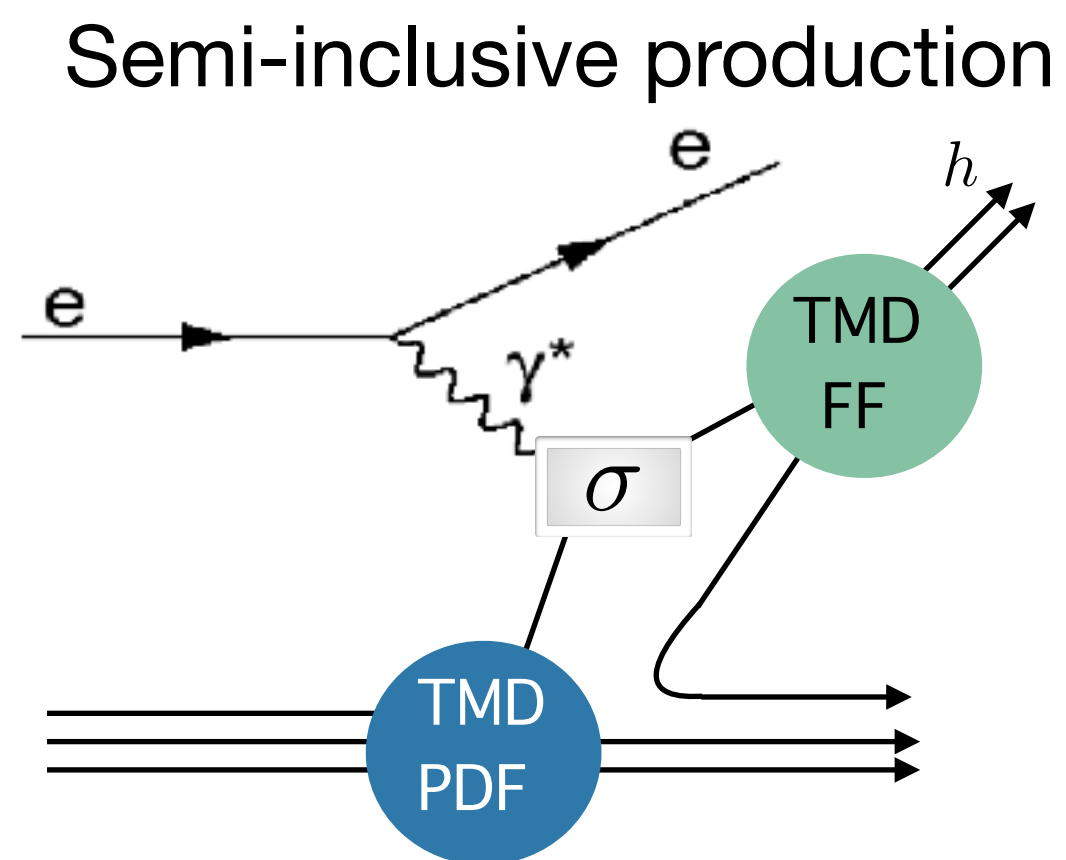
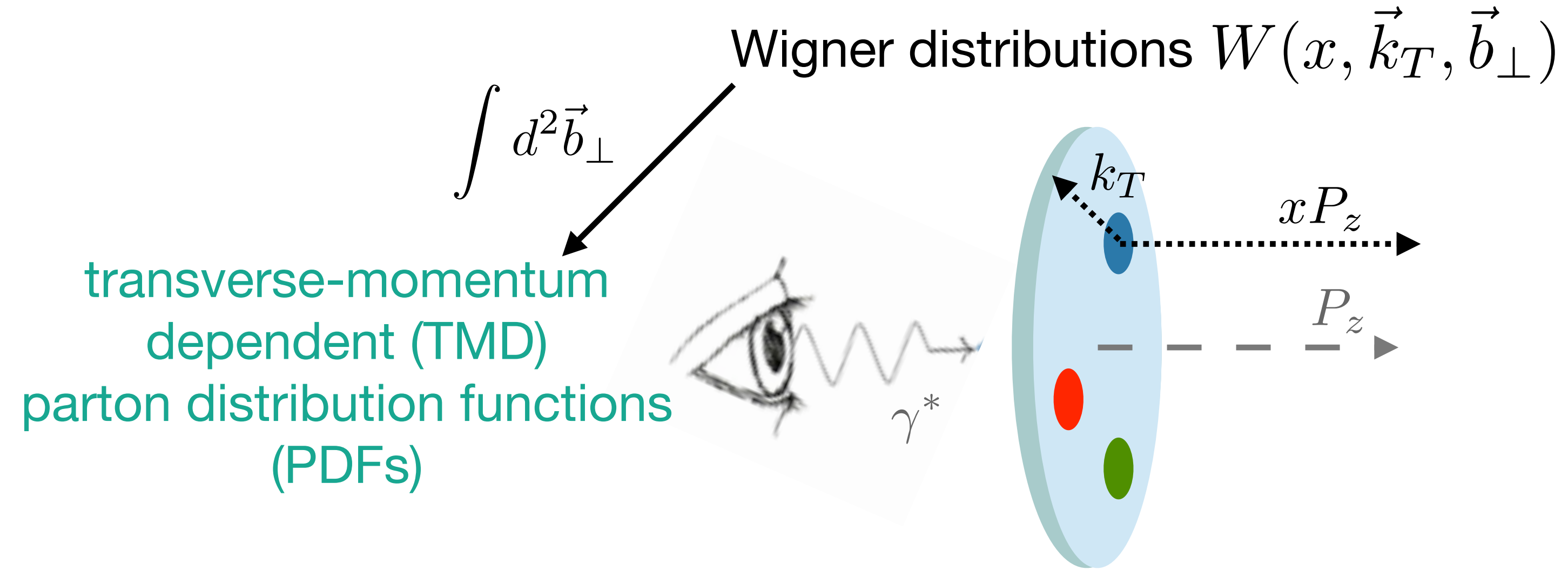
Wigner distributions $W(x, \vec{k}_T, \vec{b}_\perp)$



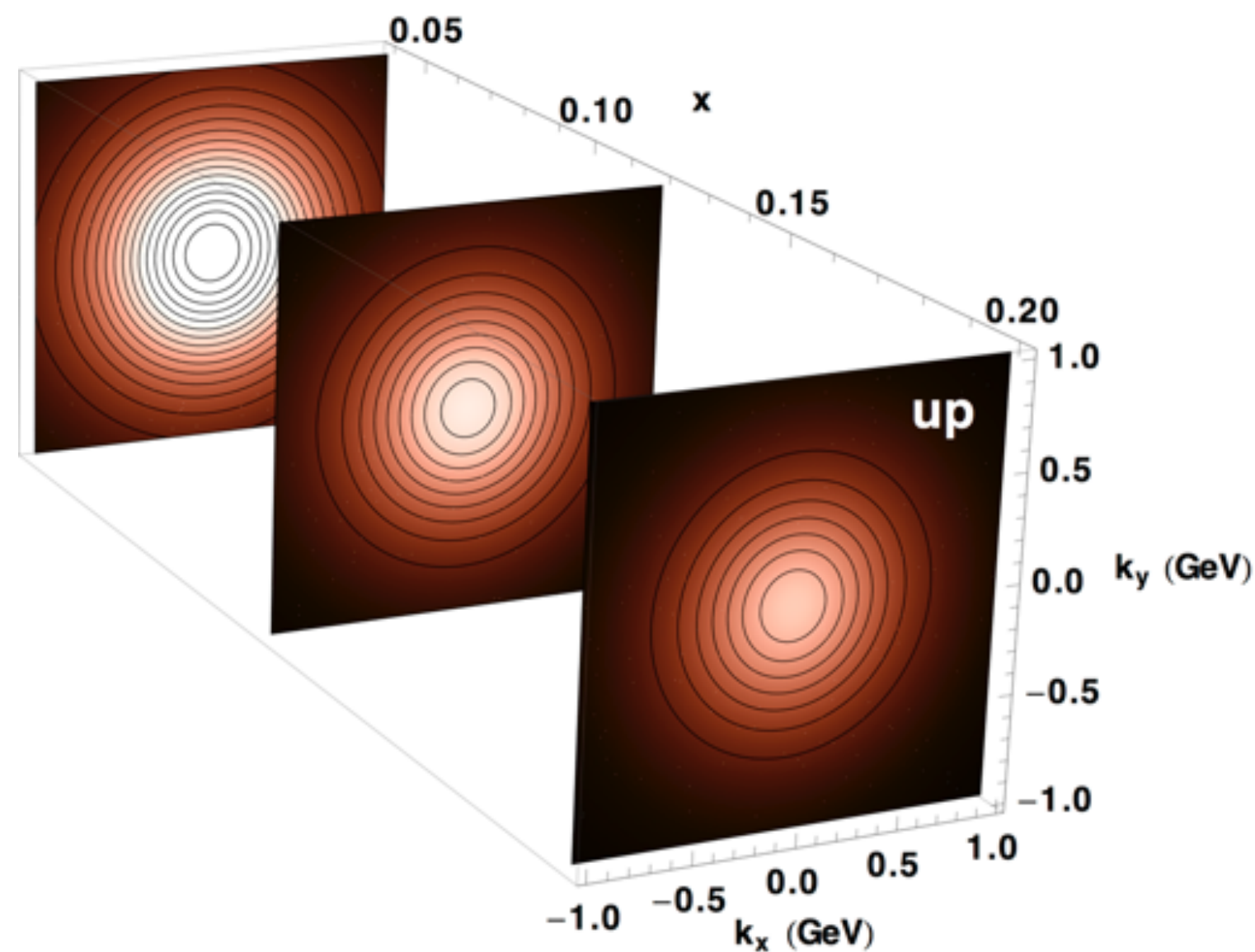
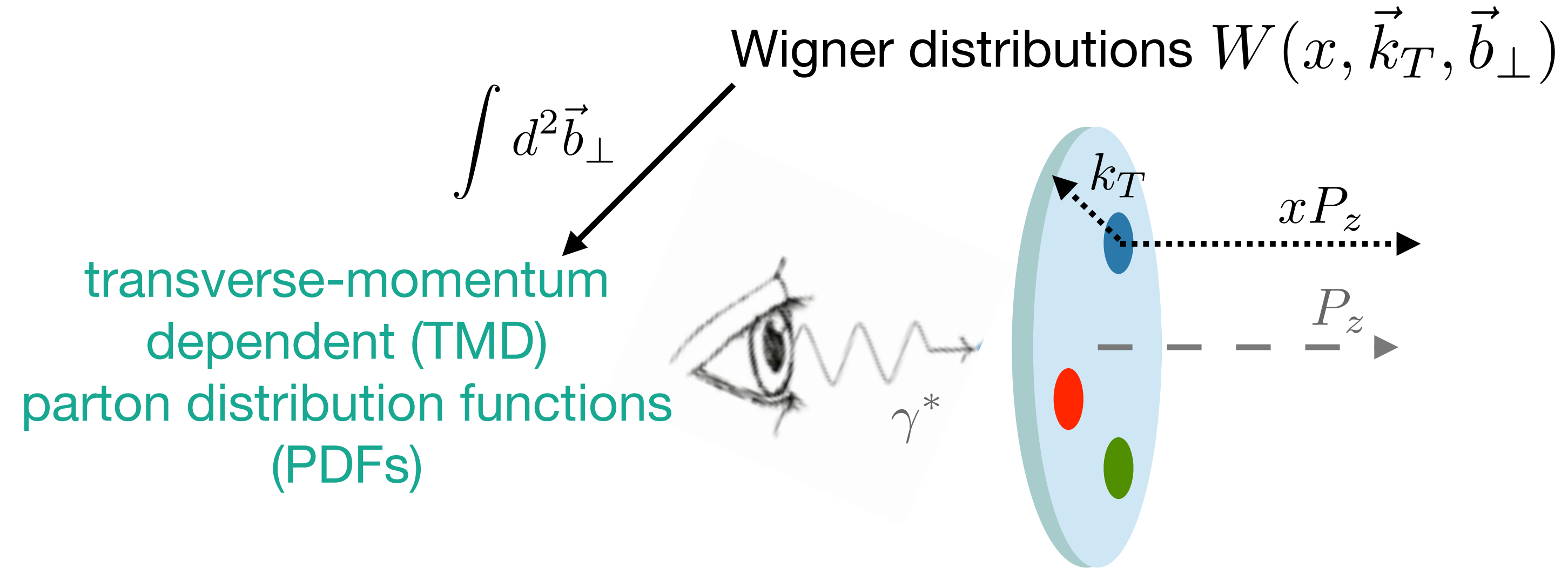
The various dimensions of the nucleon structure



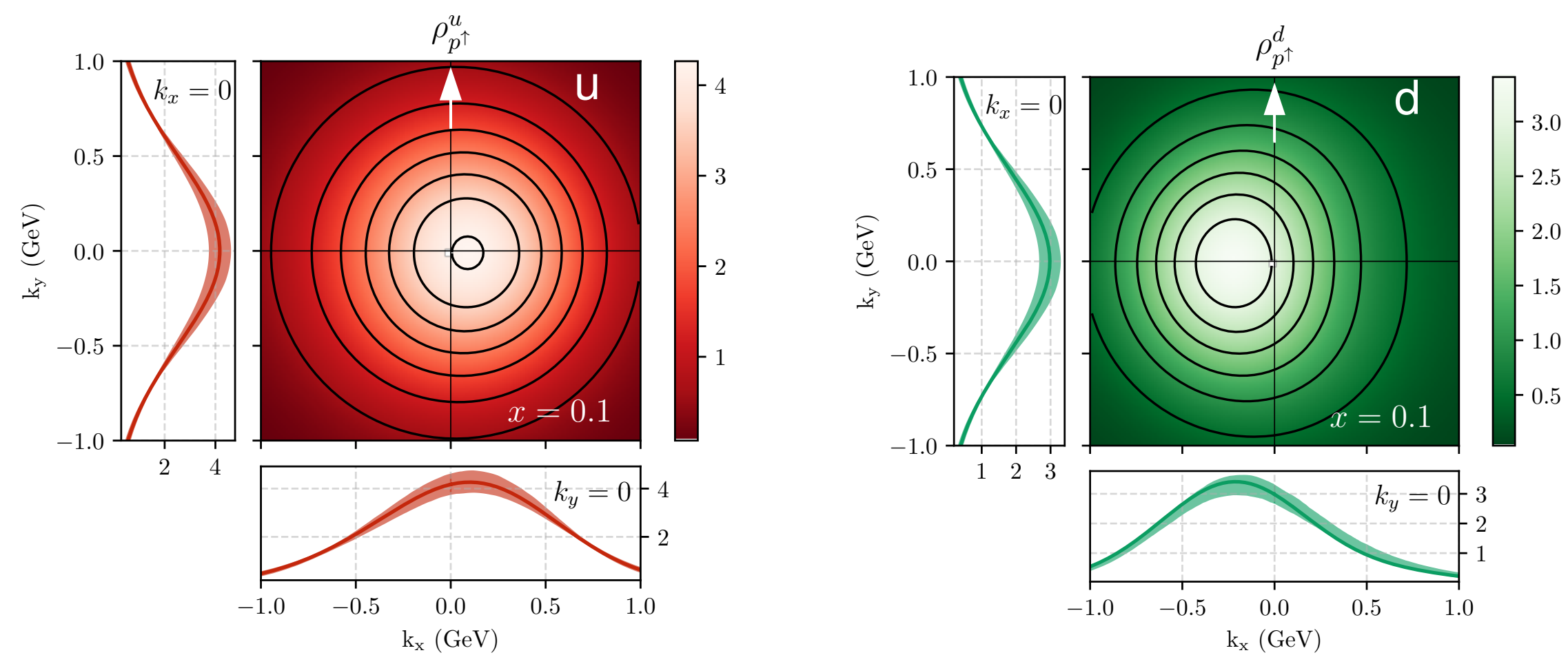
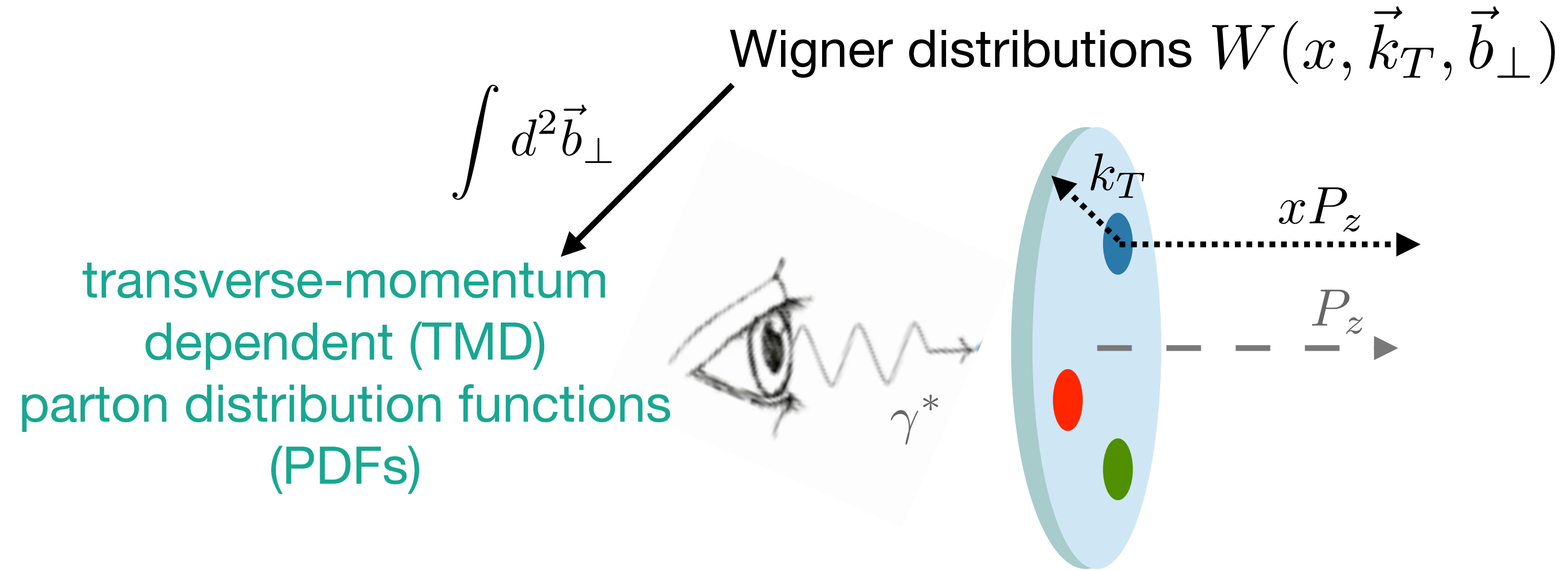
The various dimensions of the nucleon structure



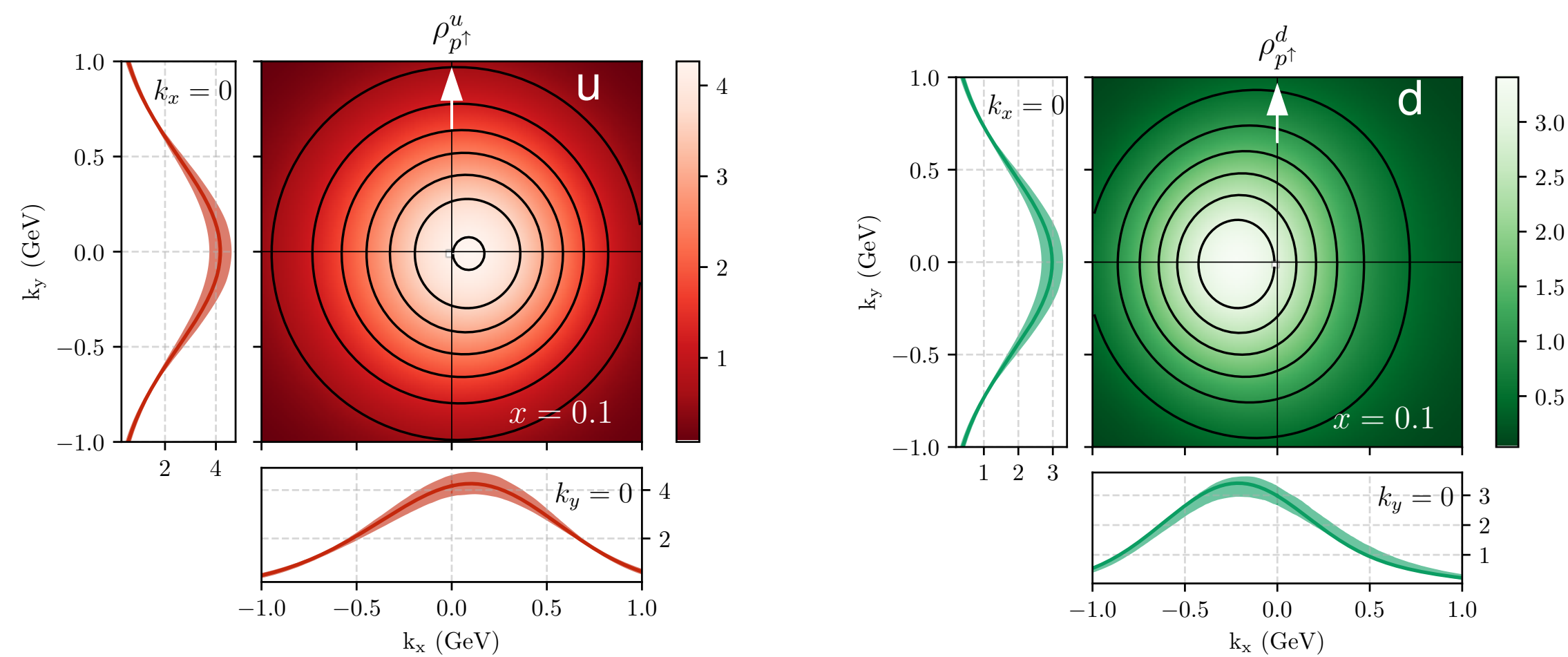
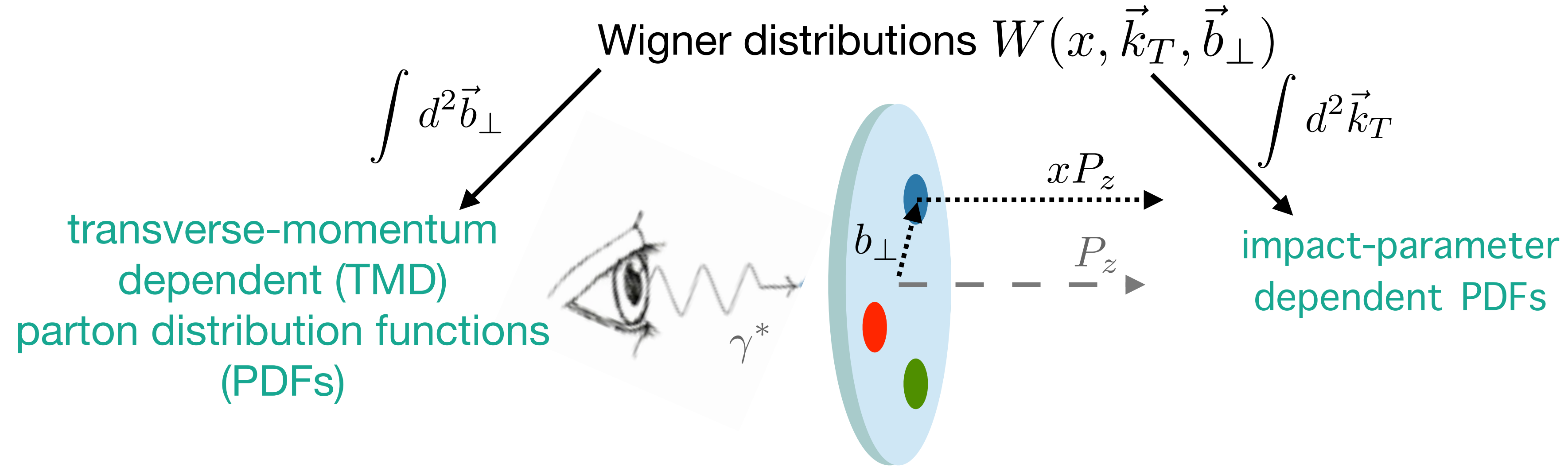
The various dimensions of the nucleon structure



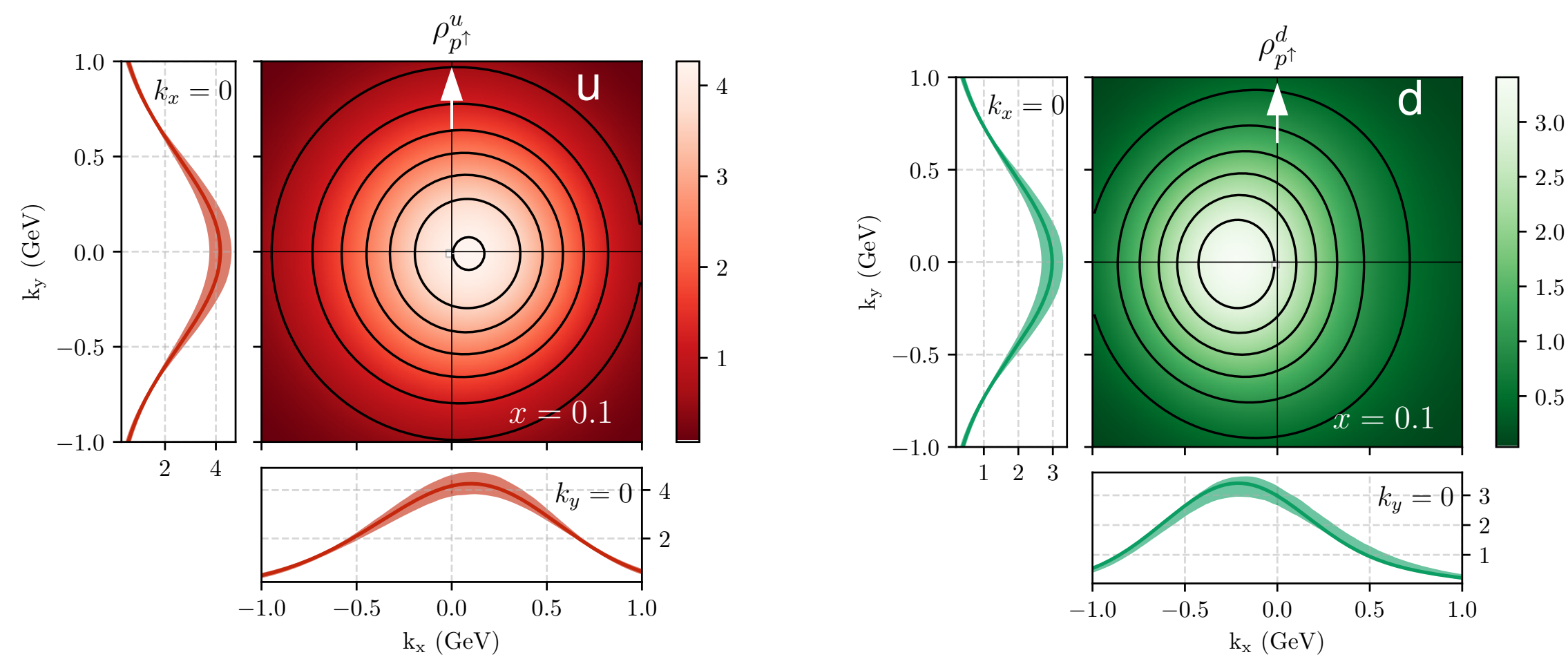
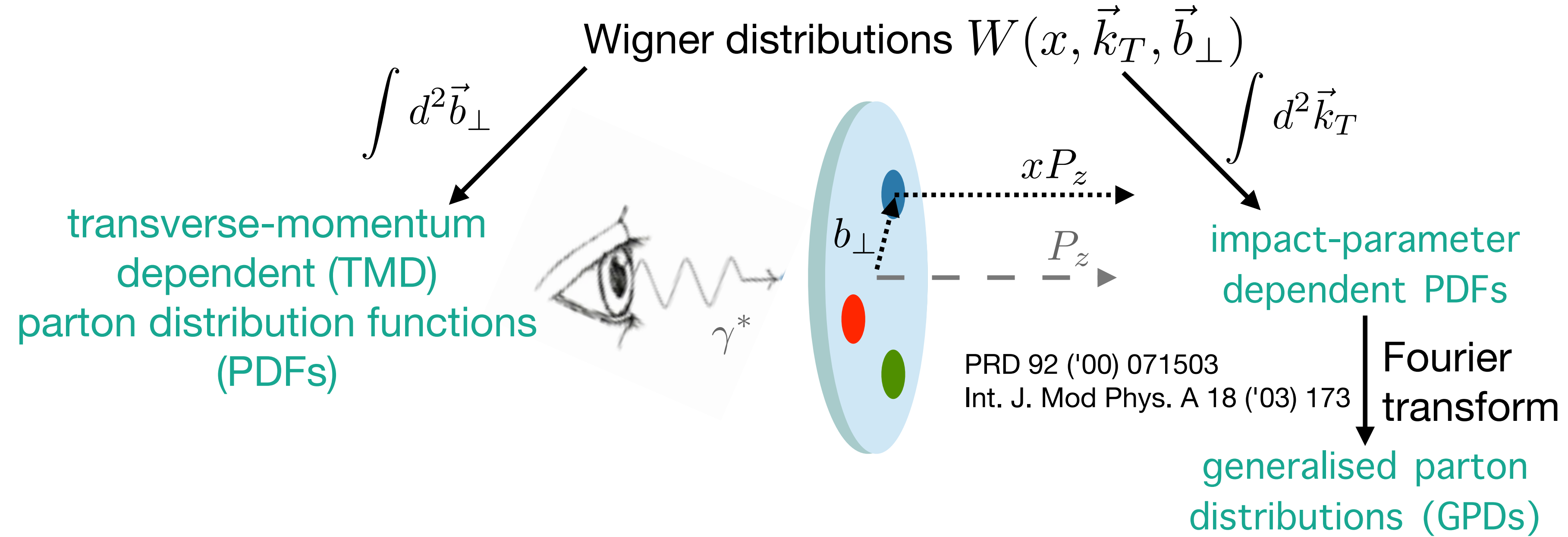
The various dimensions of the nucleon structure



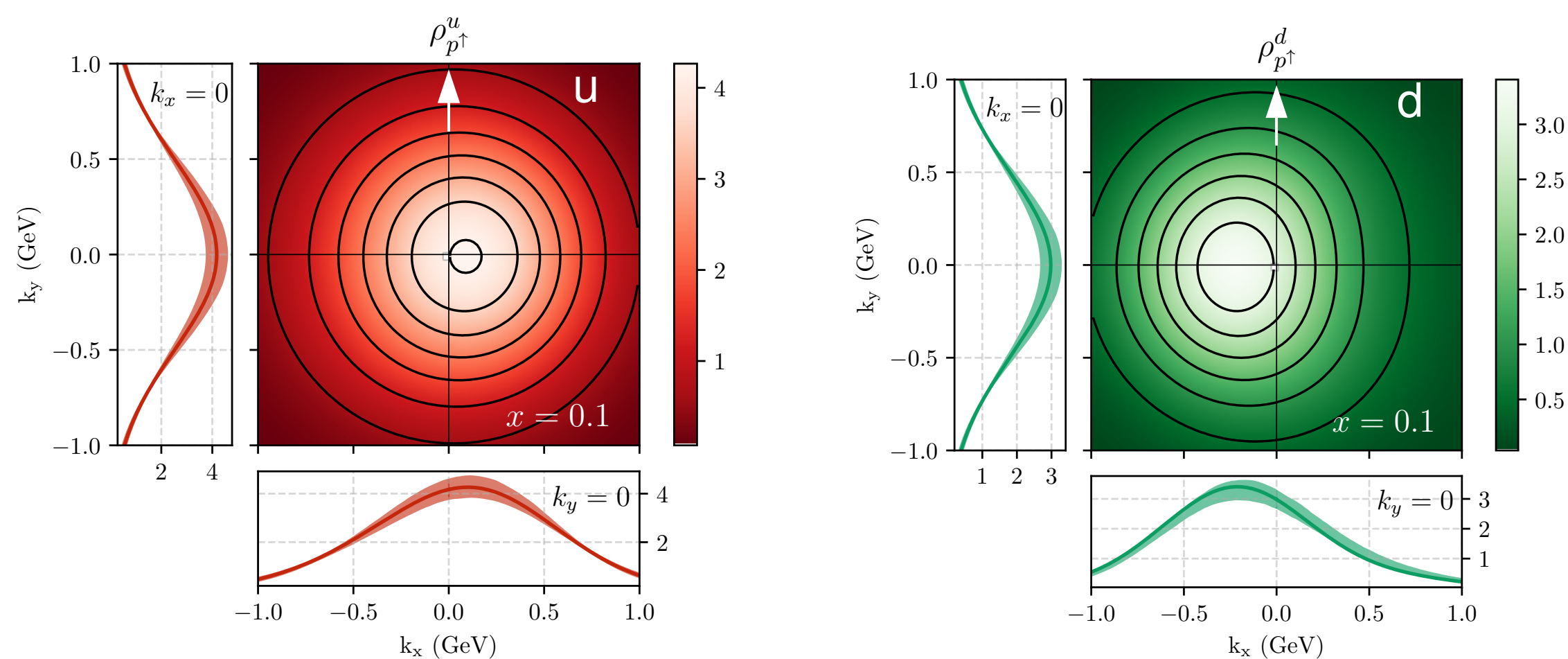
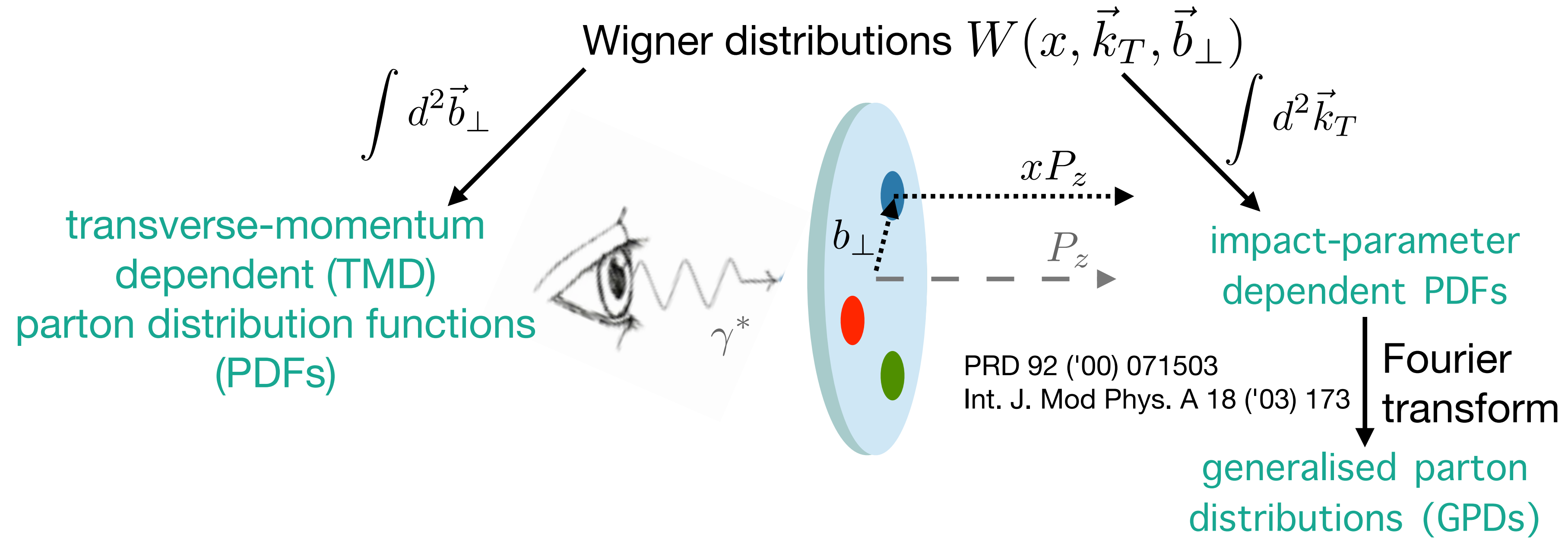
The various dimensions of the nucleon structure



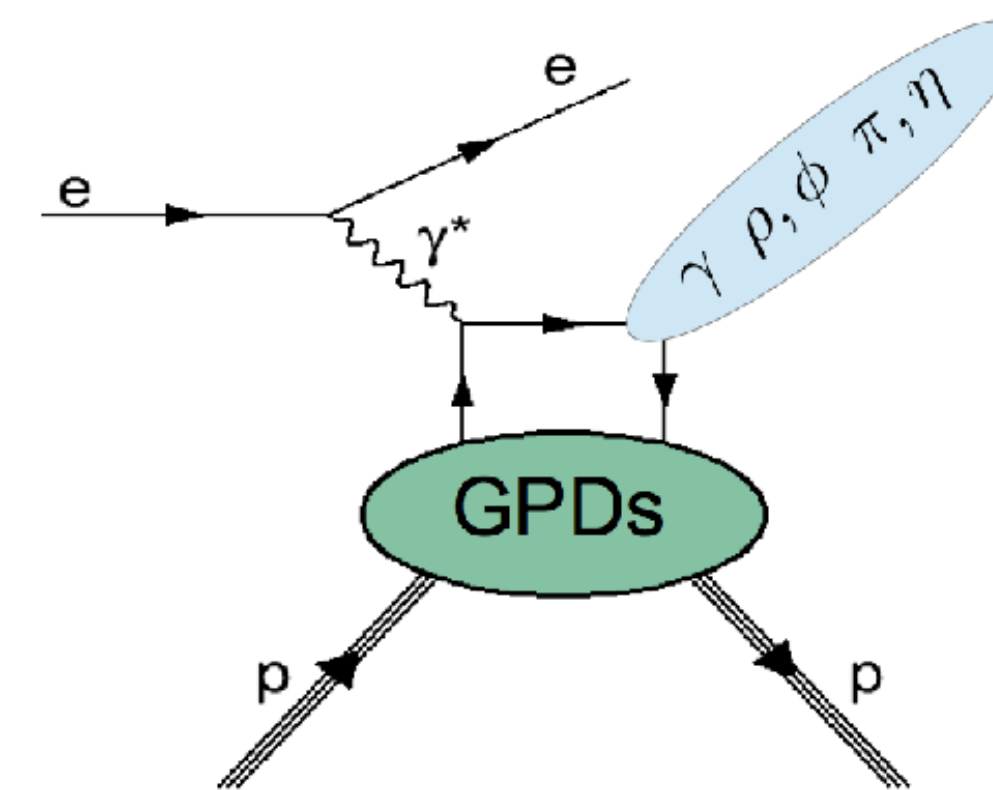
The various dimensions of the nucleon structure



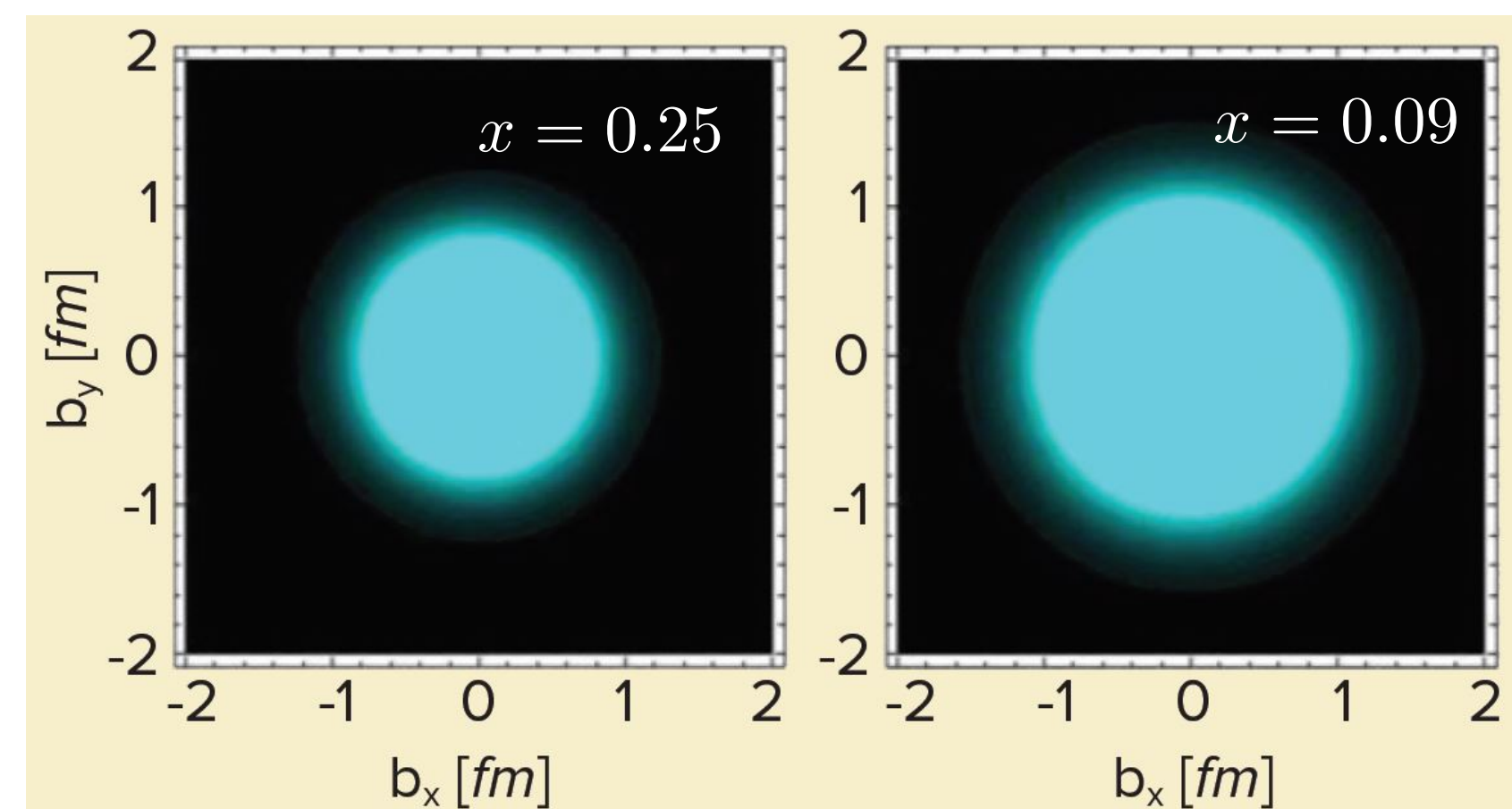
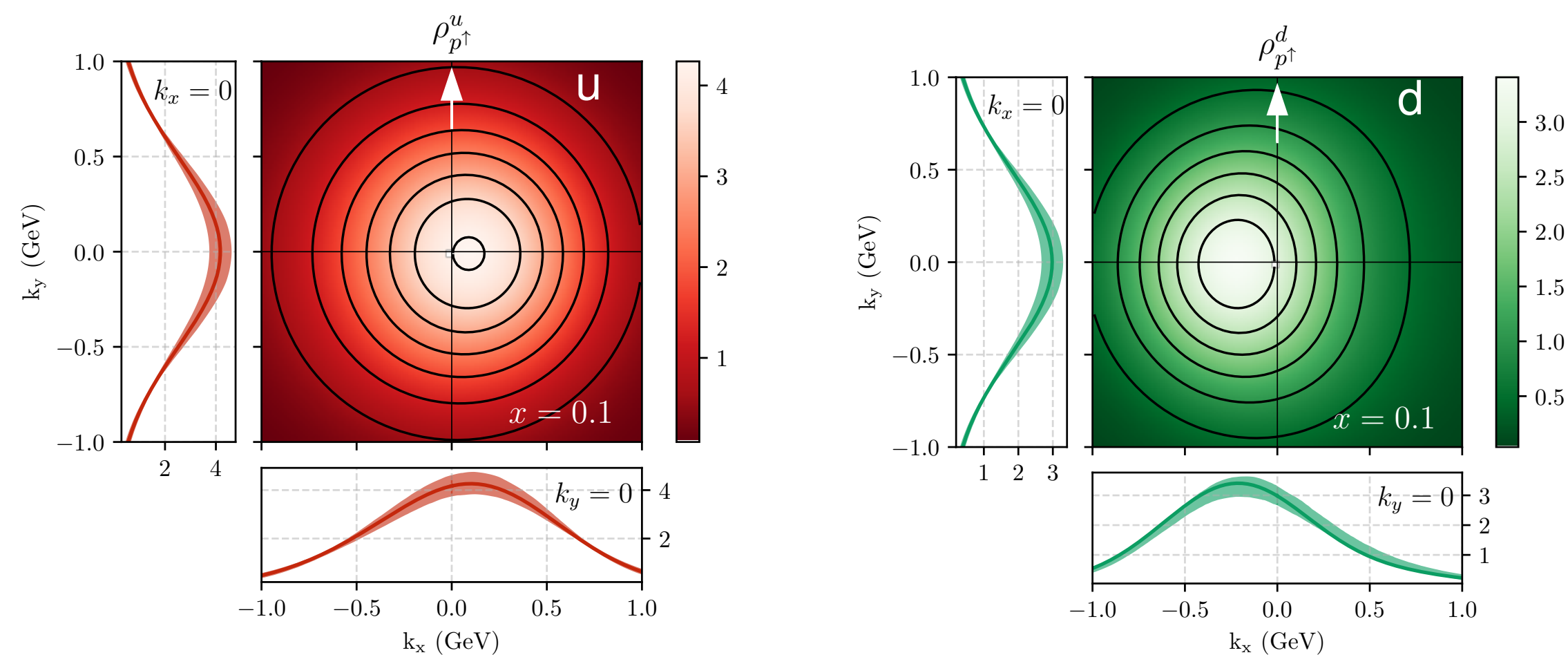
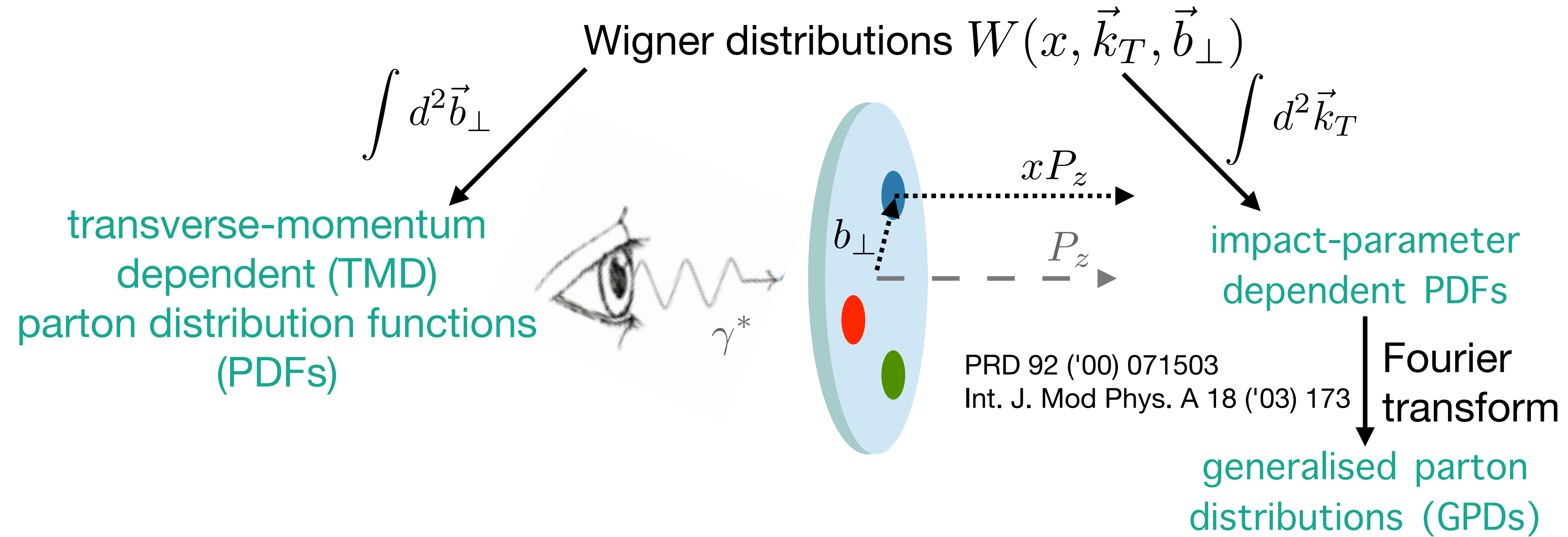
The various dimensions of the nucleon structure



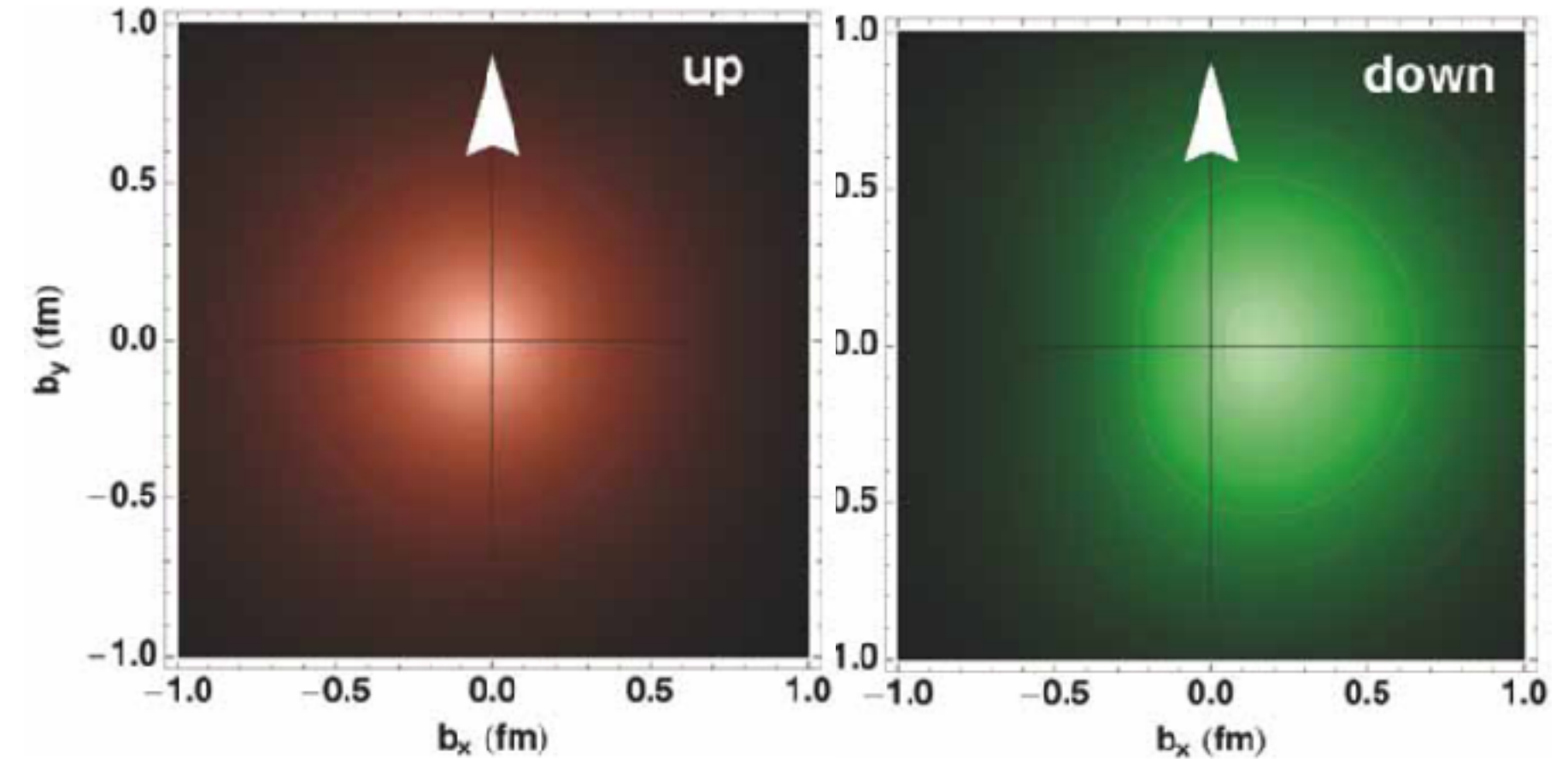
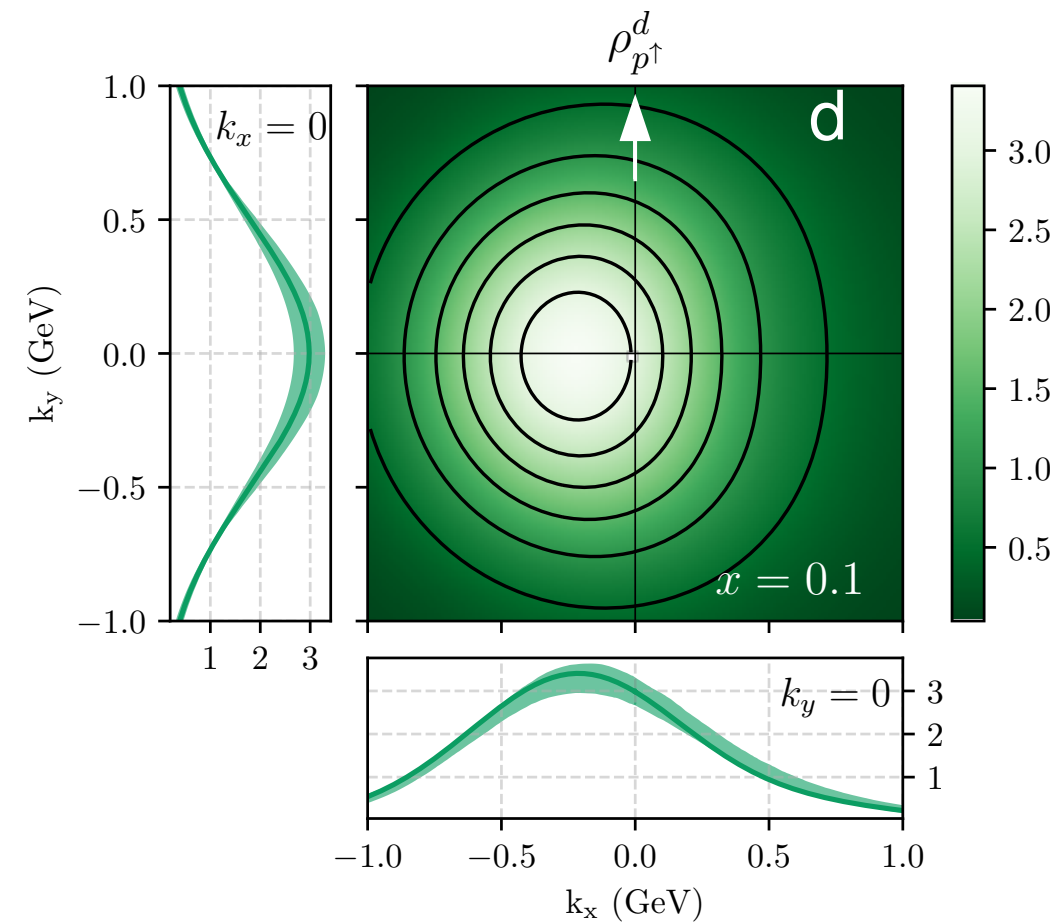
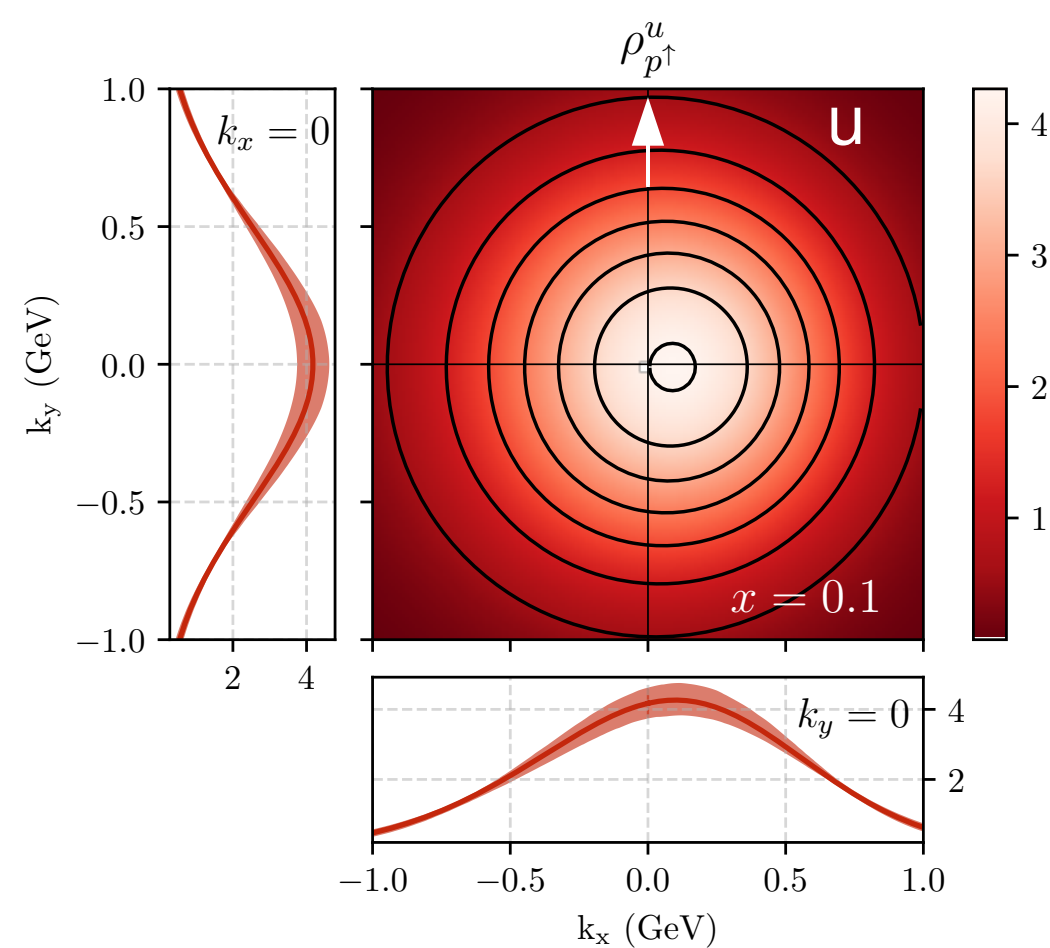
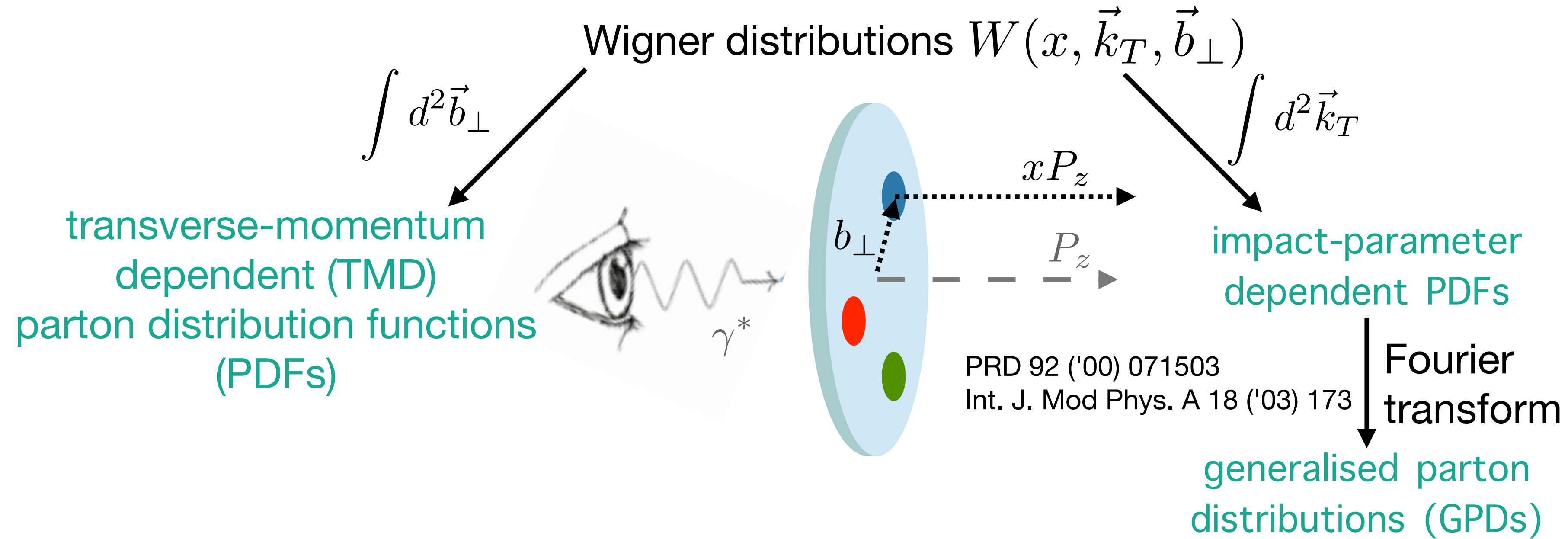
Exclusive production



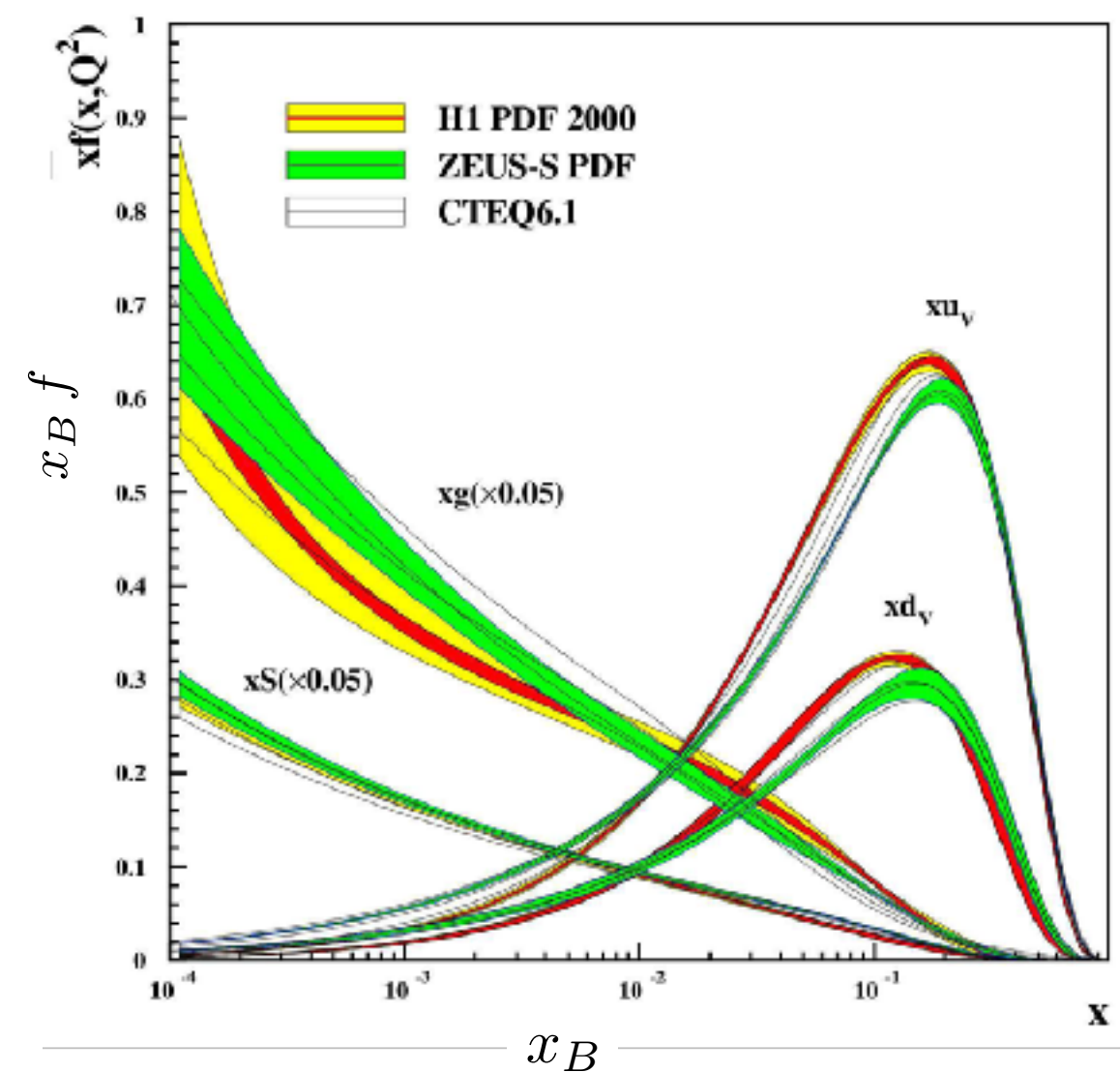
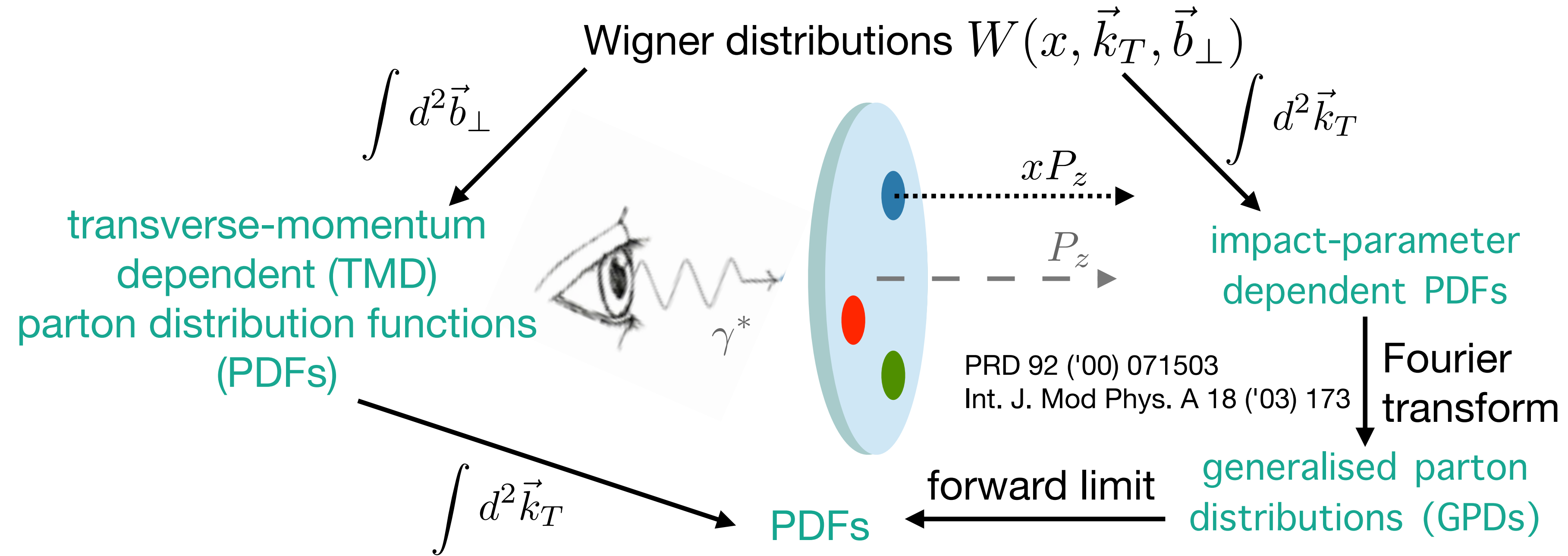
The various dimensions of the nucleon structure



The various dimensions of the nucleon structure

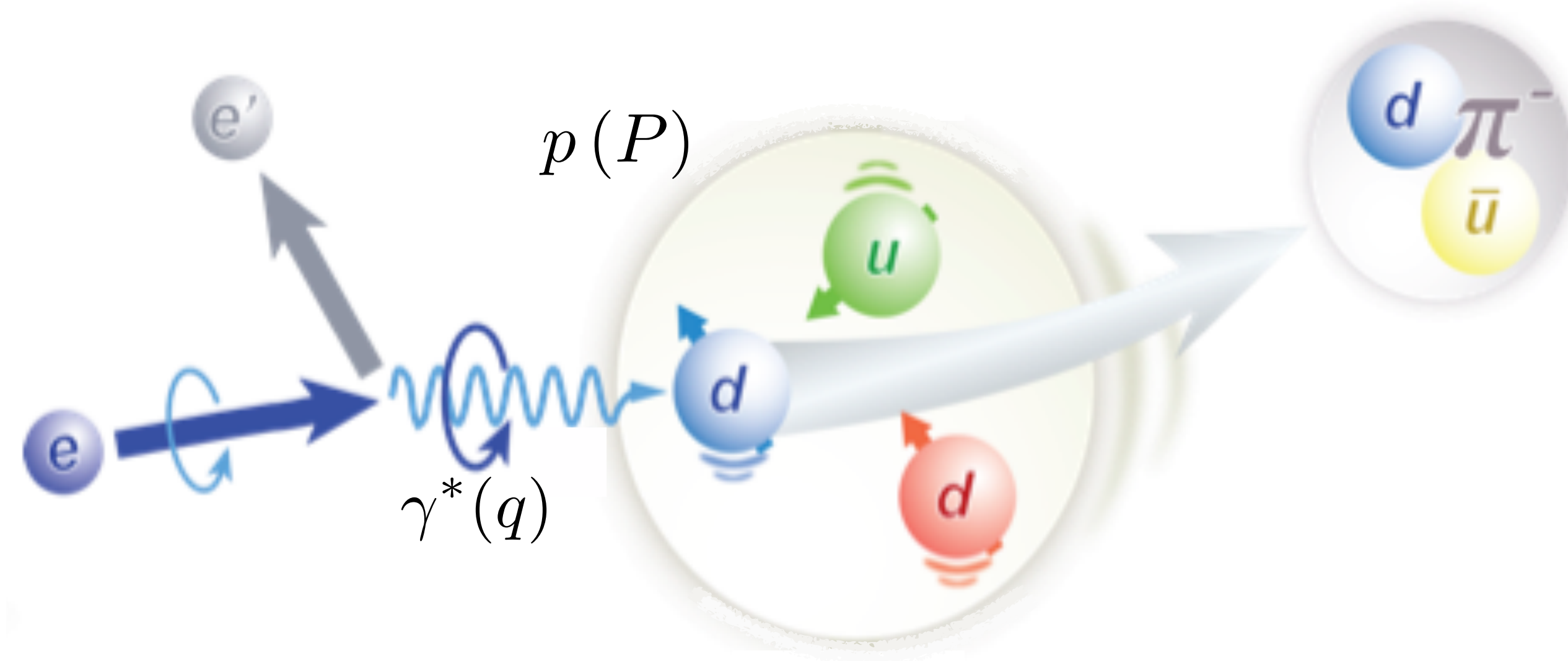


The various dimensions of the nucleon structure



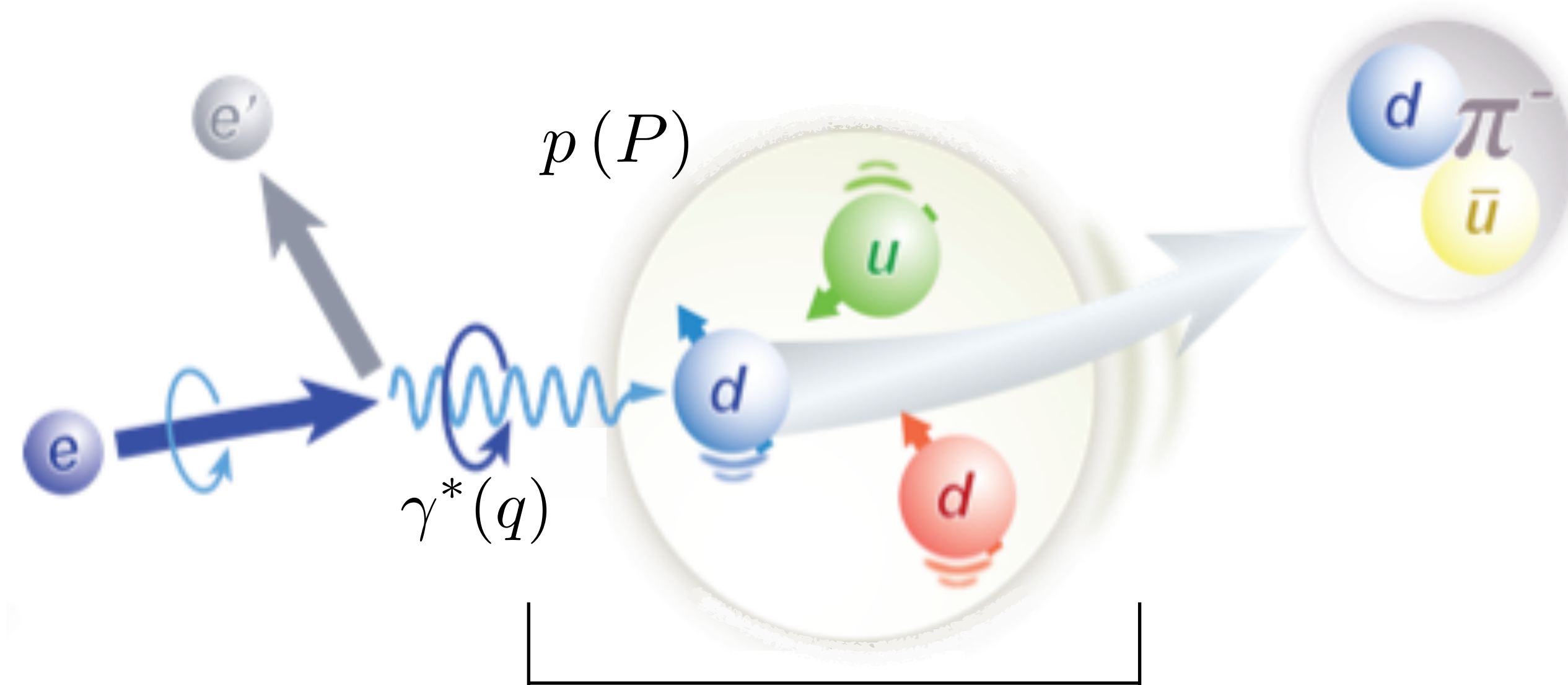
Single-hadron production in semi-inclusive DIS

$$Q^2 = -q^2$$
$$x_B = \frac{Q^2}{2P \cdot q}$$



Single-hadron production in semi-inclusive DIS

$$Q^2 = -q^2$$
$$x_B = \frac{Q^2}{2P \cdot q}$$

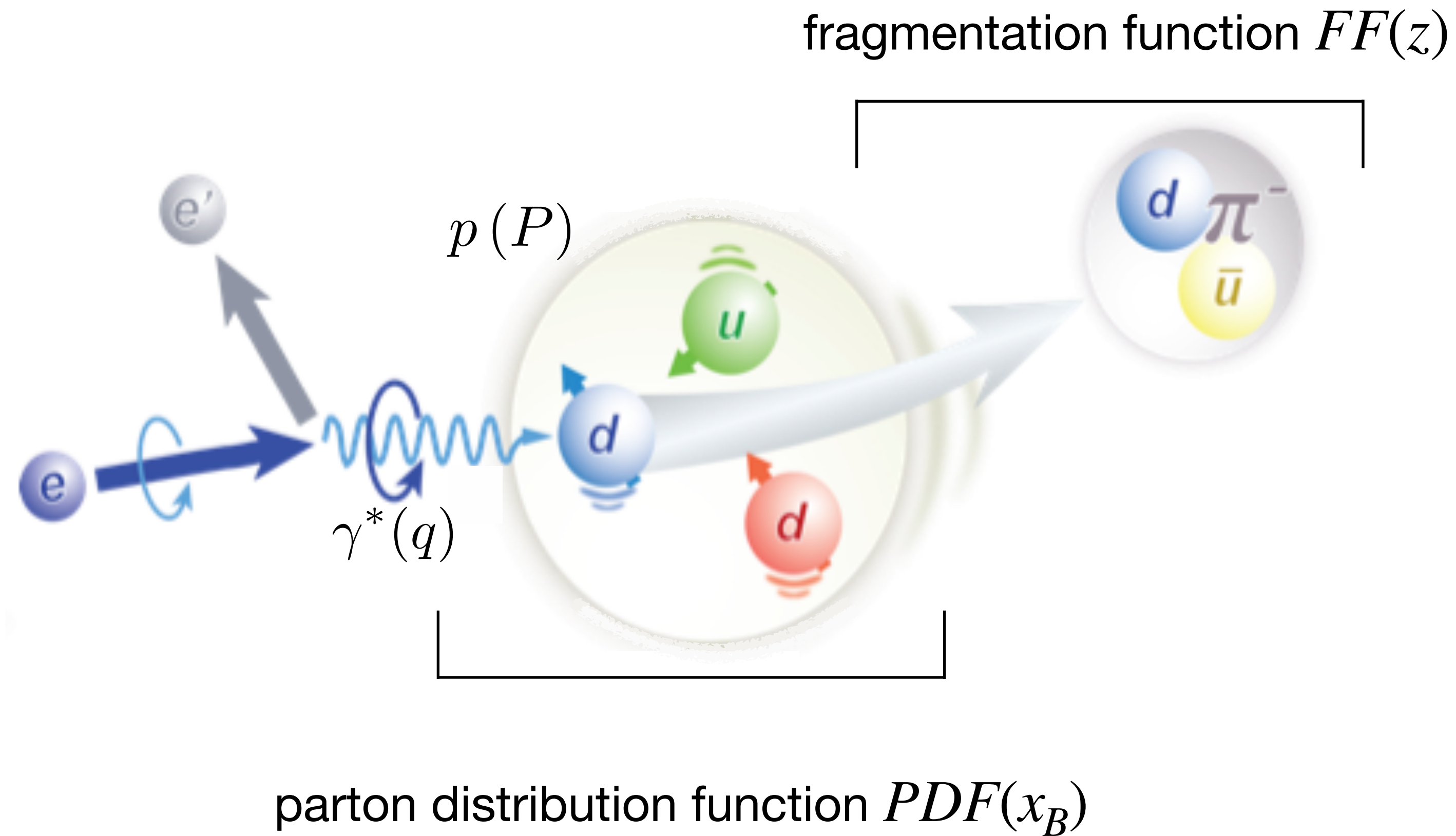


Single-hadron production in semi-inclusive DIS

$$Q^2 = -q^2$$

$$x_B = \frac{Q^2}{2P \cdot q}$$

$$z \stackrel{\text{lab}}{=} \frac{E_h}{E_{\gamma^*}}$$

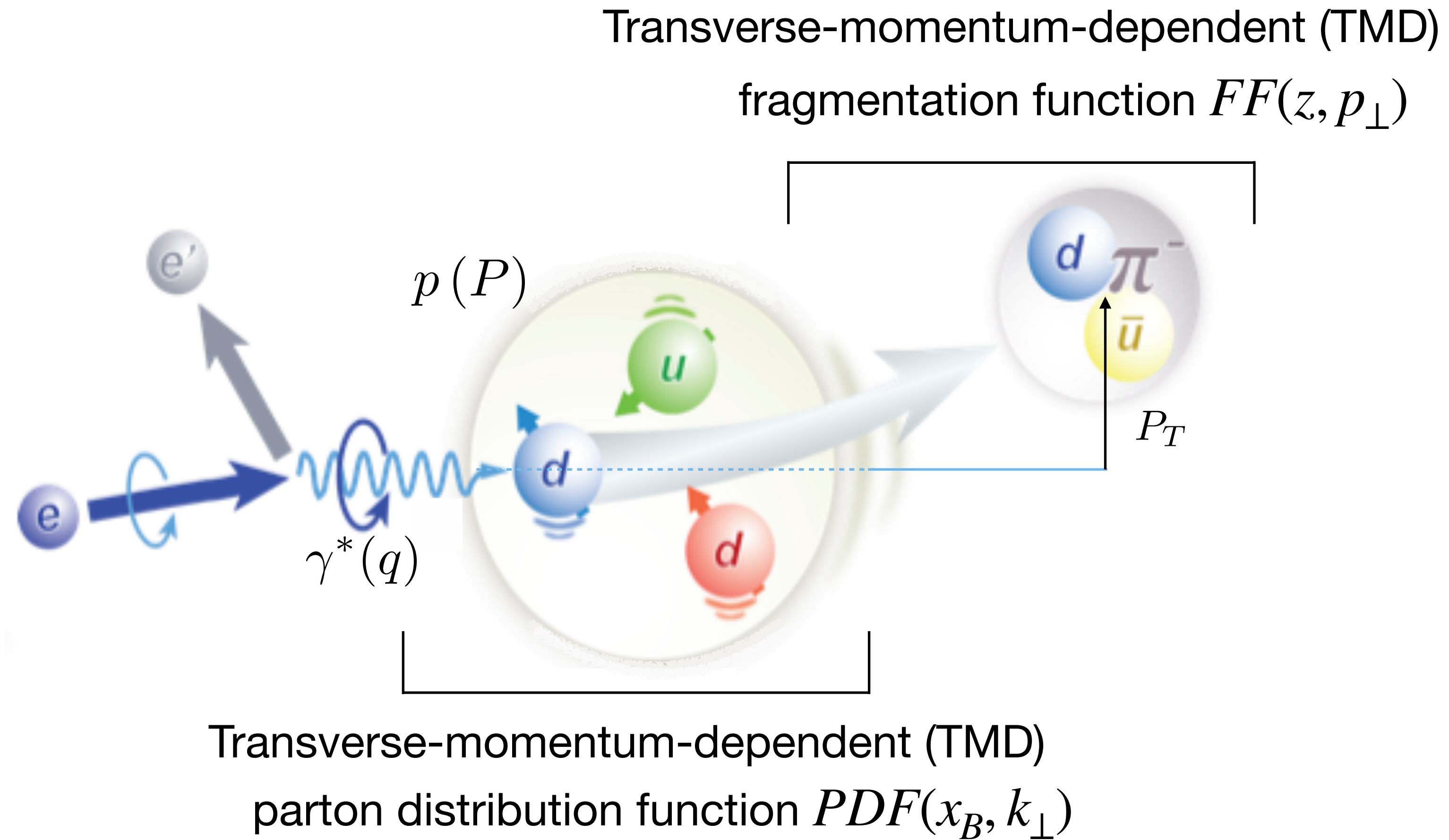


Single-hadron production in semi-inclusive DIS

$$Q^2 = -q^2$$

$$x_B = \frac{Q^2}{2P \cdot q}$$

$$z \stackrel{\text{lab}}{=} \frac{E_h}{E_{\gamma^*}}$$

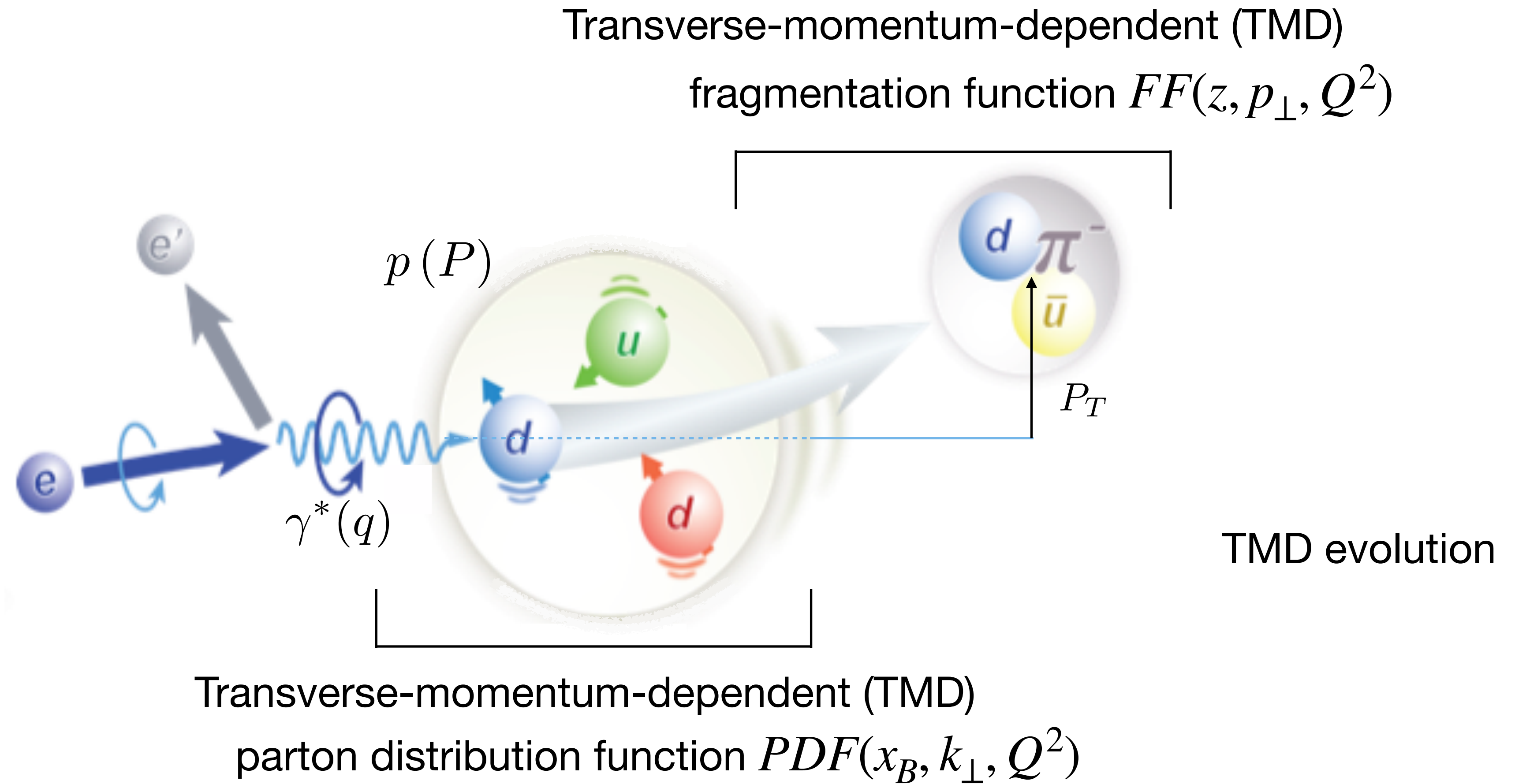


Single-hadron production in semi-inclusive DIS

$$Q^2 = -q^2$$

$$x_B = \frac{Q^2}{2P \cdot q}$$

$$z \stackrel{\text{lab}}{=} \frac{E_h}{E_{\gamma^*}}$$

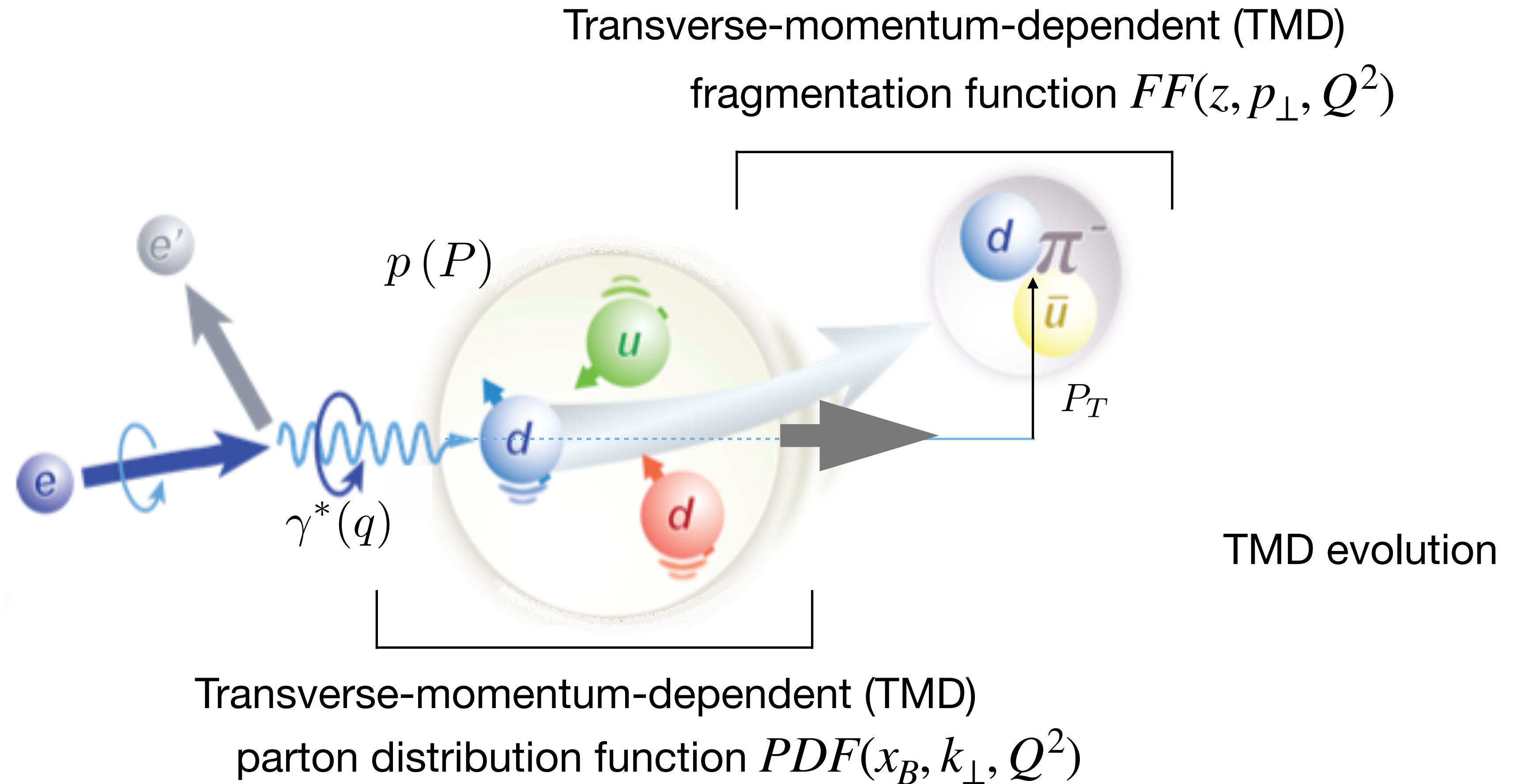


Single-hadron production in semi-inclusive DIS

$$Q^2 = -q^2$$

$$x_B = \frac{Q^2}{2P \cdot q}$$

$$z \stackrel{\text{lab}}{=} \frac{E_h}{E_{\gamma^*}}$$

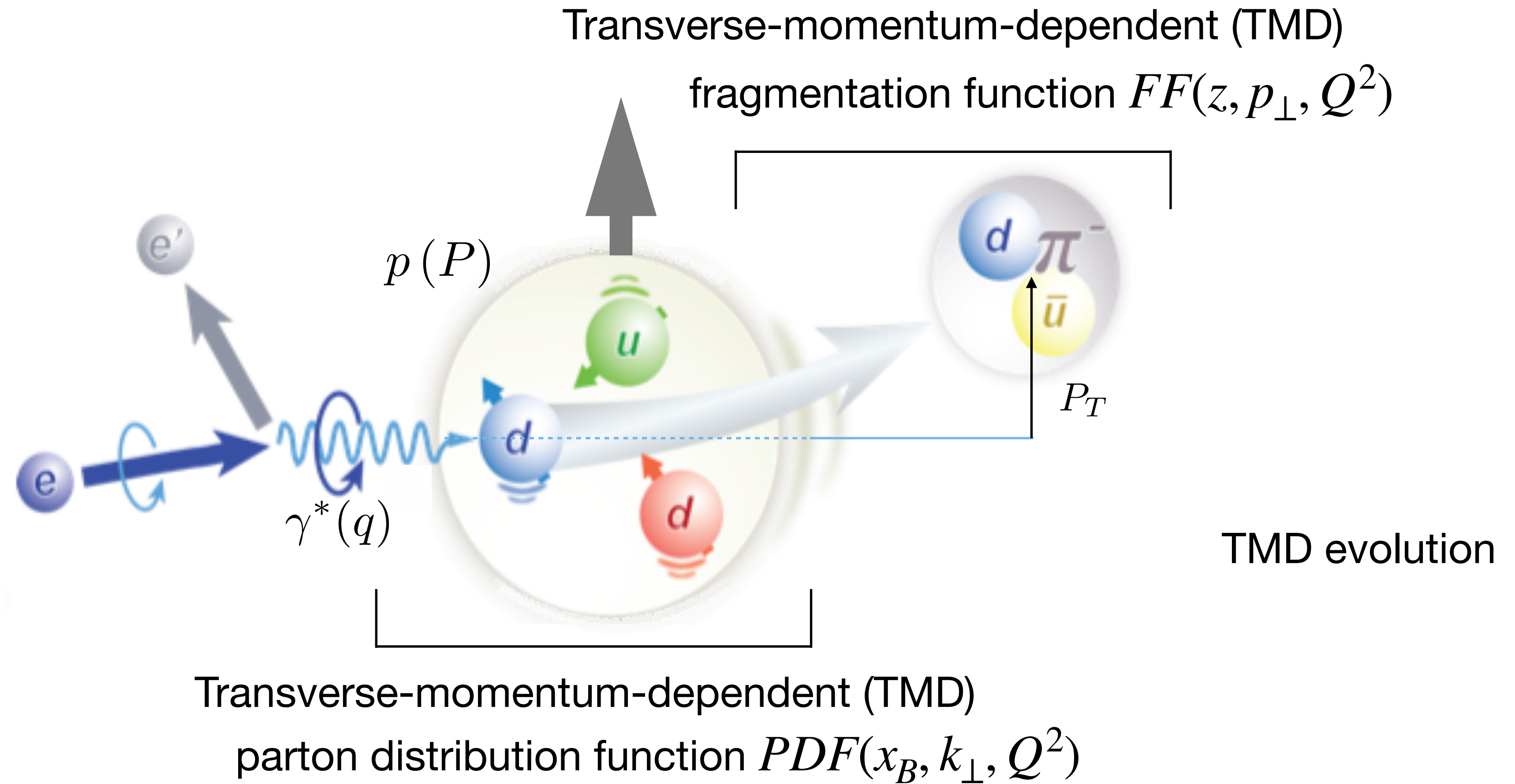


Single-hadron production in semi-inclusive DIS

$$Q^2 = -q^2$$

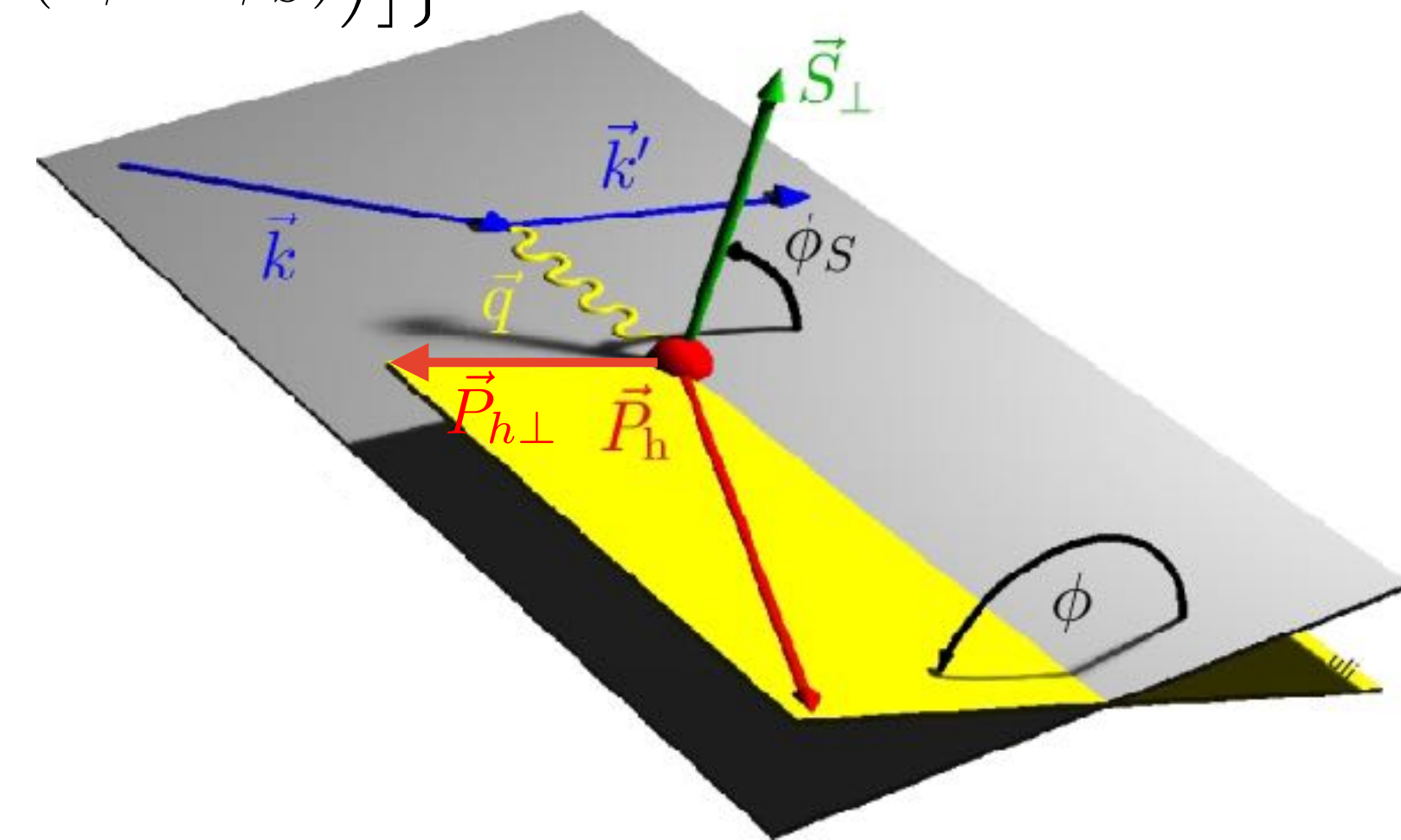
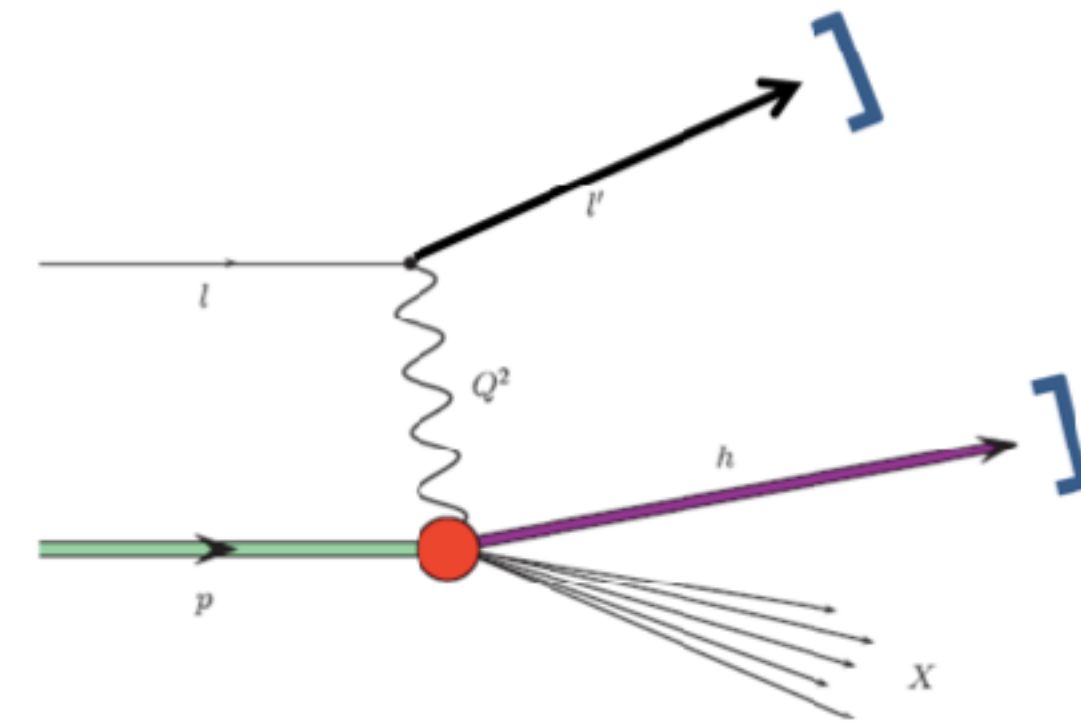
$$x_B = \frac{Q^2}{2P \cdot q}$$

$$z \stackrel{\text{lab}}{=} \frac{E_h}{E_{\gamma^*}}$$

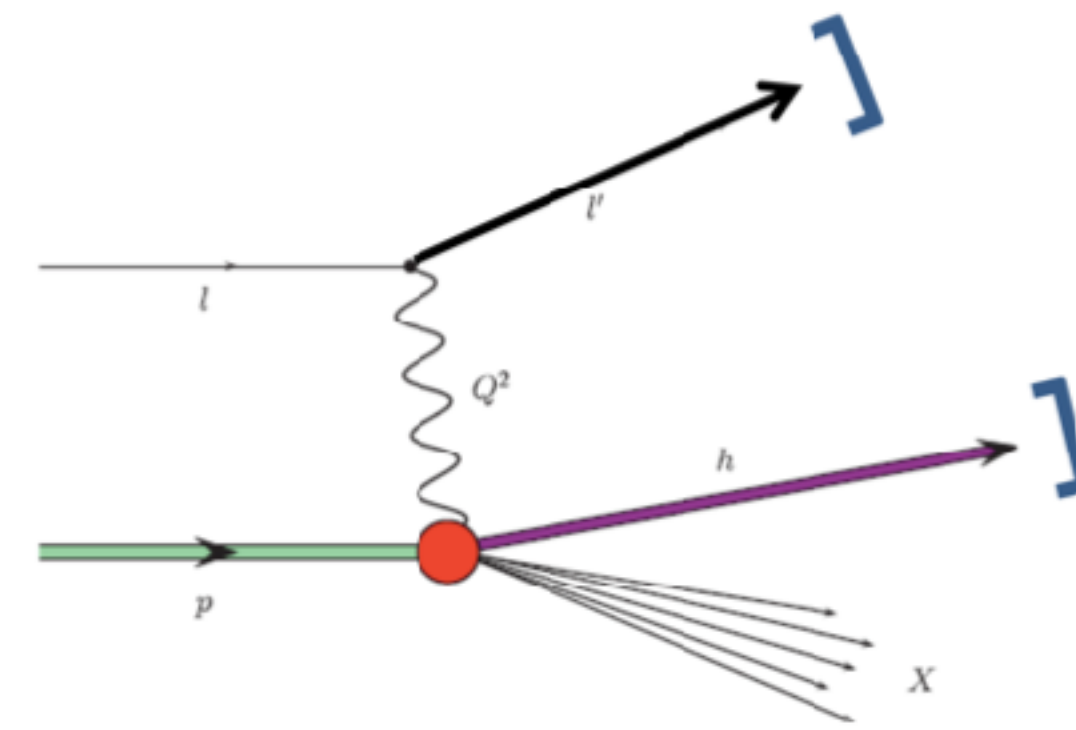


Semi-inclusive DIS cross section

$$\begin{aligned}
 \sigma^h(\phi, \phi_S) = & \sigma_{UU}^h \left\{ 1 + 2\langle \cos(\phi) \rangle_{UU}^h \cos(\phi) + 2\langle \cos(2\phi) \rangle_{UU}^h \cos(2\phi) \right. \\
 & + \lambda_l 2\langle \sin(\phi) \rangle_{LU}^h \sin(\phi) \\
 & + S_L \left[2\langle \sin(\phi) \rangle_{UL}^h \sin(\phi) + 2\langle \sin(2\phi) \rangle_{UL}^h \sin(2\phi) \right. \\
 & + \lambda_l \left(2\langle \cos(0\phi) \rangle_{LL}^h \cos(0\phi) + 2\langle \cos(\phi) \rangle_{LL}^h \cos(\phi) \right) \left. \right] \\
 & + S_T \left[2\langle \sin(\phi - \phi_S) \rangle_{UT}^h \sin(\phi - \phi_S) + 2\langle \sin(\phi + \phi_S) \rangle_{UT}^h \sin(\phi + \phi_S) \right. \\
 & + 2\langle \sin(3\phi - \phi_S) \rangle_{UT}^h \sin(3\phi - \phi_S) + 2\langle \sin(\phi_S) \rangle_{UT}^h \sin(\phi_S) \\
 & + 2\langle \sin(2\phi - \phi_S) \rangle_{UT}^h \sin(2\phi - \phi_S) \\
 & + \lambda_l \left(2\langle \cos(\phi - \phi_S) \rangle_{LT}^h \cos(\phi - \phi_S) \right. \\
 & \left. \left. + 2\langle \cos(\phi_S) \rangle_{LT}^h \cos(\phi_S) + 2\langle \cos(2\phi - \phi_S) \rangle_{LT}^h \cos(2\phi - \phi_S) \right) \right] \left. \right\}
 \end{aligned}$$

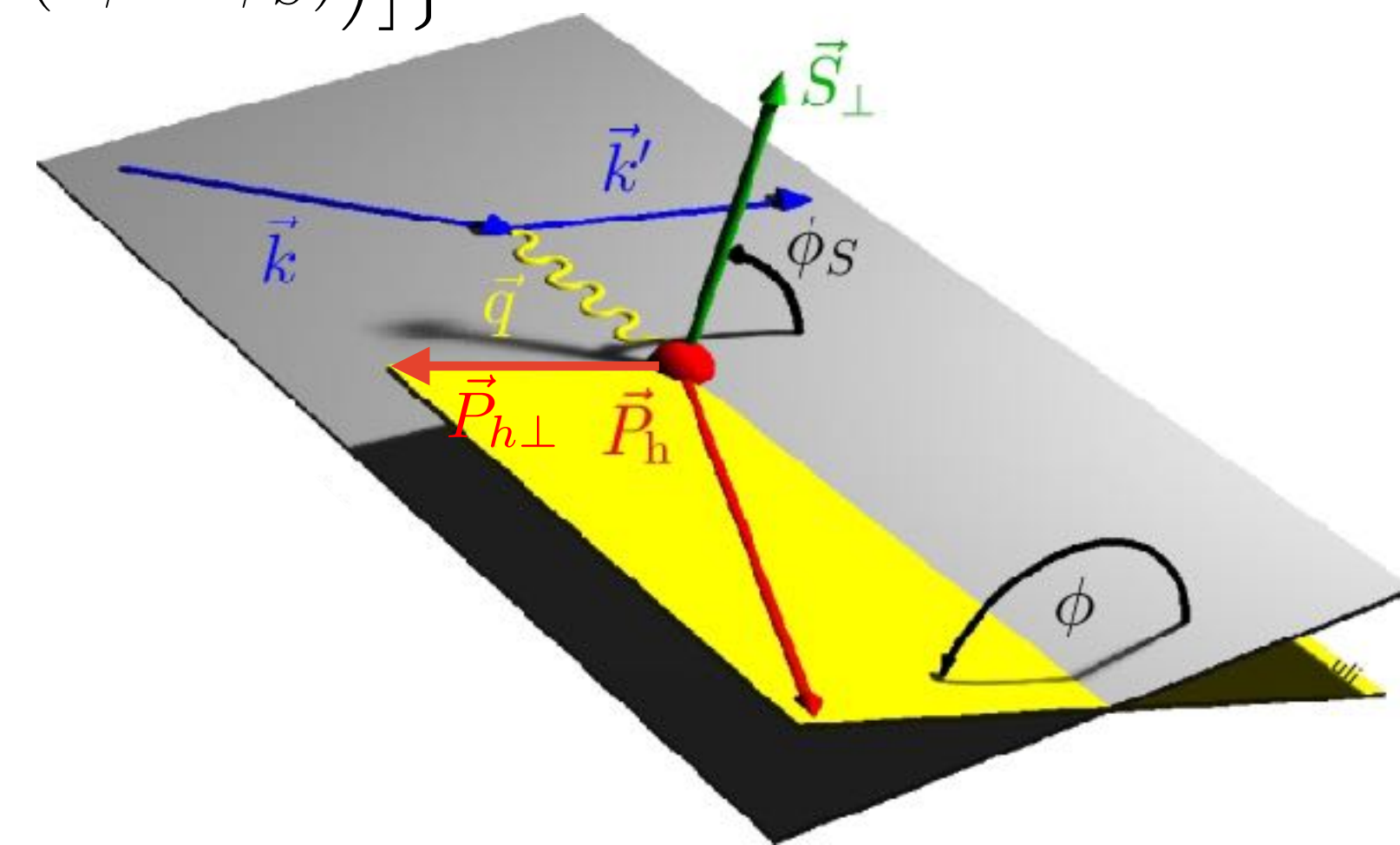


Semi-inclusive DIS cross section



$$\begin{aligned}
 \sigma^h(\phi, \phi_S) = & \sigma_{UU}^h \left\{ 1 + 2\langle \cos(\phi) \rangle_{UU}^h \cos(\phi) + 2\langle \cos(2\phi) \rangle_{UU}^h \cos(2\phi) \right. \\
 & + \lambda_l 2\langle \sin(\phi) \rangle_{LU}^h \sin(\phi) \\
 \text{longitudinal target} & \leftarrow + S_L \left[2\langle \sin(\phi) \rangle_{UL}^h \sin(\phi) + 2\langle \sin(2\phi) \rangle_{UL}^h \sin(2\phi) \right. \\
 \text{polarisation} & \left. + \lambda_l \left(2\langle \cos(0\phi) \rangle_{LL}^h \cos(0\phi) + 2\langle \cos(\phi) \rangle_{LL}^h \cos(\phi) \right) \right] \\
 \text{transverse target} & \leftarrow + S_T \left[2\langle \sin(\phi - \phi_S) \rangle_{UT}^h \sin(\phi - \phi_S) + 2\langle \sin(\phi + \phi_S) \rangle_{UT}^h \sin(\phi + \phi_S) \right. \\
 \text{polarisation} & \left. + 2\langle \sin(3\phi - \phi_S) \rangle_{UT}^h \sin(3\phi - \phi_S) + 2\langle \sin(\phi_S) \rangle_{UT}^h \sin(\phi_S) \right. \\
 & + 2\langle \sin(2\phi - \phi_S) \rangle_{UT}^h \sin(2\phi - \phi_S) \\
 \text{beam} & \leftarrow + \lambda_l \left(2\langle \cos(\phi - \phi_S) \rangle_{LT}^h \cos(\phi - \phi_S) \right. \\
 \text{polarisation} & \left. + 2\langle \cos(\phi_S) \rangle_{LT}^h \cos(\phi_S) + 2\langle \cos(2\phi - \phi_S) \rangle_{LT}^h \cos(2\phi - \phi_S) \right) \left. \right\}
 \end{aligned}$$

beam polarisation
target polarisation



TMD PDFs and fragmentation functions (FFs)

Azimuthal amplitudes related to structure functions F_{XY} :

$$2\langle \sin(\phi + \phi_S) \rangle_{UT}^h = \epsilon F_{UT}^{\sin(\phi + \phi_S)}$$

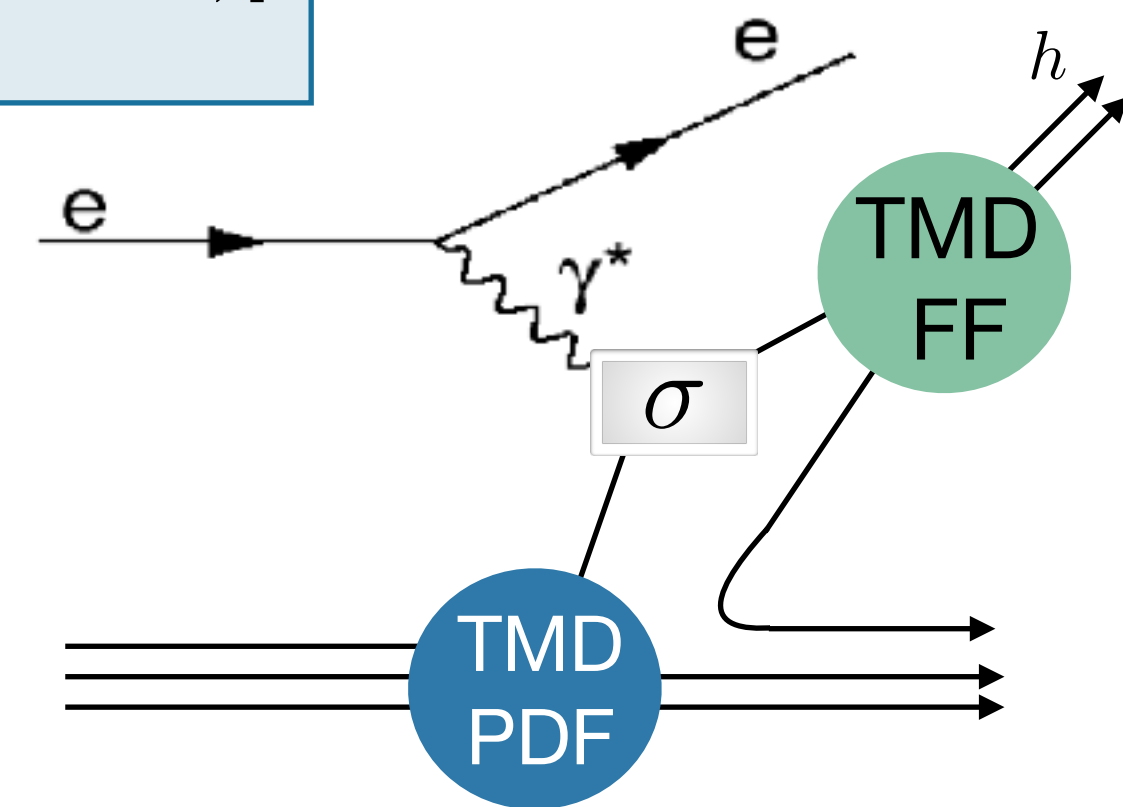
TMD PDFs and fragmentation functions (FFs)

Azimuthal amplitudes related to structure functions F_{XY} :

$$2\langle \sin(\phi + \phi_S) \rangle_{UT}^h = \epsilon F_{UT}^{\sin(\phi + \phi_S)}$$

$$F_{XY} \propto \mathcal{C} [\text{TMD PDF}(x, k_{\perp}) \times \text{TMD FF}(z, p_{\perp})]$$

$$z \stackrel{\text{lab}}{=} \frac{E_h}{E_{\gamma^*}}$$



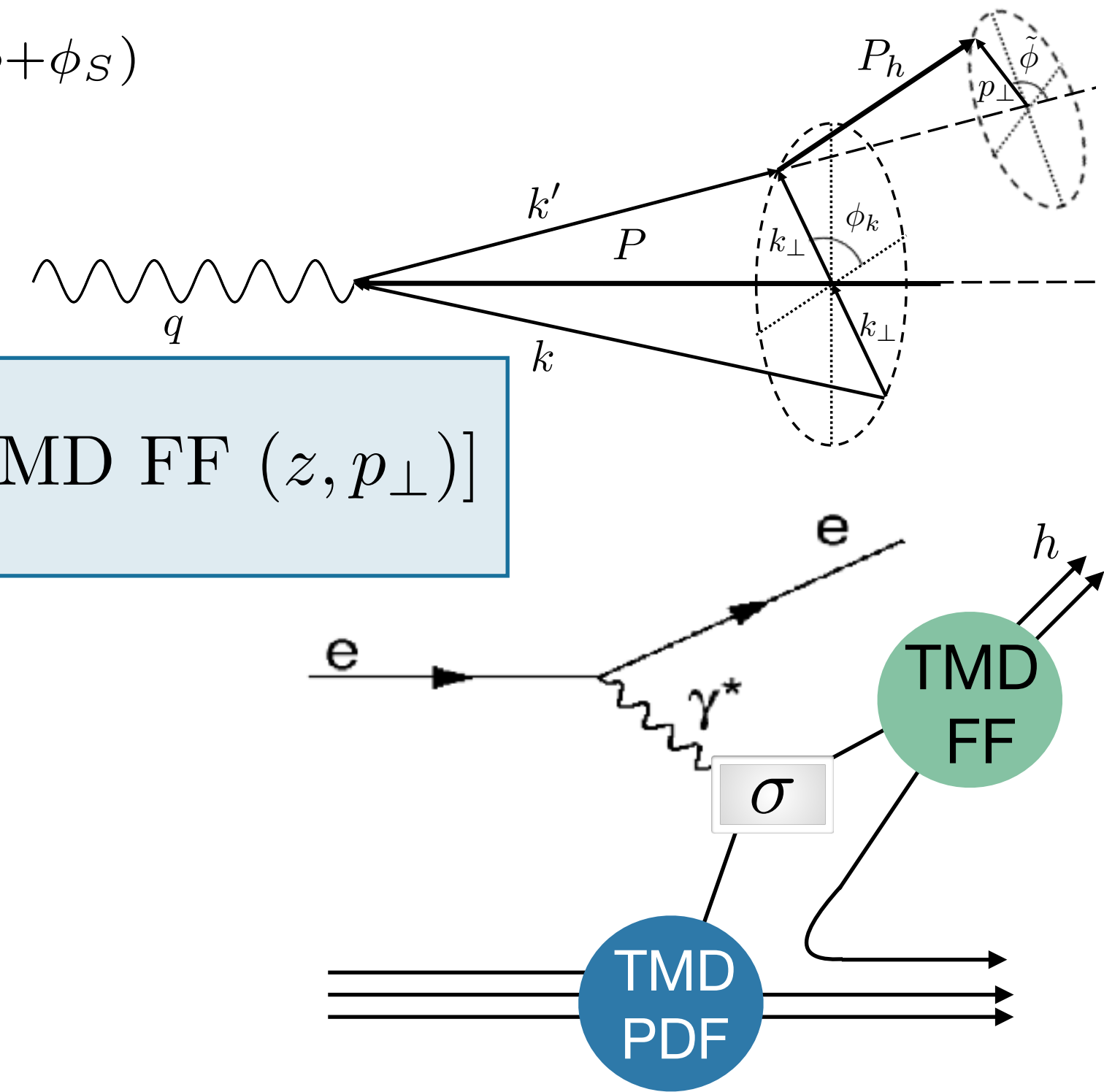
TMD PDFs and fragmentation functions (FFs)

Azimuthal amplitudes related to structure functions F_{XY} :

$$2\langle \sin(\phi + \phi_S) \rangle_{UT}^h = \epsilon F_{UT}^{\sin(\phi + \phi_S)}$$

$$F_{XY} \propto \mathcal{C} [\text{TMD PDF}(x, k_{\perp}) \times \text{TMD FF}(z, p_{\perp})]$$

$$z \stackrel{\text{lab}}{=} \frac{E_h}{E_{\gamma^*}}$$

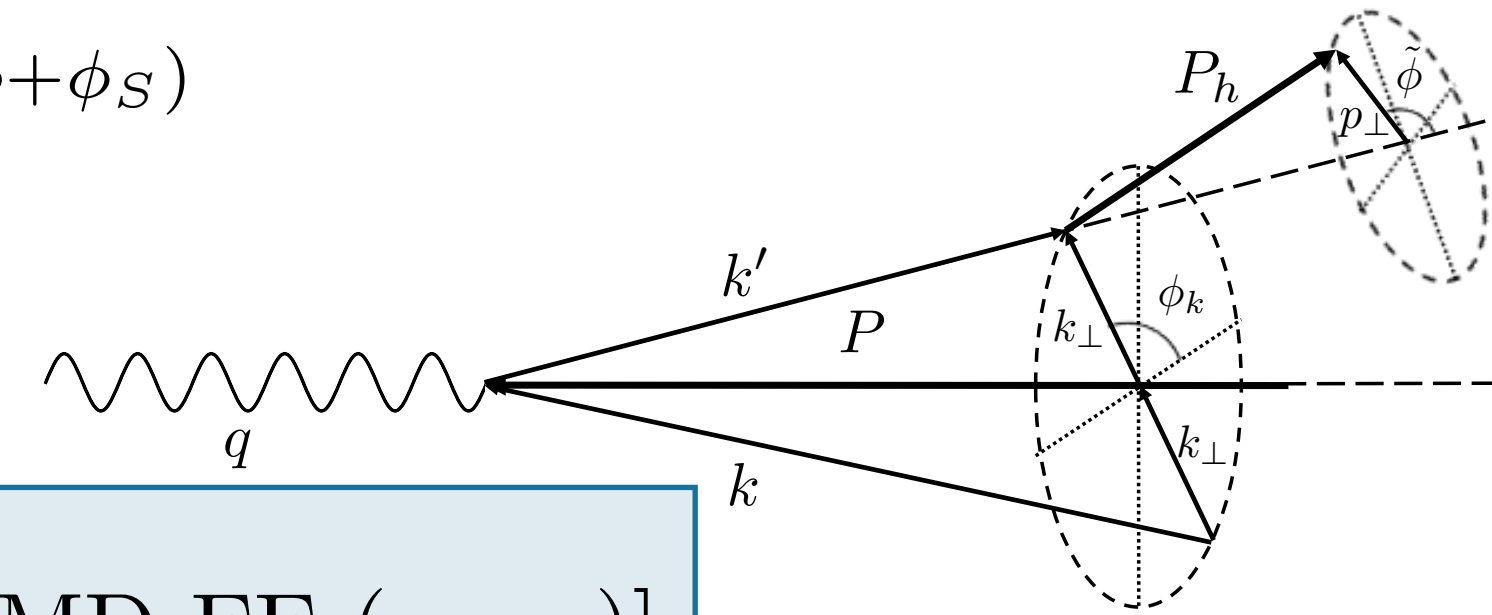


TMD PDFs and fragmentation functions (FFs)

Azimuthal amplitudes related to structure functions F_{XY} :

$$2\langle \sin(\phi + \phi_S) \rangle_{UT}^h = \epsilon F_{UT}^{\sin(\phi + \phi_S)}$$

$$F_{XY} \propto \mathcal{C} [\text{TMD PDF}(x, k_{\perp}) \times \text{TMD FF}(z, p_{\perp})]$$

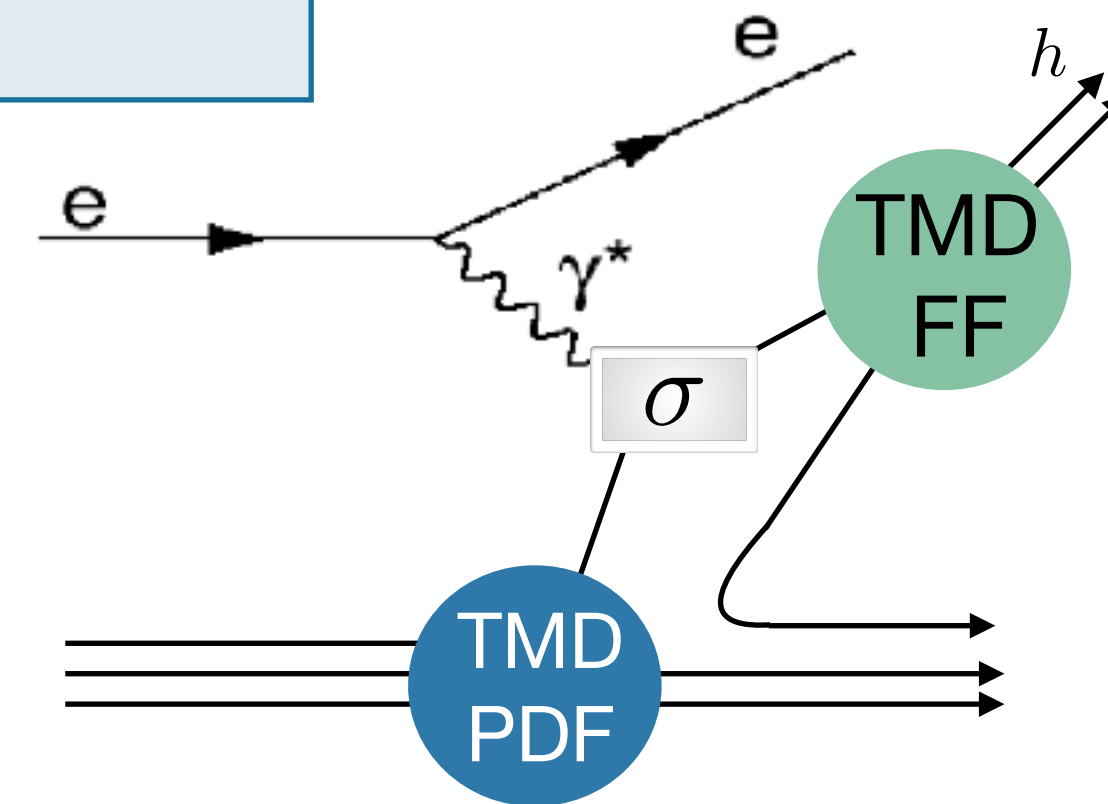


quark polarisation

nucleon polarisation		U	L	T
	U	f_1		
	L		g_{1L}	
	T			h_{1T}

survive integration of parton transverse momentum

$$z \stackrel{\text{lab}}{=} \frac{E_h}{E_{\gamma^*}}$$

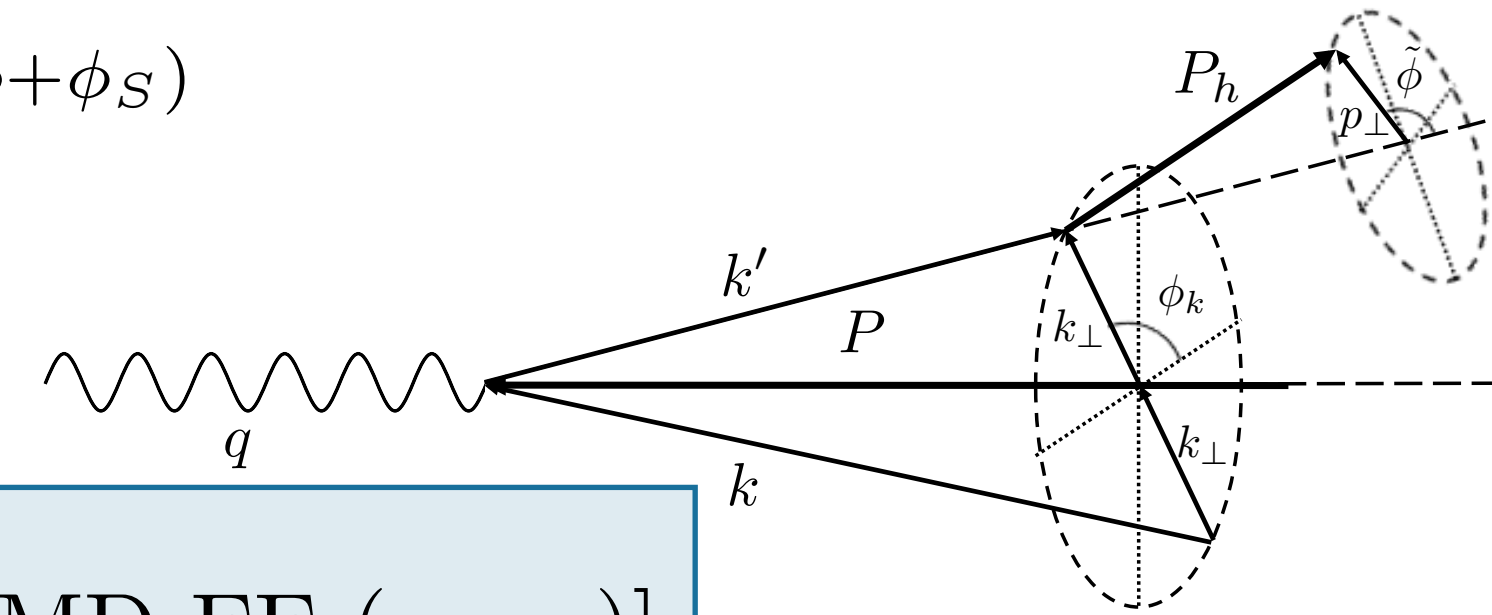


TMD PDFs and fragmentation functions (FFs)

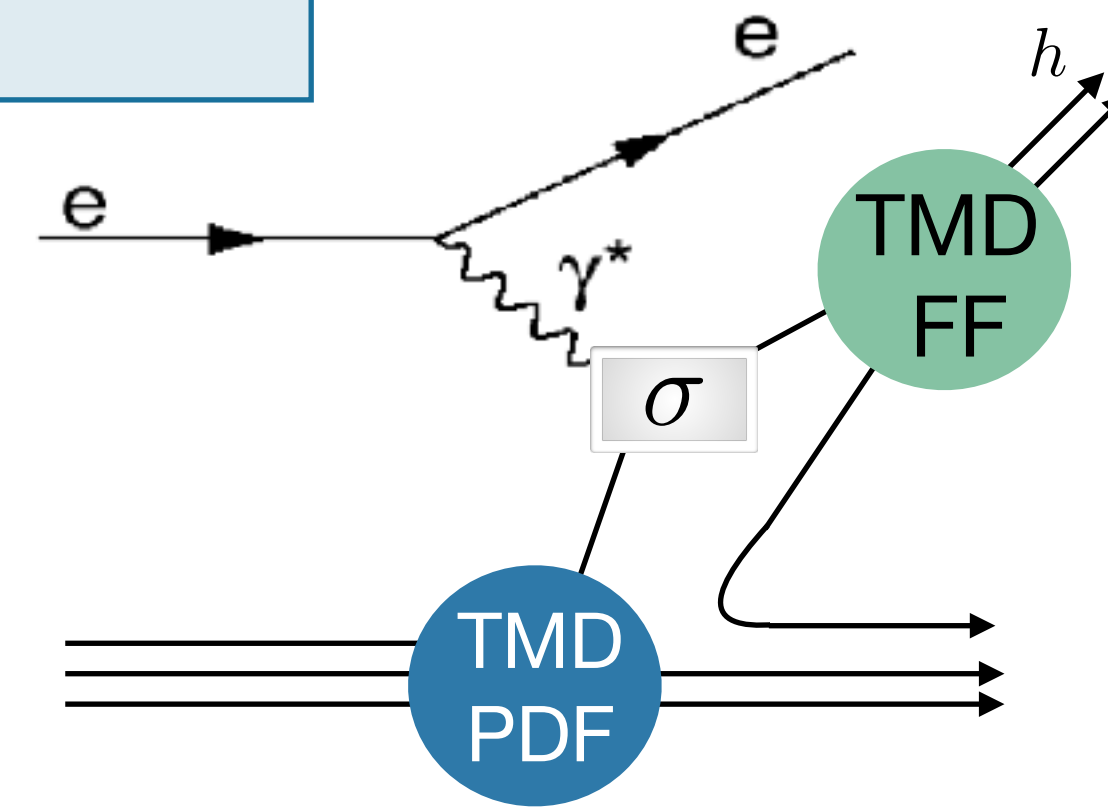
Azimuthal amplitudes related to structure functions F_{XY} :

$$2\langle \sin(\phi + \phi_S) \rangle_{UT}^h = \epsilon F_{UT}^{\sin(\phi + \phi_S)}$$

$$F_{XY} \propto \mathcal{C} [\text{TMD PDF}(x, k_{\perp}) \times \text{TMD FF}(z, p_{\perp})]$$



$$z \stackrel{\text{lab}}{=} \frac{E_h}{E_{\gamma^*}}$$



nucleon polarisation

quark polarisation

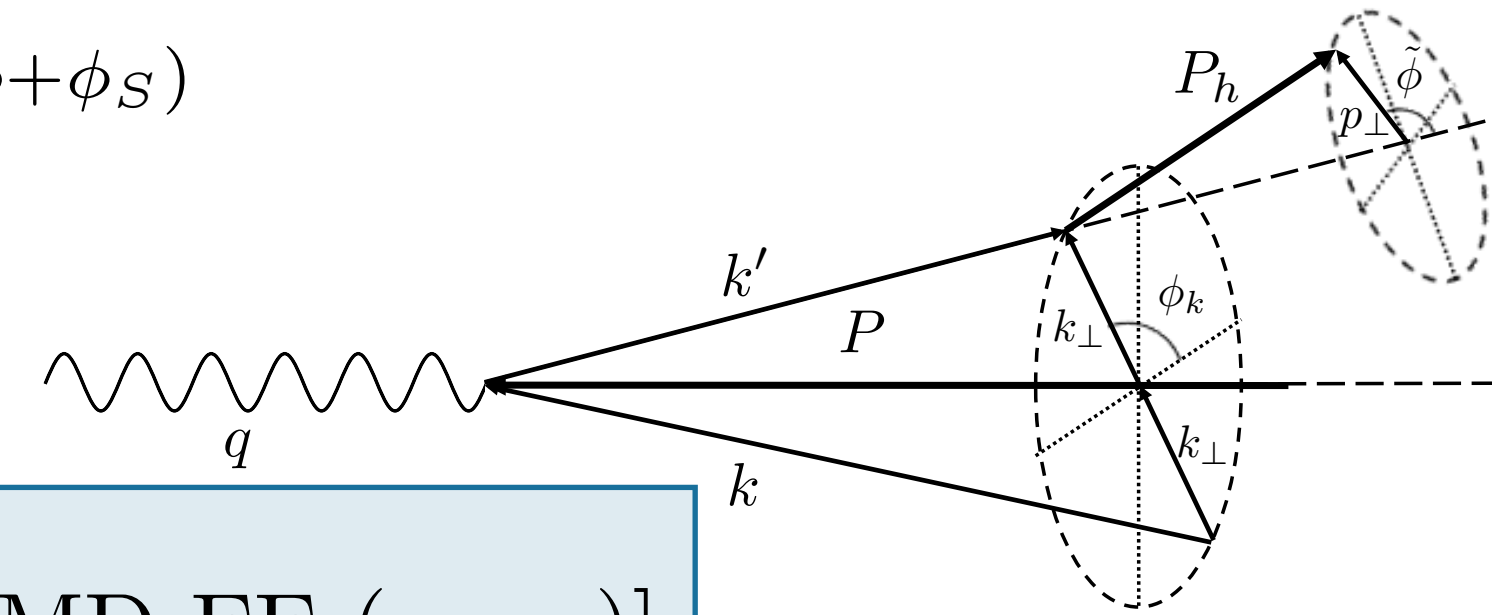
	U	L	T
U	f_1		h_1^{\perp}
L		g_{1L}	h_{1L}^{\perp}
T	f_{1T}^{\perp}	g_{1T}^{\perp}	$h_{1T} h_{1T}^{\perp}$

TMD PDFs and fragmentation functions (FFs)

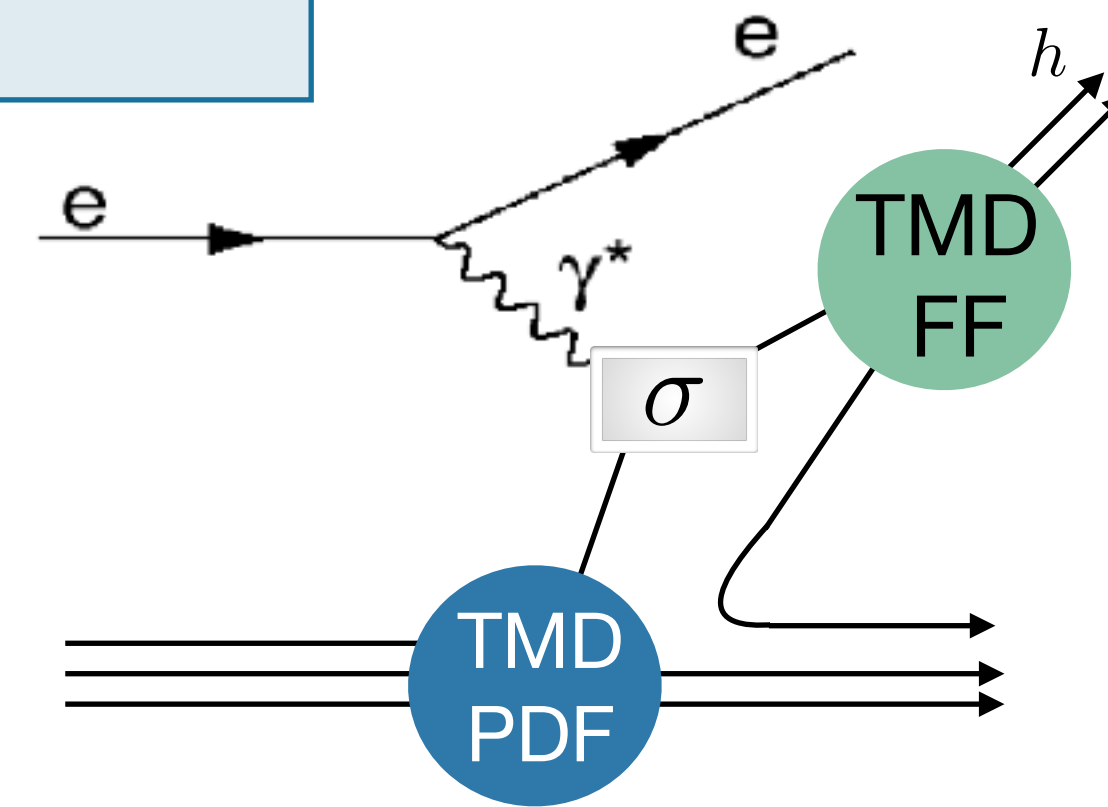
Azimuthal amplitudes related to structure functions F_{XY} :

$$2\langle \sin(\phi + \phi_S) \rangle_{UT}^h = \epsilon F_{UT}^{\sin(\phi + \phi_S)}$$

$$F_{XY} \propto \mathcal{C} [\text{TMD PDF}(x, k_{\perp}) \times \text{TMD FF}(z, p_{\perp})]$$



$$z \stackrel{\text{lab}}{=} \frac{E_h}{E_{\gamma^*}}$$



nucleon polarisation

quark polarisation

	U	L	T
U	f_1		h_1^{\perp}
L		g_{1L}	h_{1L}^{\perp}
T	f_{1T}^{\perp}	g_{1T}^{\perp}	$h_{1T} h_{1T}^{\perp}$

hadron polarisation

quark polarisation

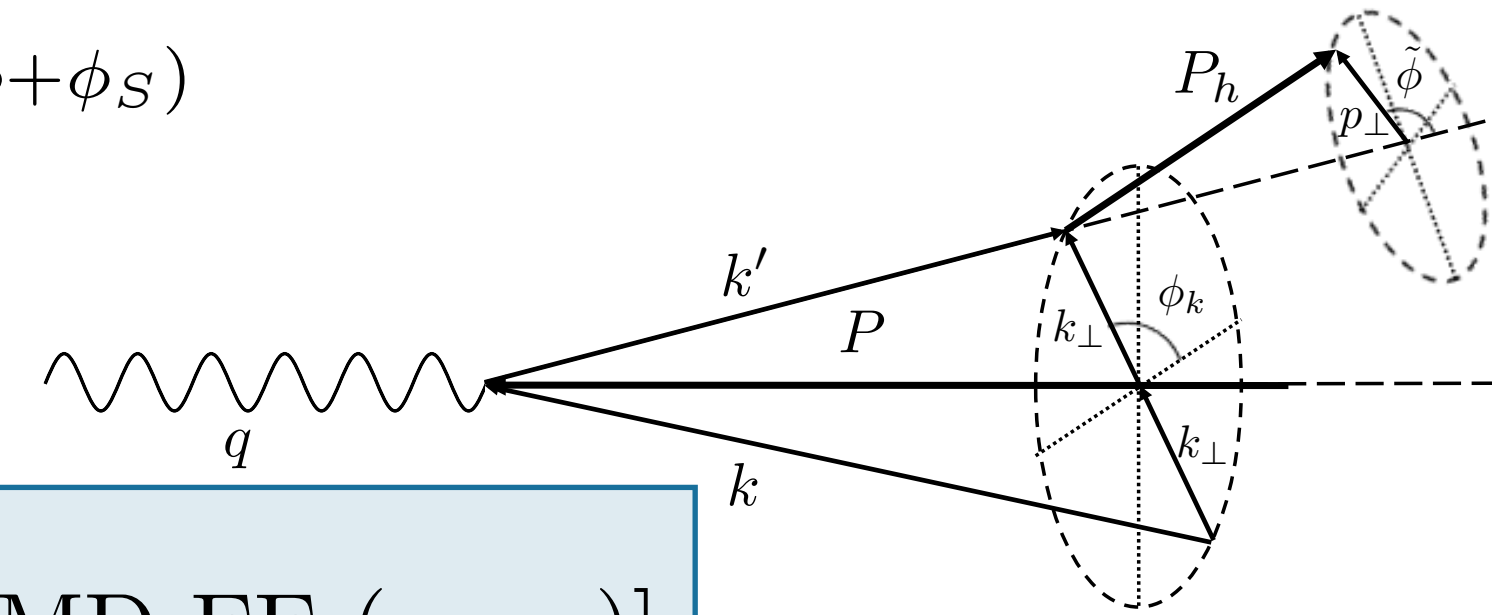
	U	L	T
U	D_1		H_1^{\perp}

TMD PDFs and fragmentation functions (FFs)

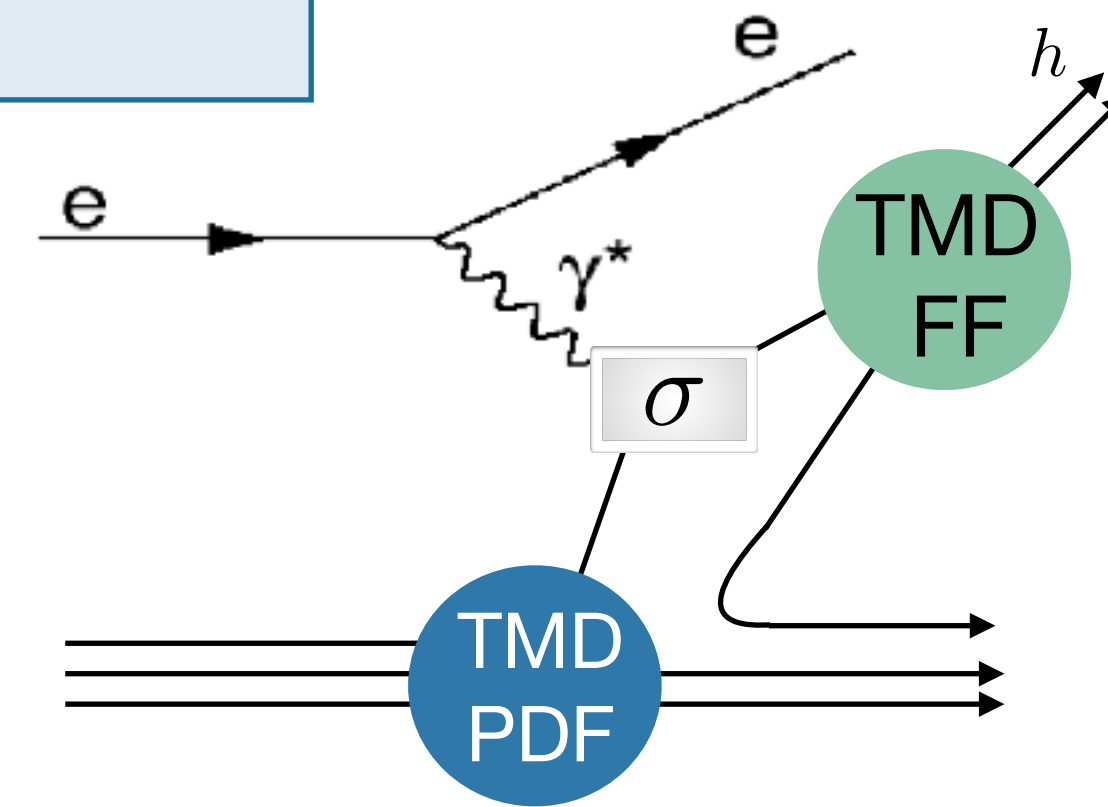
Azimuthal amplitudes related to structure functions F_{XY} :

$$2\langle \sin(\phi + \phi_S) \rangle_{UT}^h = \epsilon F_{UT}^{\sin(\phi + \phi_S)}$$

$$F_{XY} \propto \mathcal{C} [\text{TMD PDF}(x, k_{\perp}) \times \text{TMD FF}(z, p_{\perp})]$$



$$z \stackrel{\text{lab}}{=} \frac{E_h}{E_{\gamma^*}}$$



nucleon polarisation

quark polarisation

	U	L	T
U	f_1		h_1^{\perp}
L		g_{1L}	h_{1L}^{\perp}
T	f_{1T}^{\perp}	g_{1T}^{\perp}	$h_{1T} h_{1T}^{\perp}$

hadron polarisation

quark polarisation

	U	L	T
U	D_1		H_1^{\perp}

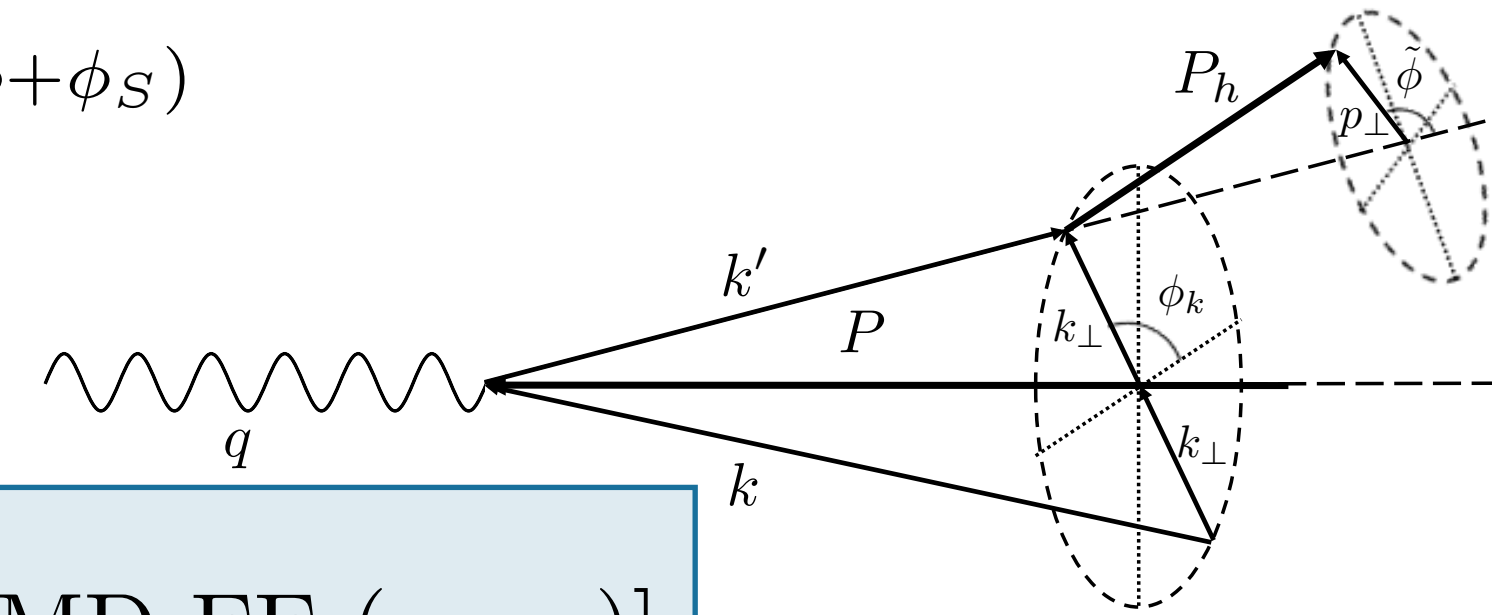
Chiral odd

TMD PDFs and fragmentation functions (FFs)

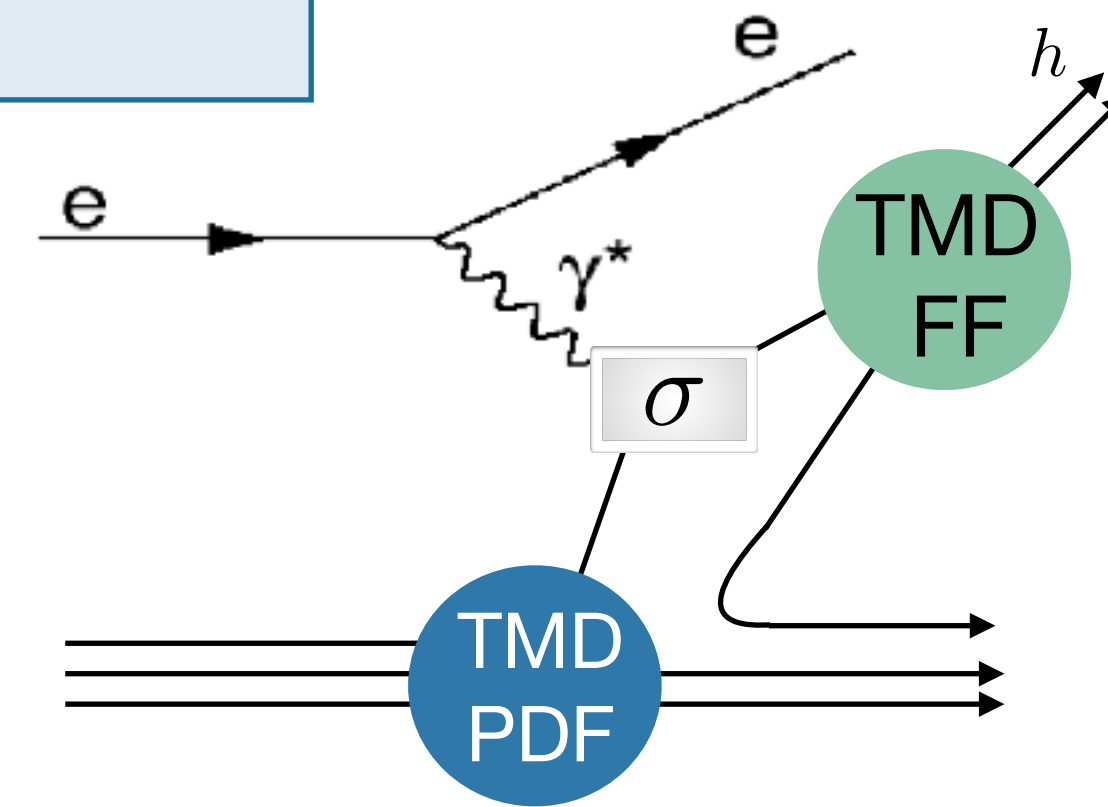
Azimuthal amplitudes related to structure functions F_{XY} :

$$2\langle \sin(\phi + \phi_S) \rangle_{UT}^h = \epsilon F_{UT}^{\sin(\phi + \phi_S)}$$

$$F_{XY} \propto \mathcal{C} [\text{TMD PDF}(x, k_{\perp}) \times \text{TMD FF}(z, p_{\perp})]$$



$$z \stackrel{\text{lab}}{=} \frac{E_h}{E_{\gamma^*}}$$



quark polarisation

	U	L	T
U	f_1		h_1^{\perp}
L		g_{1L}	h_{1L}^{\perp}
T	f_{1T}^{\perp}	g_{1T}^{\perp}	$h_{1T} h_{1T}^{\perp}$

nucleon polarisation

quark polarisation

	U	L	T
U	D_1		H_1^{\perp}

hadron polarisation

Chiral odd

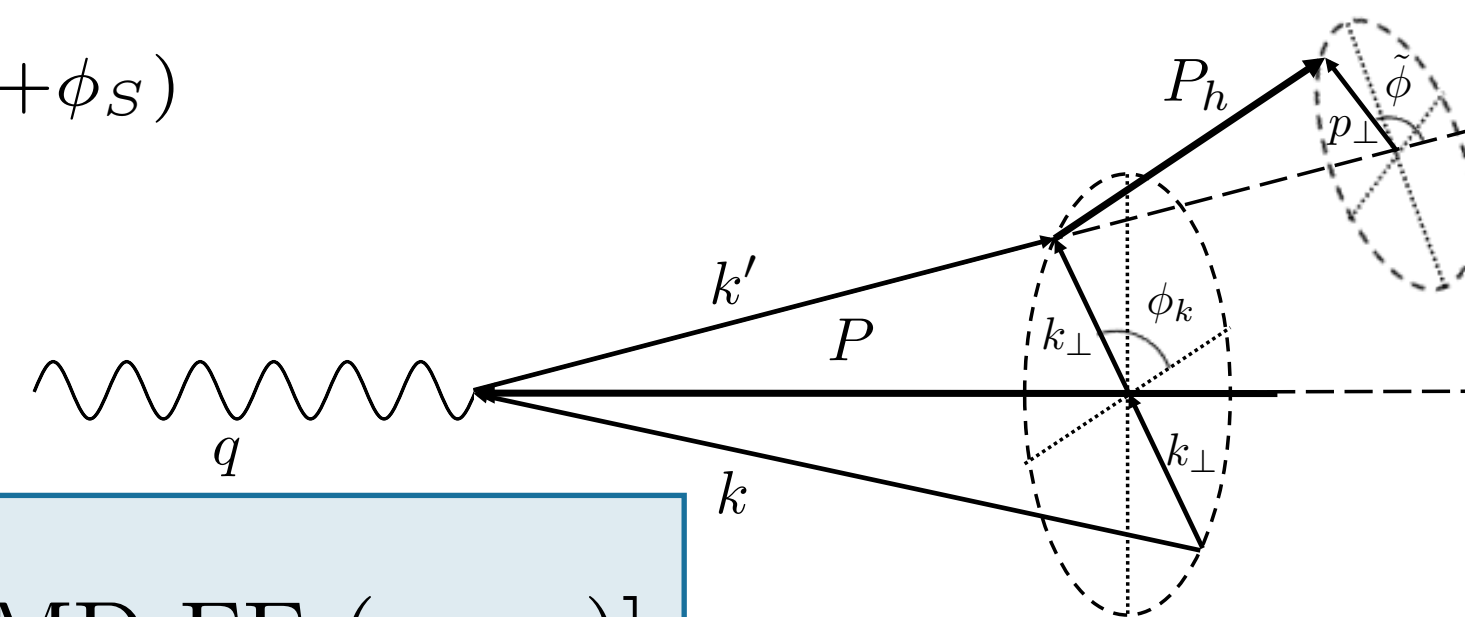
Naive T-odd

TMD PDFs and fragmentation functions (FFs)

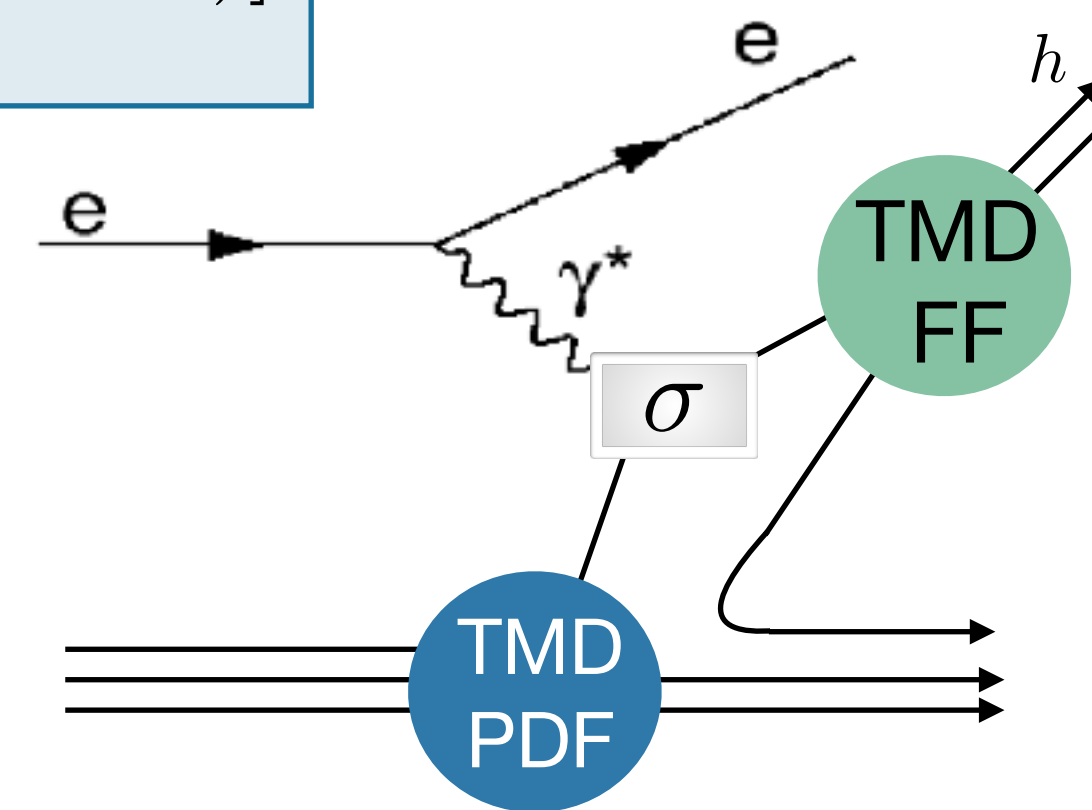
Azimuthal amplitudes related to structure functions F_{XY} :

$$2\langle \sin(\phi + \phi_S) \rangle_{UT}^h = \epsilon F_{UT}^{\sin(\phi + \phi_S)}$$

$$F_{XY} \propto \mathcal{C} [\text{TMD PDF}(x, k_{\perp}) \times \text{TMD FF}(z, p_{\perp})]$$



$$z \stackrel{\text{lab}}{=} \frac{E_h}{E_{\gamma^*}}$$



quark polarisation

	U	L	T
U	f_1		h_1^{\perp}
L		g_{1L}	h_{1L}^{\perp}
T	f_{1T}^{\perp}	g_{1T}^{\perp}	$h_{1T} h_{1T}^{\perp}$

nucleon polarisation

quark polarisation

	U	L	T
U	D_1		H_1^{\perp}

hadron polarisation

Chiral odd

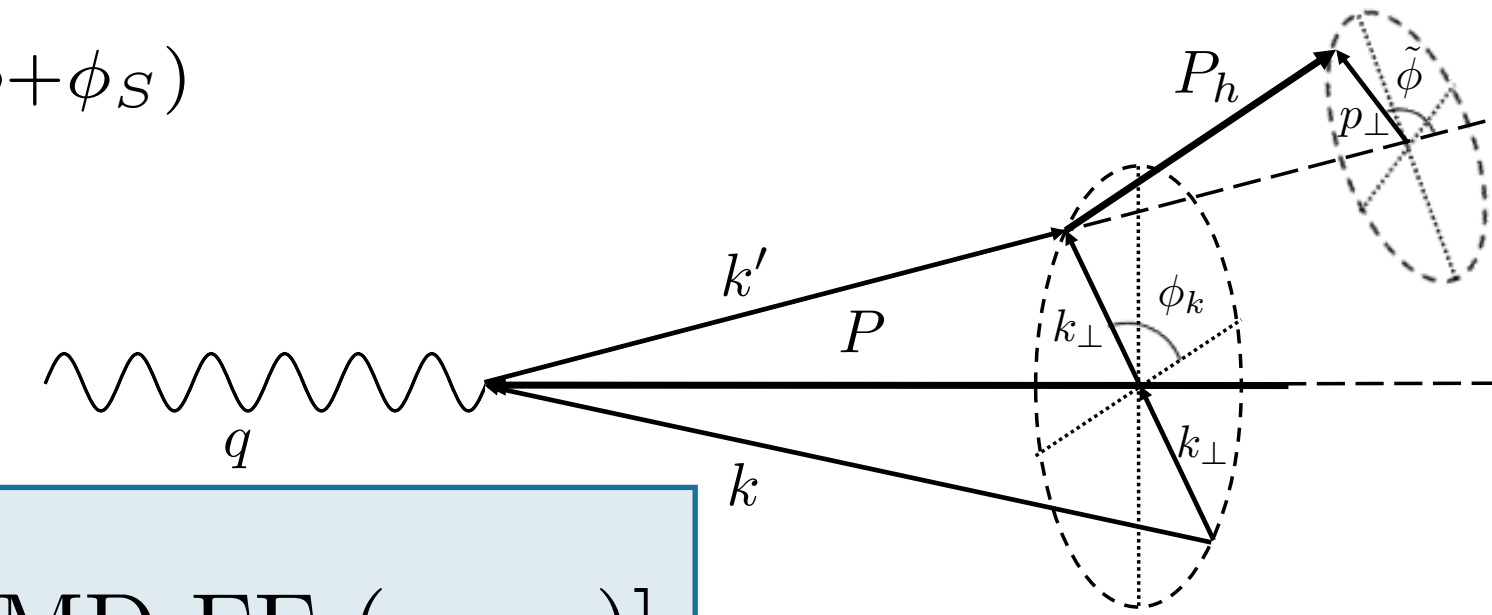
Naive T-odd

TMD PDFs and fragmentation functions (FFs)

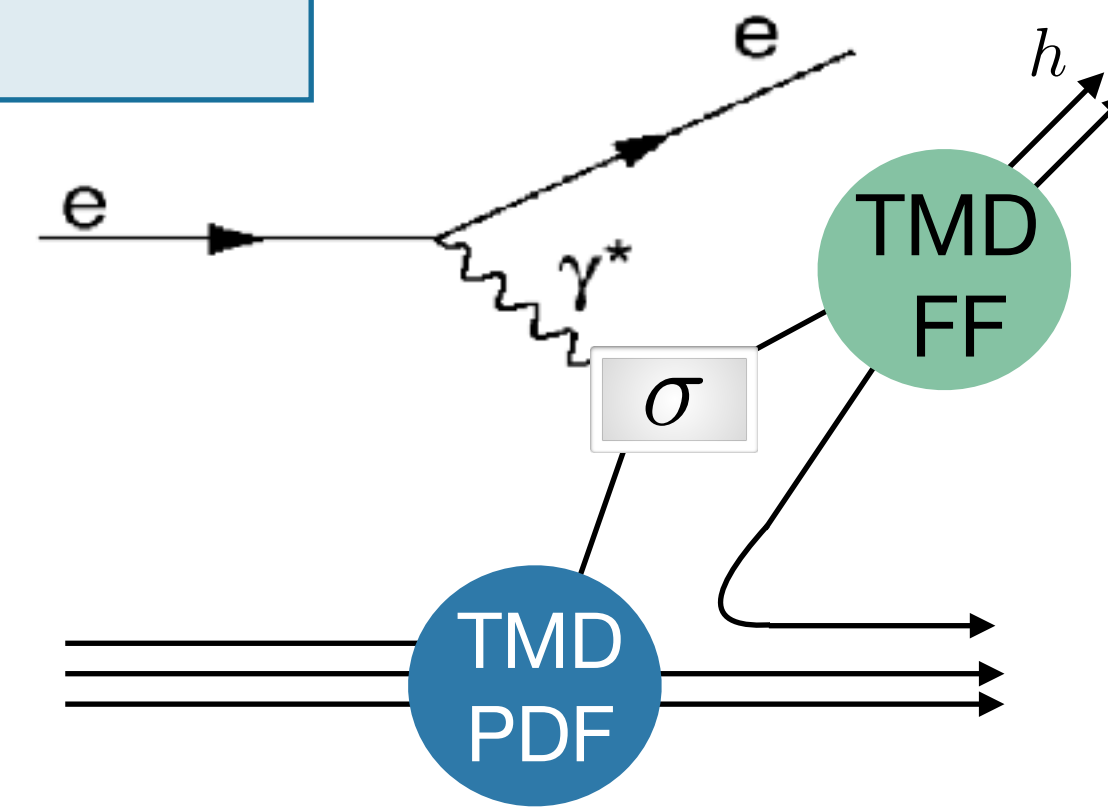
Azimuthal amplitudes related to structure functions F_{XY} :

$$2\langle \sin(\phi + \phi_S) \rangle_{UT}^h = \epsilon F_{UT}^{\sin(\phi + \phi_S)}$$

$$F_{XY} \propto \mathcal{C} [\text{TMD PDF}(x, k_{\perp}) \times \text{TMD FF}(z, p_{\perp})]$$



$$z = \frac{\text{lab } E_h}{E_{\gamma^*}}$$



quark polarisation

	U	L	T
U	f_1		h_1^{\perp}
L		g_{1L}	h_{1L}^{\perp}
T	f_{1T}^{\perp}	g_{1T}^{\perp}	$h_{1T} h_{1T}^{\perp}$

nucleon polarisation

quark polarisation

	U	L	T
U	D_1		H_1^{\perp}

hadron polarisation

Chiral odd

Naive T-odd

Semi-inclusive DIS cross section

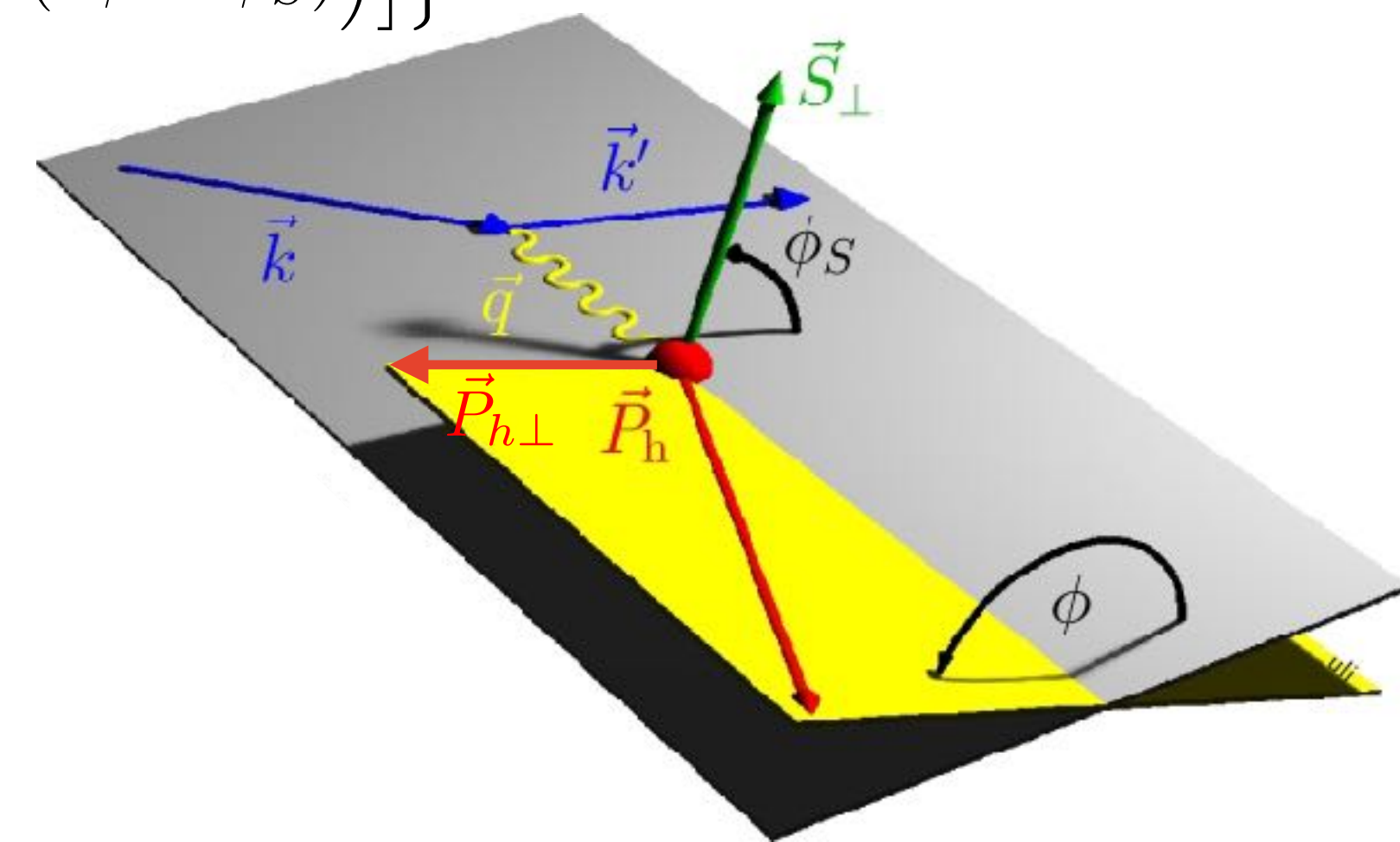
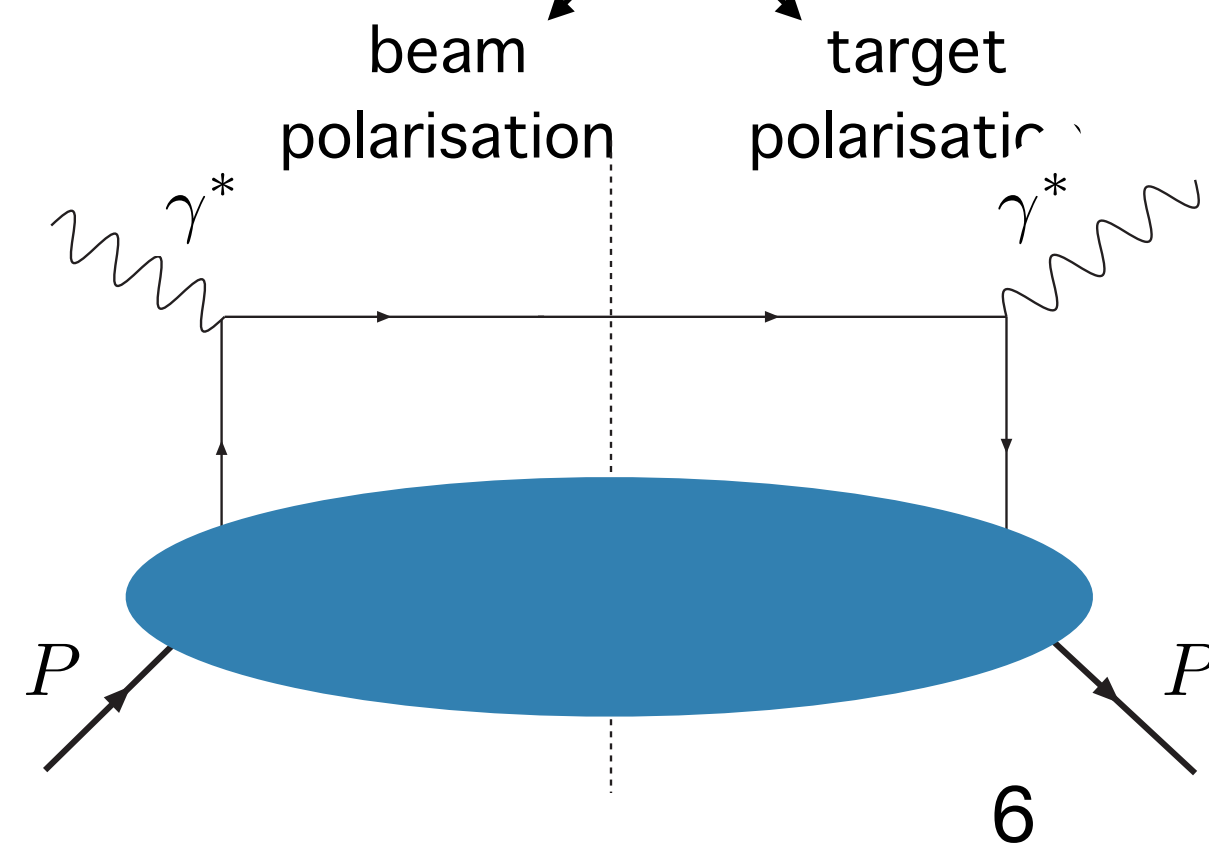
$$\begin{aligned}
 \sigma^h(\phi, \phi_S) = & \sigma_{UU}^h \left\{ 1 + 2\langle \cos(\phi) \rangle_{UU}^h \cos(\phi) + 2\langle \cos(2\phi) \rangle_{UU}^h \cos(2\phi) \right. \\
 & + \lambda_l 2\langle \sin(\phi) \rangle_{LU}^h \sin(\phi) \\
 & + S_L \left[2\langle \sin(\phi) \rangle_{UL}^h \sin(\phi) + 2\langle \sin(2\phi) \rangle_{UL}^h \sin(2\phi) \right. \\
 & \left. + \lambda_l \left(2\langle \cos(0\phi) \rangle_{LL}^h \cos(0\phi) + 2\langle \cos(\phi) \rangle_{LL}^h \cos(\phi) \right) \right] \\
 & + S_T \left[2\langle \sin(\phi - \phi_S) \rangle_{UT}^h \sin(\phi - \phi_S) + 2\langle \sin(\phi + \phi_S) \rangle_{UT}^h \sin(\phi + \phi_S) \right. \\
 & + 2\langle \sin(3\phi - \phi_S) \rangle_{UT}^h \sin(3\phi - \phi_S) + 2\langle \sin(\phi_S) \rangle_{UT}^h \sin(\phi_S) \\
 & + 2\langle \sin(2\phi - \phi_S) \rangle_{UT}^h \sin(2\phi - \phi_S) \\
 & + \lambda_l \left(2\langle \cos(\phi - \phi_S) \rangle_{LT}^h \cos(\phi - \phi_S) \right. \\
 & \left. + 2\langle \cos(\phi_S) \rangle_{LT}^h \cos(\phi_S) + 2\langle \cos(2\phi - \phi_S) \rangle_{LT}^h \cos(2\phi - \phi_S) \right) \left. \right\}
 \end{aligned}$$

longitudinal target polarisation

transverse target polarisation

beam polarisation

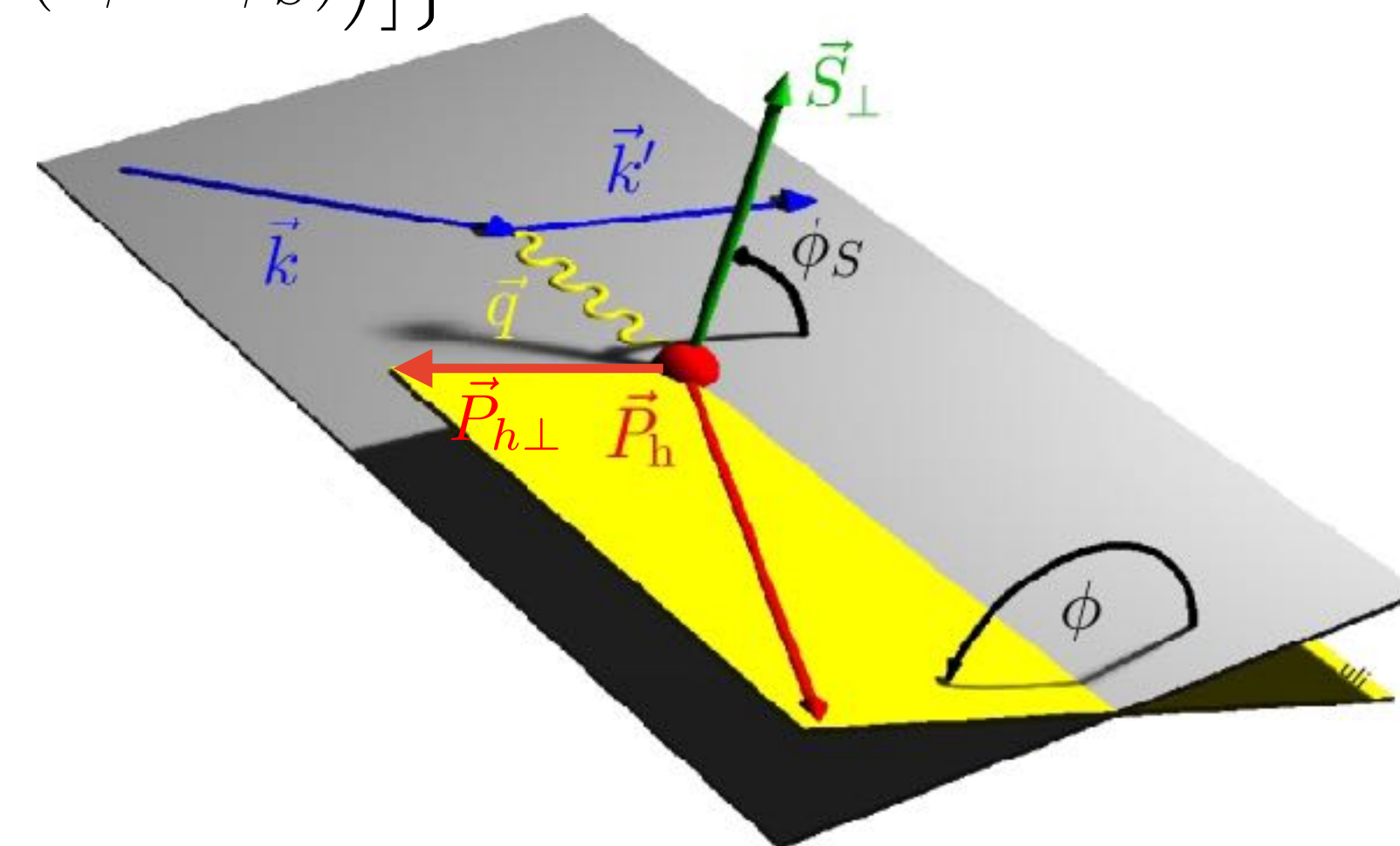
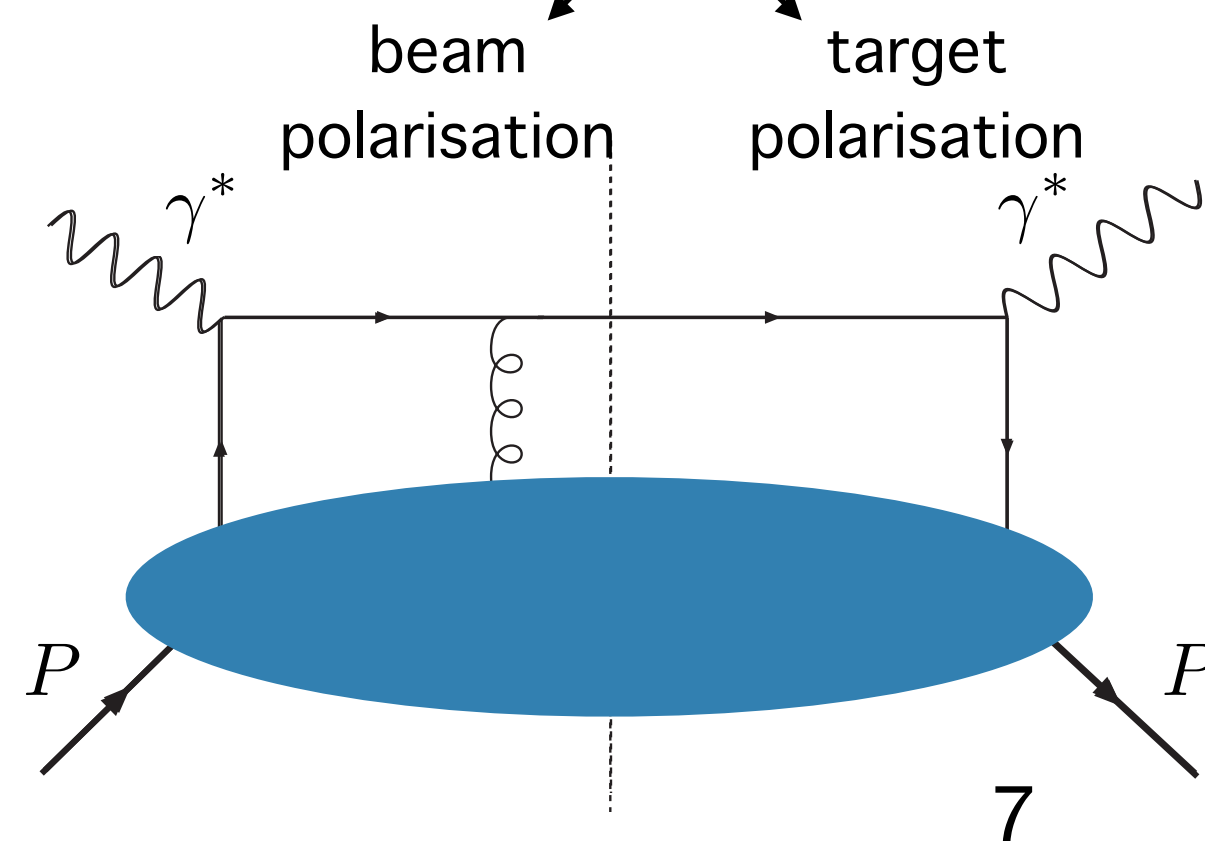
leading twist



Semi-inclusive DIS cross section

$$\begin{aligned}
 \sigma^h(\phi, \phi_S) = & \sigma_{UU}^h \left\{ 1 + 2\langle \cos(\phi) \rangle_{UU}^h \cos(\phi) + 2\langle \cos(2\phi) \rangle_{UU}^h \cos(2\phi) \right. \\
 & + \lambda_l 2\langle \sin(\phi) \rangle_{LU}^h \sin(\phi) \\
 \text{longitudinal target} & \leftarrow + S_L \left[2\langle \sin(\phi) \rangle_{UL}^h \sin(\phi) + 2\langle \sin(2\phi) \rangle_{UL}^h \sin(2\phi) \right. \\
 \text{polarisation} & \leftarrow + \lambda_l \left(2\langle \cos(0\phi) \rangle_{LL}^h \cos(0\phi) + 2\langle \cos(\phi) \rangle_{LL}^h \cos(\phi) \right) \\
 & + S_T \left[2\langle \sin(\phi - \phi_S) \rangle_{UT}^h \sin(\phi - \phi_S) + 2\langle \sin(\phi + \phi_S) \rangle_{UT}^h \sin(\phi + \phi_S) \right. \\
 \text{transverse target} & \leftarrow + 2\langle \sin(3\phi - \phi_S) \rangle_{UT}^h \sin(3\phi - \phi_S) + 2\langle \sin(\phi_S) \rangle_{UT}^h \sin(\phi_S) \\
 & + 2\langle \sin(2\phi - \phi_S) \rangle_{UT}^h \sin(2\phi - \phi_S) \\
 \text{beam} & \leftarrow + \lambda_l \left(2\langle \cos(\phi - \phi_S) \rangle_{LT}^h \cos(\phi - \phi_S) \right. \\
 \text{polarisation} & \leftarrow + 2\langle \cos(\phi_S) \rangle_{LT}^h \cos(\phi_S) + 2\langle \cos(2\phi - \phi_S) \rangle_{LT}^h \cos(2\phi - \phi_S) \left. \right\}
 \end{aligned}$$

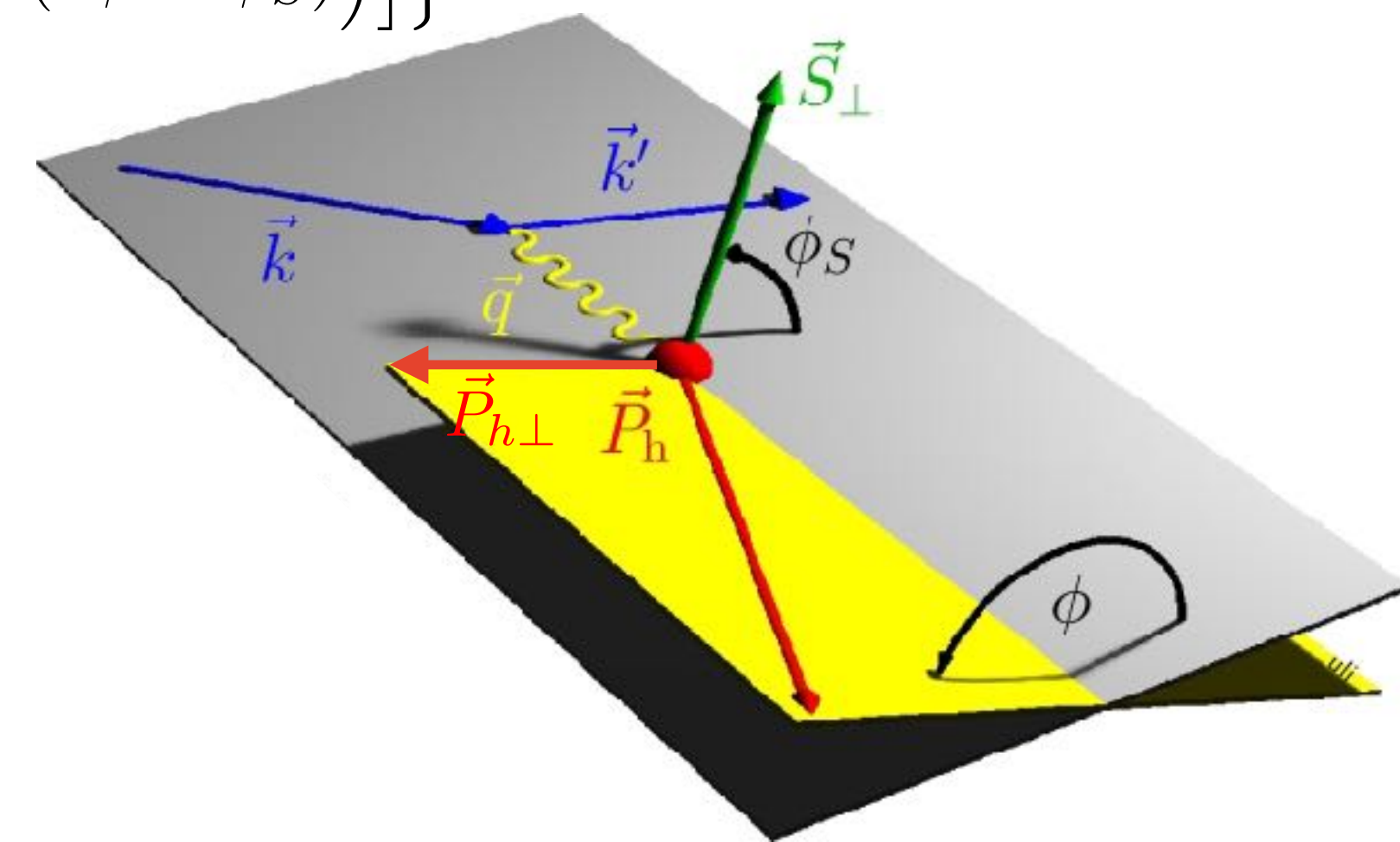
sub-leading twist



Presented amplitudes

$$\begin{aligned}
 \sigma^h(\phi, \phi_S) = & \sigma_{UU}^h \left\{ 1 + 2\langle \cos(\phi) \rangle_{UU}^h \cos(\phi) + 2\langle \cos(2\phi) \rangle_{UU}^h \cos(2\phi) \right. \\
 & + \lambda_l 2\langle \sin(\phi) \rangle_{LU}^h \sin(\phi) \\
 & + S_L \left[2\langle \sin(\phi) \rangle_{UL}^h \sin(\phi) + 2\langle \sin(2\phi) \rangle_{UL}^h \sin(2\phi) \right. \\
 & + \lambda_l \left(2\langle \cos(0\phi) \rangle_{LL}^h \cos(0\phi) + 2\langle \cos(\phi) \rangle_{LL}^h \cos(\phi) \right) \left. \right] \\
 & + S_T \left[2\langle \sin(\phi - \phi_S) \rangle_{UT}^h \sin(\phi - \phi_S) + 2\langle \sin(\phi + \phi_S) \rangle_{UT}^h \sin(\phi + \phi_S) \right. \\
 & + 2\langle \sin(3\phi - \phi_S) \rangle_{UT}^h \sin(3\phi - \phi_S) + 2\langle \sin(\phi_S) \rangle_{UT}^h \sin(\phi_S) \\
 & + 2\langle \sin(2\phi - \phi_S) \rangle_{UT}^h \sin(2\phi - \phi_S) \\
 & + \lambda_l \left(2\langle \cos(\phi - \phi_S) \rangle_{LT}^h \cos(\phi - \phi_S) \right. \\
 & \left. \left. + 2\langle \cos(\phi_S) \rangle_{LT}^h \cos(\phi_S) + 2\langle \cos(2\phi - \phi_S) \rangle_{LT}^h \cos(2\phi - \phi_S) \right) \right] \left. \right\}
 \end{aligned}$$

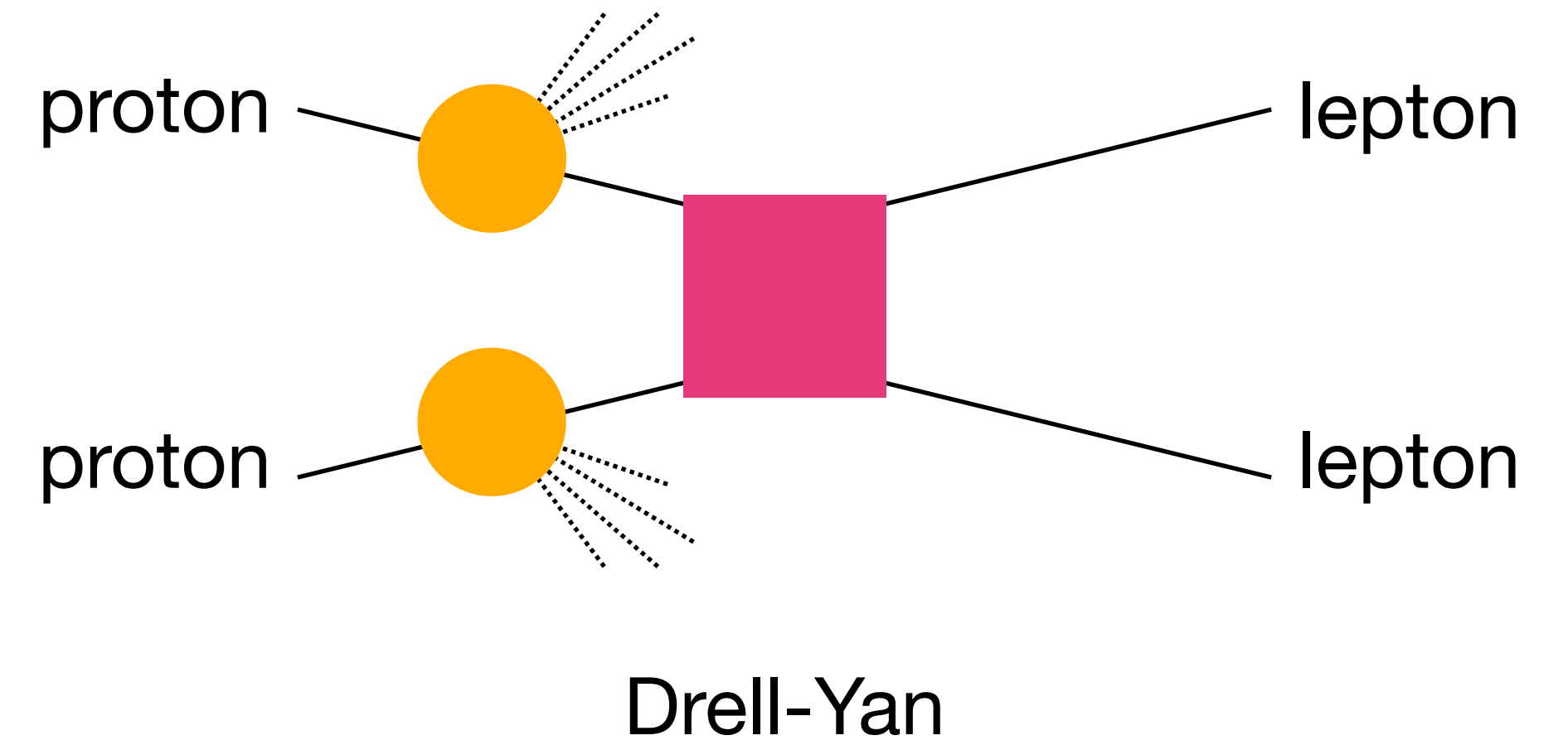
Presented here



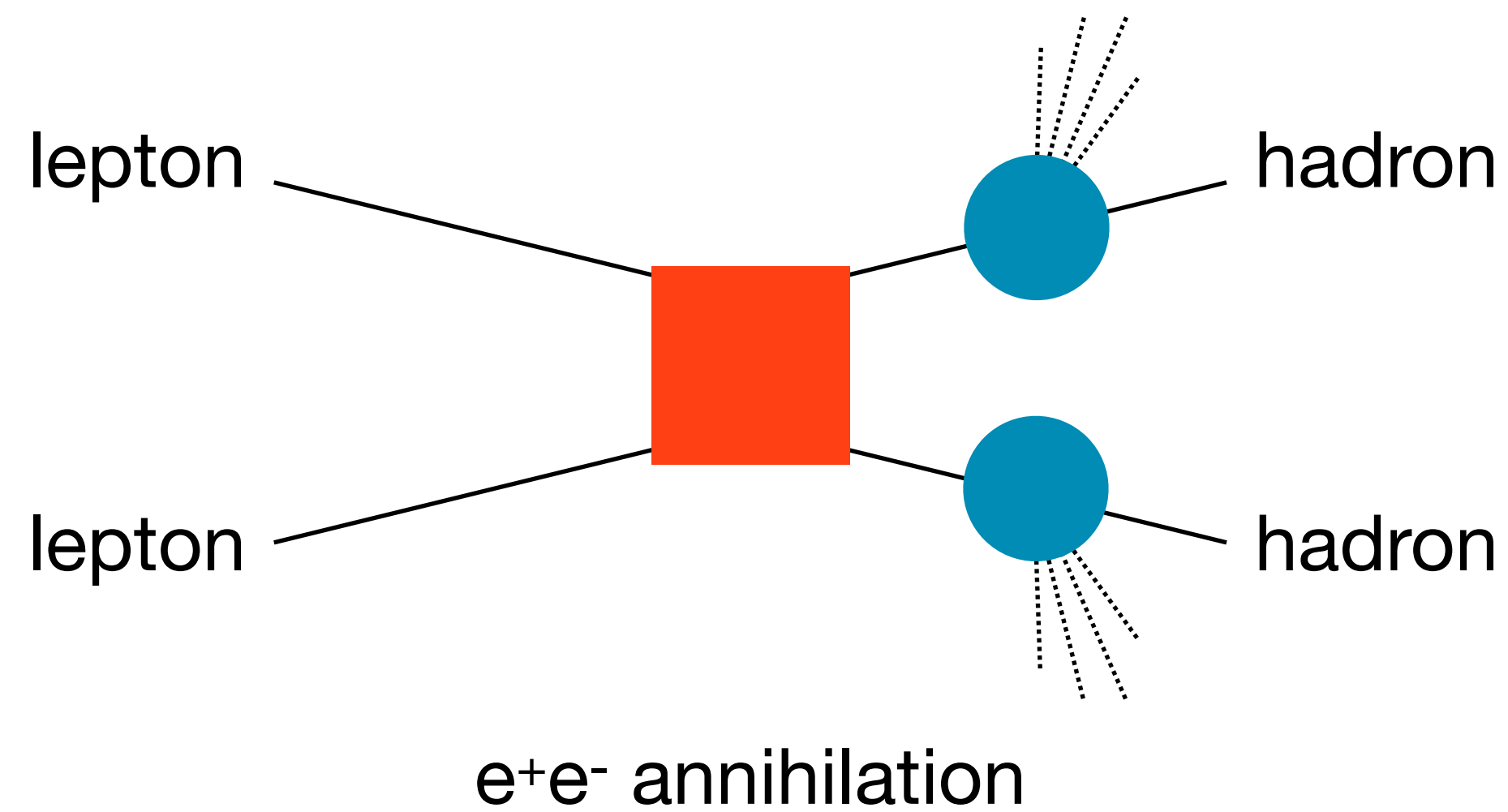
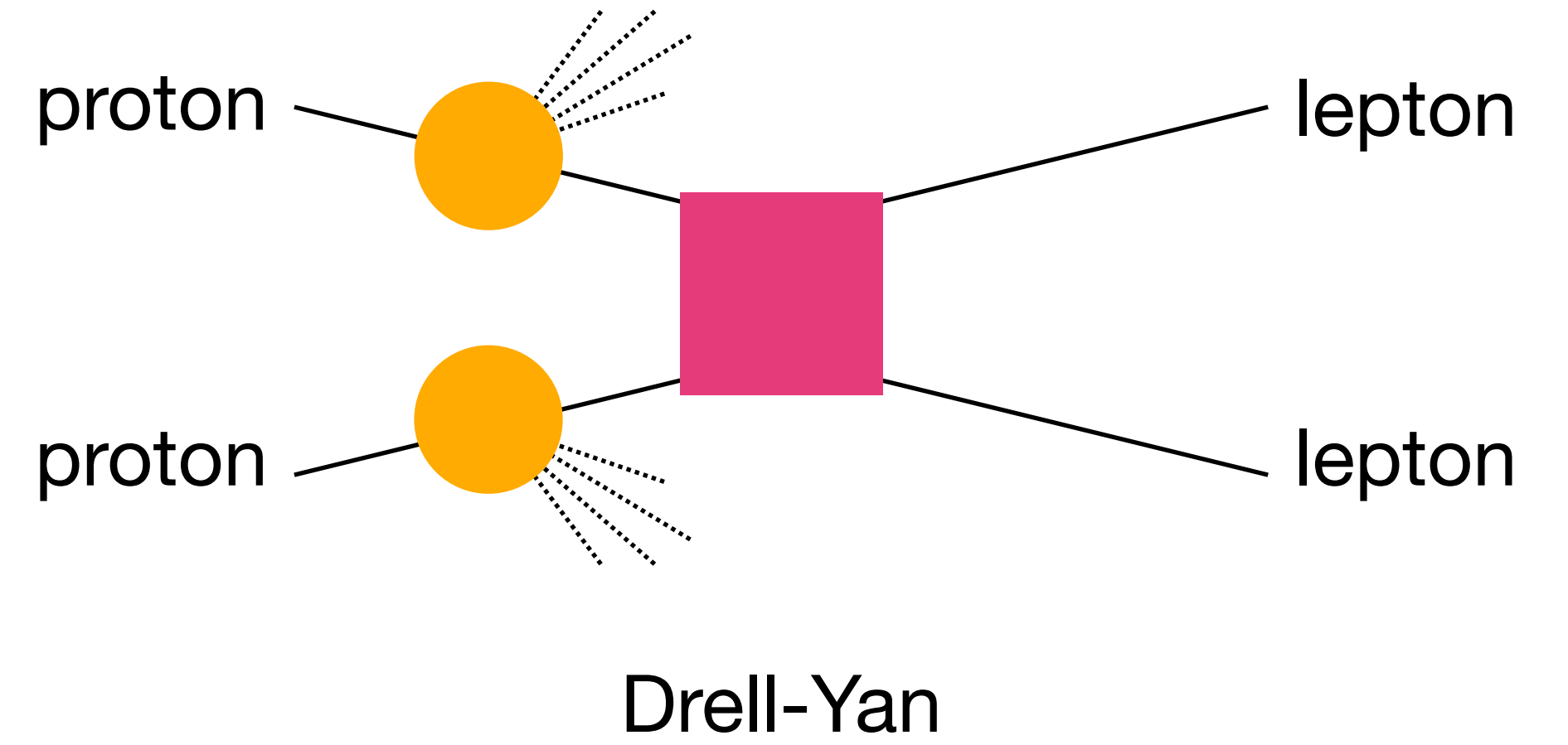
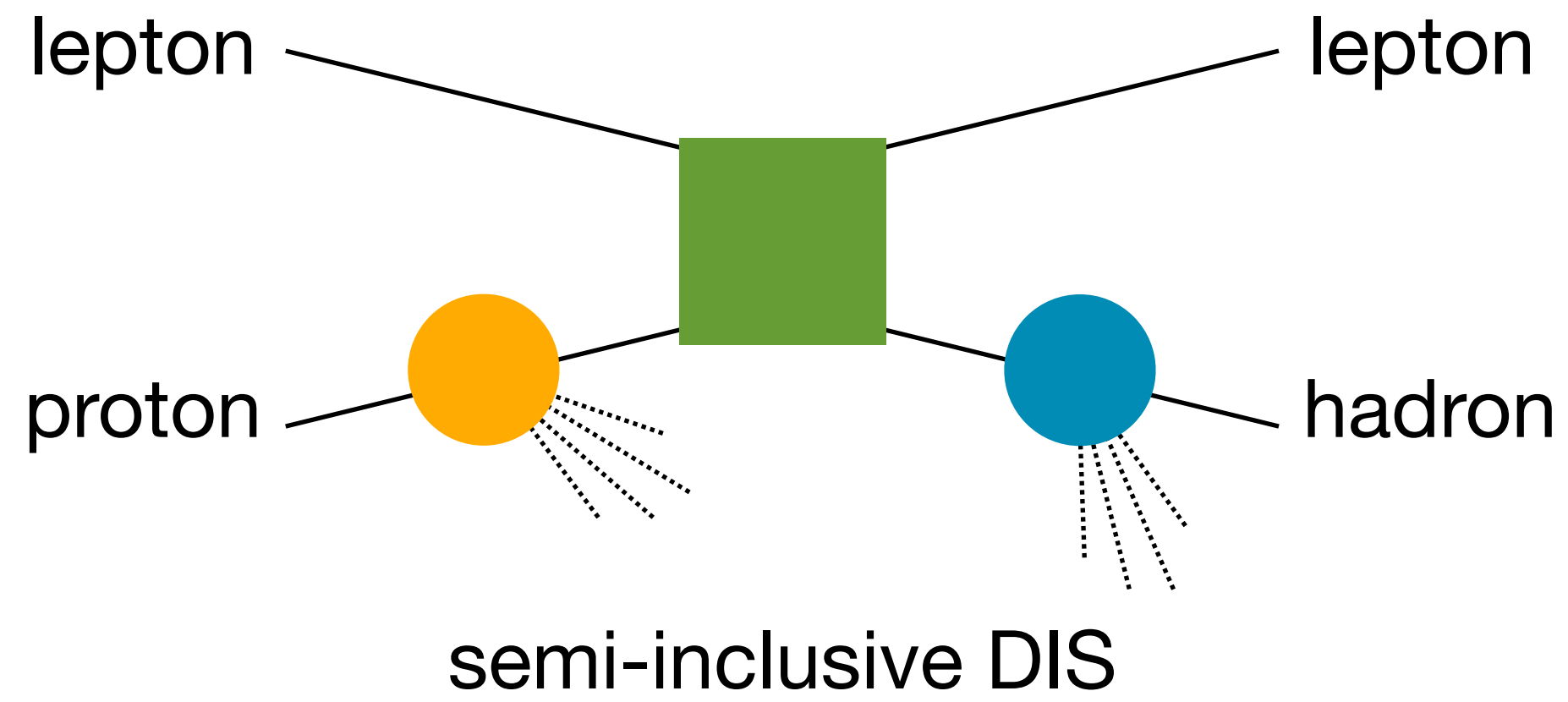
Factorisation and universality



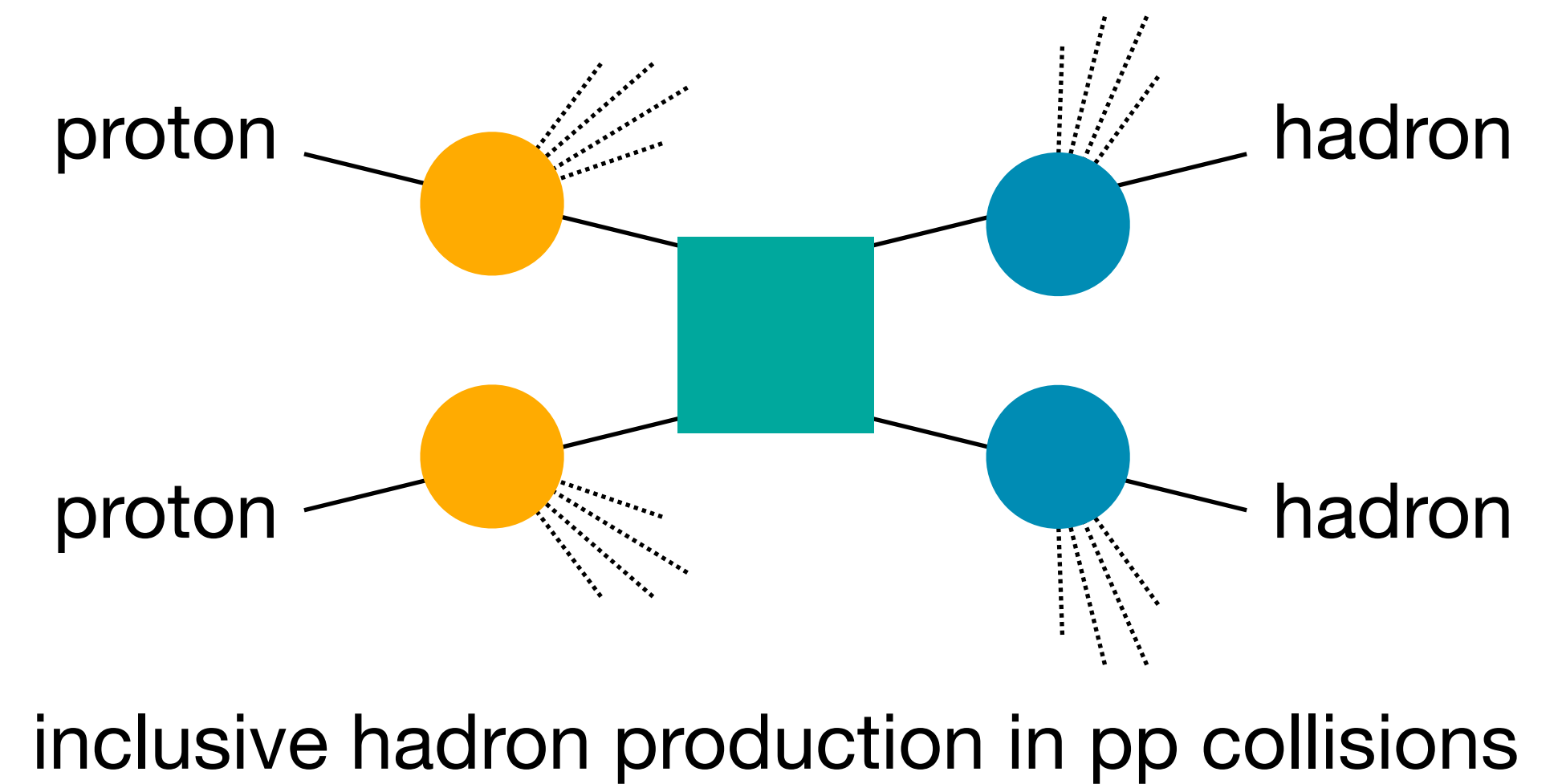
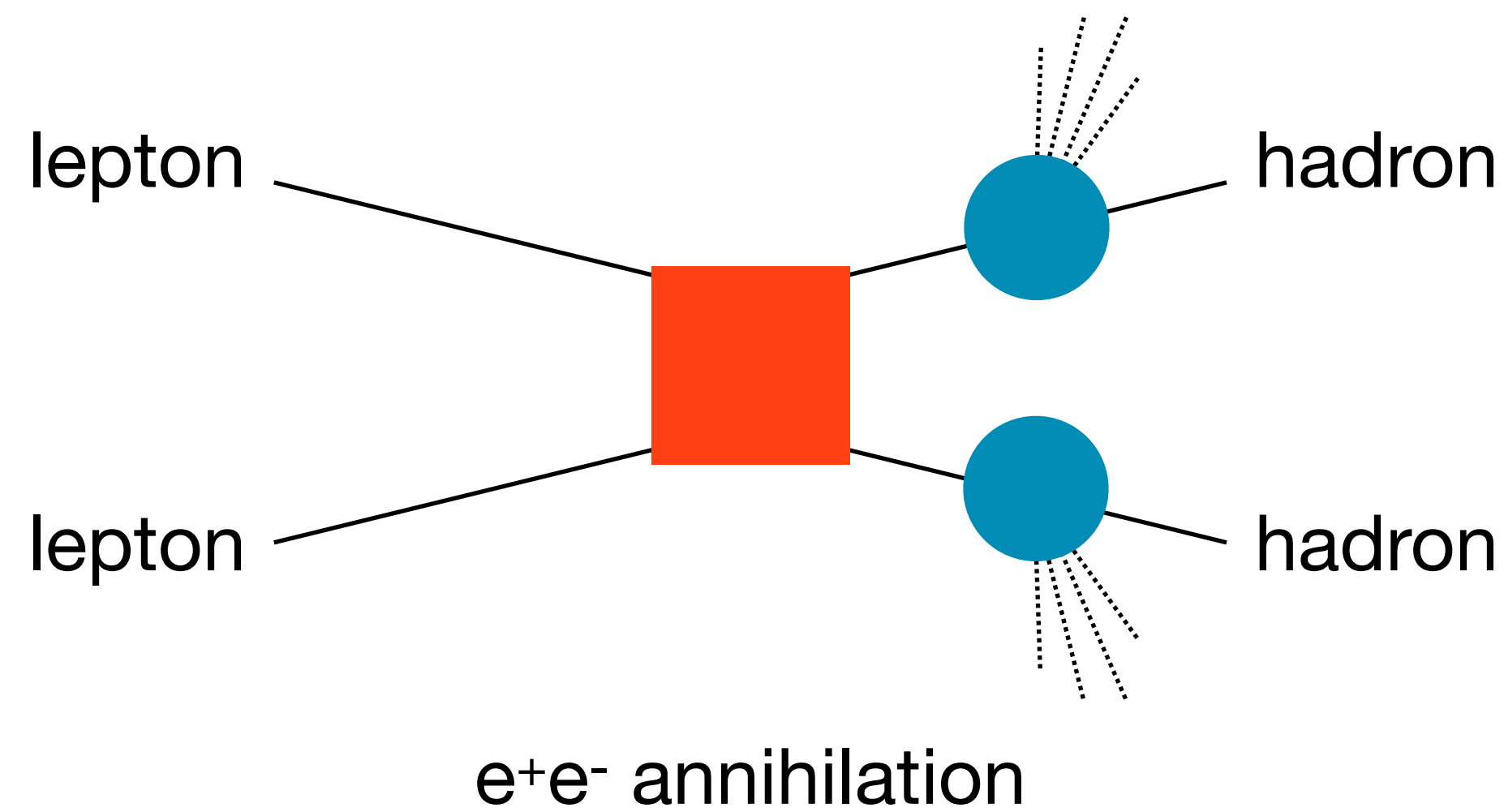
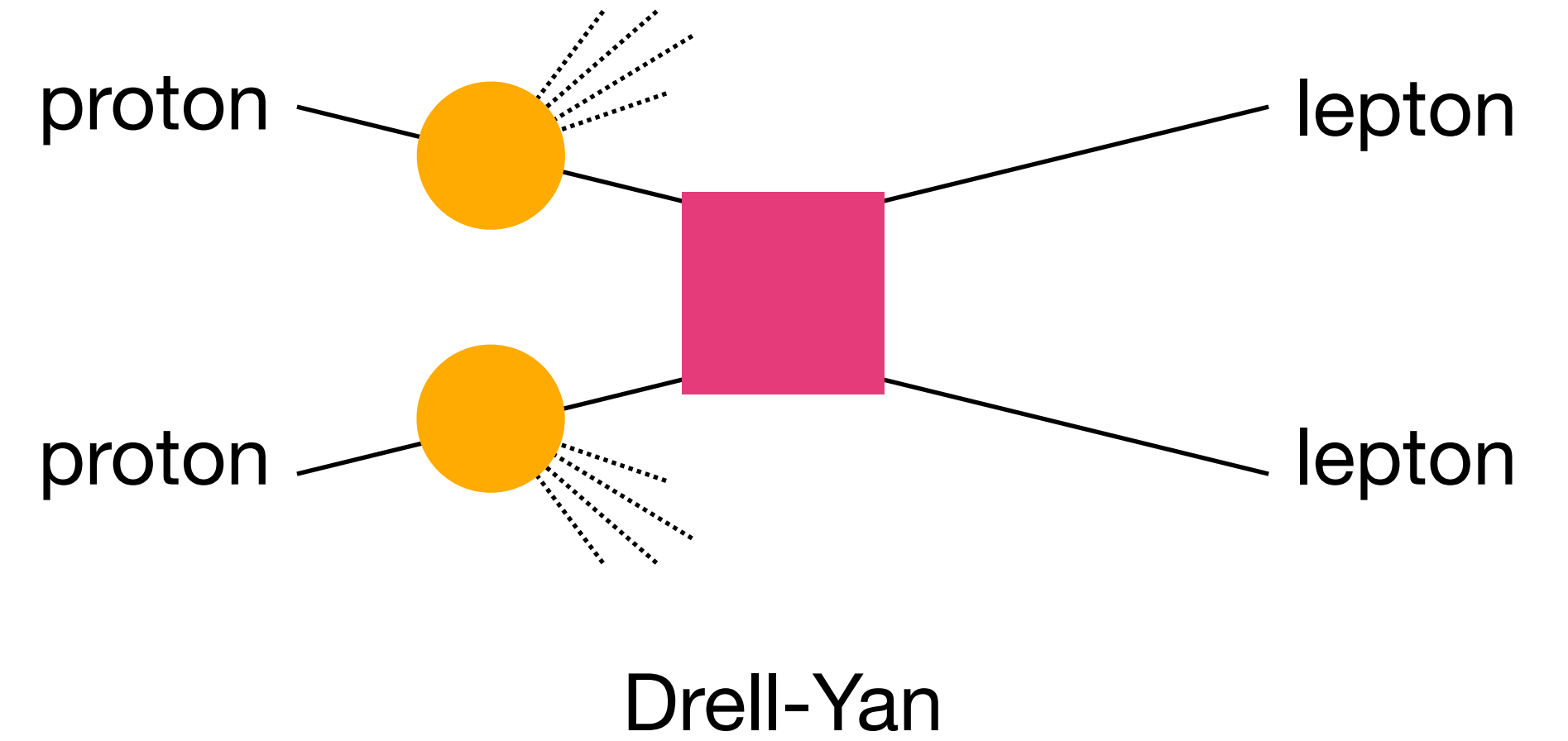
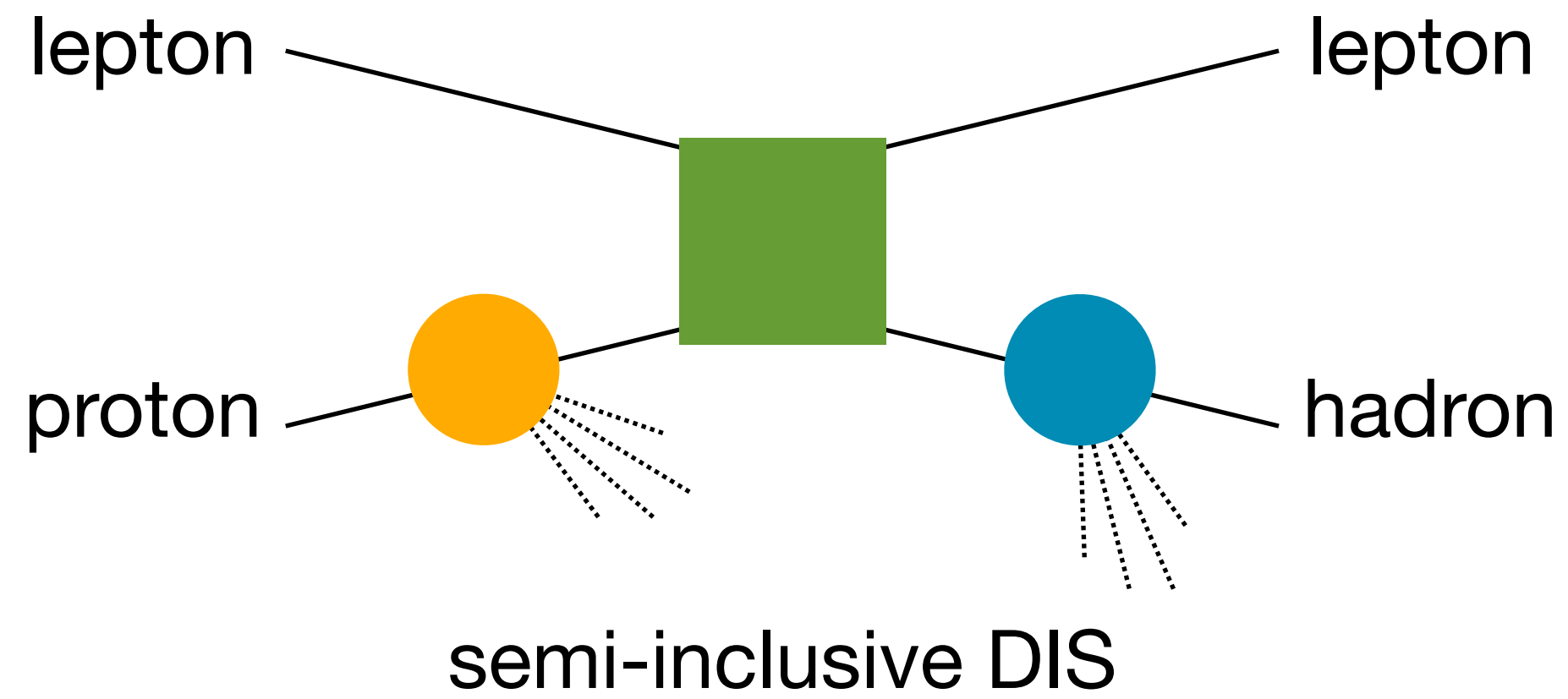
Factorisation and universality



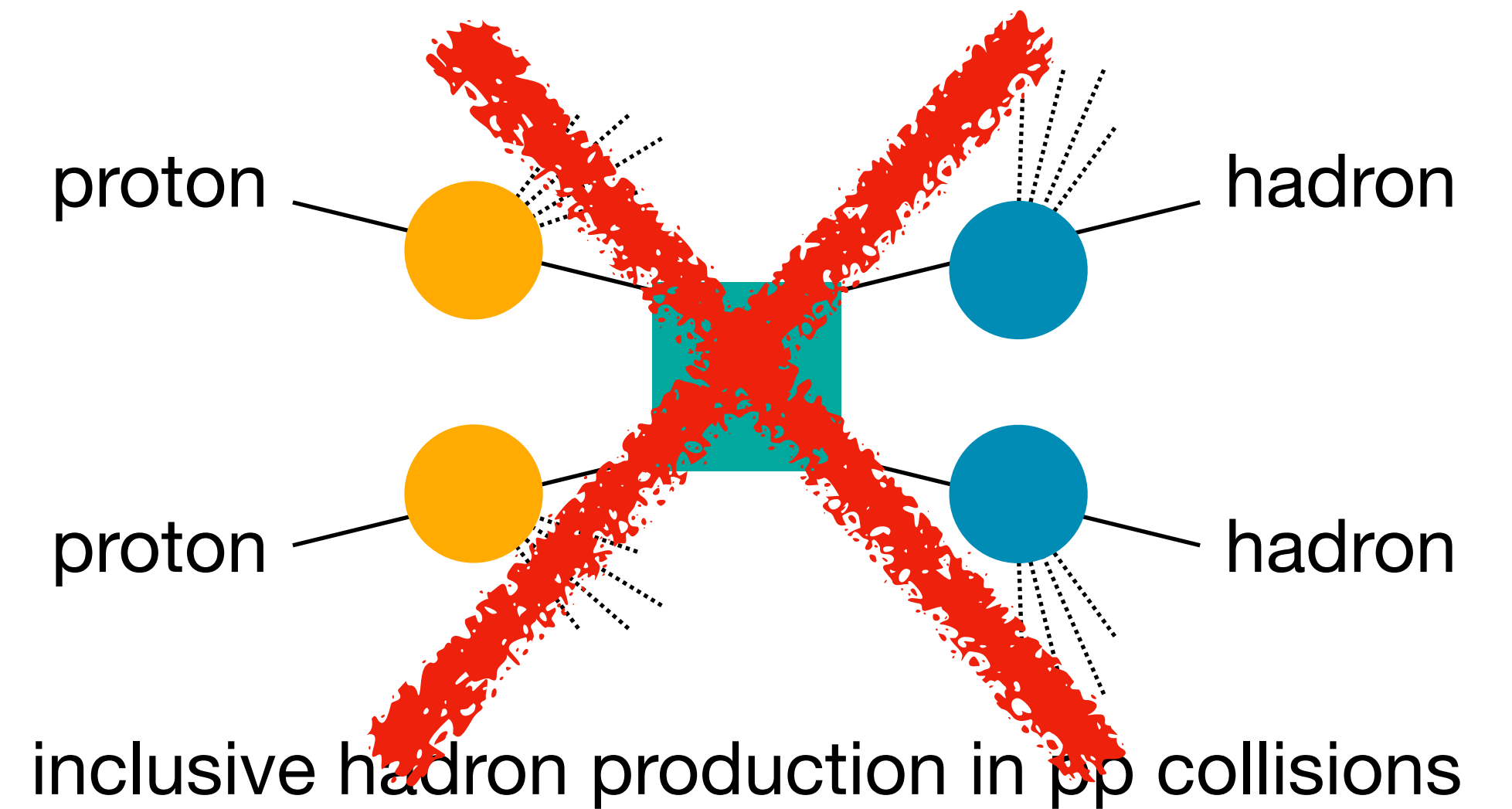
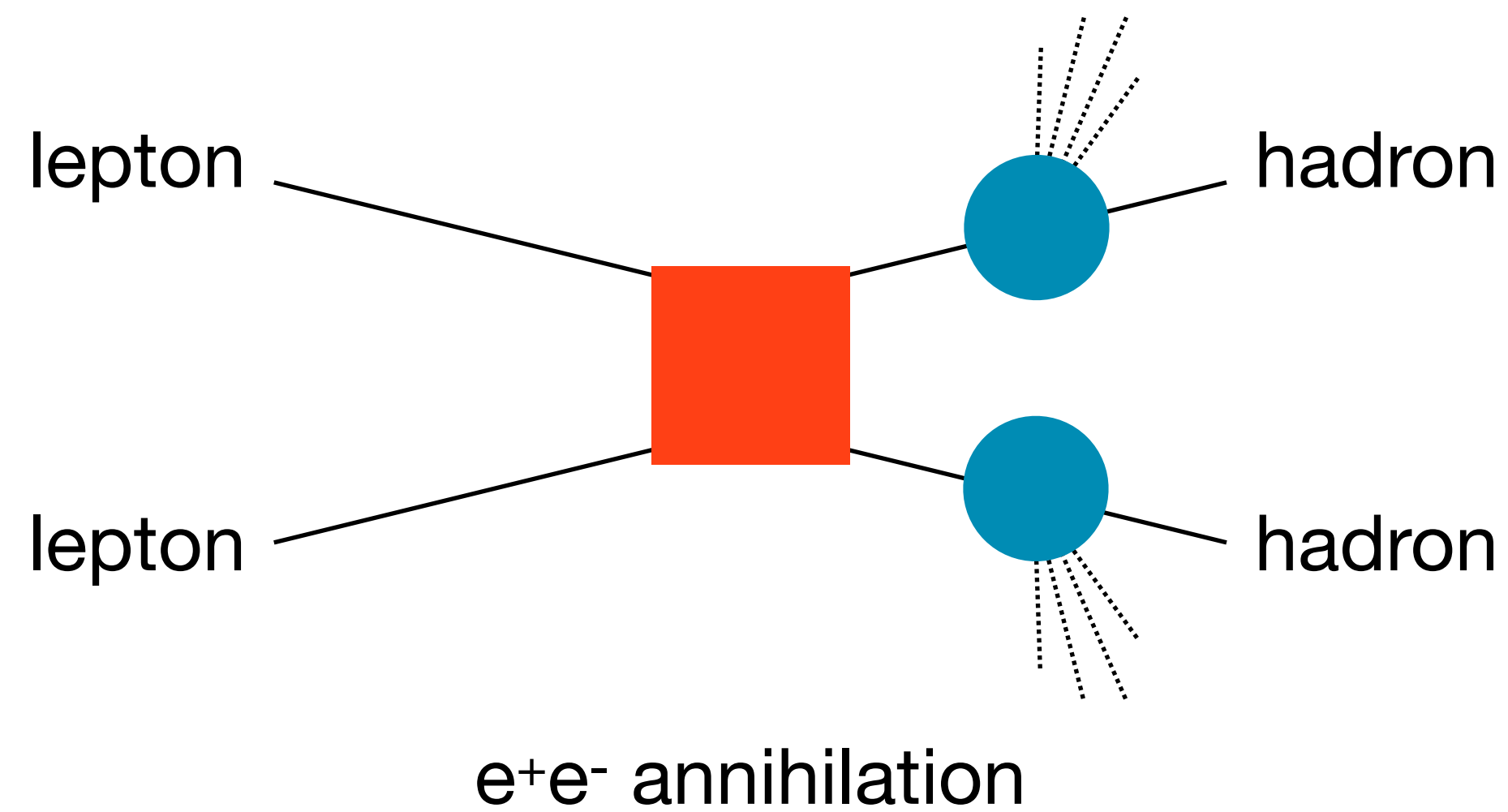
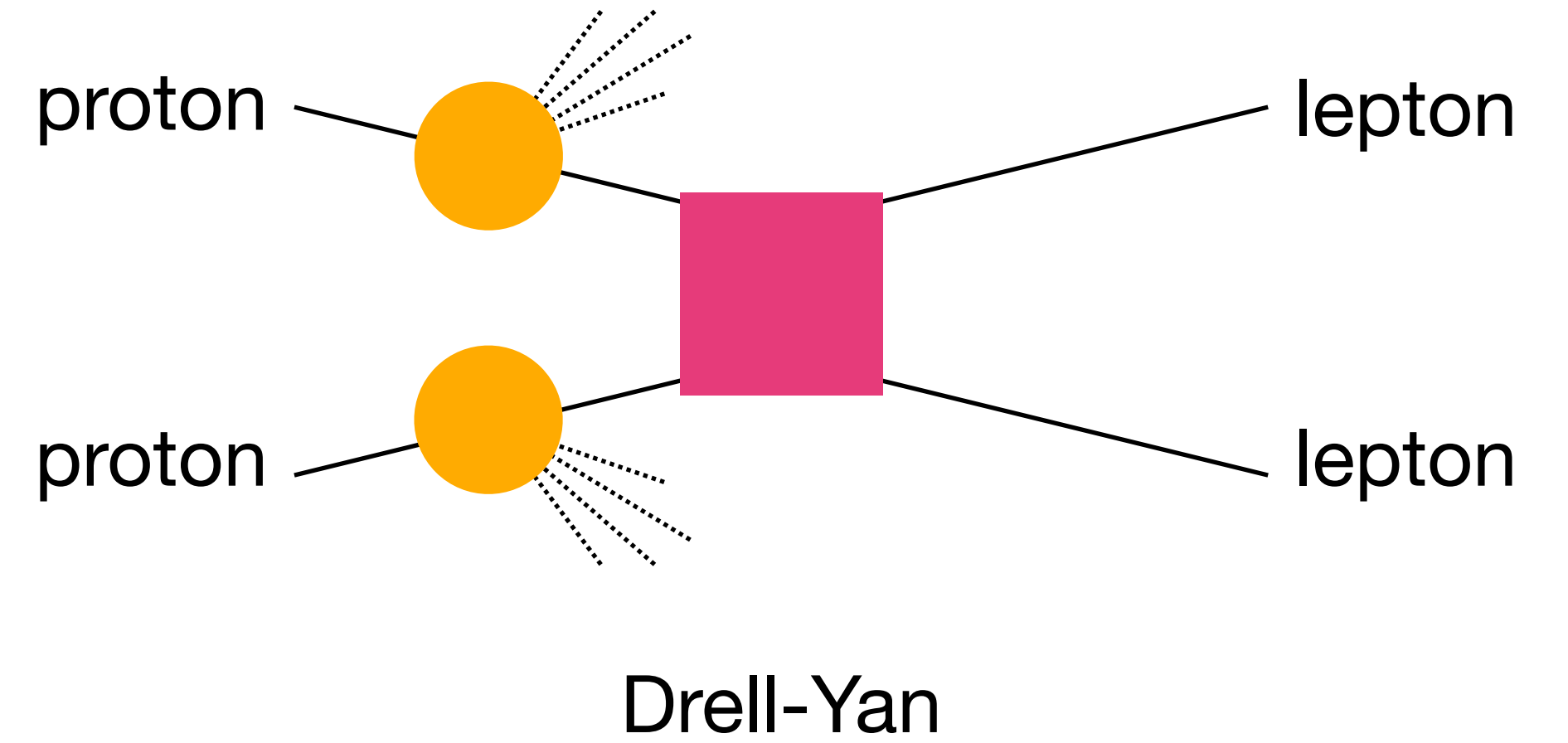
Factorisation and universality



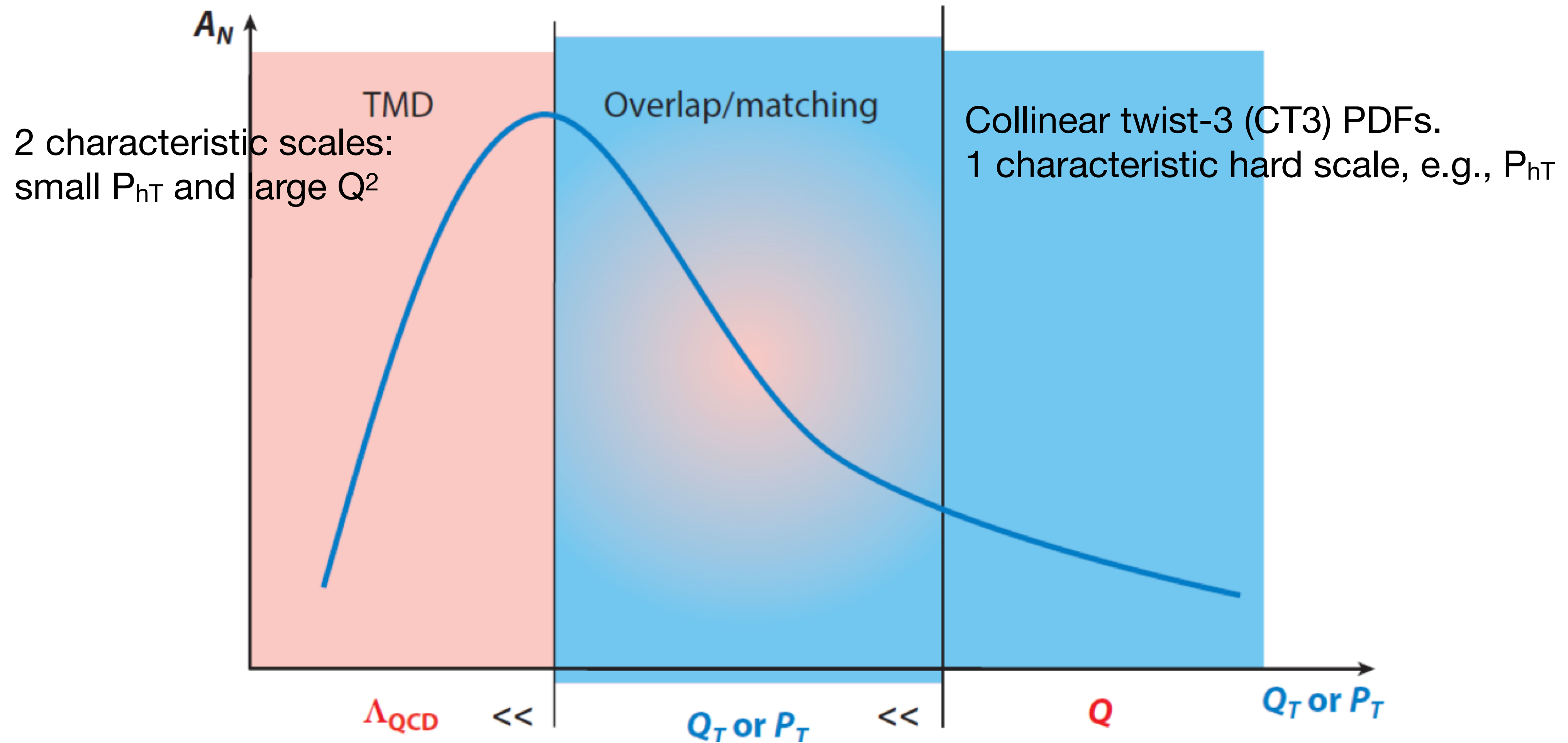
Factorisation and universality



Factorisation and universality



Validity of TMD description



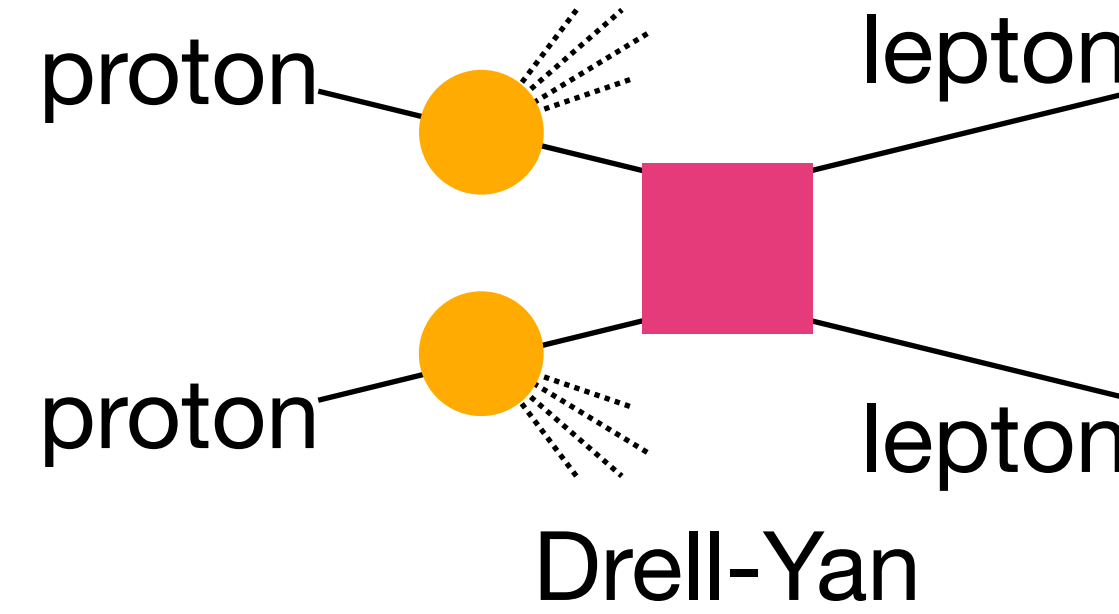
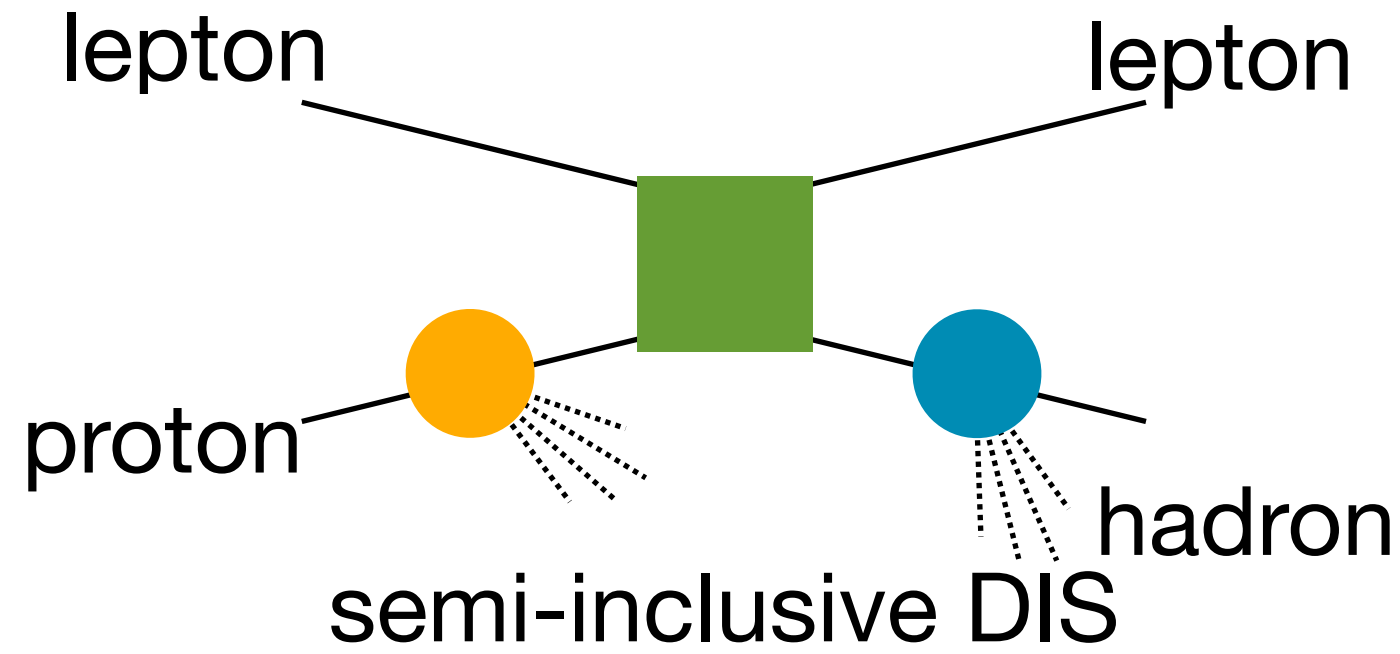
Consistent results for TMD
and CT3 in overlap region

Experiments investigating TMD PDFs and TMD FFs



Spin-independent TMD PDFs: global analysis

I. Scimemi, A. Vladimirov JHEP **06** (2020)137

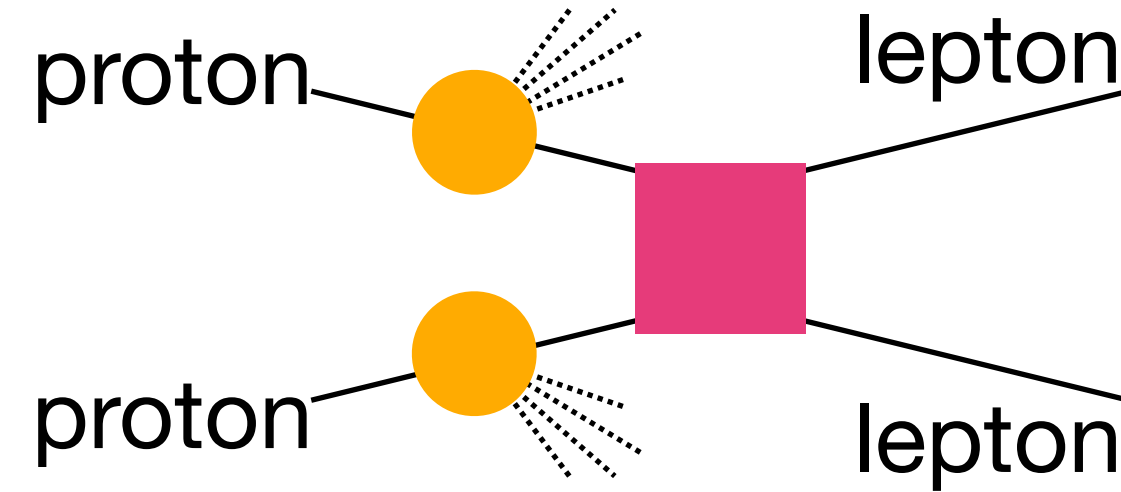
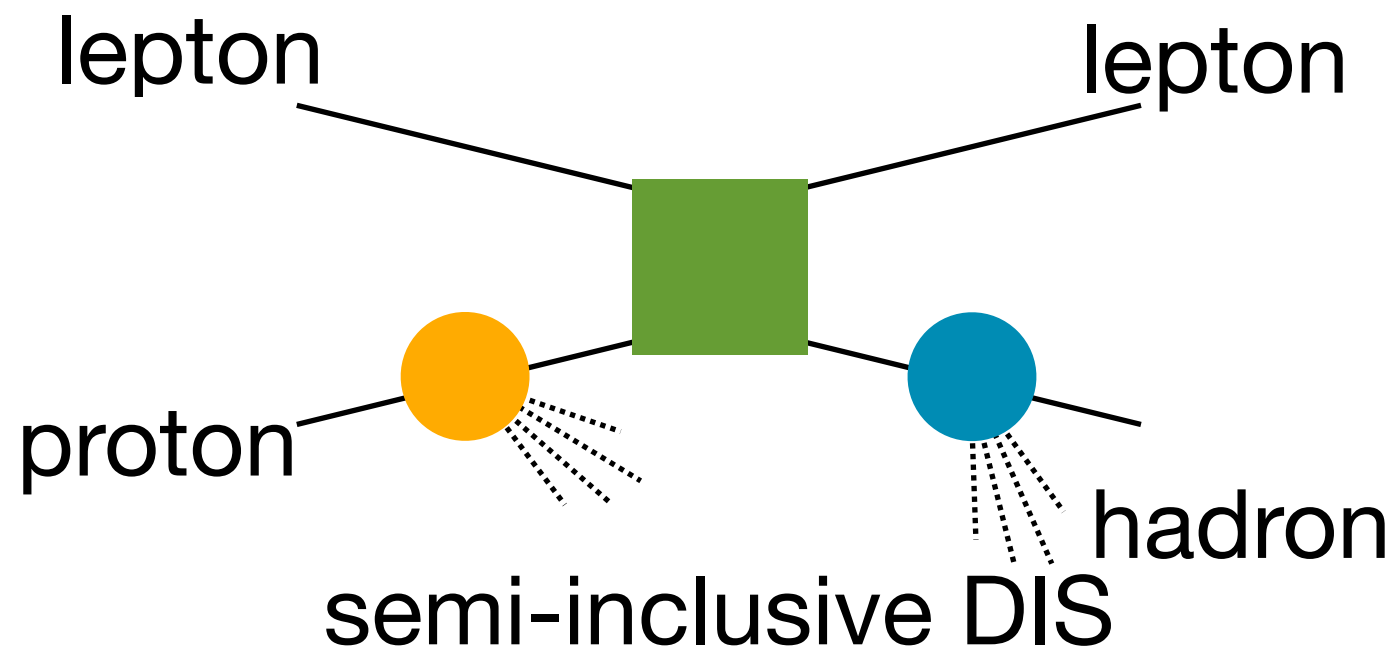


Experiment	Reaction	ref.	Kinematics	N_{pt} after cuts
HERMES	$p \rightarrow \pi^+$	[67]	$0.023 < x < 0.6$ (6 bins) $0.2 < z < 0.8$ (6 bins) $1.0 < Q < \sqrt{20} \text{ GeV}$	24
	$p \rightarrow \pi^-$			24
	$p \rightarrow K^+$			24
	$p \rightarrow K^-$			24
	$D \rightarrow \pi^+$		$W^2 > 10 \text{ GeV}^2$ $0.1 < y < 0.85$	24
	$D \rightarrow \pi^-$			24
	$D \rightarrow K^+$			24
	$D \rightarrow K^-$			24
COMPASS	$d \rightarrow h^+$	[68]	$0.003 < x < 0.4$ (8 bins)	195
	$d \rightarrow h^-$		$0.2 < z < 0.8$ (4 bins) $1.0 < Q \simeq 9 \text{ GeV}$ (5 bins)	195
Total				582

Experiment	ref.	\sqrt{s} [GeV]	Q [GeV]	y/x_F	fiducial region	N_{pt} after cuts
F288 (200)	[73]	19.4	4–9 in 1 GeV bins*	$0.1 < x_F < 0.7$		43
E288 (300)	[73]	23.8	4–12 in 1 GeV bins*	$-0.09 < x_F < 0.51$	—	53
E288 (400)	[73]	27.4	5–14 in 1 GeV bins*	$-0.27 < x_F < 0.33$	—	76
E605	[74]	38.8	7–18 in 5 bins*	$-0.1 < x_F < 0.2$	—	53
E772	[75]	38.8	5–15 in 8 bins*	$0.1 < x_F < 0.3$	—	35
PHENIX	[76]	200	4.8–8.2	$1.2 < y < 2.2$	—	3
CDF (run1)	[77]	1800	66–116	—	—	33
CDF (run2)	[78]	1960	66–116	—	—	39
D0 (run1)	[79]	1800	75–105	—	—	16
D0 (run2)	[80]	1960	70–110	—	—	8
D0 (run2) $_{\mu}$	[81]	1960	65–115	$ y < 1.7$	$p_T > 15 \text{ GeV}$ $ \eta < 1.7$	3
ATLAS (7 TeV)	[47]	7000	66–116	$ y < 1$ $1 < y < 2$ $2 < y < 2.4$	$p_T > 20 \text{ GeV}$ $ \eta < 2.4$	15
ATLAS (8 TeV)	[48]	8000	66–116	$ y < 2.4$ in 6 bins	$p_T > 20 \text{ GeV}$ $ \eta < 2.4$	30
ATLAS (8 TeV)	[48]	8000	46–66	$ y < 2.4$	$p_T > 20 \text{ GeV}$ $ \eta < 2.4$	3
ATLAS (8 TeV)	[48]	8000	116–150	$ y < 2.4$	$p_T > 20 \text{ GeV}$ $ \eta < 2.1$	7
CMS (7 TeV)	[49]	7000	60–120	$ y < 2.1$	$p_T > 20 \text{ GeV}$ $ \eta < 2.1$	8
CMS (8 TeV)	[50]	8000	60–120	$ y < 2.1$	$p_T > 20 \text{ GeV}$ $ \eta < 2.1$	8
LHCb (7 TeV)	[82]	7000	60–120	$2 < y < 4.5$	$p_T > 20 \text{ GeV}$ $2 < \eta < 4.5$	8
LHCb (8 TeV)	[83]	8000	60–120	$2 < y < 4.5$	$p_T > 20 \text{ GeV}$ $2 < \eta < 4.5$	7
LHCb (13 TeV)	[84]	13000	60–120	$2 < y < 4.5$	$p_T > 20 \text{ GeV}$ $2 < \eta < 4.5$	9
Total						457

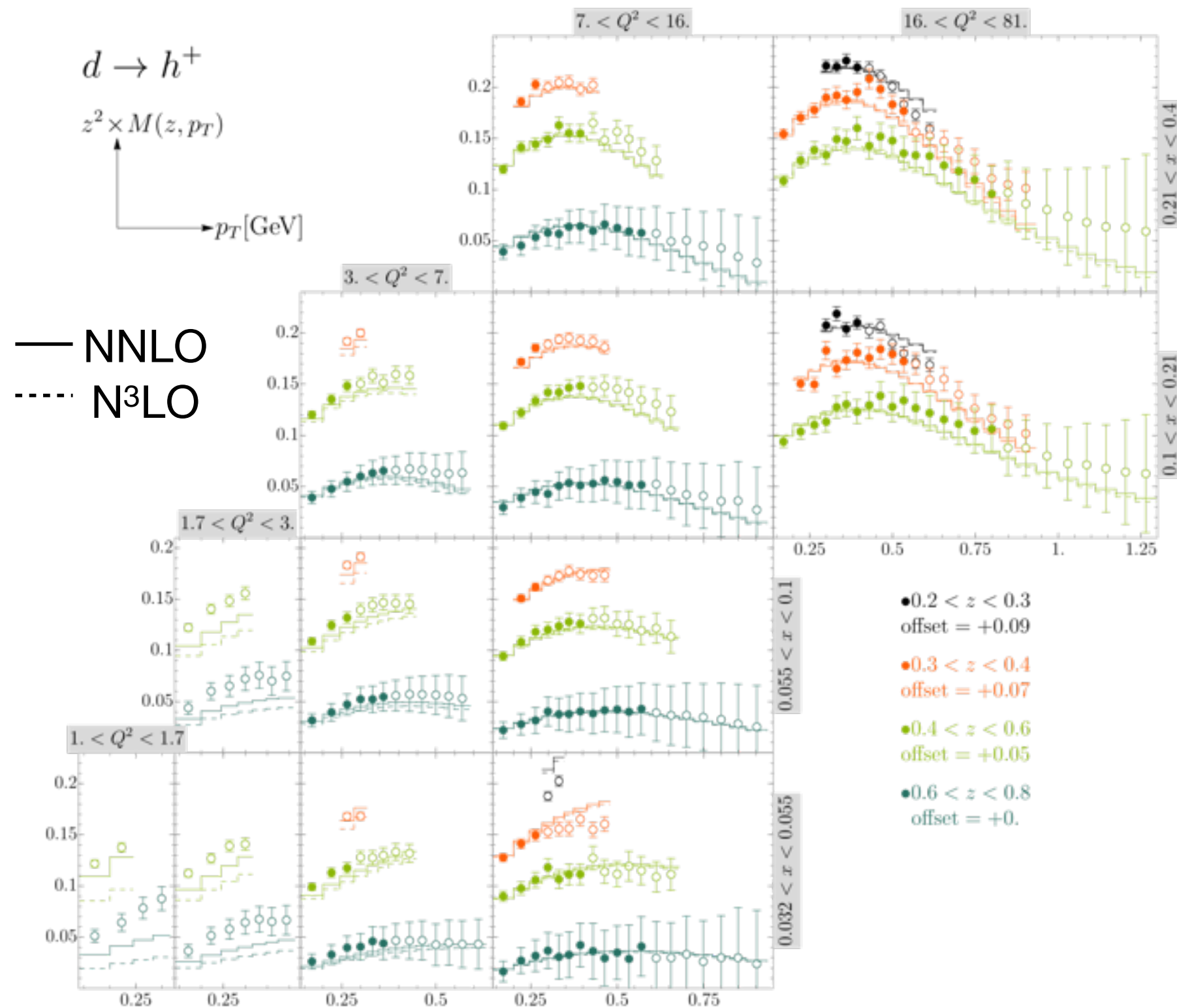
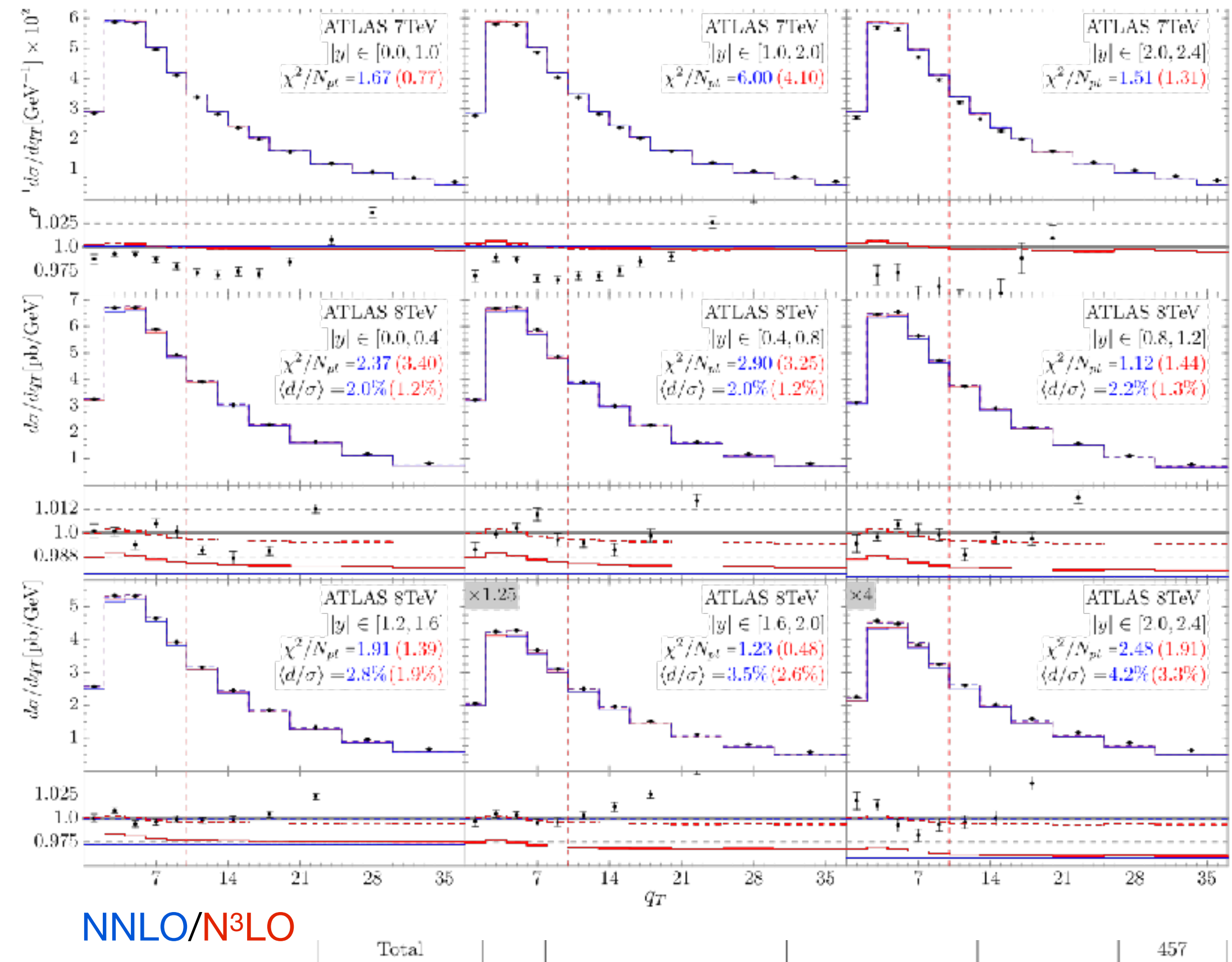
Spin-independent TMD PDFs: global analysis

I. Scimemi, A. Vladimirov JHEP 06 (2020)137

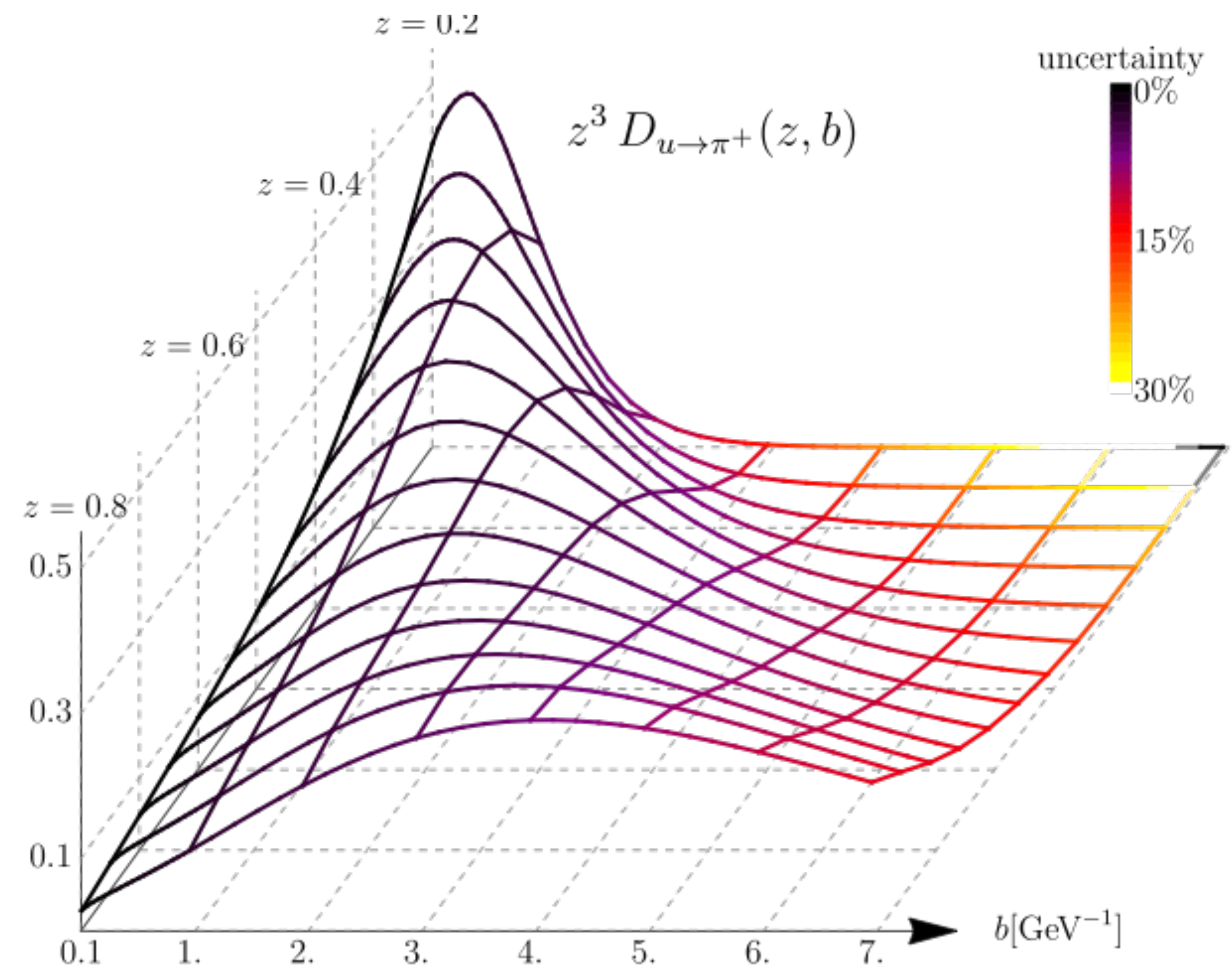
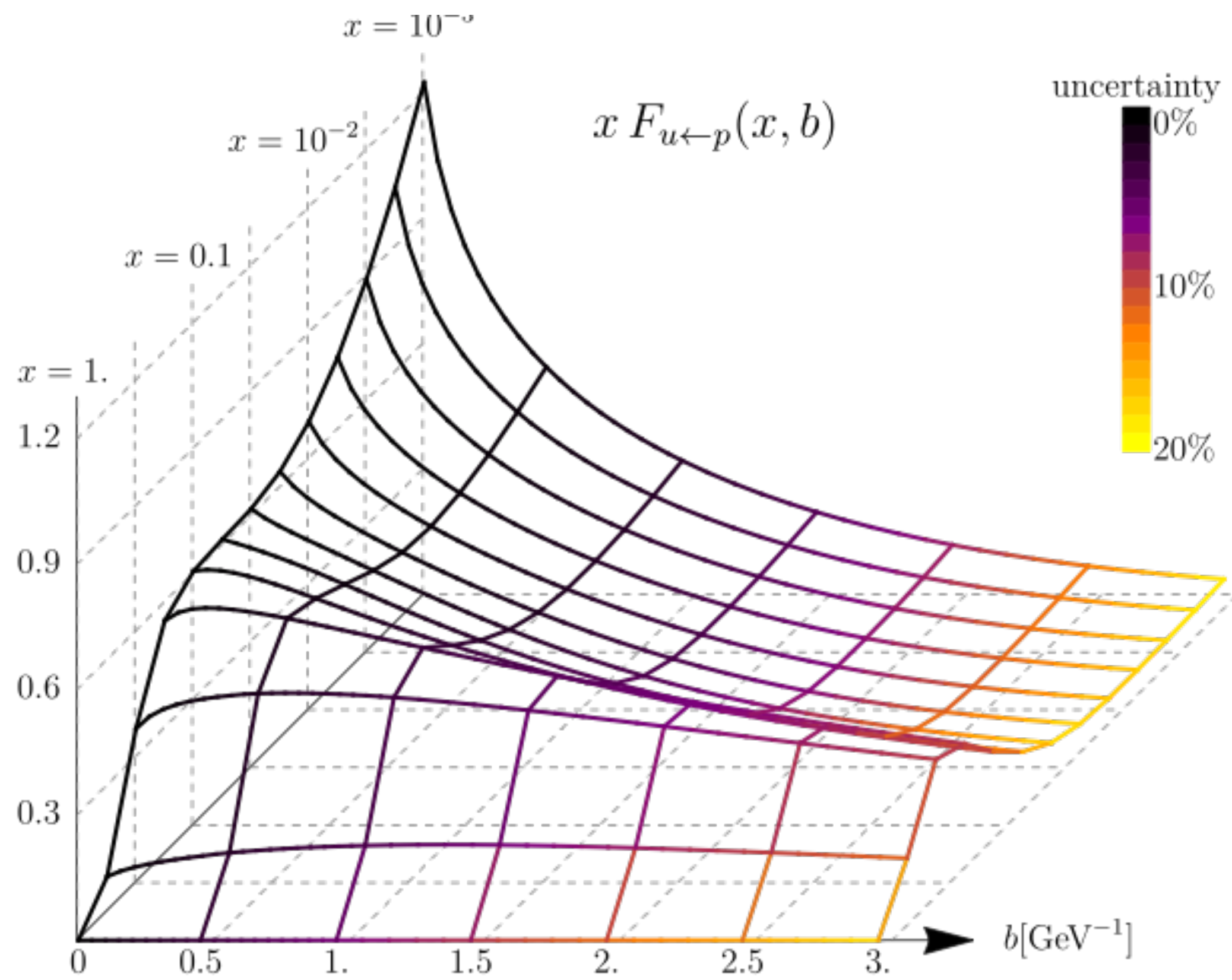


Experiment	ref.	\sqrt{s} [GeV]	Q [GeV]	y/x_F	fiducial region	N_{pt} after cuts
F288 (200)	[73]	19.4	4–9 in 1 GeV bins*	$0.1 < x_F < 0.7$	—	43
E288 (300)	[73]	23.8	4–12 in 1 GeV bins*	$-0.09 < x_F < 0.51$	—	53
ATLAS (7TeV)	[73]	37.2	5–14 in 1 GeV bins*	$0.07 < x_F < 0.93$	—	70

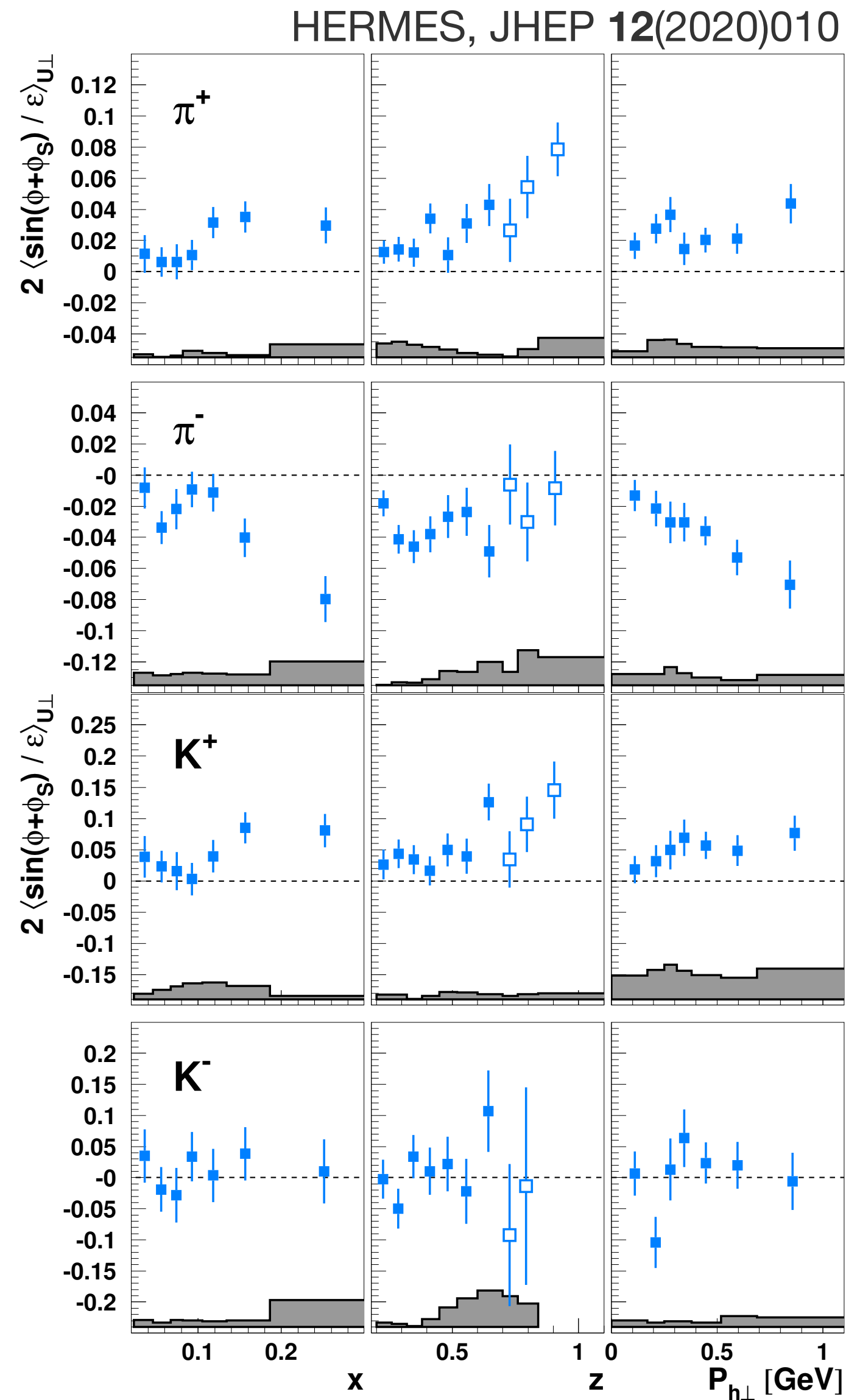
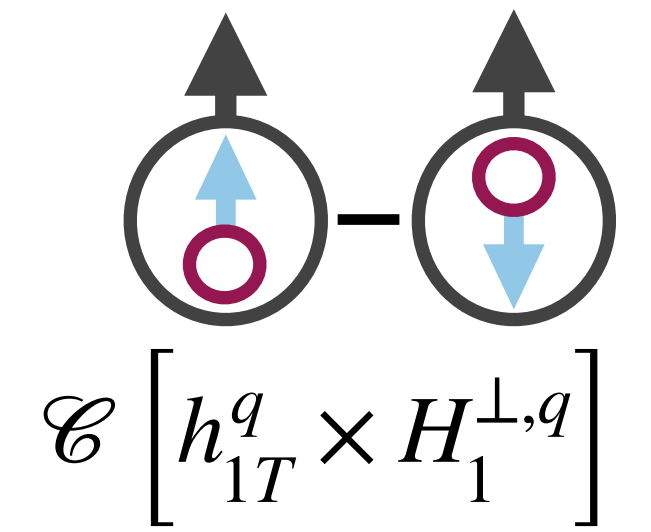
Description of the data



Spin-independent TMD PDFs: global analysis



Collins amplitudes



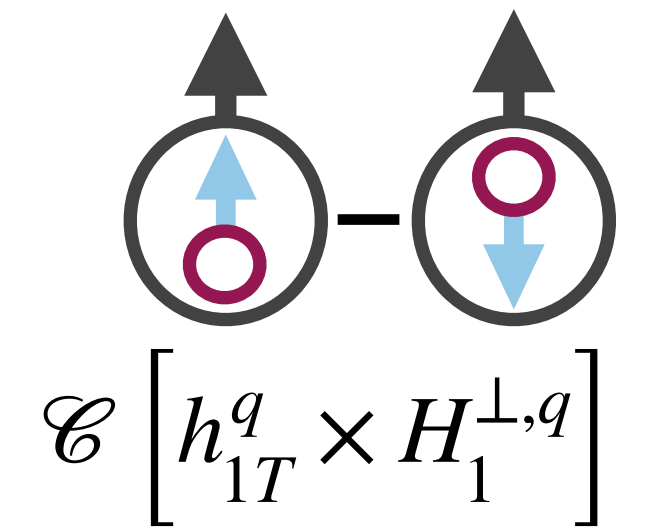
- Oppositely signed amplitudes for π^+ and π^- :

$$H_1^{\perp, u \rightarrow \pi^+} \approx -H_1^{\perp, u \rightarrow \pi^-}$$

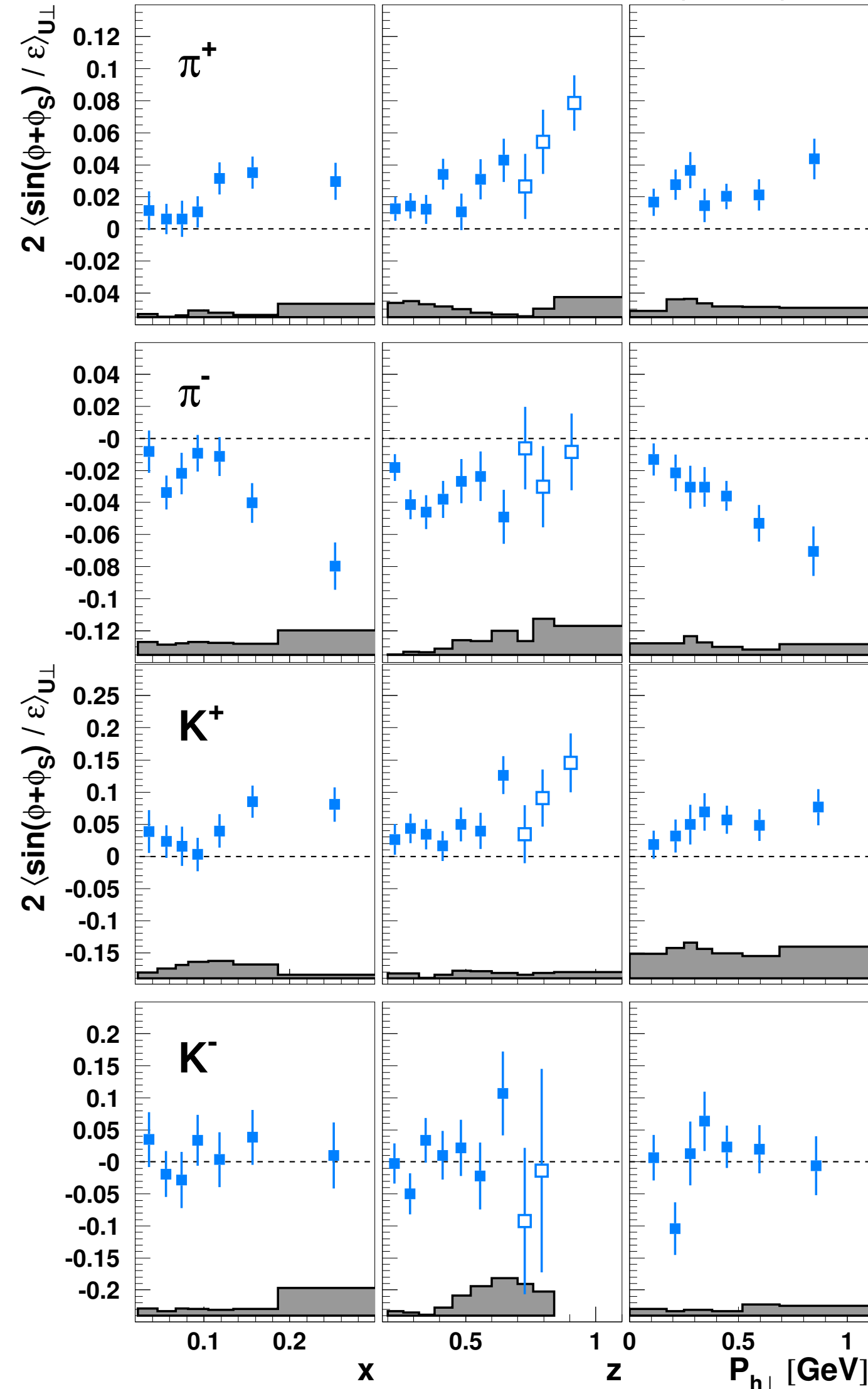
- Amplitudes for K^+ larger than for π^+ :

$$H_1^{\perp, u \rightarrow K^+} > H_1^{\perp, u \rightarrow \pi^+}$$

Collins amplitudes



HERMES, JHEP 12(2020)010

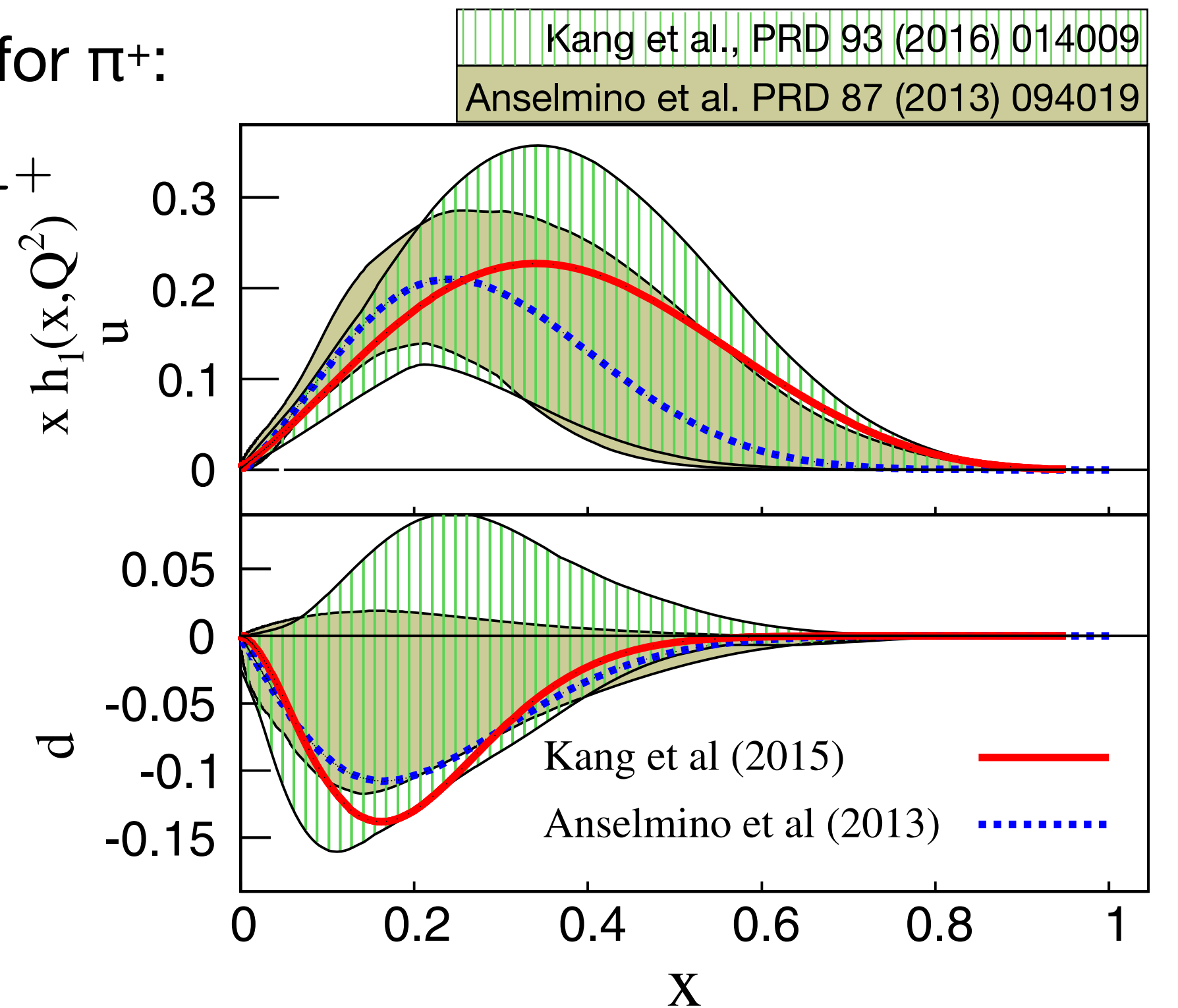


- Oppositely signed amplitudes for π^+ and π^- :

$$H_1^{\perp, u \rightarrow \pi^+} \approx -H_1^{\perp, u \rightarrow \pi^-}$$

- Amplitudes for K^+ larger than for π^+ :

$$H_1^{\perp, u \rightarrow K^+} > H_1^{\perp, u \rightarrow \pi^+}$$

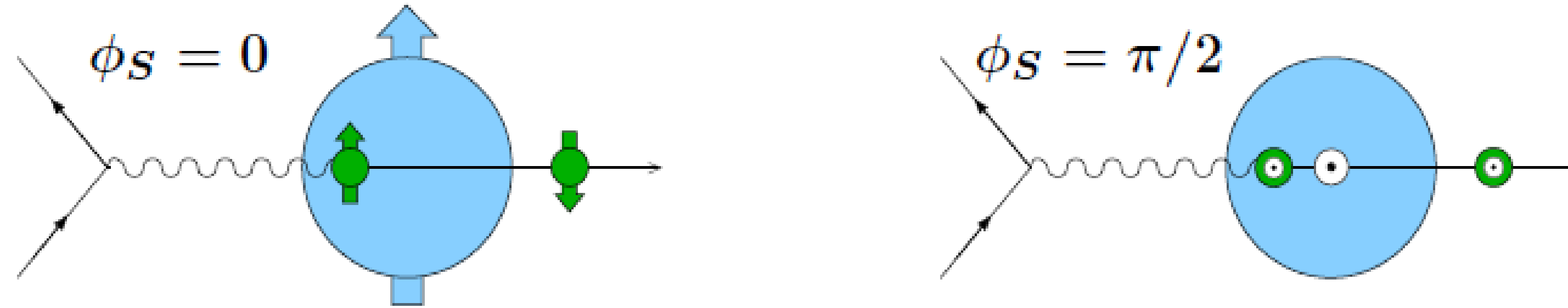


data from Belle, Babar, COMPASS, HERMES, Jefferson Lab Hall A

Artru model

X. Artru et al., Z. Phys. C73 (1997) 527

polarisation component in lepton scattering plane reversed by photoabsorption:



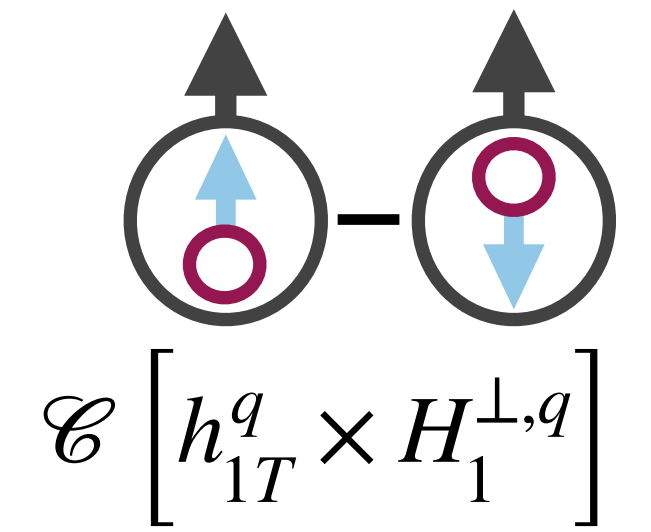
string break, quark-antiquark pair with vacuum numbers:



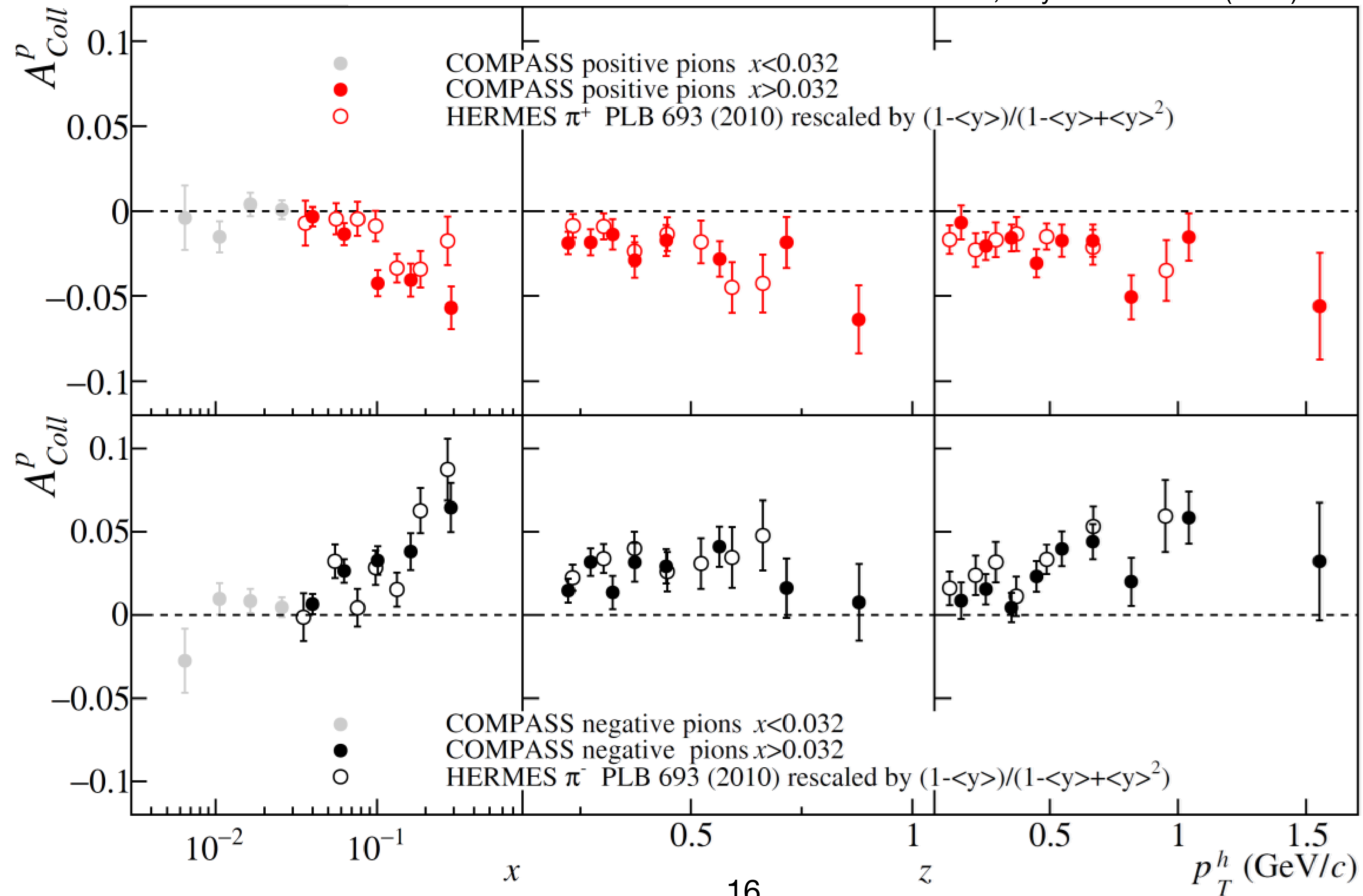
orbital angular momentum creates transverse momentum:



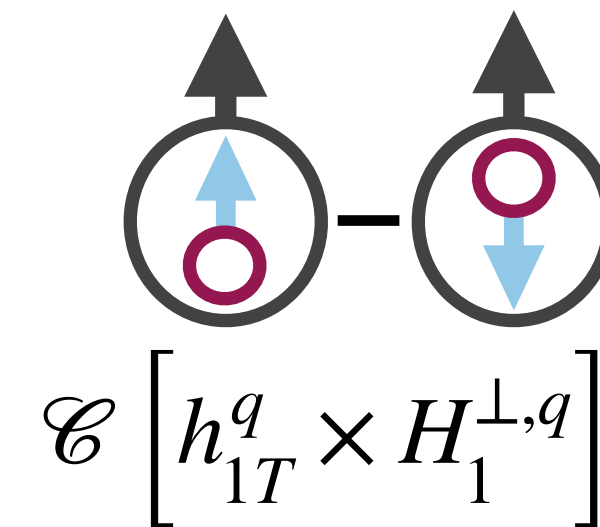
Collins amplitudes: QCD evolution



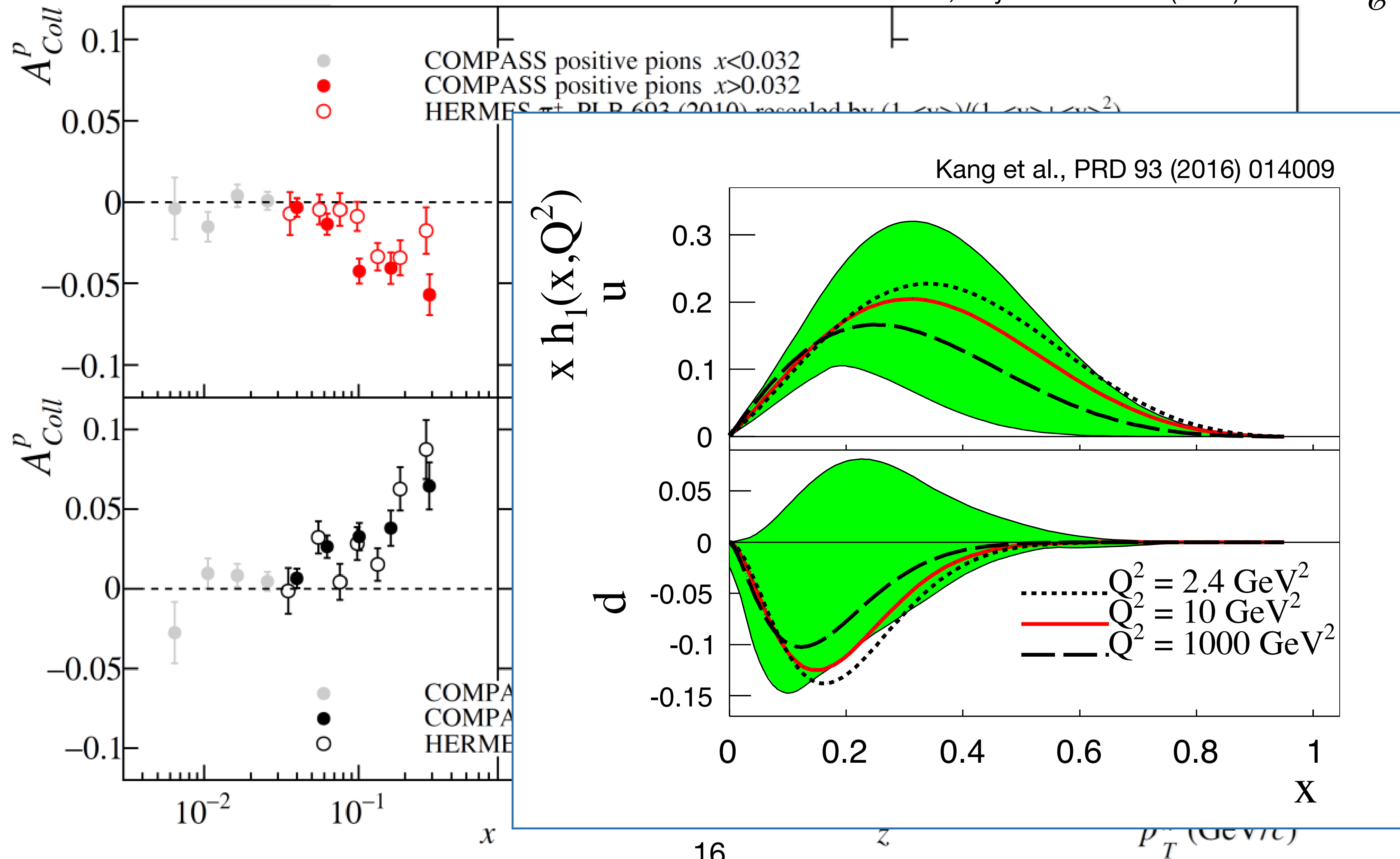
COMPASS, Phys. Lett. **B 744** (2015) 250



Collins amplitudes: QCD evolution

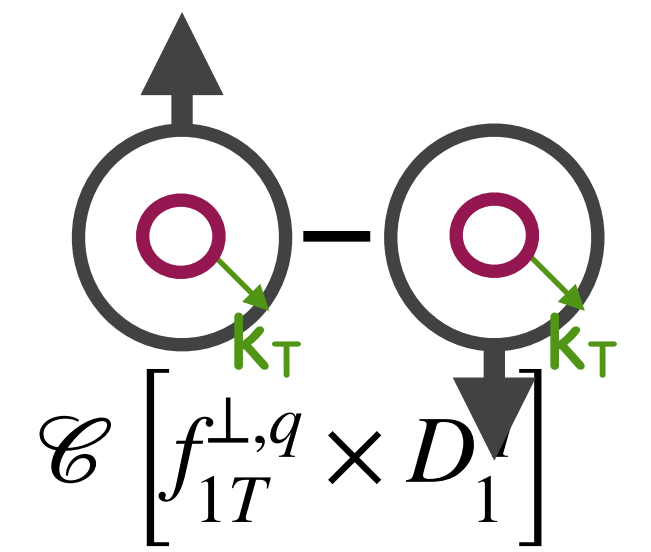


COMPASS, Phys. Lett. **B 744** (2015) 250



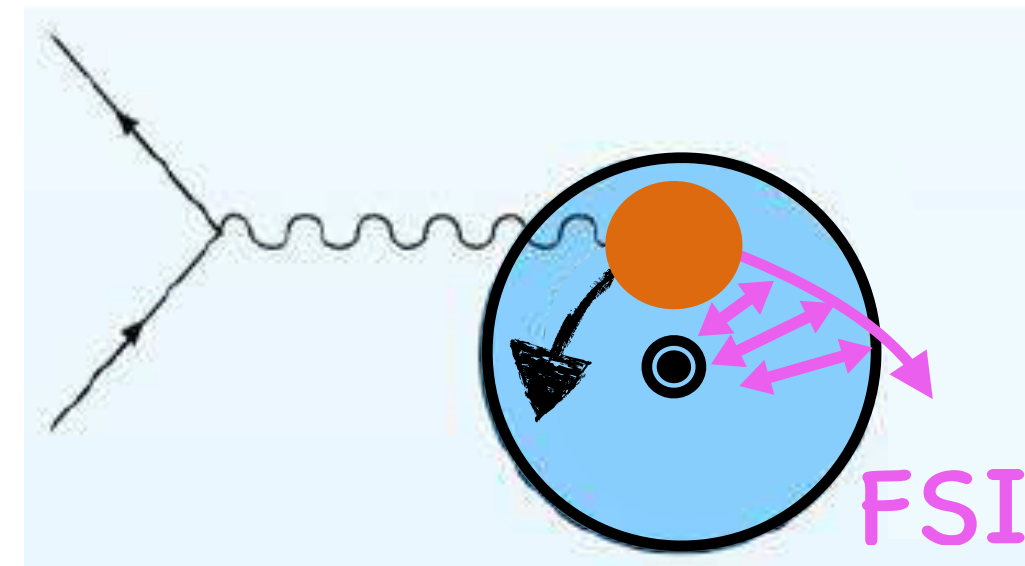
Kang et al., PRD 93 (2016) 014009

Sivers amplitudes

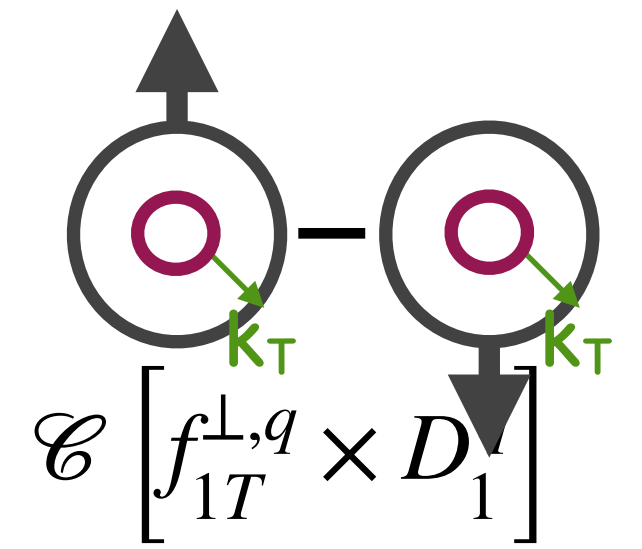


The diagram shows two nucleons, represented by circles with a smaller inner circle. The left nucleon has an upward-pointing spin vector (black arrow) and a green arrow labeled k_T pointing to the right. The right nucleon has a downward-pointing spin vector (black arrow) and a green arrow labeled k_T pointing to the left. Below the nucleons is the mathematical expression $\mathcal{C} [f_{1T}^{\perp,q} \times D_1]$.

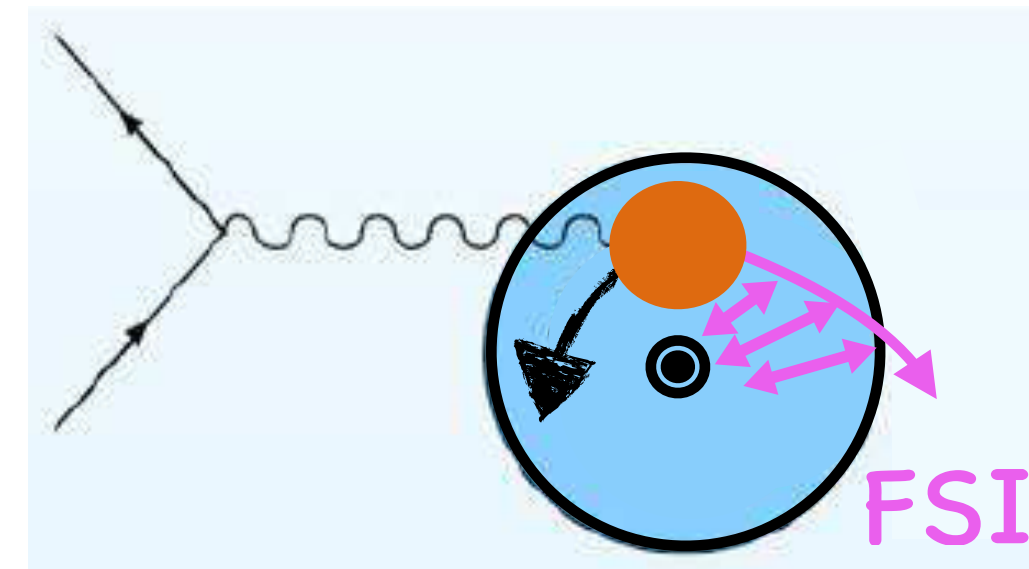
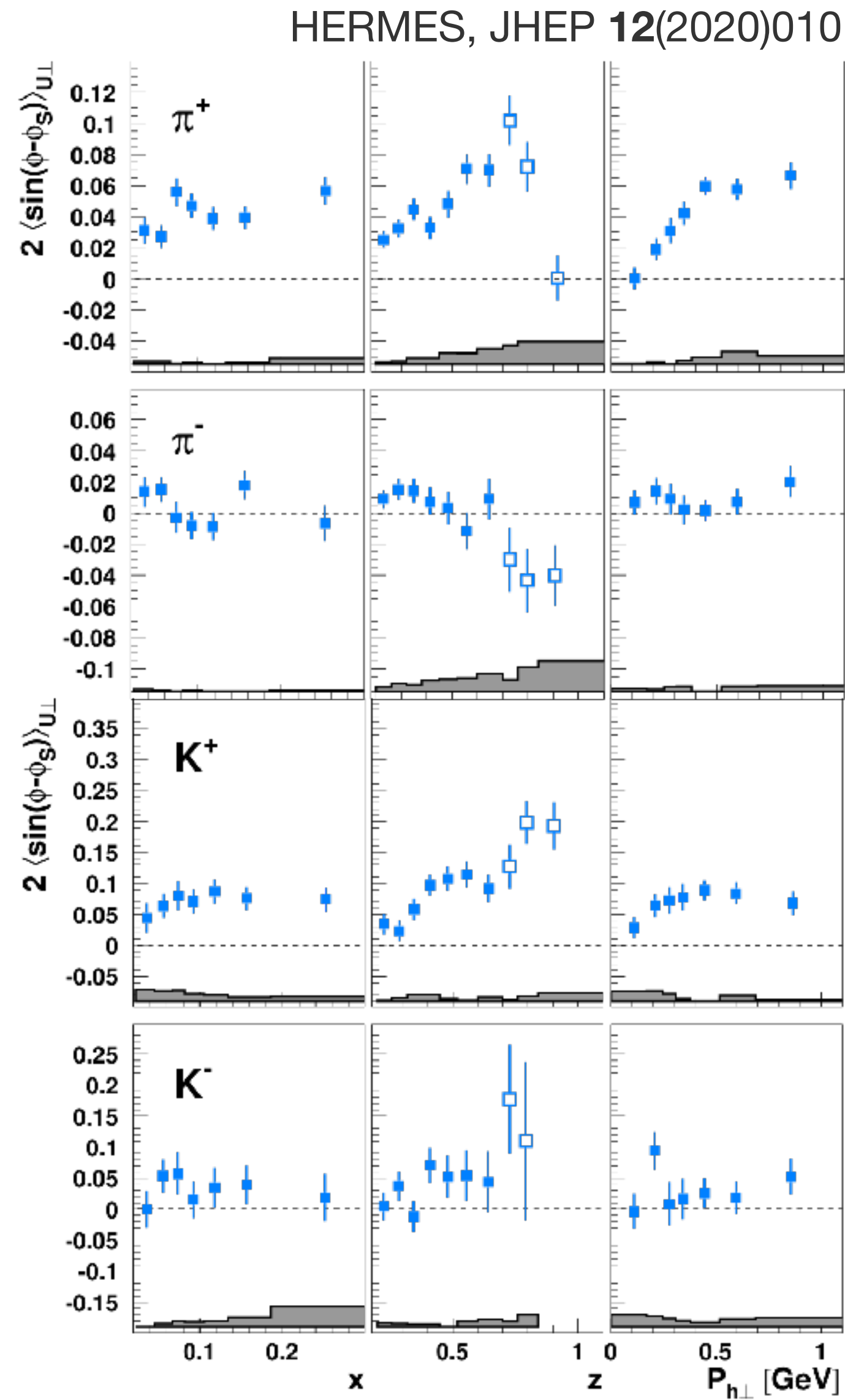
- Sivers function:
 - requires non-zero orbital angular momentum
 - final-state interactions \rightarrow azimuthal asymmetries



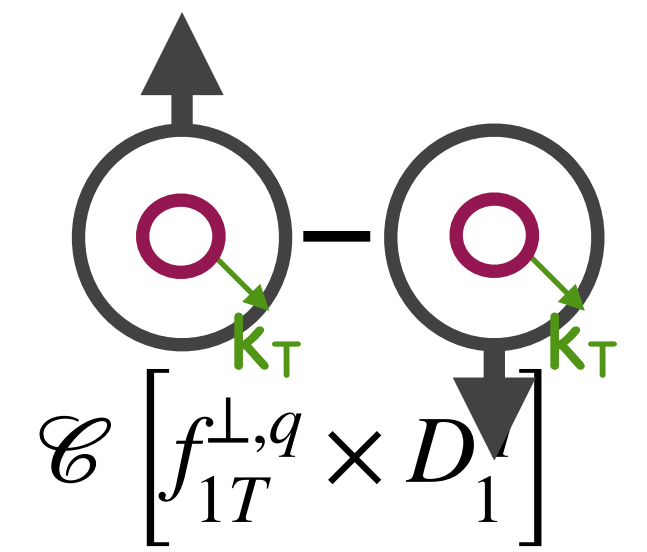
Sivers amplitudes



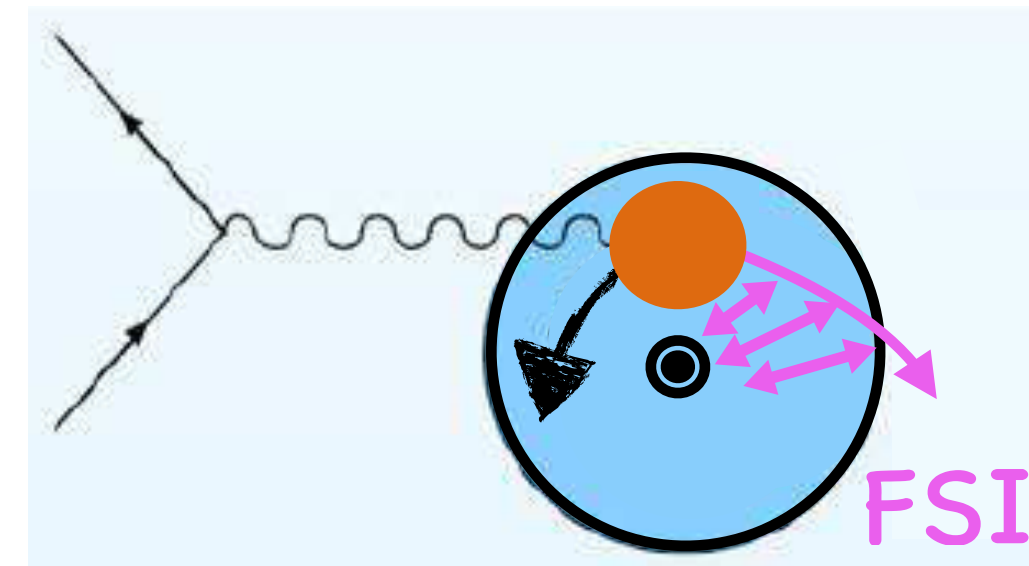
- Sivers function:
 - requires non-zero orbital angular momentum
 - final-state interactions \rightarrow azimuthal asymmetries



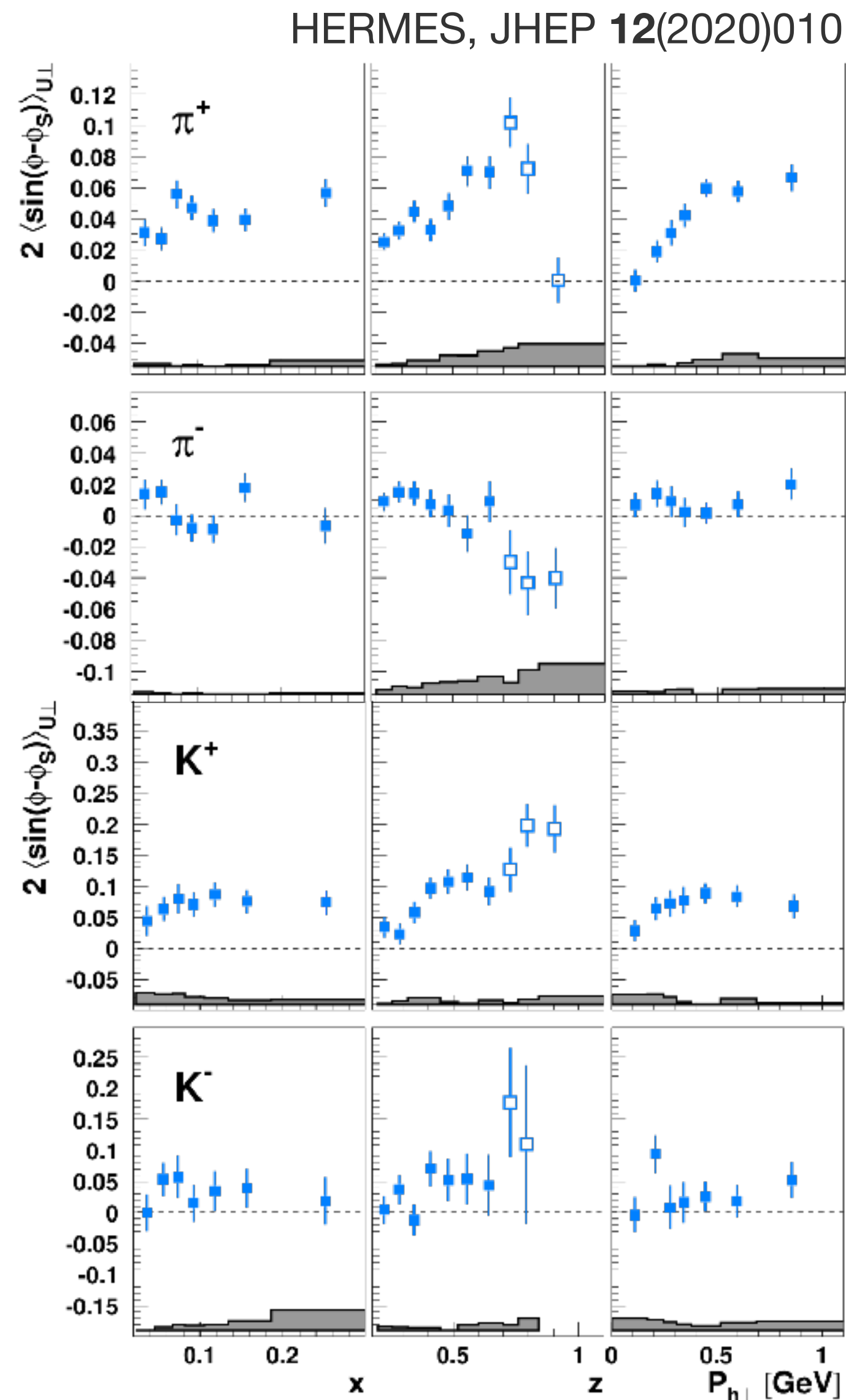
Sivers amplitudes



- Sivers function:
 - requires non-zero orbital angular momentum
 - final-state interactions \rightarrow azimuthal asymmetries

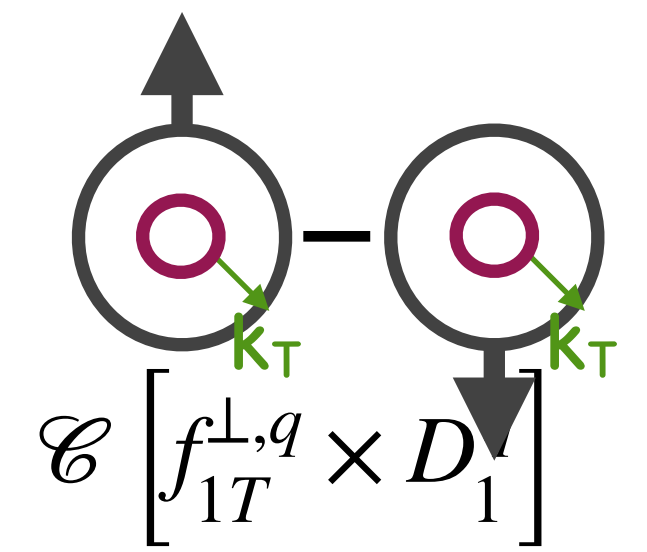
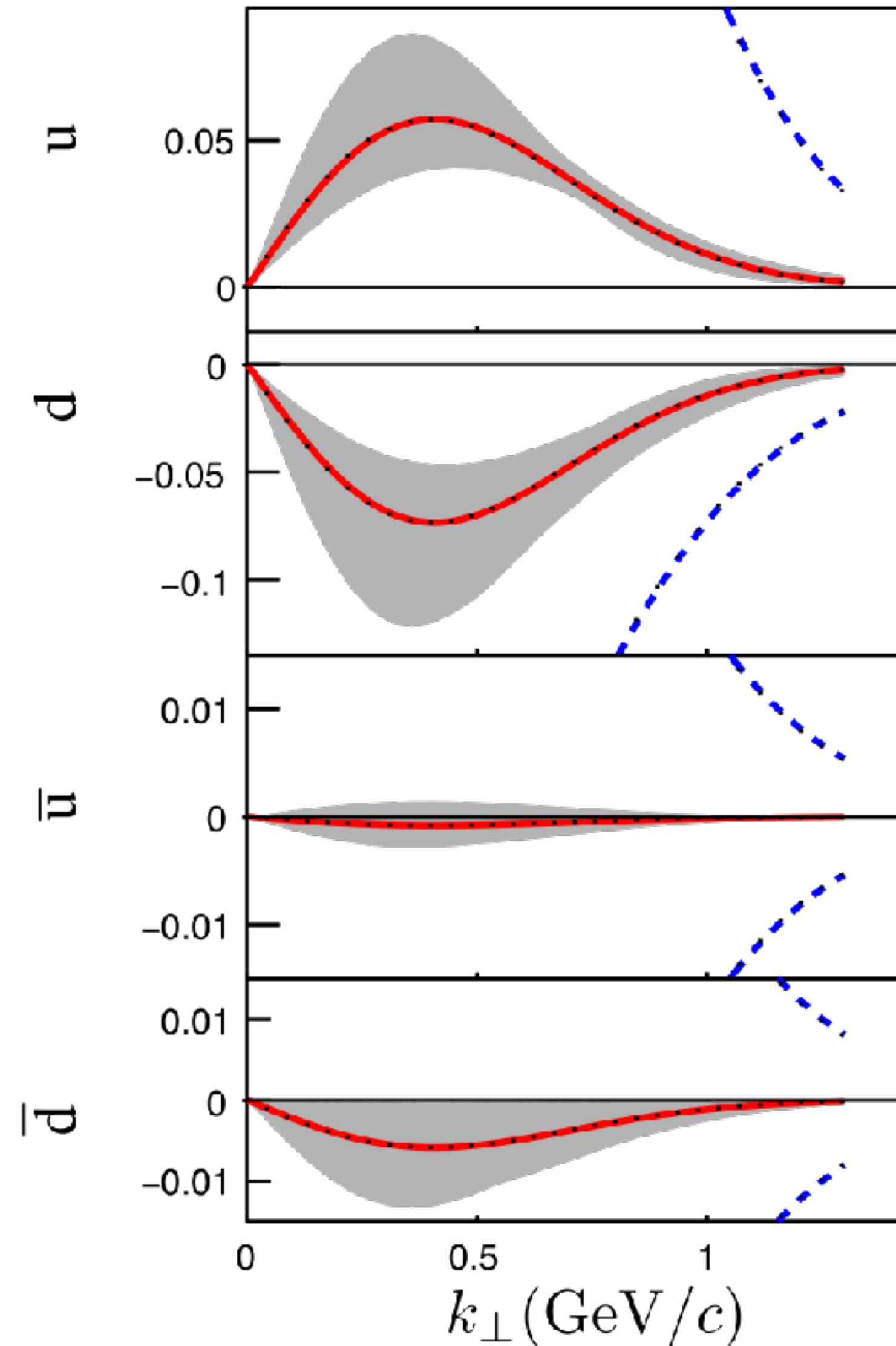


- π^+ :
 - positive \rightarrow non-zero orbital angular momentum
- π^- :
 - consistent with zero $\rightarrow u$ and d quark cancelation



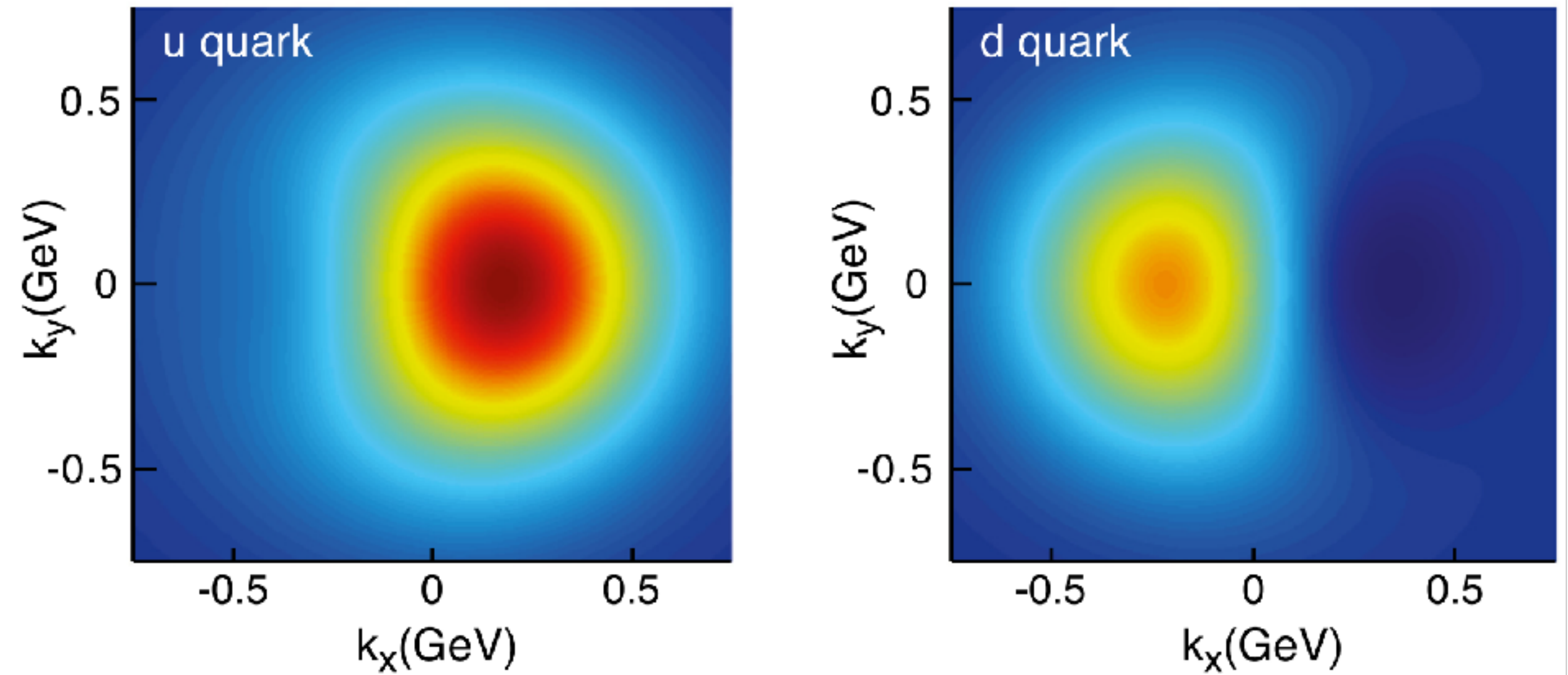
Sivers function

M. Anselmino et al., JHEP **04** (2017) 046



$x f_1(x, k_T, S_T)$

A. Accardi et al.,
Eur. Phys. J. A **52** (2016) 268

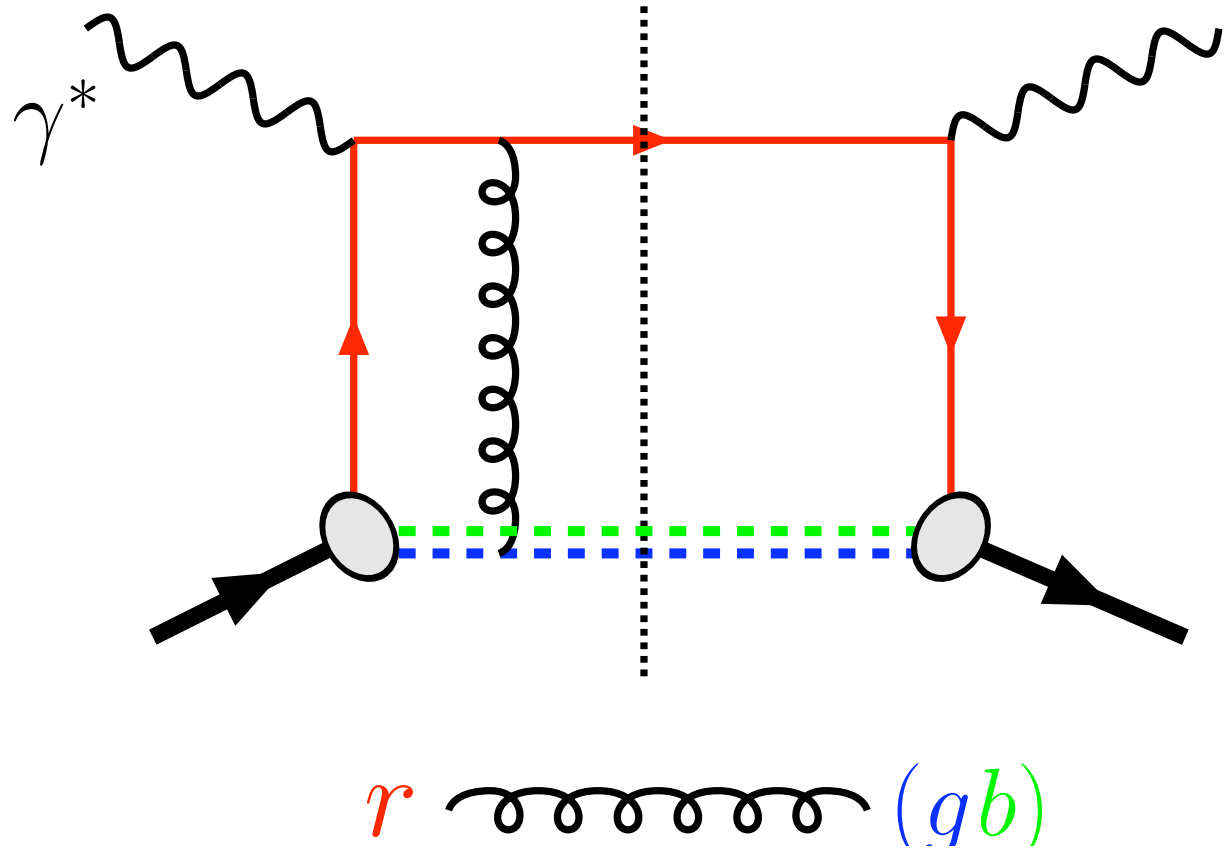
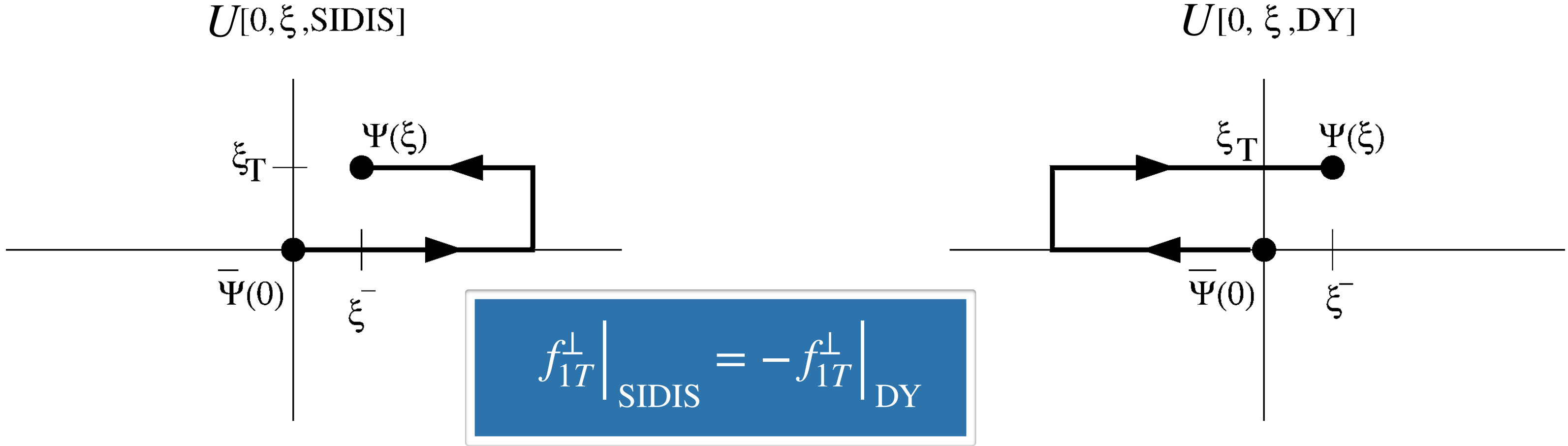


nucleon polarised along \hat{y}

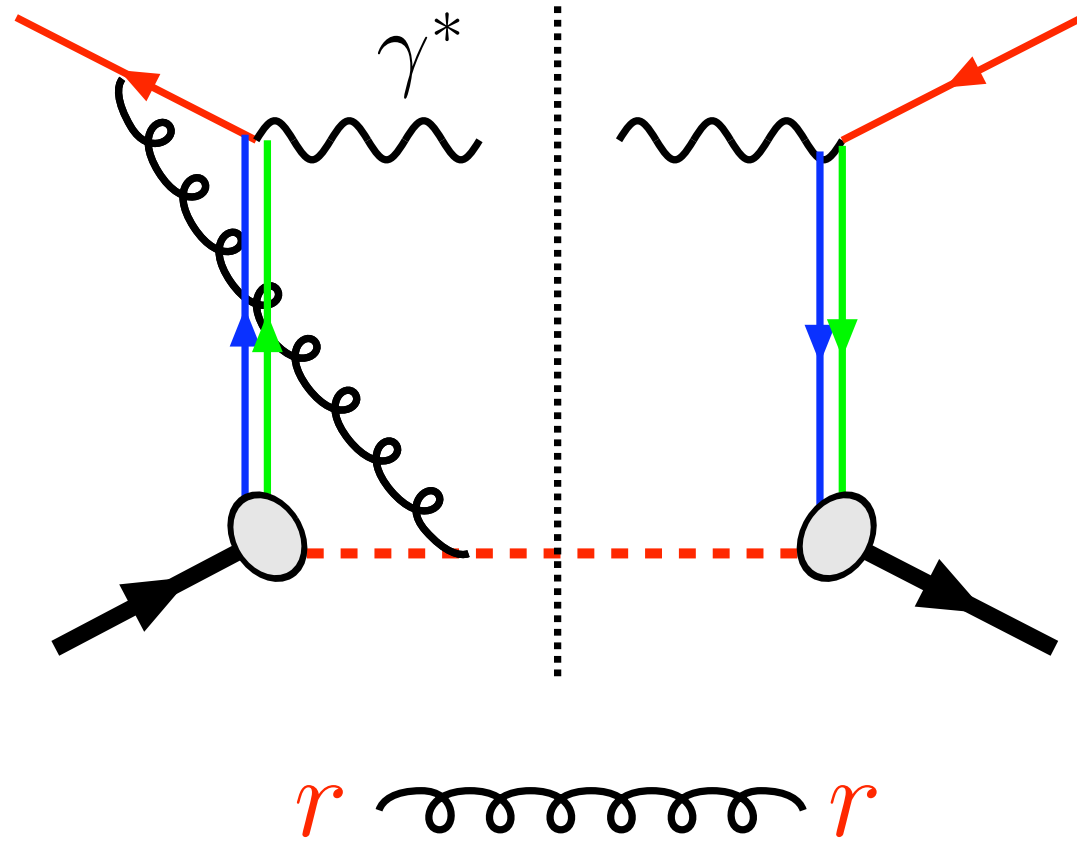
Predicted Sivvers sign change for SIDIS and Drell-Yan

J. C. Collins, Phys. Lett. B 536 (2002) 43

$$\Phi_{ij}(p, P, S) = \frac{1}{(2\pi)^4} \int d^4\xi e^{ip \cdot \xi} \langle P, S | \bar{\psi}_j(0) U_{[0, \xi]} \psi_i(\xi) | P, S \rangle$$

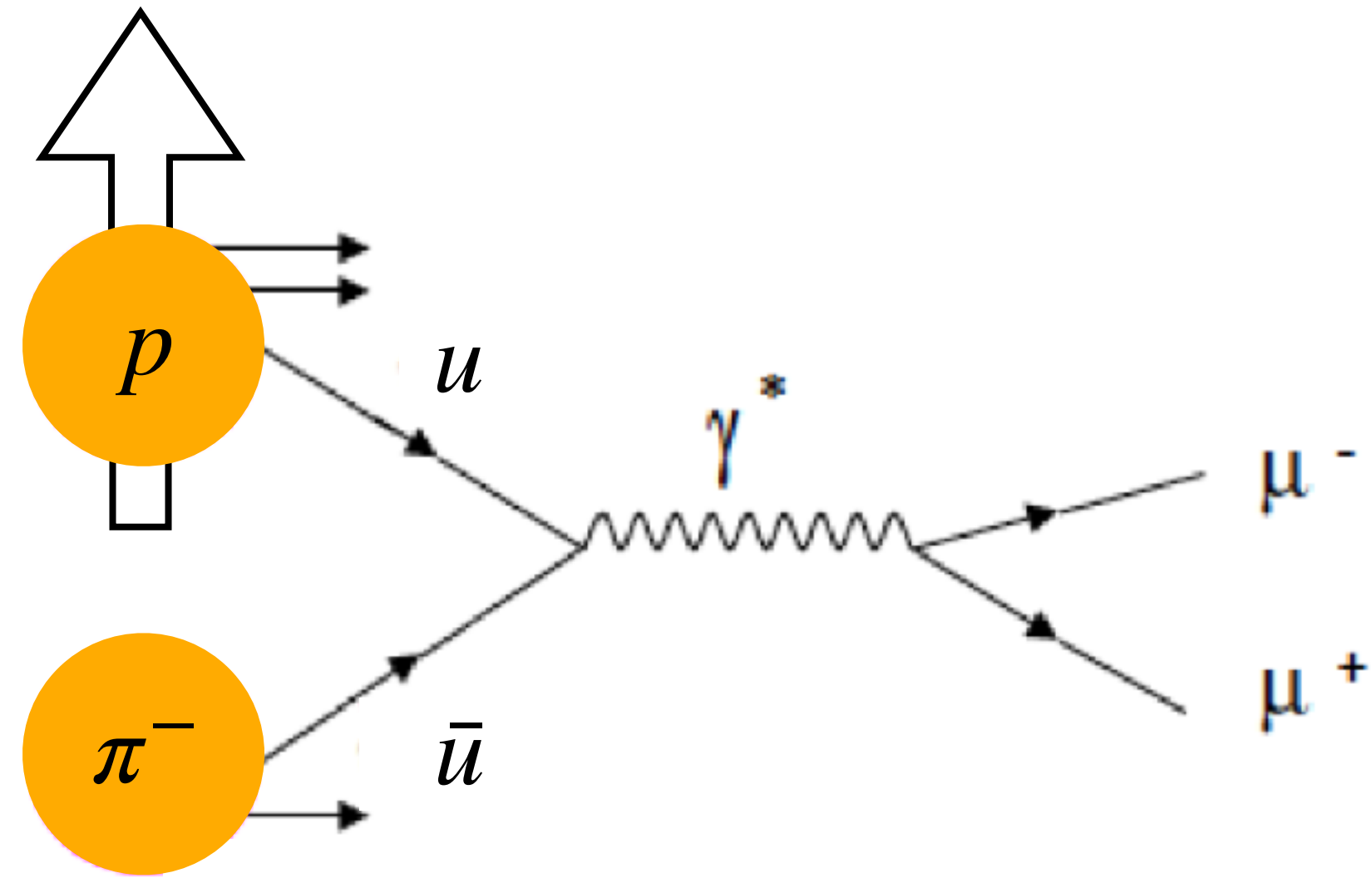


SIDIS

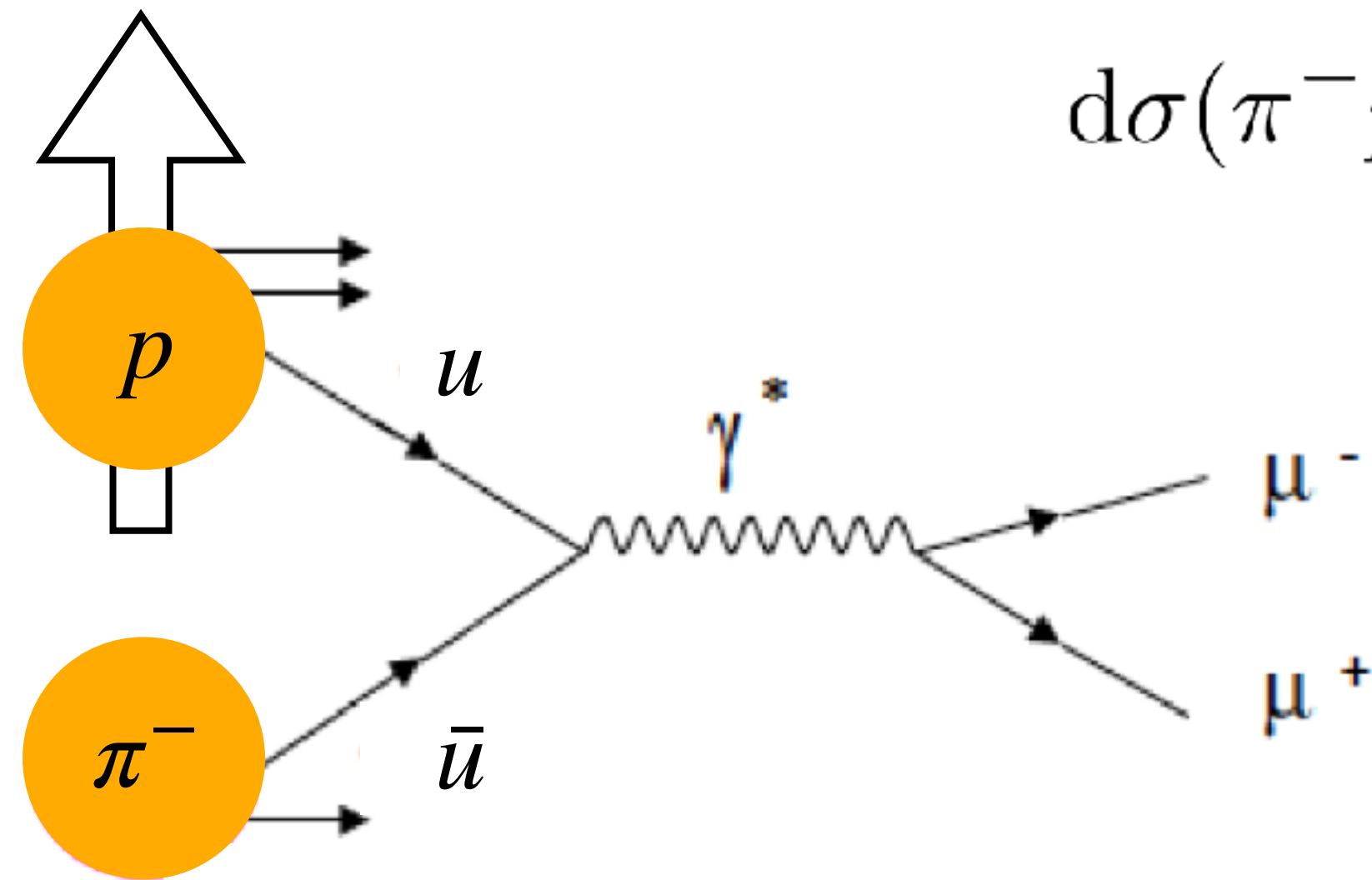


Drell-Yan

Experimental access to Sivers in Drell-Yan



Experimental access to Sivers in Drell-Yan

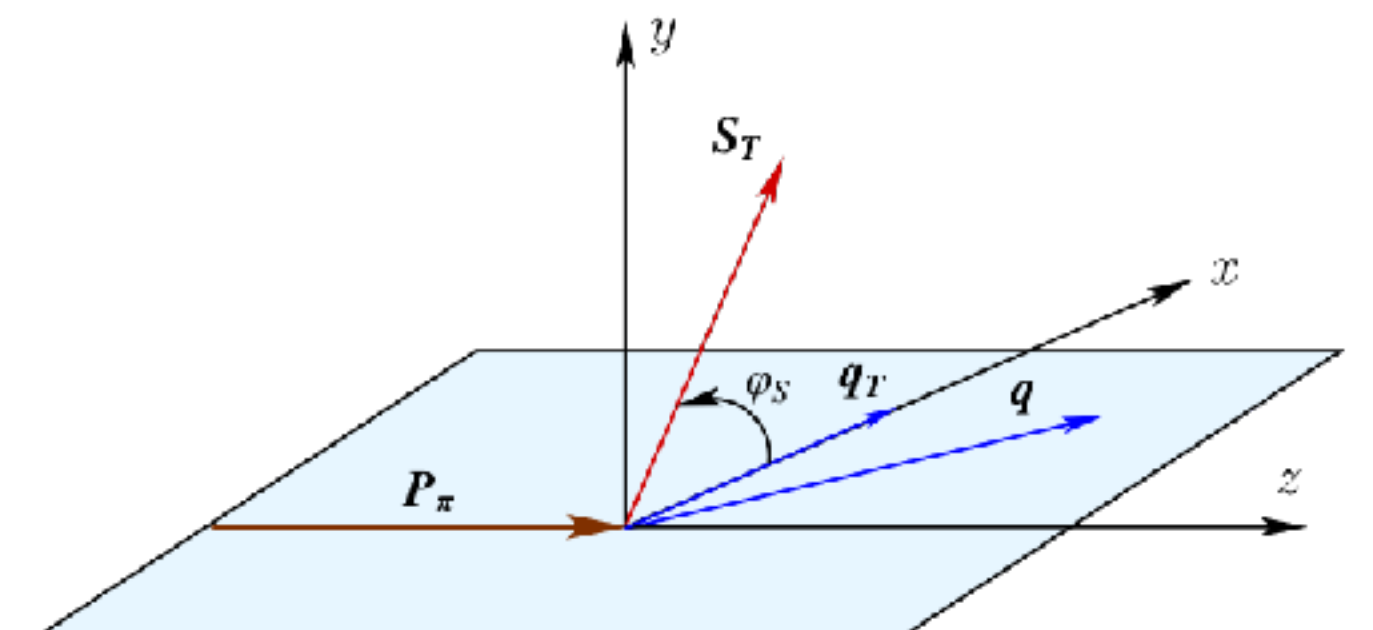
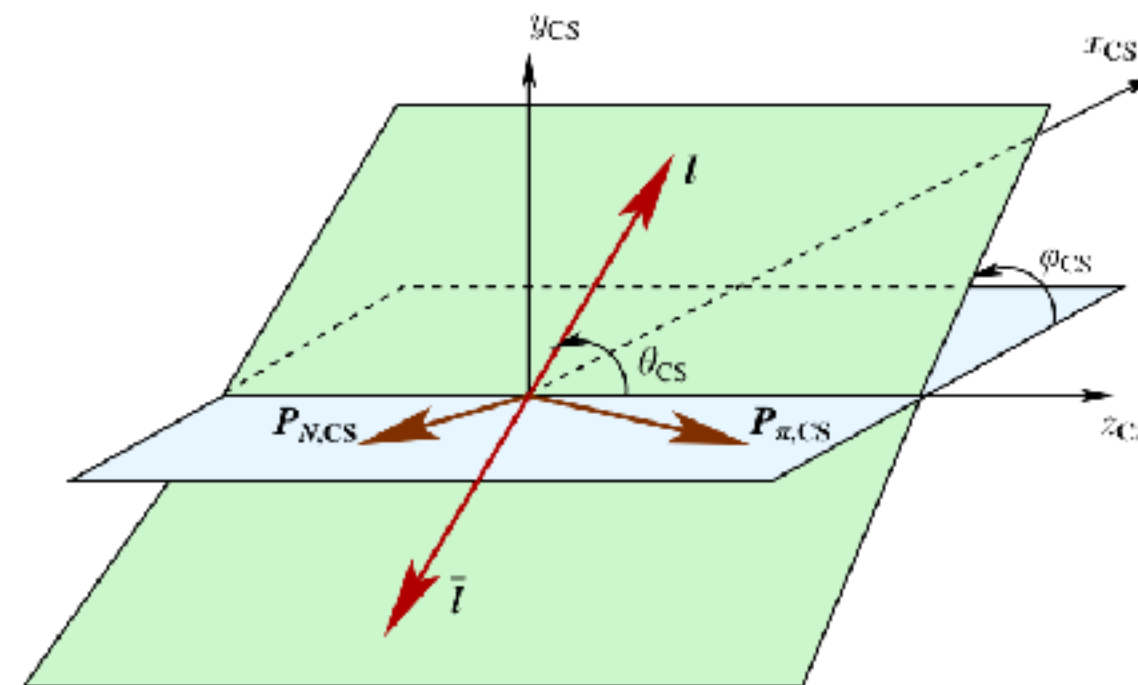


$$d\sigma(\pi^- p^\uparrow \rightarrow \mu^+ \mu^- X) \sim 1 + \bar{h}_1^\perp \otimes h_1^\perp \cos(2\phi)$$

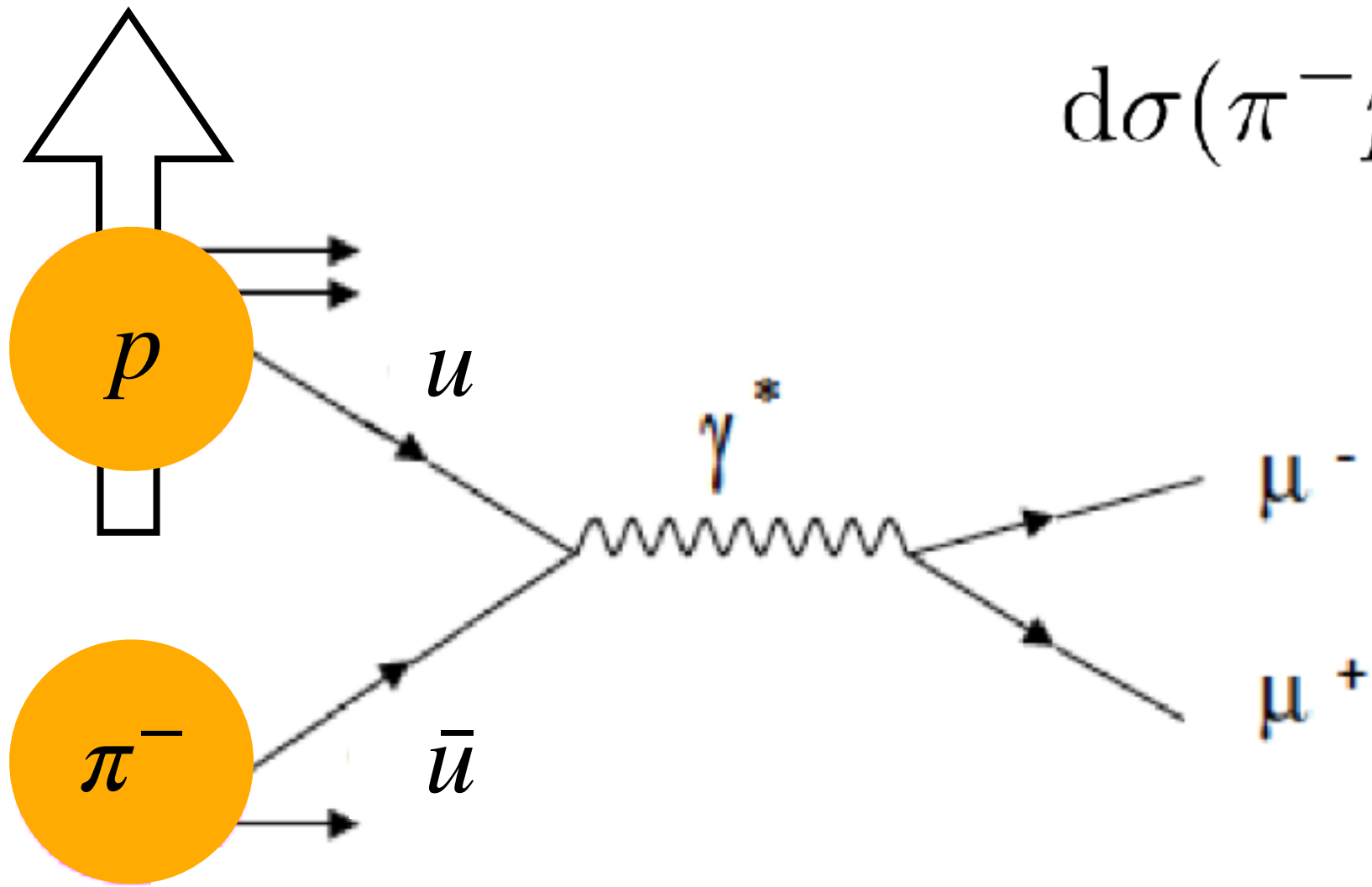
$$+ |S_T| \bar{f}_1 \otimes f_{1T}^\perp \sin \phi_S$$

$$+ |S_T| \bar{h}_1^\perp \otimes h_{1T}^\perp \sin(2\phi + \phi_S)$$

$$+ |S_T| \bar{h}_1^\perp \otimes h_{1T} \sin(2\phi - \phi_S)$$



Experimental access to Sivers in Drell-Yan

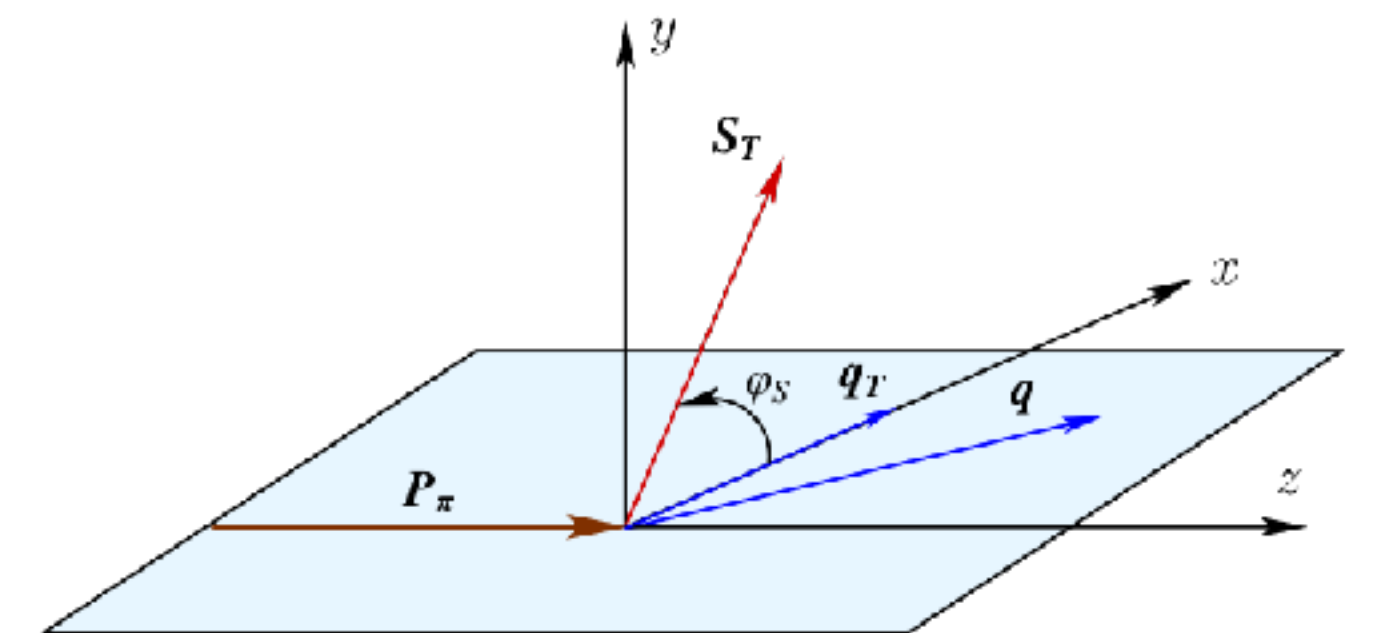
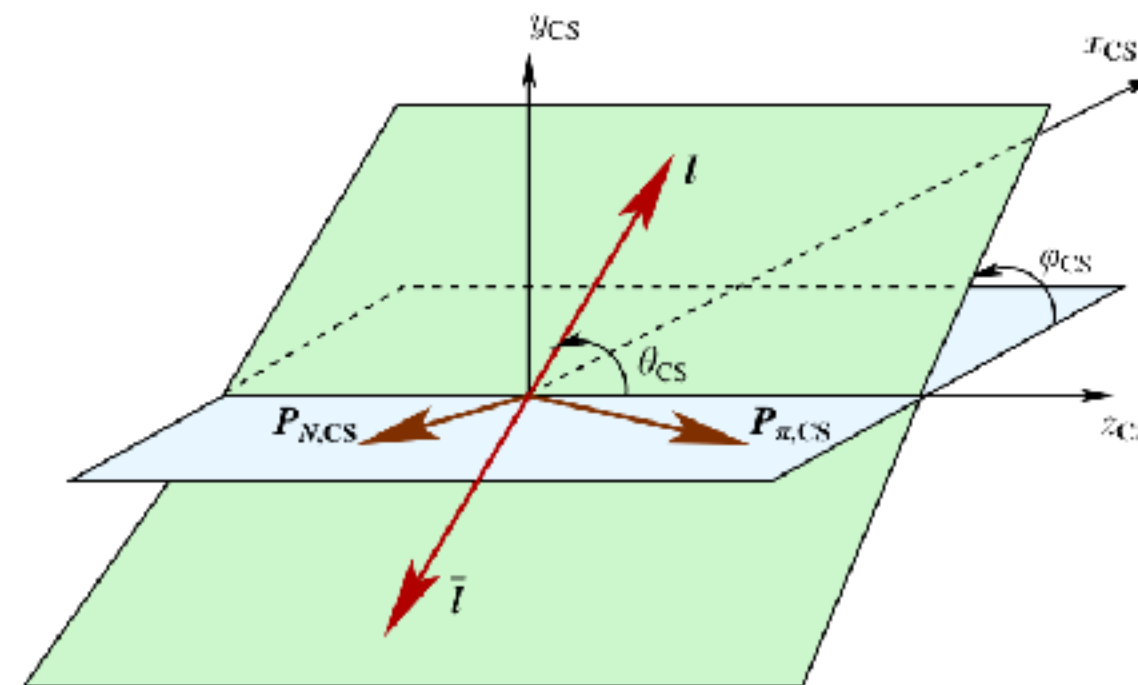


$$d\sigma(\pi^- p^\uparrow \rightarrow \mu^+ \mu^- X) \sim 1 + \bar{h}_1^\perp \otimes h_1^\perp \cos(2\phi)$$

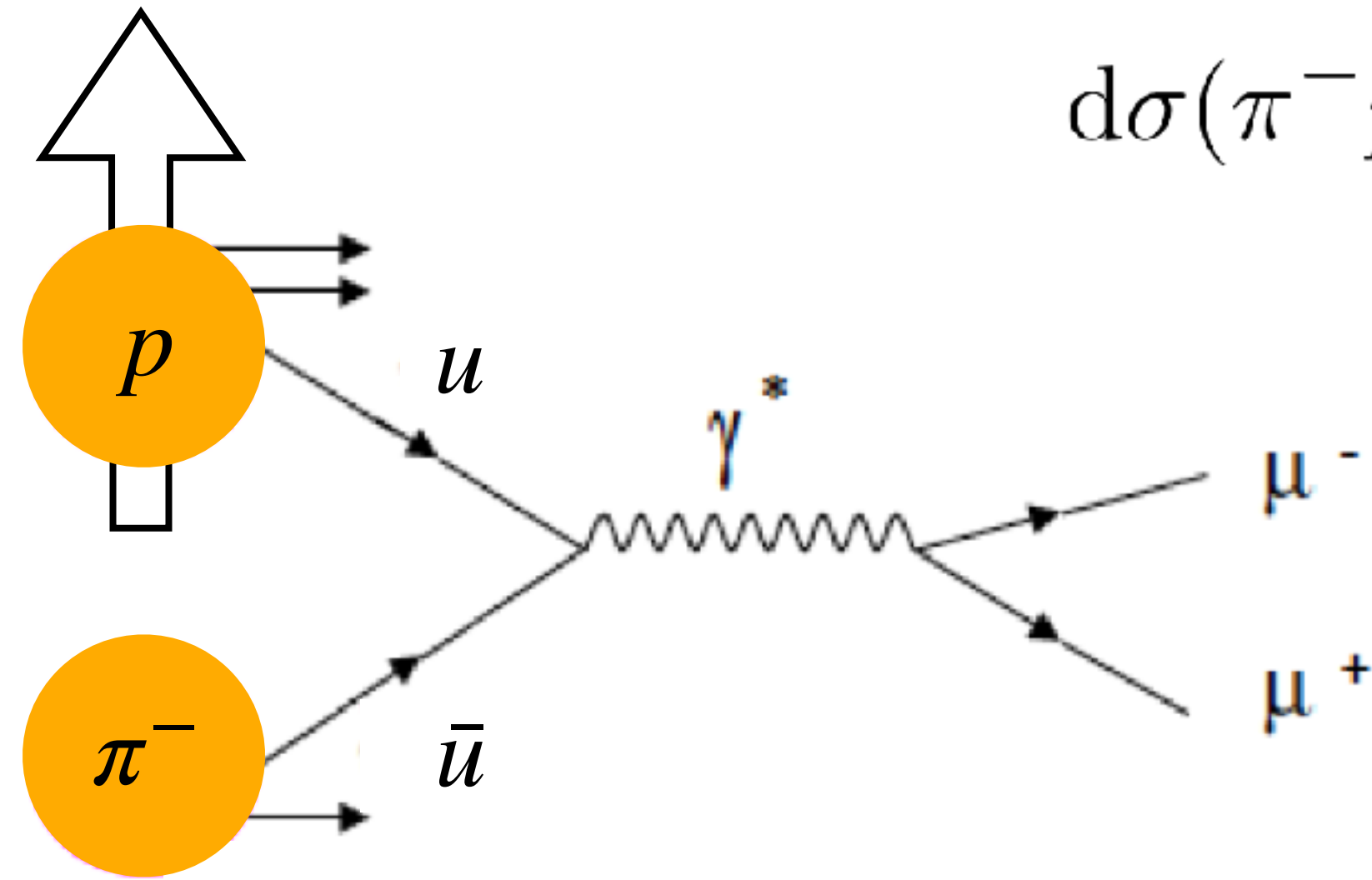
$$+ |S_T| \bar{f}_1 \otimes f_{1T}^\perp \sin \phi_S$$

$$+ |S_T| \bar{h}_1^\perp \otimes h_{1T}^\perp \sin(2\phi + \phi_S)$$

$$+ |S_T| \underbrace{\bar{h}_1^\perp}_{\pi^-} \otimes \underbrace{h_{1T}^\perp}_p \sin(2\phi - \phi_S)$$



Experimental access to Sivers in Drell-Yan

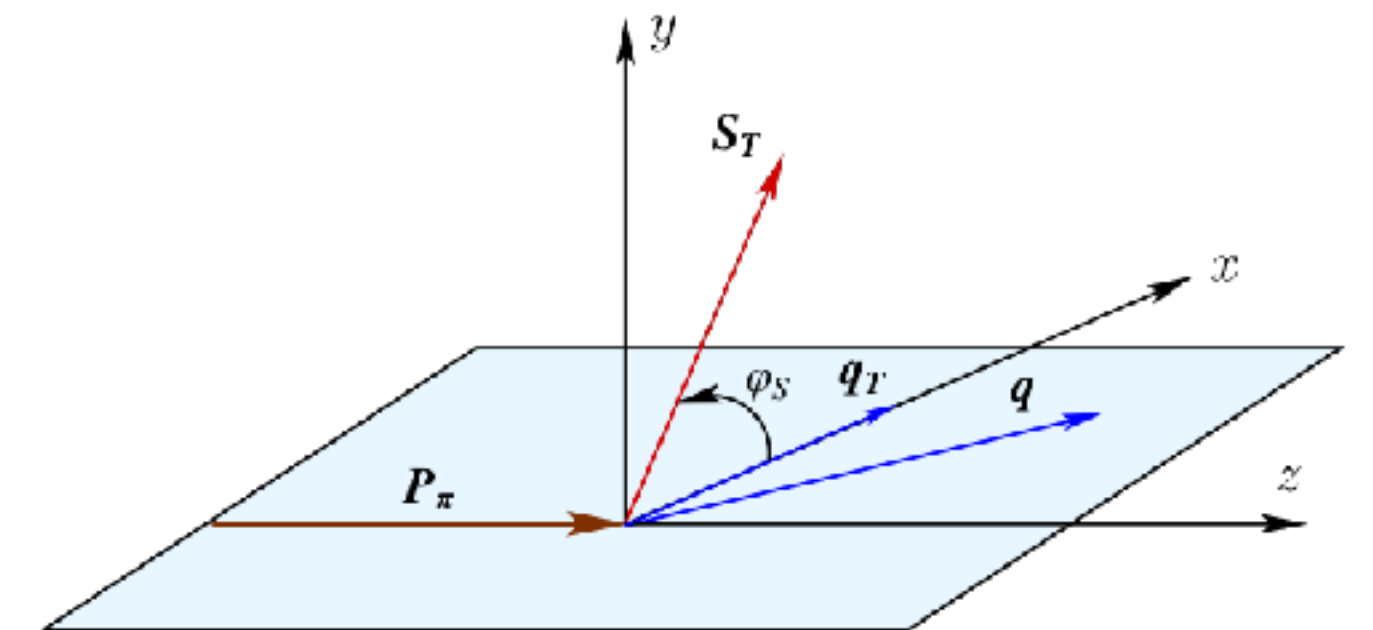
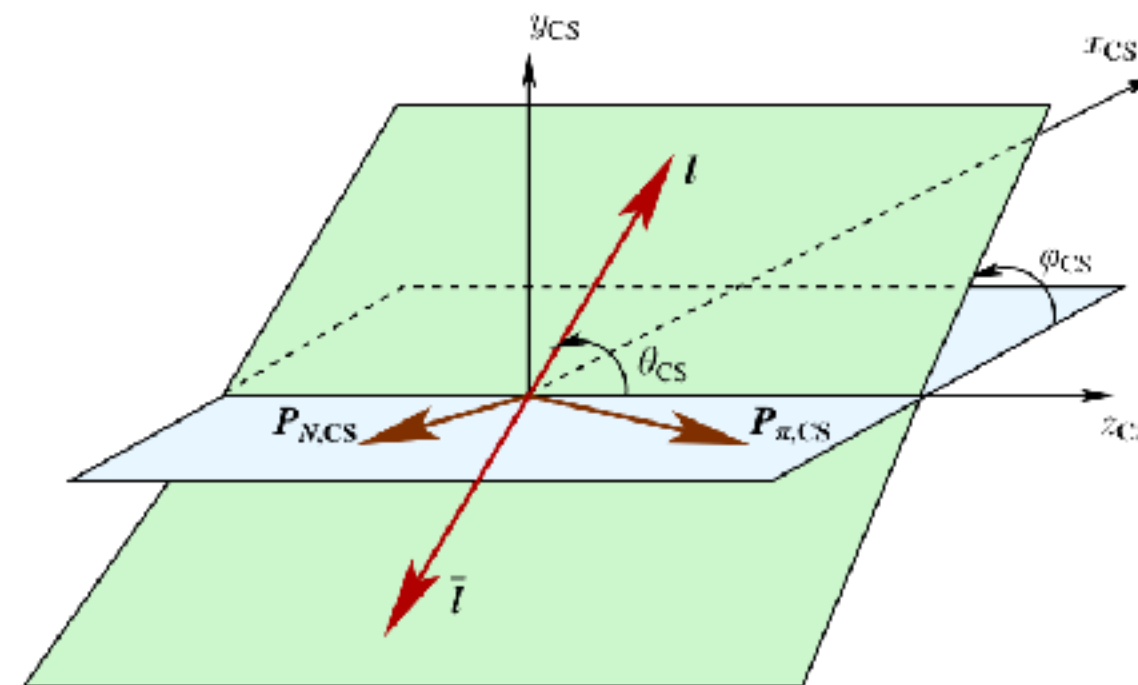


$$d\sigma(\pi^- p^\uparrow \rightarrow \mu^+ \mu^- X) \sim 1 + \bar{h}_1^\perp \otimes h_1^\perp \cos(2\phi)$$

$$+ |S_T| \bar{f}_1 \otimes \bar{f}_{1T} \sin \phi_S$$

$$+ |S_T| \bar{h}_1^\perp \otimes h_{1T}^\perp \sin(2\phi + \phi_S)$$

$$+ |S_T| \underbrace{\bar{h}_1^\perp}_{\pi^-} \otimes \underbrace{h_{1T}^\perp}_p \sin(2\phi - \phi_S)$$



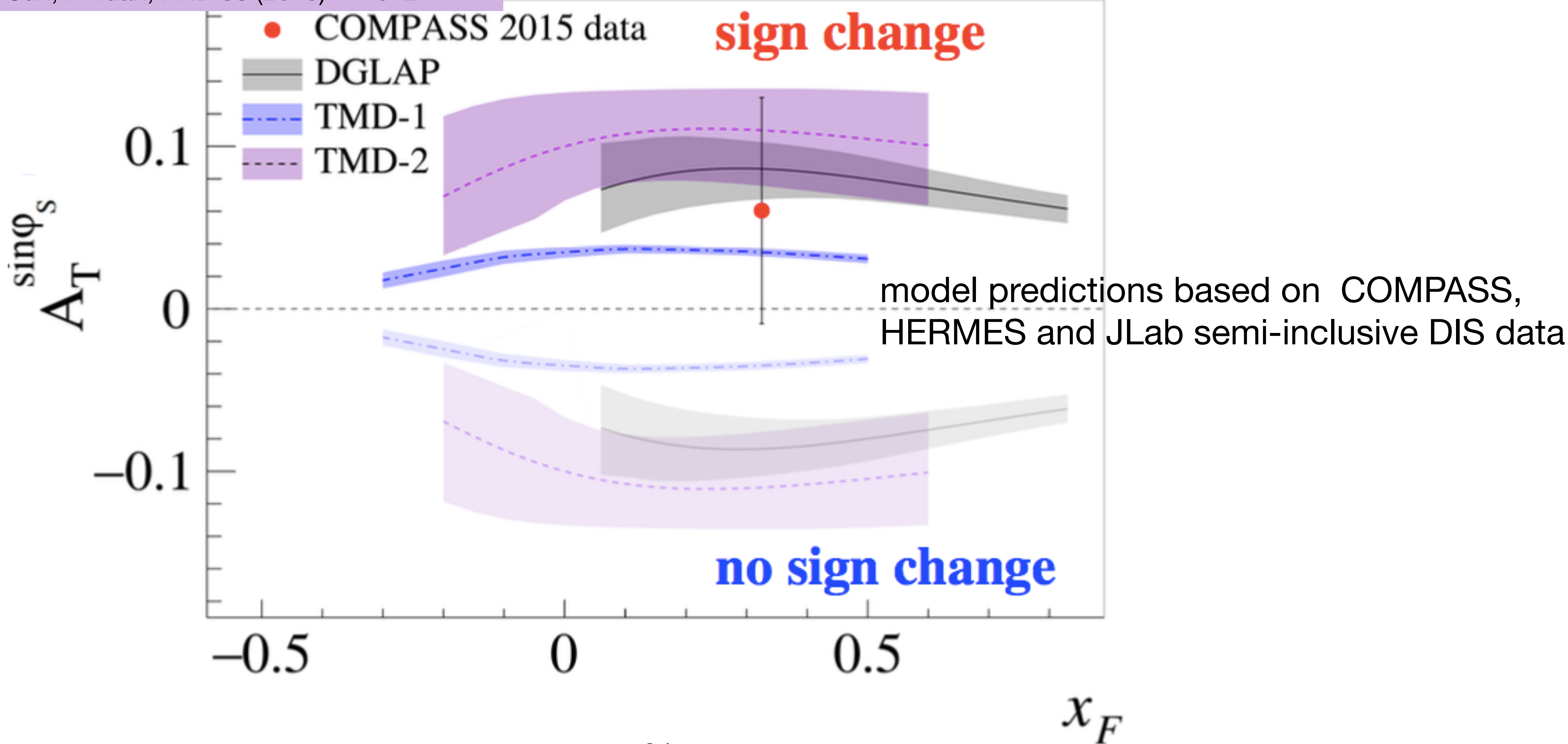
Investigation of the Sivers sign change in $p^\uparrow \pi^-$ collisions

M. Anselmino et al., JHEP **04** (2017) 046

M. G. Echevarria et al. PRD **89** (2014)074013

P. Sun, F. Yuan, PRD **88** (2013) 114012

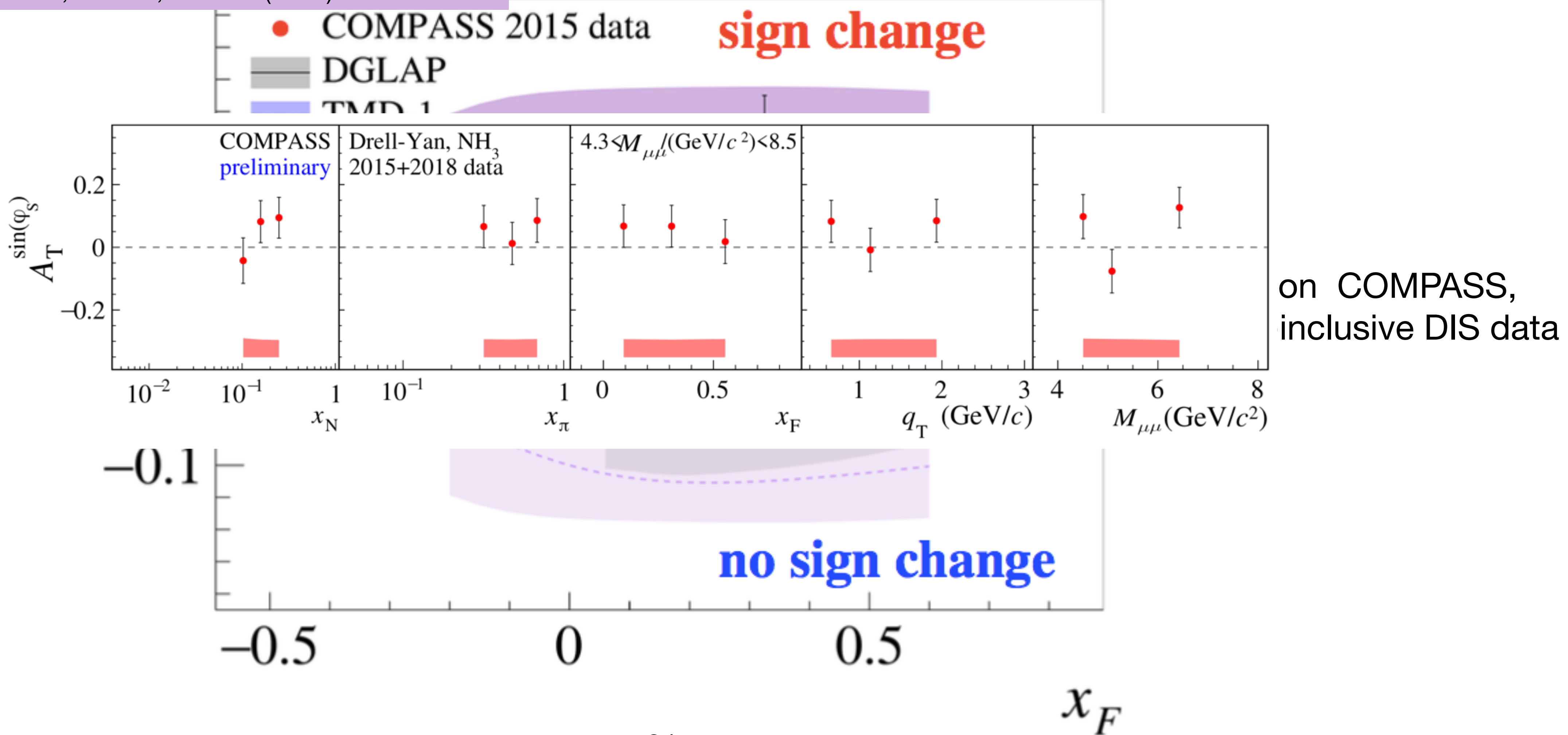
COMPASS, PRL **119** (2017) 112002



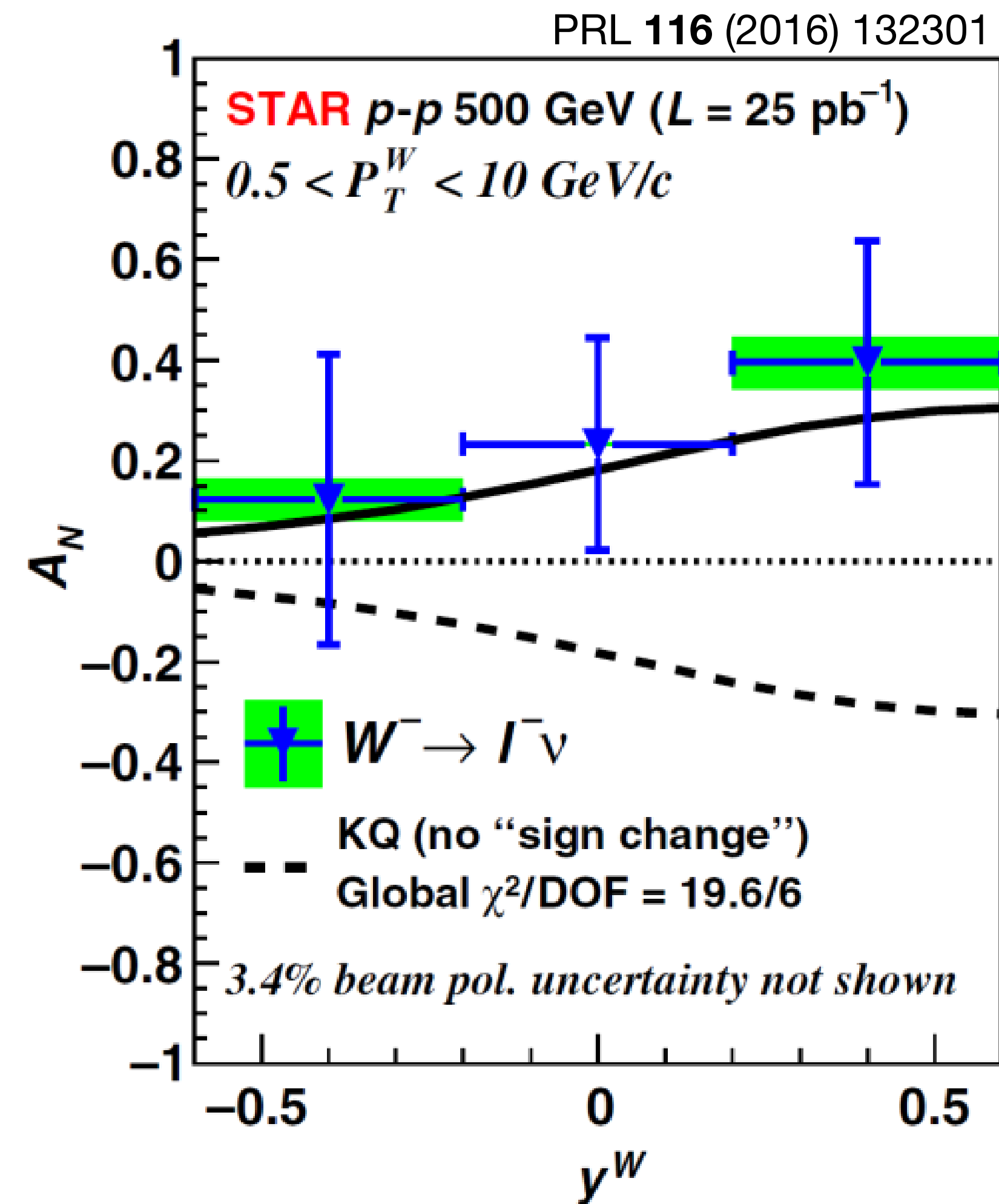
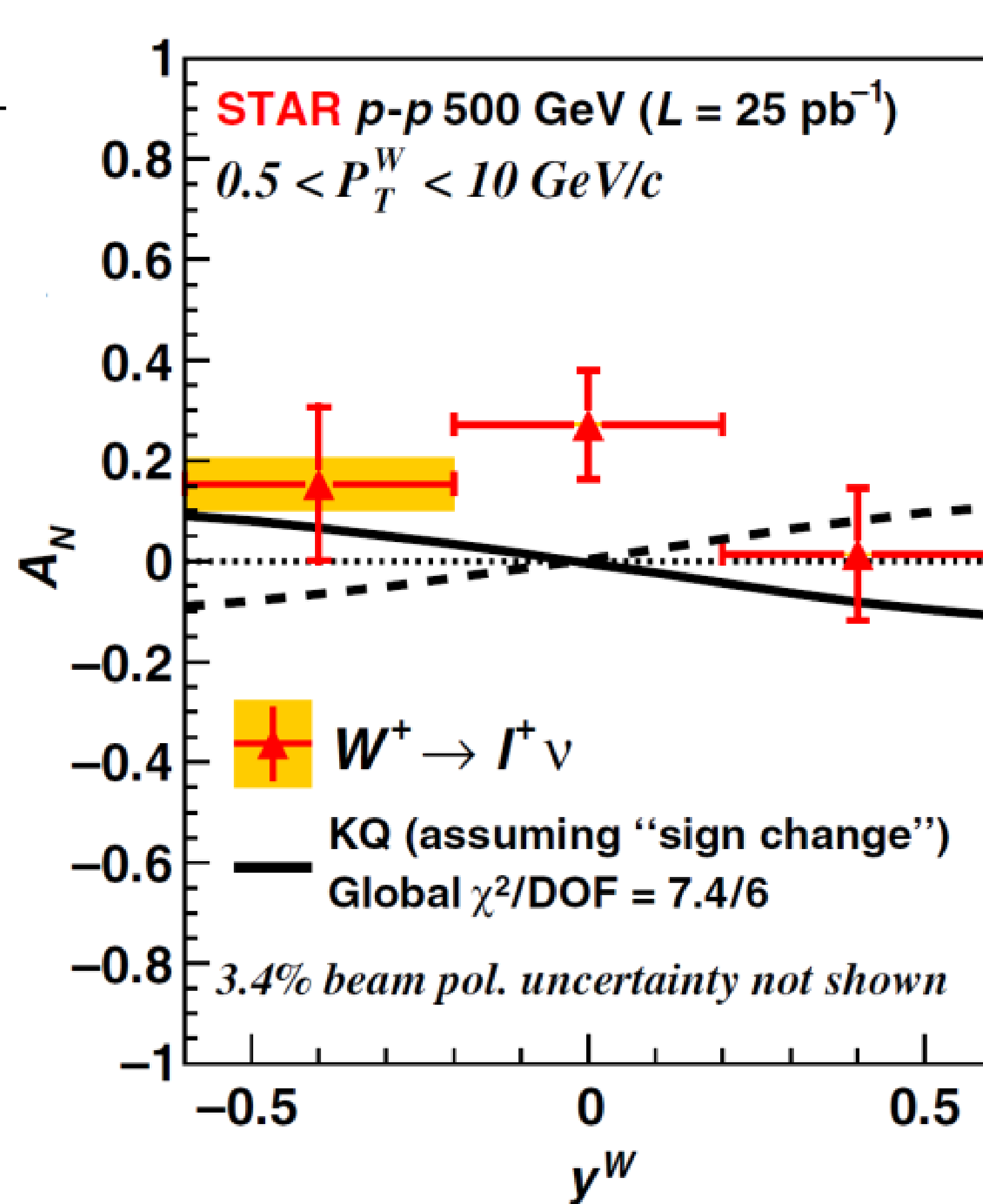
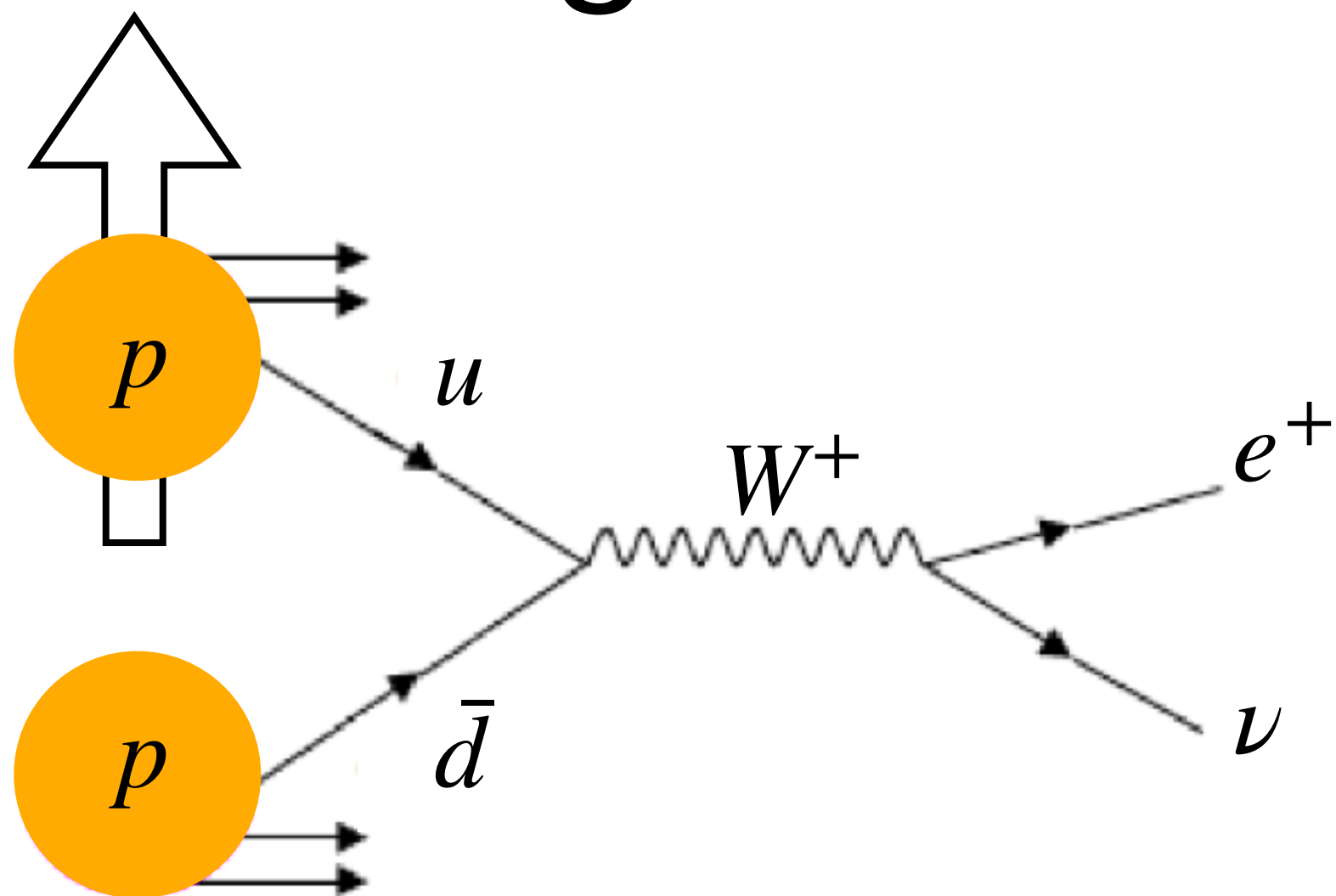
Investigation of the Sivers sign change in $p^\uparrow \pi^-$ collisions

M. Anselmino et al., JHEP **04** (2017) 046
 M. G. Echevarria et al. PRD **89** (2014)074013
 P. Sun, F. Yuan, PRD **88** (2013) 114012

COMPASS, PRL **119** (2017) 112002

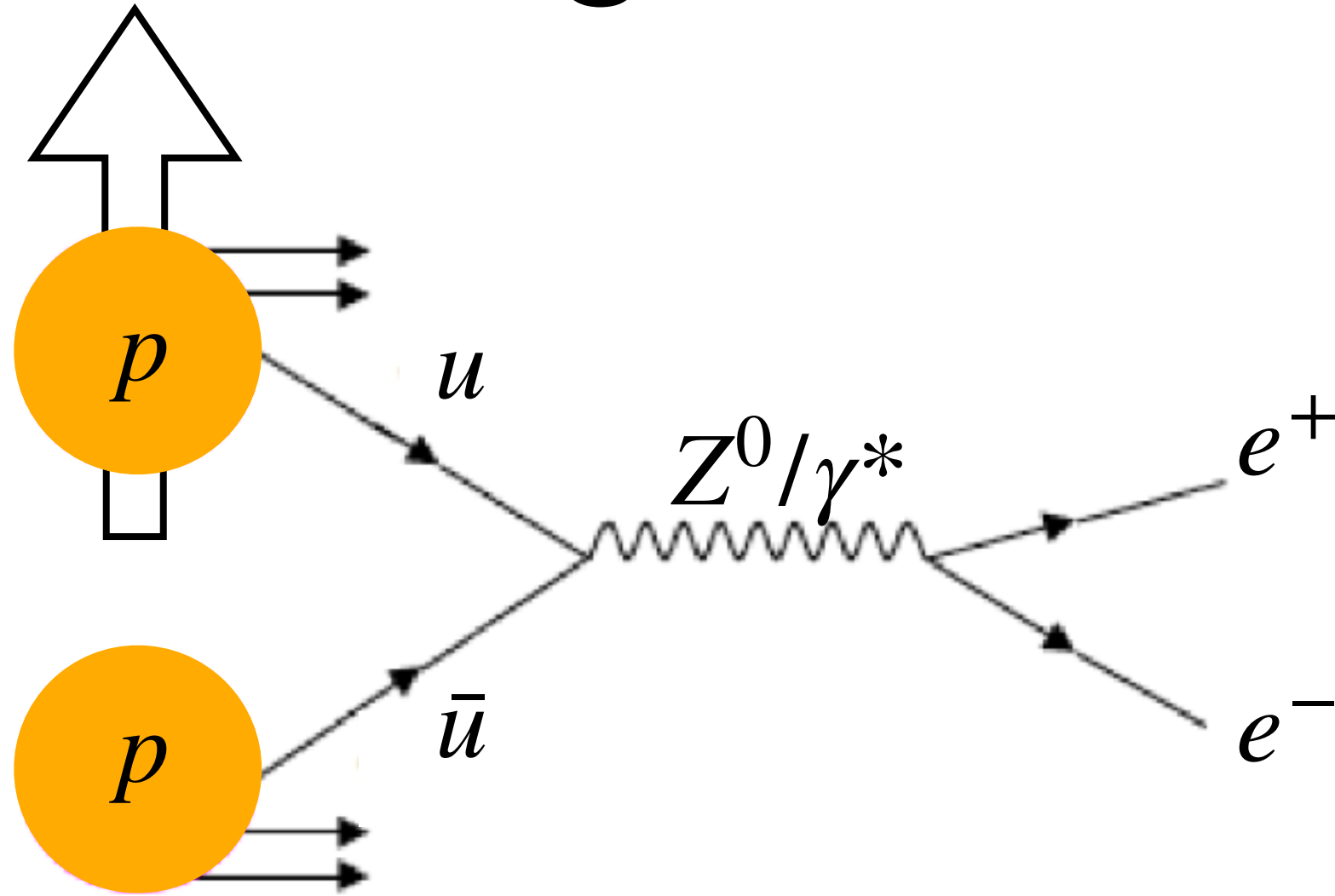


Investigation of the Sivers sign change in $p^\uparrow p$ collisions

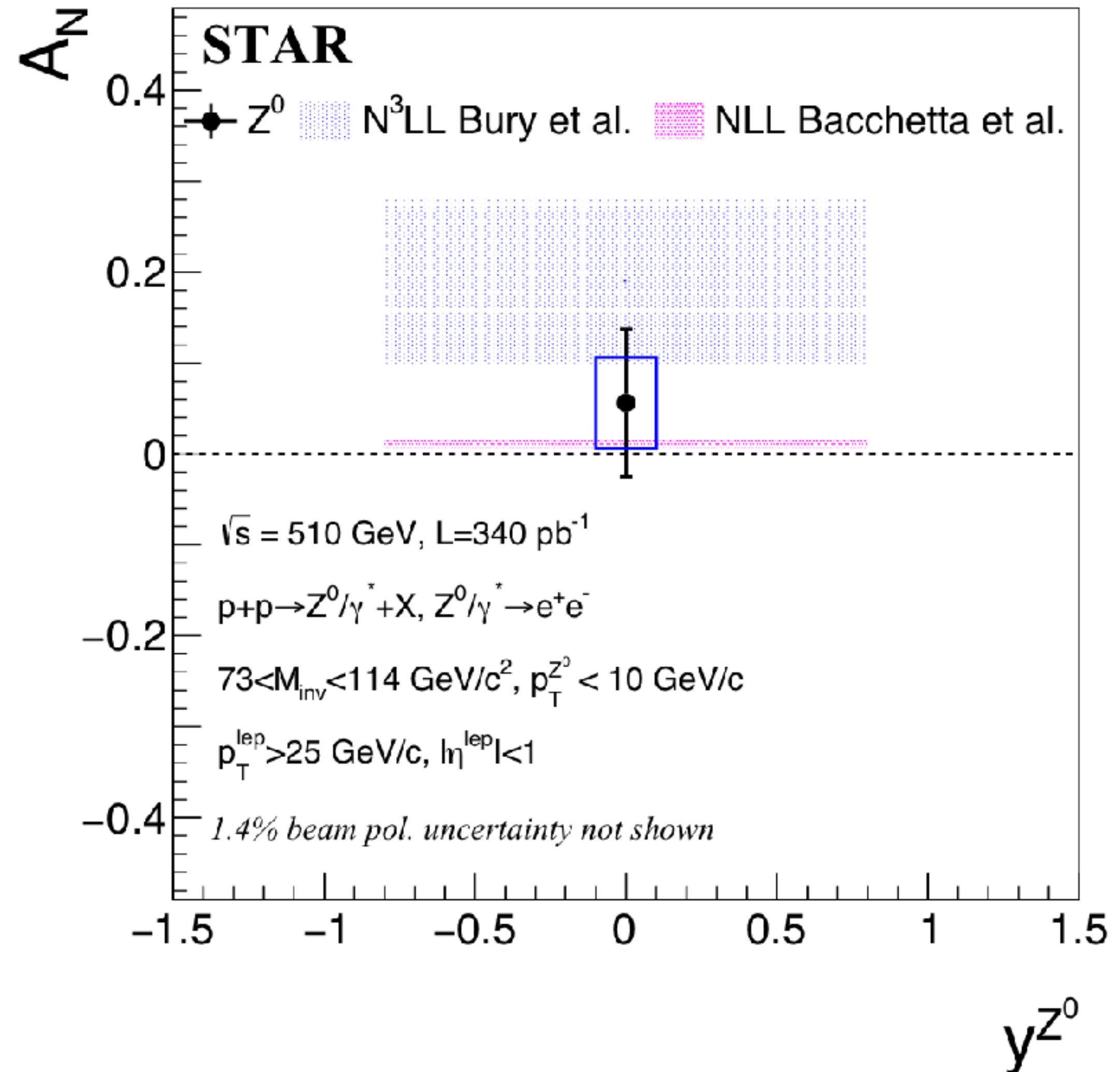


$$x_{1,2} = \frac{Q}{\sqrt{s}} e^{\pm y}$$

Investigation of the Sivers sign change in $p^\uparrow p$ collisions

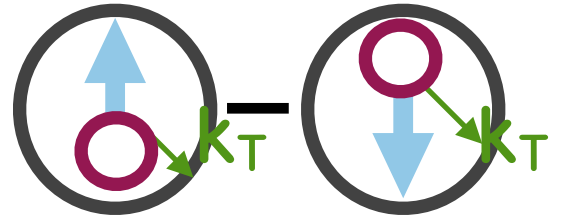


arXiv:2308.15496v1



Boer-Mulders asymmetries

Spin-dependence with unpolarised hadrons!


$$\mathcal{C} \left[h_1^{\perp,q} \times H_1^{\perp,q} \right]$$

Boer-Mulders asymmetries

Spin-dependence with unpolarised hadrons!

Measurement in ep: $\langle \cos(2\phi_h) \rangle_{Born}(j)$ $\langle \cos(2\phi_h) \rangle_{meas}(i)$



The diagram shows two circles representing hadrons. The left circle contains a blue arrow pointing up and a pink arrow pointing right, with a green arrow labeled k_T pointing right. The right circle contains a blue arrow pointing down and a pink arrow pointing right, with a green arrow labeled k_T pointing right. A minus sign is between the two circles. Below the diagram is the equation $\mathcal{C} [h_1^{\perp,q} \times H_1^{\perp,q}]$.

$$\mathcal{C} [h_1^{\perp,q} \times H_1^{\perp,q}]$$

Boer-Mulders asymmetries

Spin-dependence with unpolarised hadrons!

Measurement in ep: $\langle \cos(2\phi_h) \rangle_{Born}(j)$ $\langle \cos(2\phi_h) \rangle_{meas}(i)$

- QED radiate effects

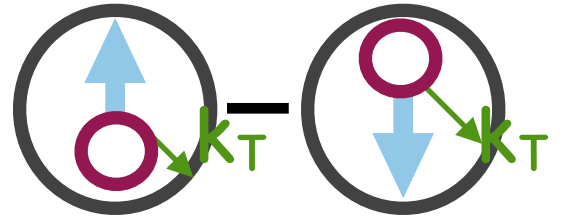


The diagram shows two circular nodes. The left node contains a blue upward arrow and a pink circle, with a green arrow labeled k_T pointing to the right. The right node contains a blue downward arrow and a pink circle, with a green arrow labeled k_T pointing to the right. A minus sign is between the two nodes.

$$\mathcal{C} \left[h_1^{\perp,q} \times H_1^{\perp,q} \right]$$

Boer-Mulders asymmetries

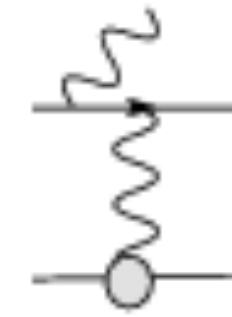
Spin-dependence with unpolarised hadrons!


$$\mathcal{C} \left[h_1^{\perp,q} \times H_1^{\perp,q} \right]$$

Measurement in ep: $\langle \cos(2\phi_h) \rangle_{Born}(j)$ $\langle \cos(2\phi_h) \rangle_{meas}(i)$



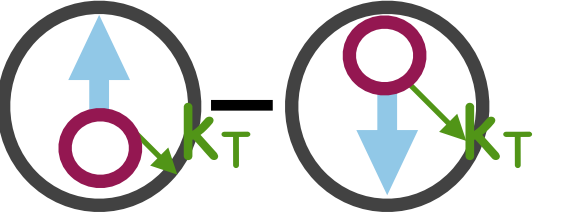
- QED radiate effects



- limited geometric and kinematic acceptance of detector

Boer-Mulders asymmetries

Spin-dependence with unpolarised hadrons!


$$\mathcal{C} \left[h_1^{\perp,q} \times H_1^{\perp,q} \right]$$

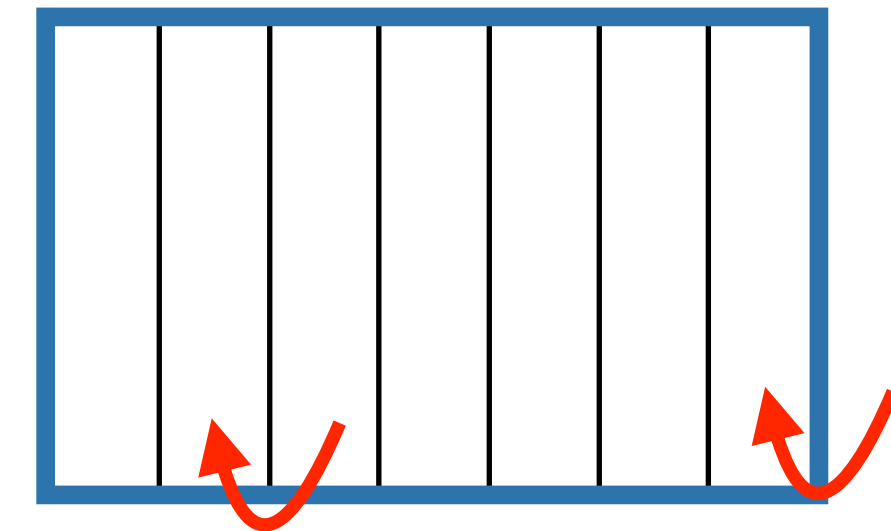
Measurement in ep: $\langle \cos(2\phi_h) \rangle_{Born}(j)$ $\langle \cos(2\phi_h) \rangle_{meas}(i)$



- QED radiate effects

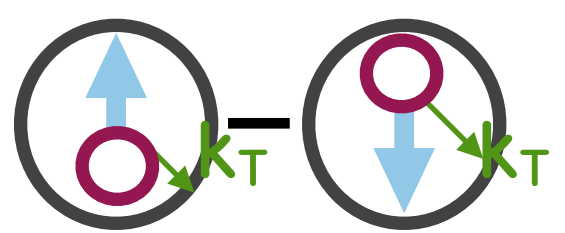


- limited geometric and kinematic acceptance of detector
- limited detector resolution



Boer-Mulders asymmetries

Spin-dependence with unpolarised hadrons!

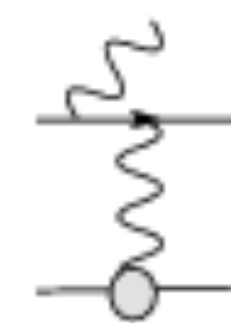


$$\mathcal{C} \left[h_1^{\perp,q} \times H_1^{\perp,q} \right]$$

Measurement in ep: $\langle \cos(2\phi_h) \rangle_{Born}(j)$ $\langle \cos(2\phi_h) \rangle_{meas}(i)$

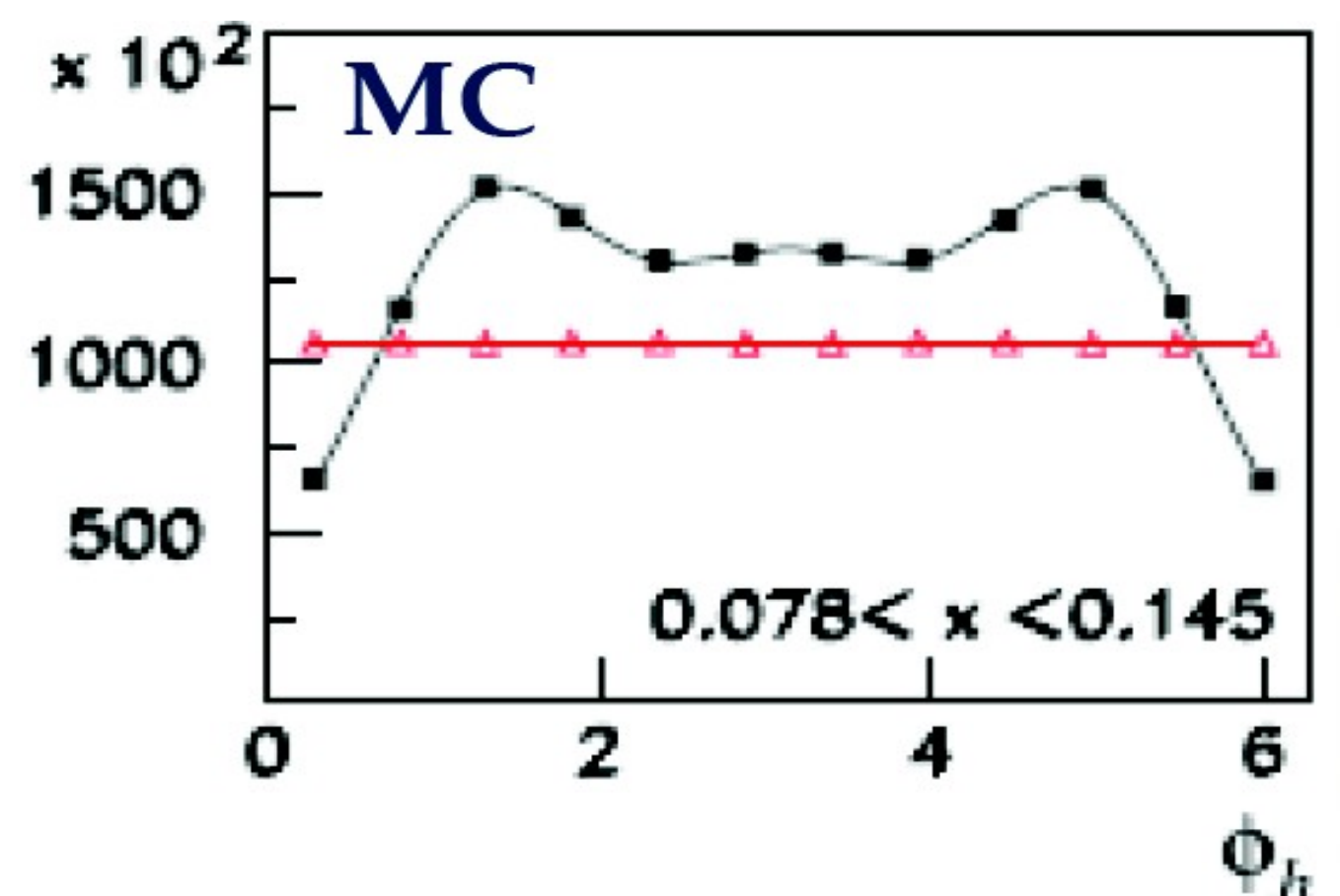
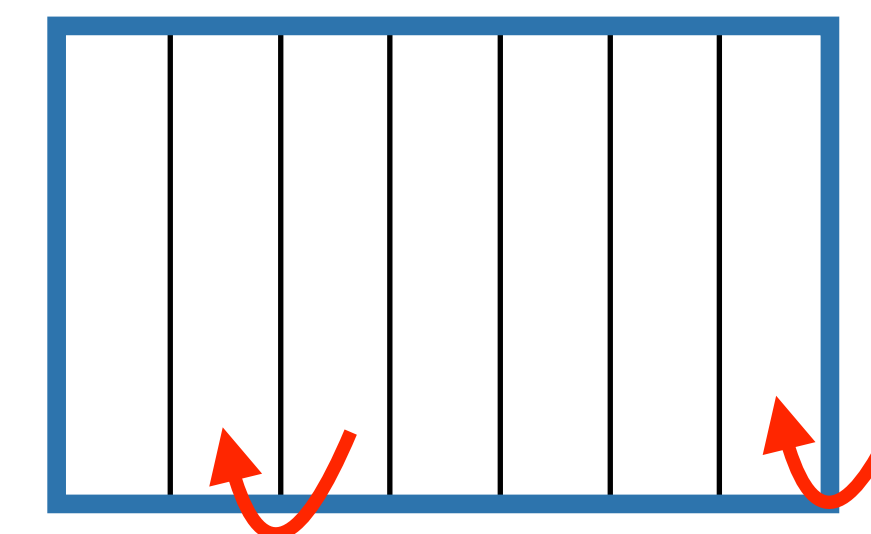




- QED radiate effects



- limited geometric and kinematic acceptance of detector

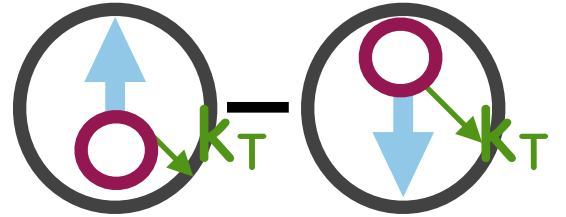
- limited detector resolution



 generated in 4π
 inside acceptance

Boer-Mulders asymmetries

Spin-dependence with unpolarised hadrons!



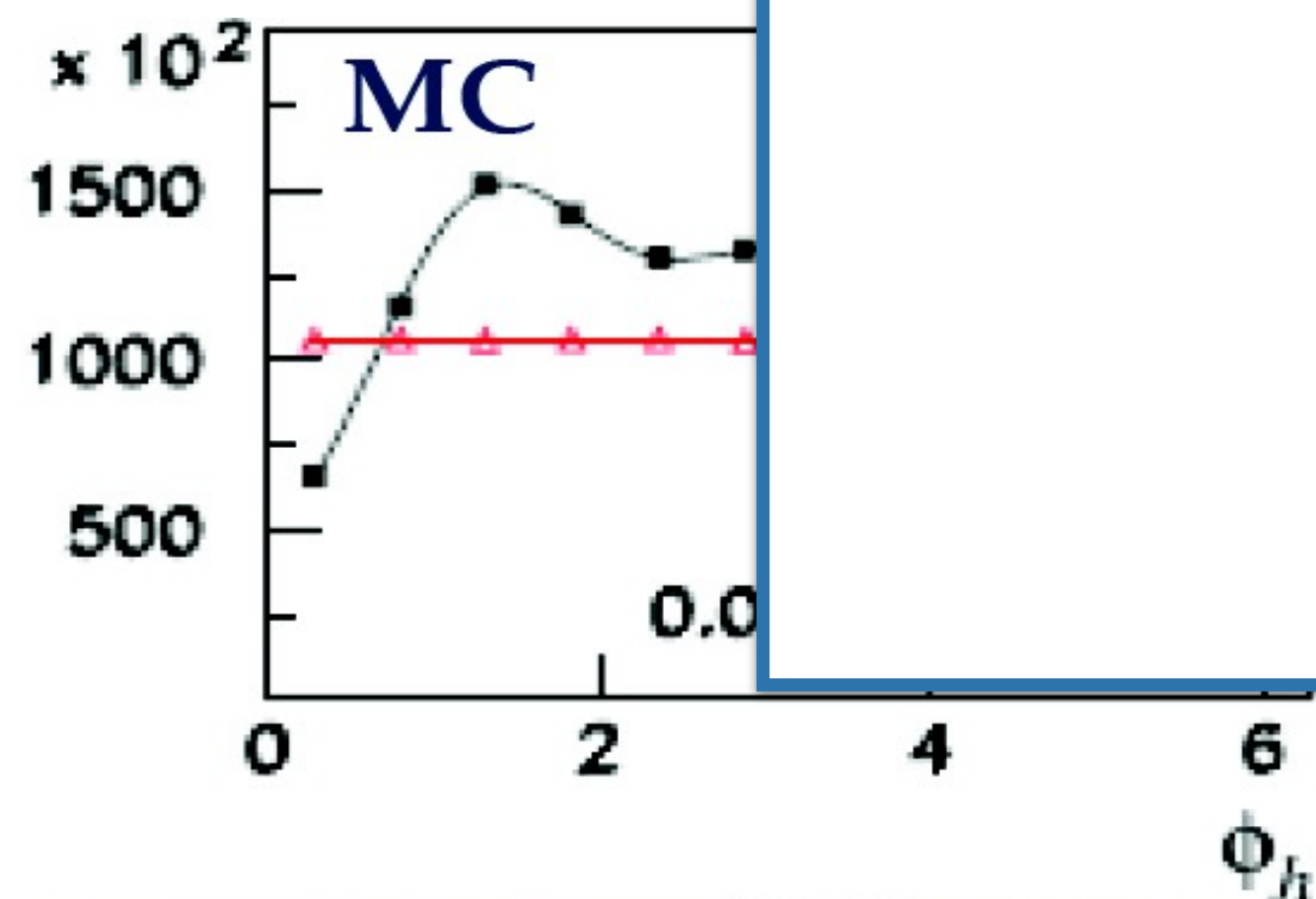
$$\mathcal{C} \left[h_1^{\perp,q} \times H_1^{\perp,q} \right]$$

Measurement in ep:

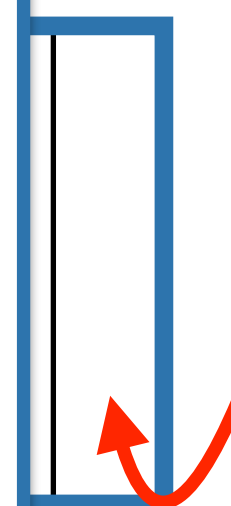
4D

Fully differential analysis
Unfolding in 400 x 12 bins

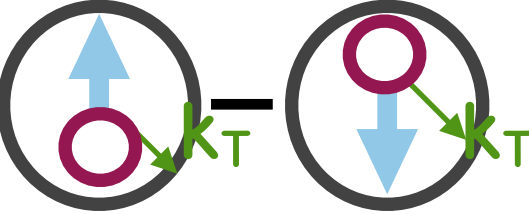
BINNING							
400 kinematic bins x 12 ϕ -bins							
Variable	Bin limits						#
x	0.023	0.042	0.078	0.145	0.27	1	5
y	0.3	0.45	0.6	0.7	0.85		4
z	0.2	0.3	0.45	0.6	0.75	1	5
P_{hT}	0.05	0.2	0.35	0.5	0.75		4



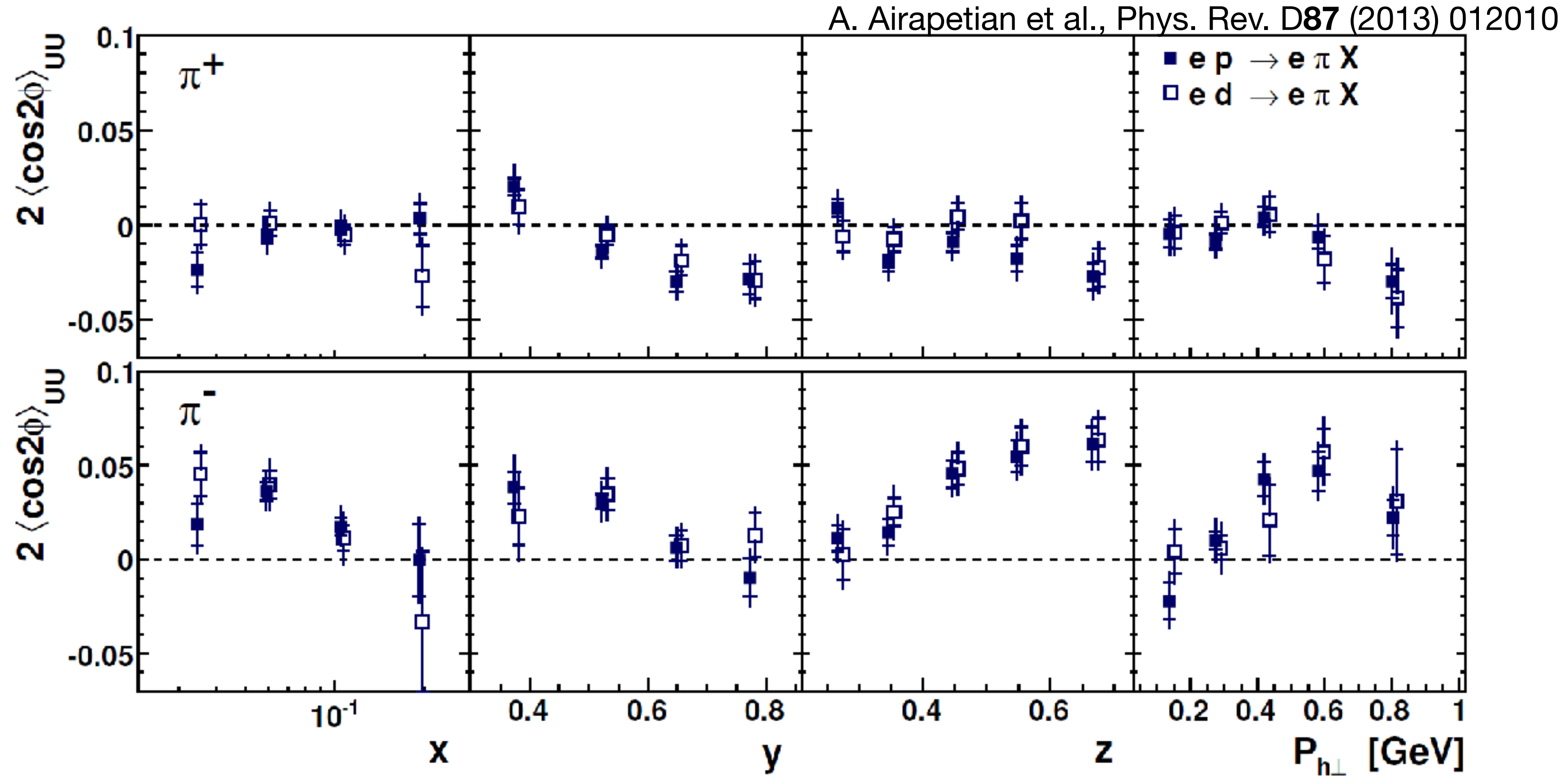
tector



Boer-Mulders asymmetries



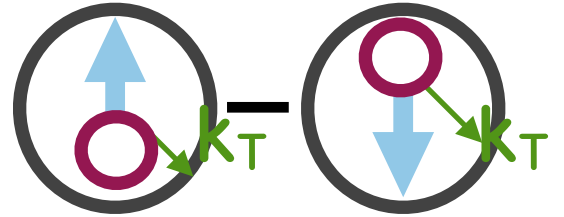
$$\mathcal{C} \left[h_1^{\perp,q} \times H_1^{\perp,q} \right]$$



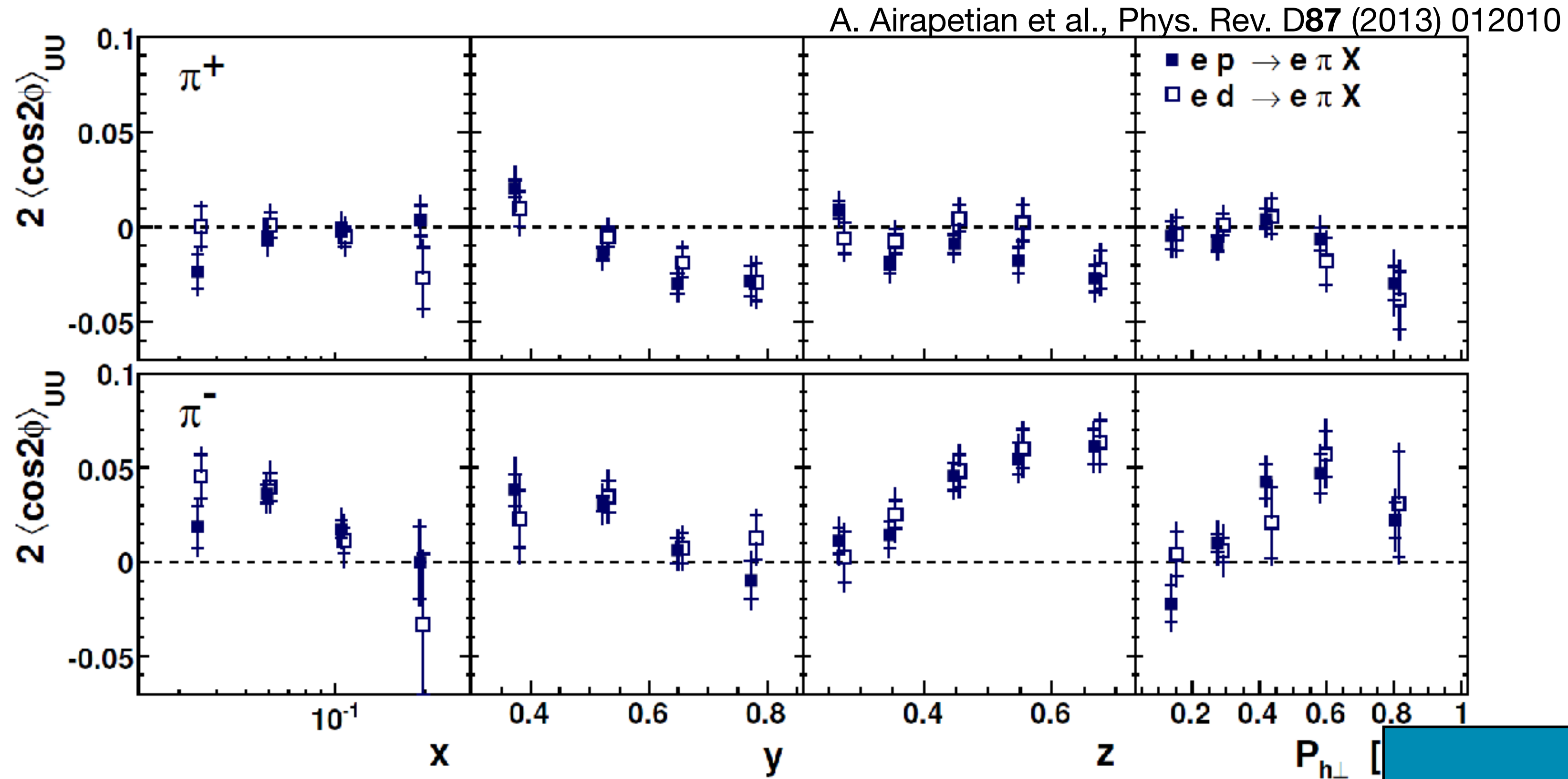
H-D comparison: $h_1^{\perp,u} \approx h_1^{\perp,d}$

Negative for π^+ ; positive for $\pi^- \rightarrow H_1^{\perp,fav} \approx -H_1^{\perp,disfav}$

Boer-Mulders asymmetries



$$\mathcal{C} \left[h_1^{\perp,q} \times H_1^{\perp,q} \right]$$



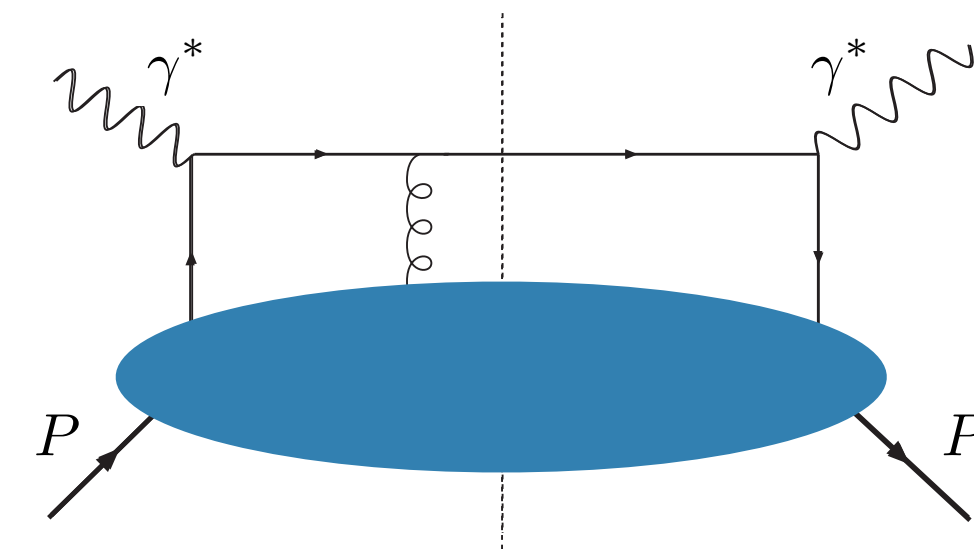
H-D comparison: $h_1^{\perp,u} \approx h_1^{\perp,d}$

Negative for π^+ ; positive for $\pi^- \rightarrow H_1^{\perp,fav} \approx -H_1^{\perp,disfav}$

Measurement also possible in Drell Yan.

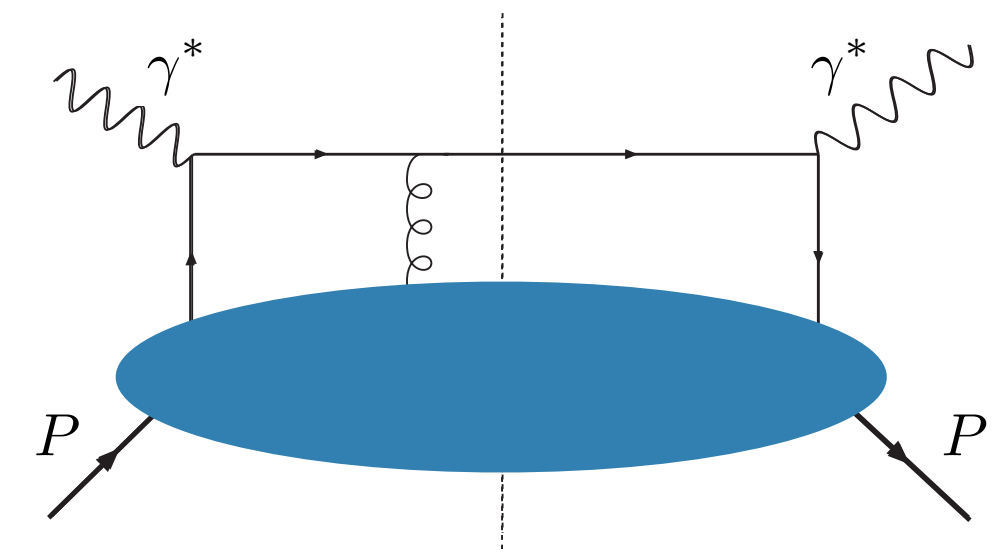
Twist-3: $\langle \sin(\phi) \rangle_{LU}^h$

$$\langle \sin(\phi) \rangle_{LU}^h \propto \mathcal{C} \left[h_1^\perp \times \tilde{E}, e \times H_1^\perp, g^\perp \times D_1, f_1 \times \tilde{G}^\perp \right]$$

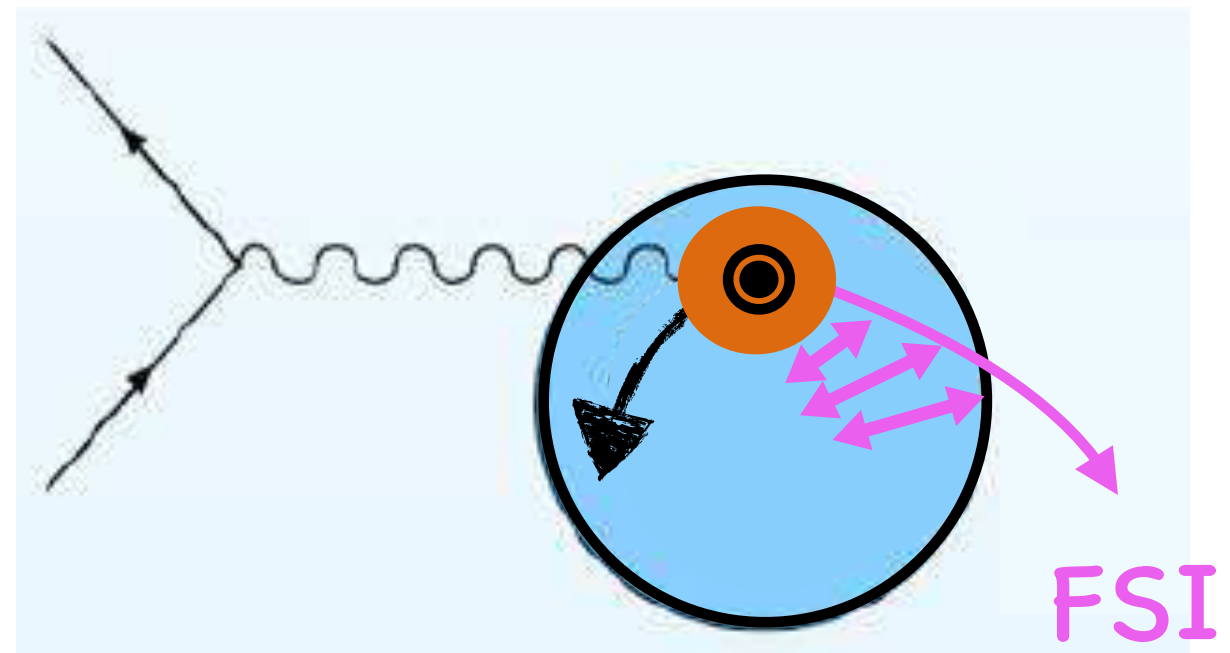


Twist-3: $\langle \sin(\phi) \rangle_{LU}^h$

$$\langle \sin(\phi) \rangle_{LU}^h \propto \mathcal{C} \left[h_1^\perp \times \tilde{E}, e \times H_1^\perp, g^\perp \times D_1, f_1 \times \tilde{G}^\perp \right]$$



Boer-Mulders PDF

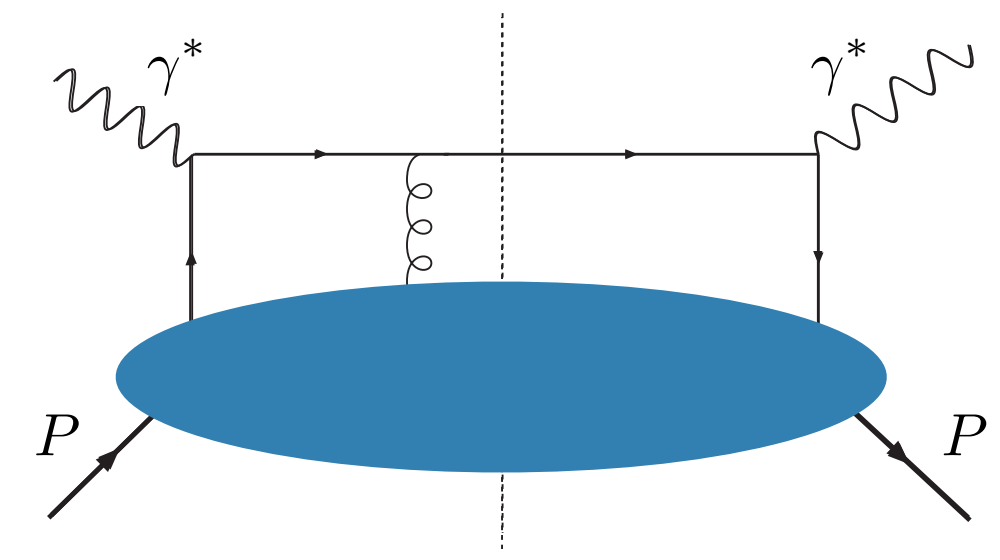


Twist-3: $\langle \sin(\phi) \rangle_{LU}^h$

$$\langle \sin(\phi) \rangle_{LU}^h \propto \mathcal{C} \left[h_1^\perp \times \tilde{E}, e \times H_1^\perp, g^\perp \times D_1, f_1 \times \tilde{G}^\perp \right]$$

Chiral-odd T-even
twist-3 PDF

Collins FF



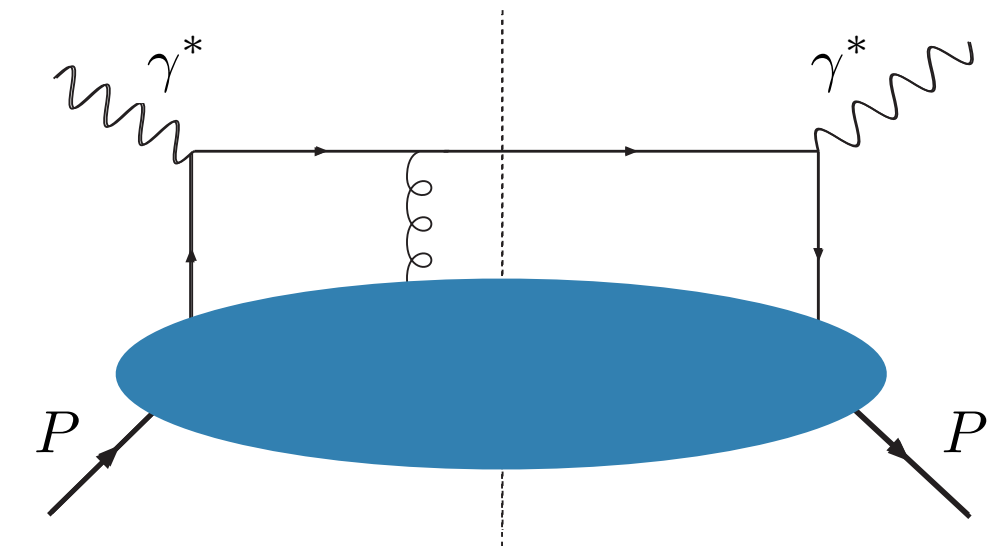
Twist-3: $\langle \sin(\phi) \rangle_{LU}^h$

$$\langle \sin(\phi) \rangle_{LU}^h \propto \mathcal{C} \left[h_1^\perp \times \tilde{E}, e \times H_1^\perp, g^\perp \times D_1, f_1 \times \tilde{G}^\perp \right]$$

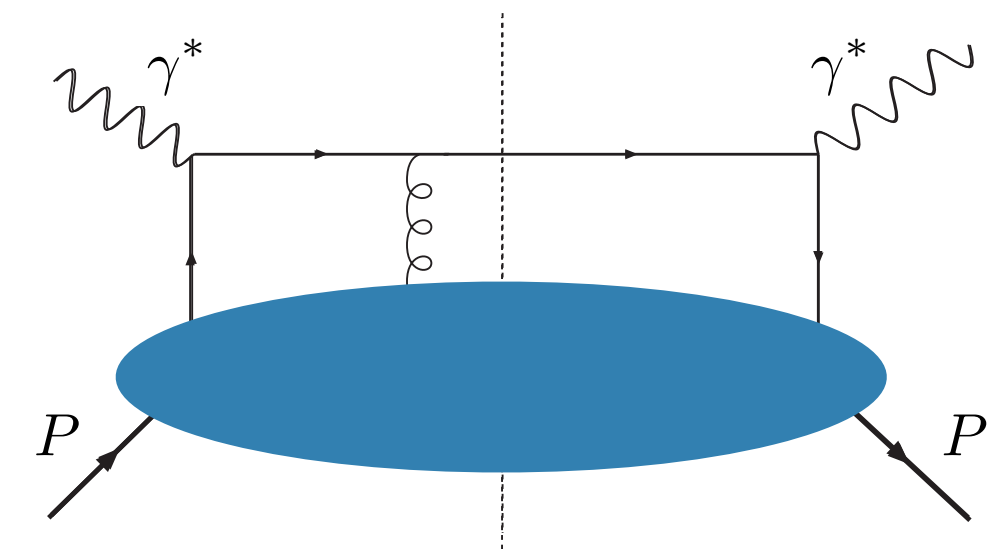
Chiral-odd T-even
twist-3 PDF

Collins FF

$$e(x) = e^{\text{WW}}(x) + \bar{e}(x)$$



Twist-3: $\langle \sin(\phi) \rangle_{LU}^h$



$$\langle \sin(\phi) \rangle_{LU}^h \propto \mathcal{C} \left[h_1^\perp \times \tilde{E}, e \times H_1^\perp, g^\perp \times D_1, f_1 \times \tilde{G}^\perp \right]$$

Chiral-odd T-even
twist-3 PDF

Collins FF

$$e(x) = e^{WW}(x) + \bar{e}(x)$$

$$e_2 \equiv \int_0^1 dx x^2 \bar{e}(x)$$

force on struck quark at t=0
M. Burkardt, arXiv:0810.3589

Boer-Mulders PDF

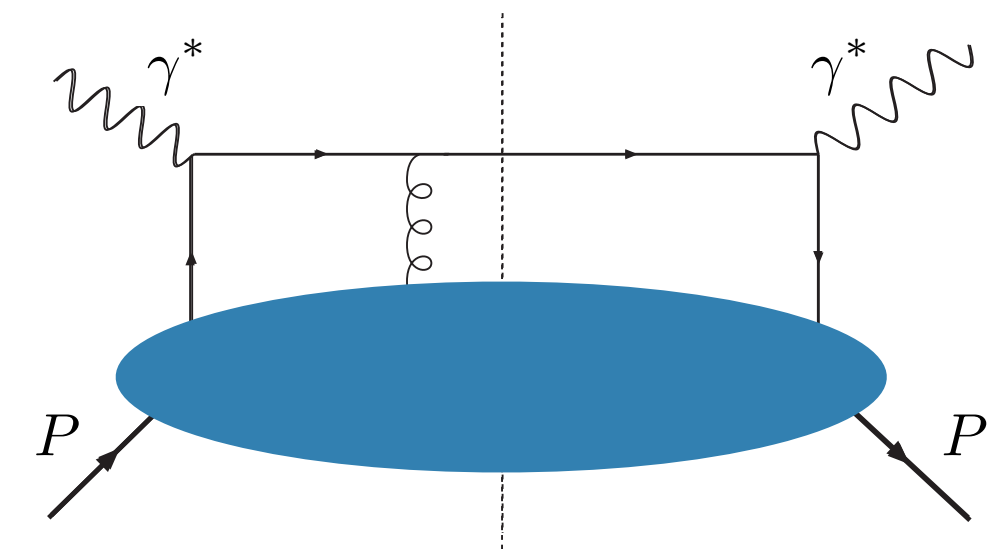
FSI: $t=0 \rightarrow \infty$

Twist-3: $\langle \sin(\phi) \rangle_{LU}^h$

$$\langle \sin(\phi) \rangle_{LU}^h \propto \mathcal{C} \left[h_1^\perp \times \tilde{E}, e \times H_1^\perp, g^\perp \times D_1, f_1 \times \tilde{G}^\perp \right]$$

Chiral-even T-odd
twist-3 PDF

spin-independent
FF



Twist-3: $\langle \sin(\phi) \rangle_{LU}^h$

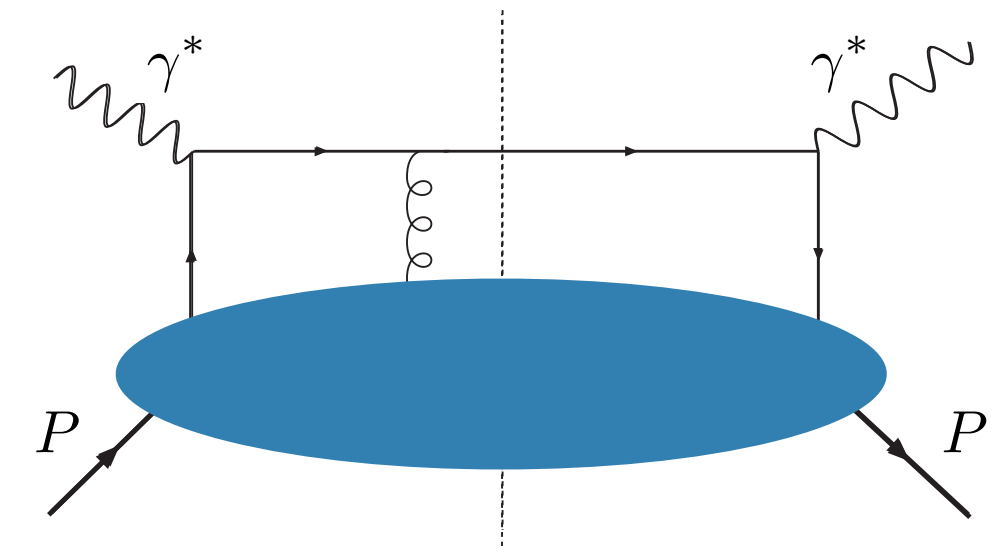
$$\langle \sin(\phi) \rangle_{LU}^h \propto \mathcal{C} \left[h_1^\perp \times \tilde{E}, e \times H_1^\perp, g^\perp \times D_1, f_1 \times \tilde{G}^\perp \right]$$

Chiral-even T-odd
twist-3 PDF

spin-independent
FF

Only term to survive in TMD single-jet inclusive DIS

$$e + p \rightarrow e' + \text{jet} + X$$

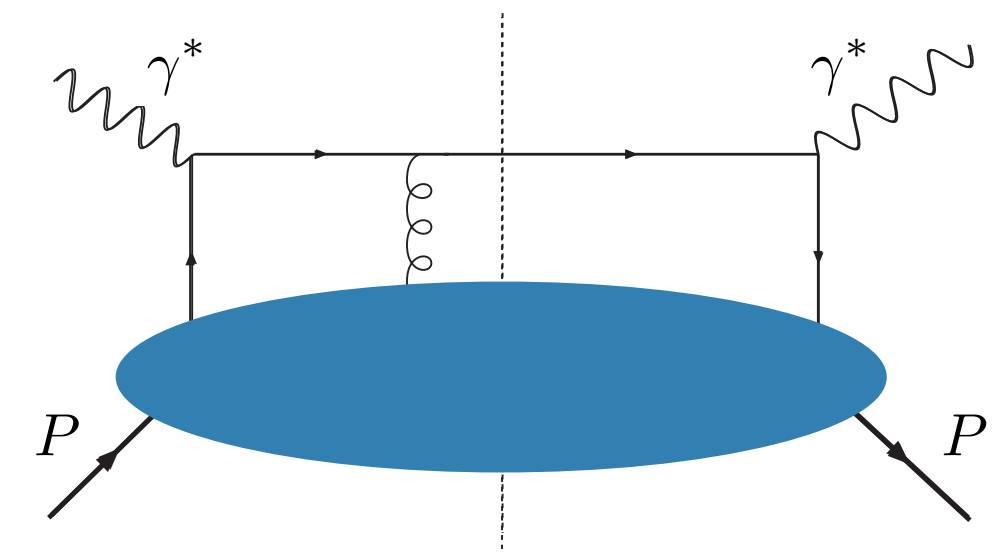


Twist-3: $\langle \sin(\phi) \rangle_{LU}^h$

$$\langle \sin(\phi) \rangle_{LU}^h \propto \mathcal{C} \left[h_1^\perp \times \tilde{E}, e \times H_1^\perp, g^\perp \times D_1, f_1 \times \tilde{G}^\perp \right]$$

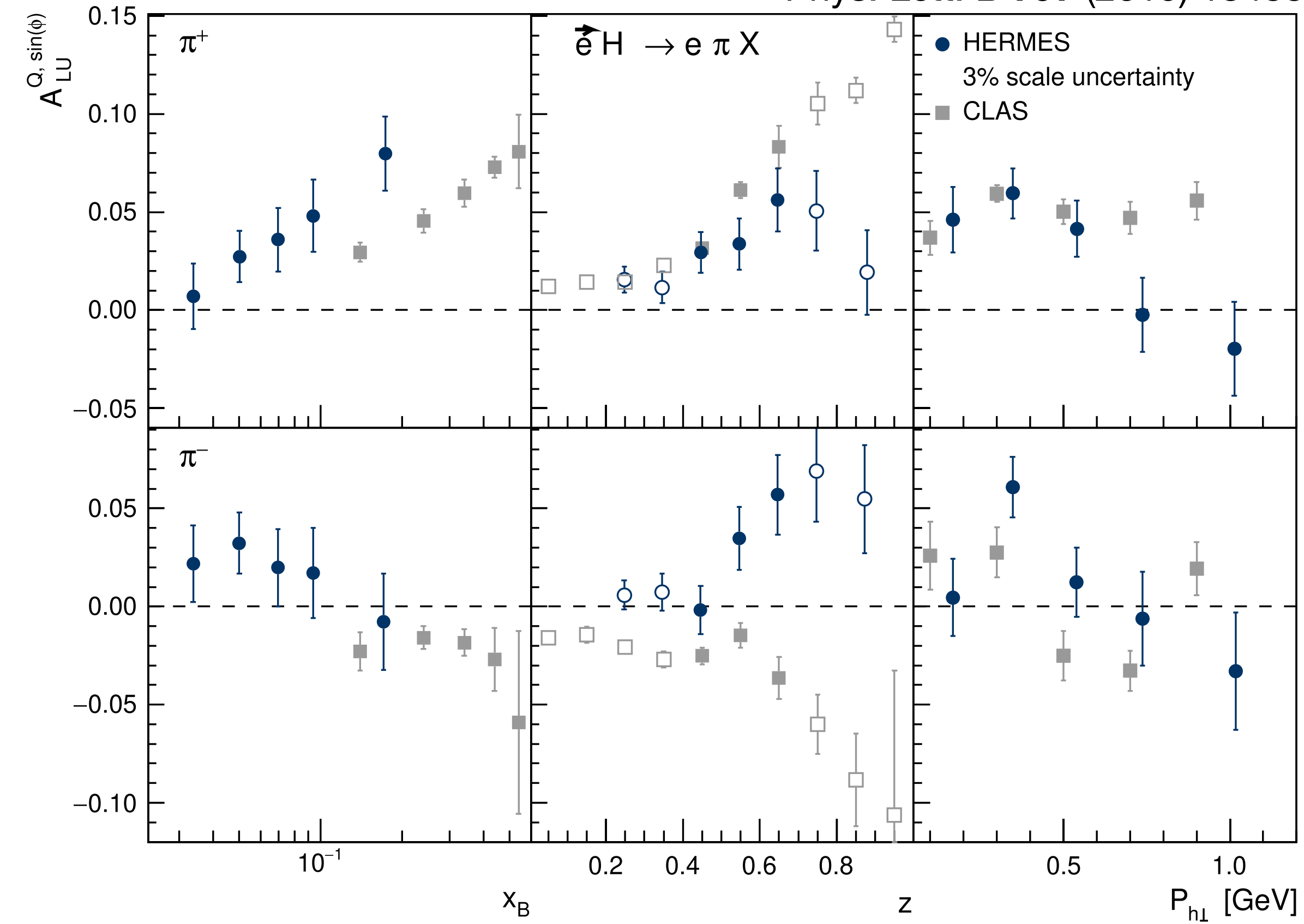
spin-independent
PDF

chiral-even, T-odd
twist-3 FF



Twist-3: $\langle \sin(\phi) \rangle_{LU}^h$

Phys. Lett. B **797** (2019) 134886



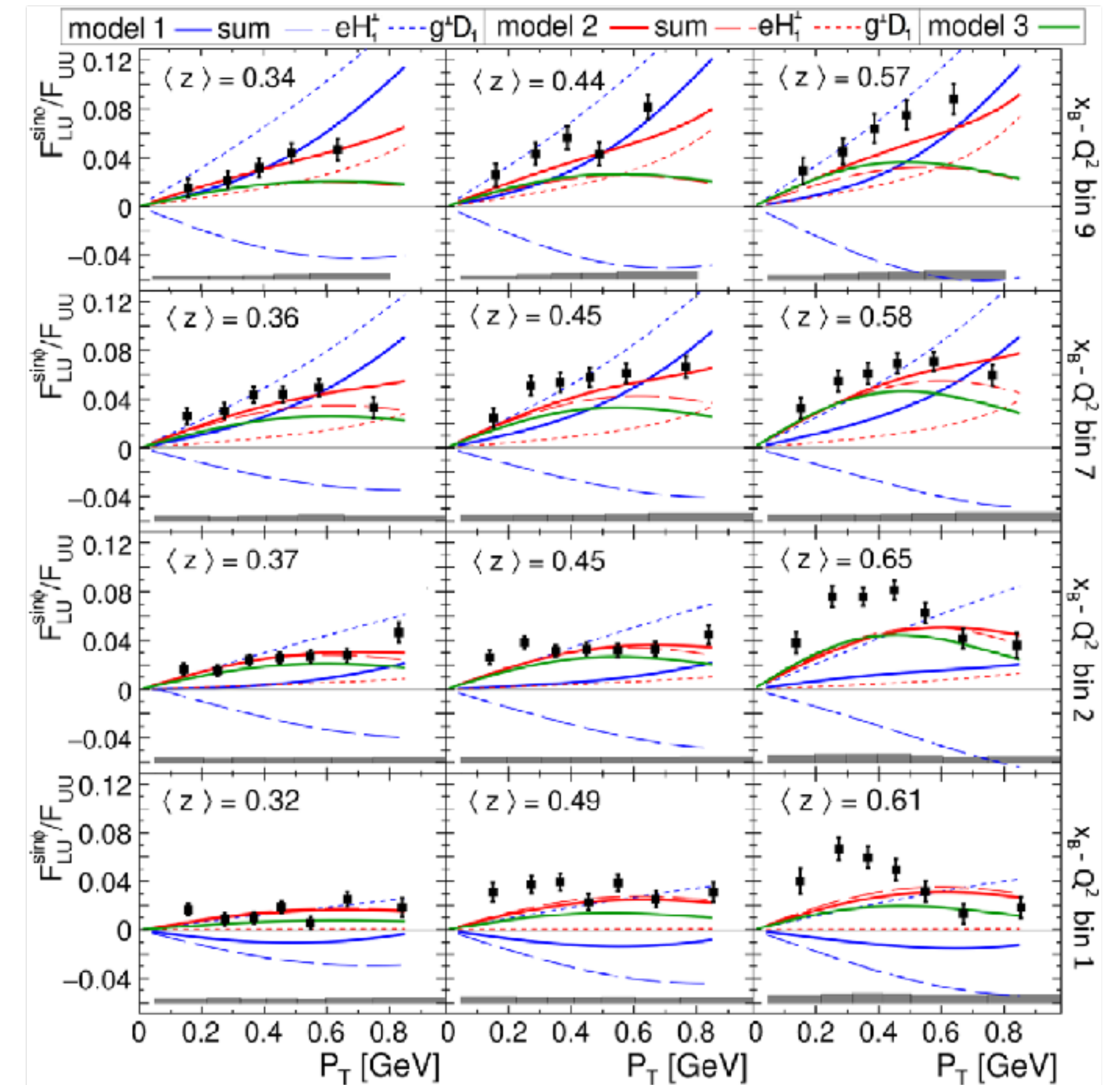
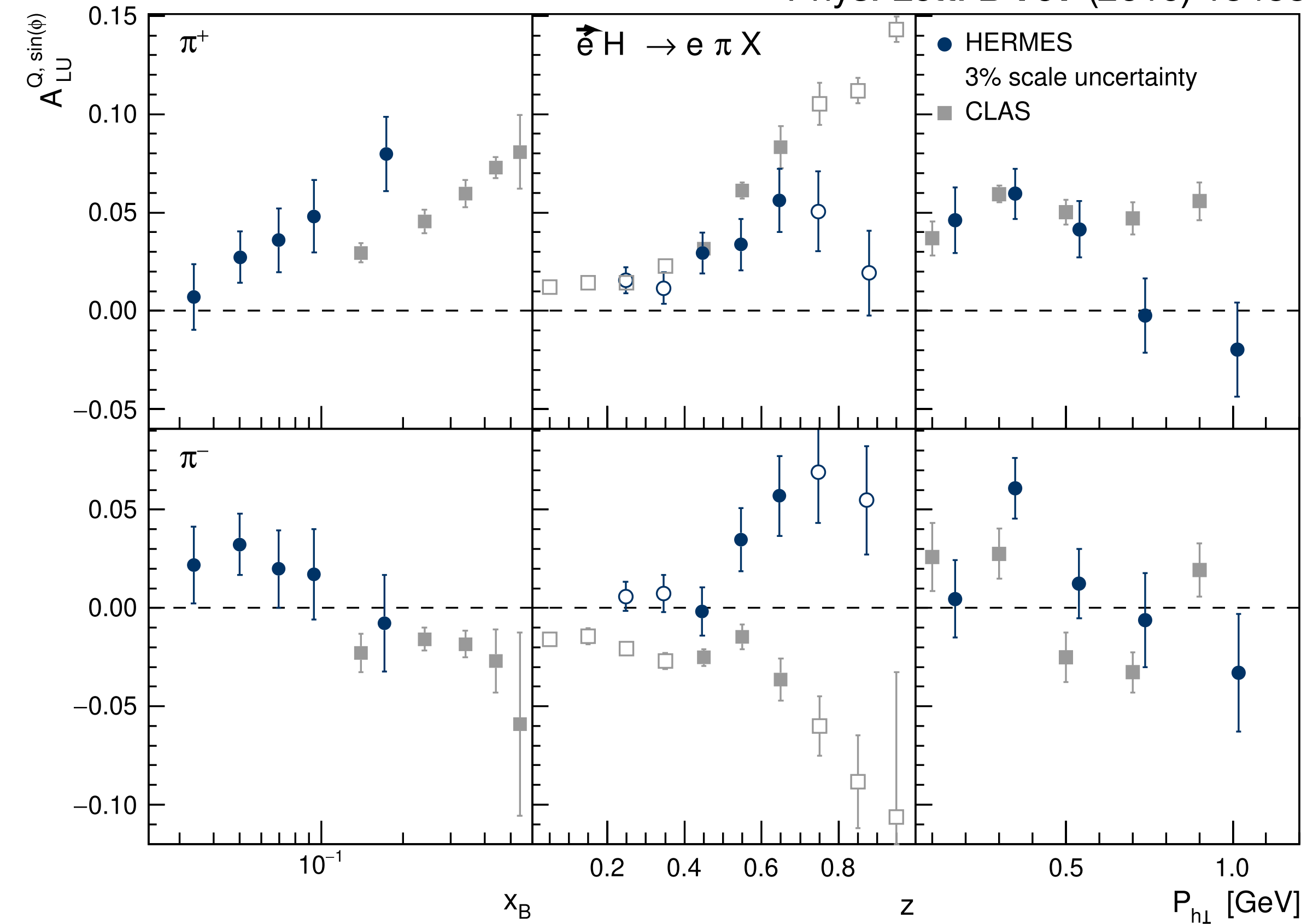
- Opposite behaviour for π^- z projection due to different x range probed
- CLAS probes higher x region: more sensitive to $e \times H_1^\perp$?

$$\langle \sin(\phi) \rangle_{LU}^h \propto \mathcal{C} \left[h_1^\perp \times \tilde{E}, x e \times H_1^\perp, x g^\perp \times D_1, f_1 \times \tilde{G}^\perp \right]$$

Twist-3: $\langle \sin(\phi) \rangle_{LU}^h$

CLAS12, Phys. Rev. Lett. **128** (2022) 062005

Phys. Lett. B **797** (2019) 134886



- Opposite behaviour for π^- z projection due to different x range probed
- CLAS probes higher x region: more sensitive to $e \times H_1^\perp$?

$$\langle \sin(\phi) \rangle_{LU}^h \propto \mathcal{C} \left[h_1^\perp \times \tilde{E}, \boxed{x e \times H_1^\perp}, x g^\perp \times D_1, f_1 \times \tilde{G}^\perp \right]$$

Gluons

GLUONS	<i>unpolarized</i>	<i>circular</i>	<i>linear</i>
U	f_1^g		$h_1^{\perp g}$
L		g_{1L}^g	$h_{1L}^{\perp g}$
T	$f_{1T}^{\perp g}$	g_{1T}^g	$h_{1T}^g, h_{1T}^{\perp g}$

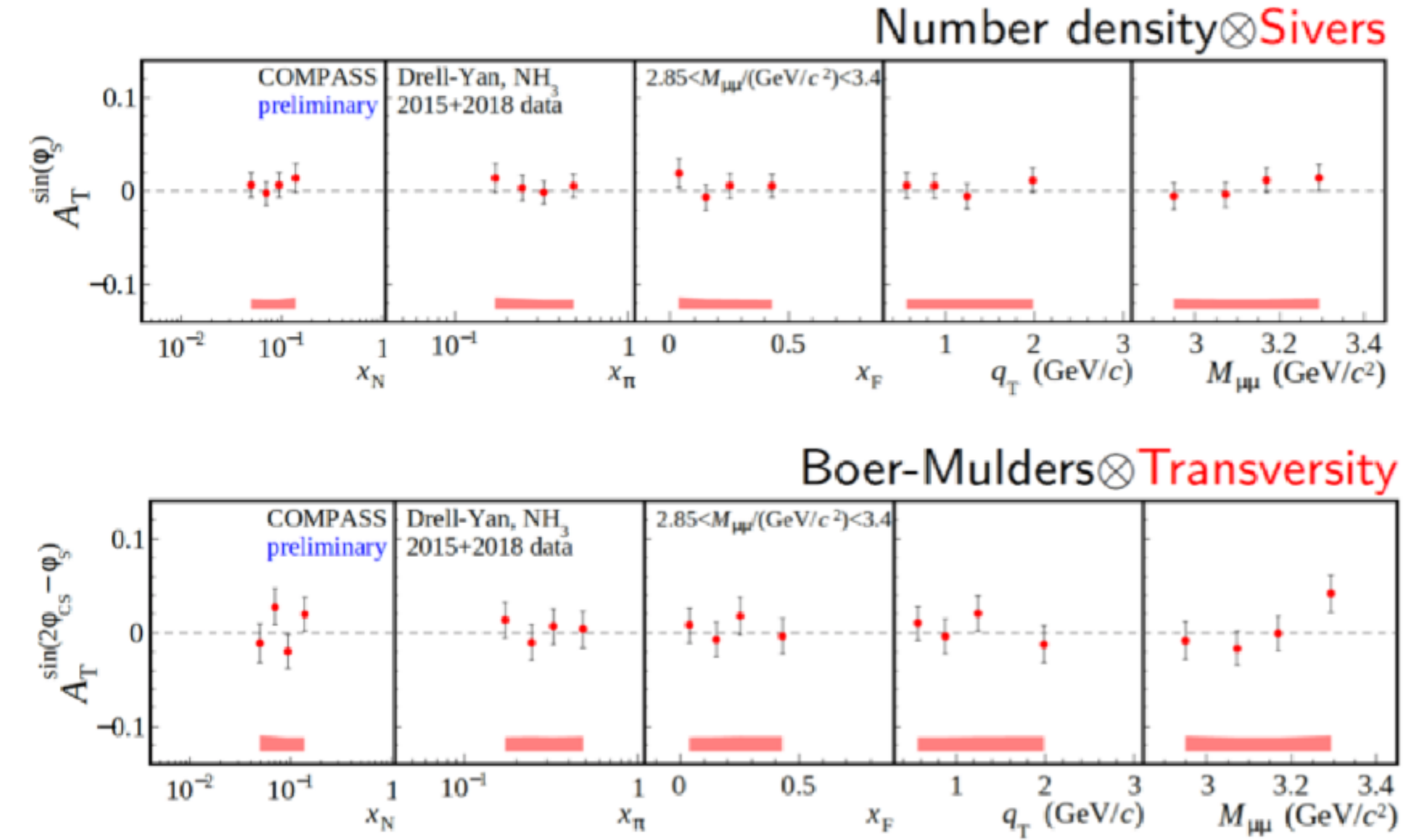
- In contrast to quark TMDs, gluon TMDs are almost unknown
- Accessible through production of dijets, high- P_T hadron pairs, quarkonia

Gluons

GLUONS	<i>unpolarized</i>	<i>circular</i>	<i>linear</i>
U	f_1^g		$h_1^{\perp g}$
L		g_{1L}^g	$h_{1L}^{\perp g}$
T	$f_{1T}^{\perp g}$	g_{1T}^g	$h_{1T}^g, h_{1T}^{\perp g}$

- In contrast to quark TMDs, gluon TMDs are almost unknown
- Accessible through production of dijets, high- P_T hadron pairs, quarkonia

Drell-Yan with lepton pair in J/ψ mass region:
 $q\bar{q}$ annihilation or gluon-gluon fusion

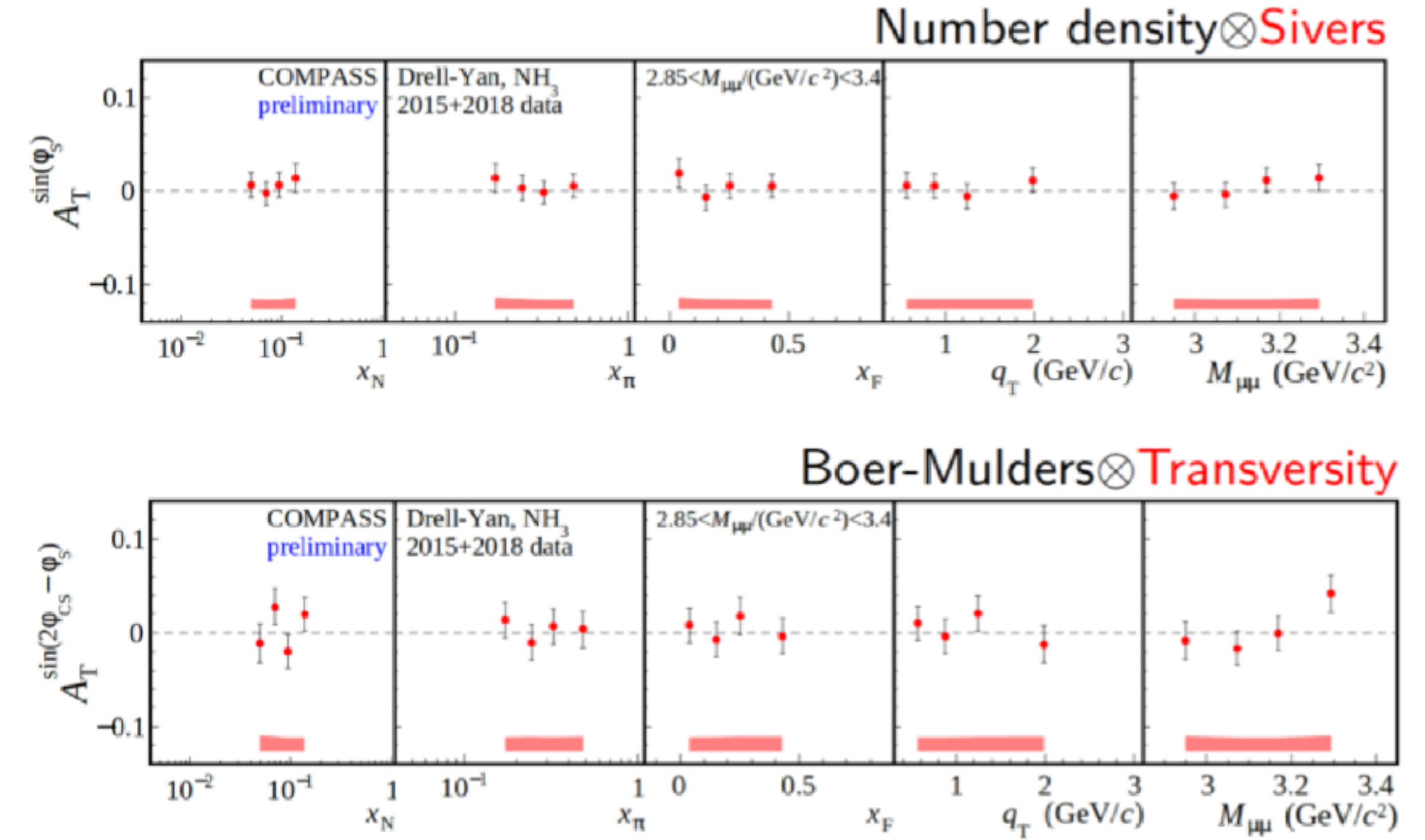


Gluons

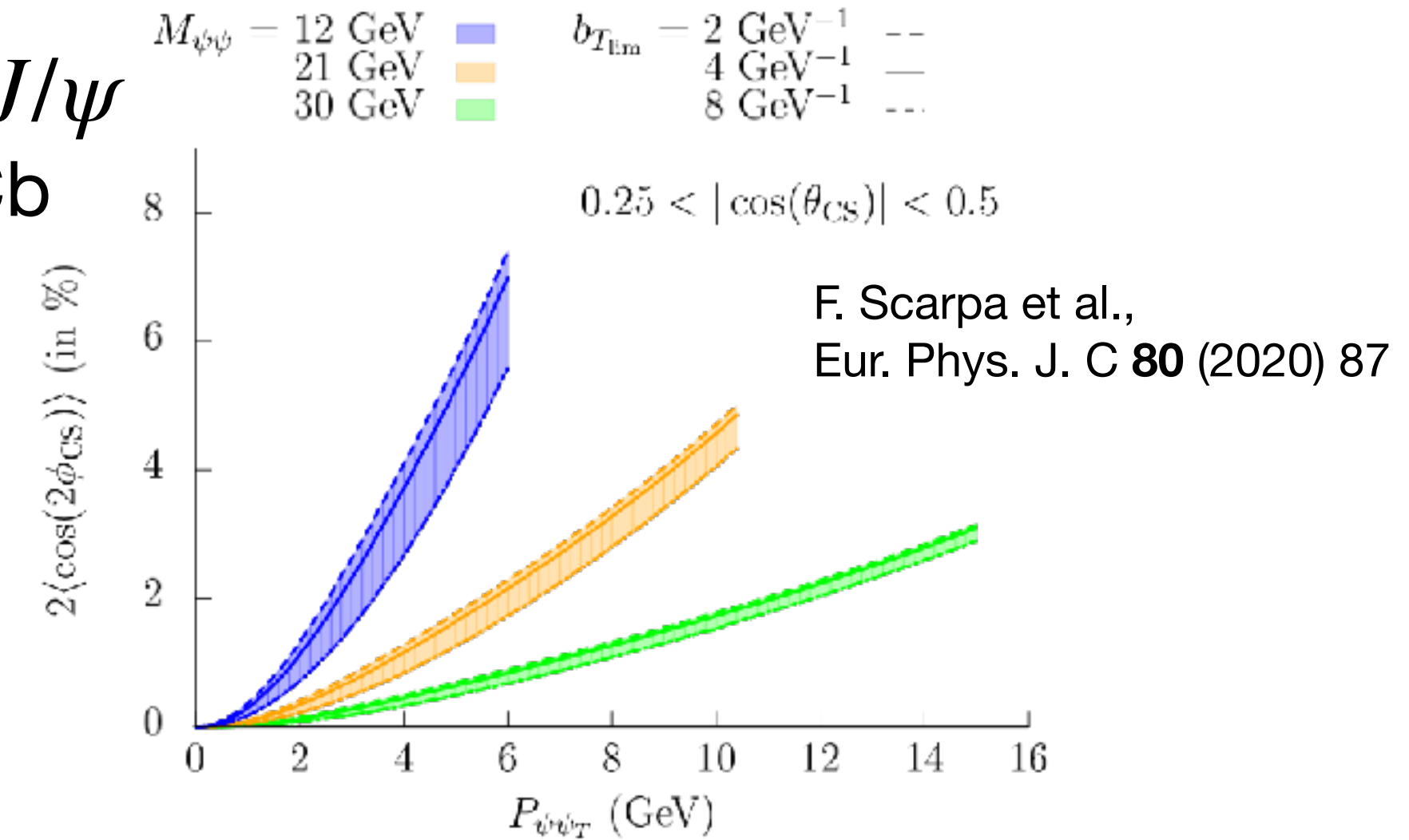
GLUONS	<i>unpolarized</i>	<i>circular</i>	<i>linear</i>
U	f_1^g		$h_1^{\perp g}$
L		g_{1L}^g	$h_{1L}^{\perp g}$
T	$f_{1T}^{\perp g}$	g_{1T}^g	$h_{1T}^g, h_{1T}^{\perp g}$

- In contrast to quark TMDs, gluon TMDs are almost unknown
- Accessible through production of dijets, high- P_T hadron pairs, quarkonia

Drell-Yan with lepton pair in J/ψ mass region:
 $q\bar{q}$ annihilation or gluon-gluon fusion



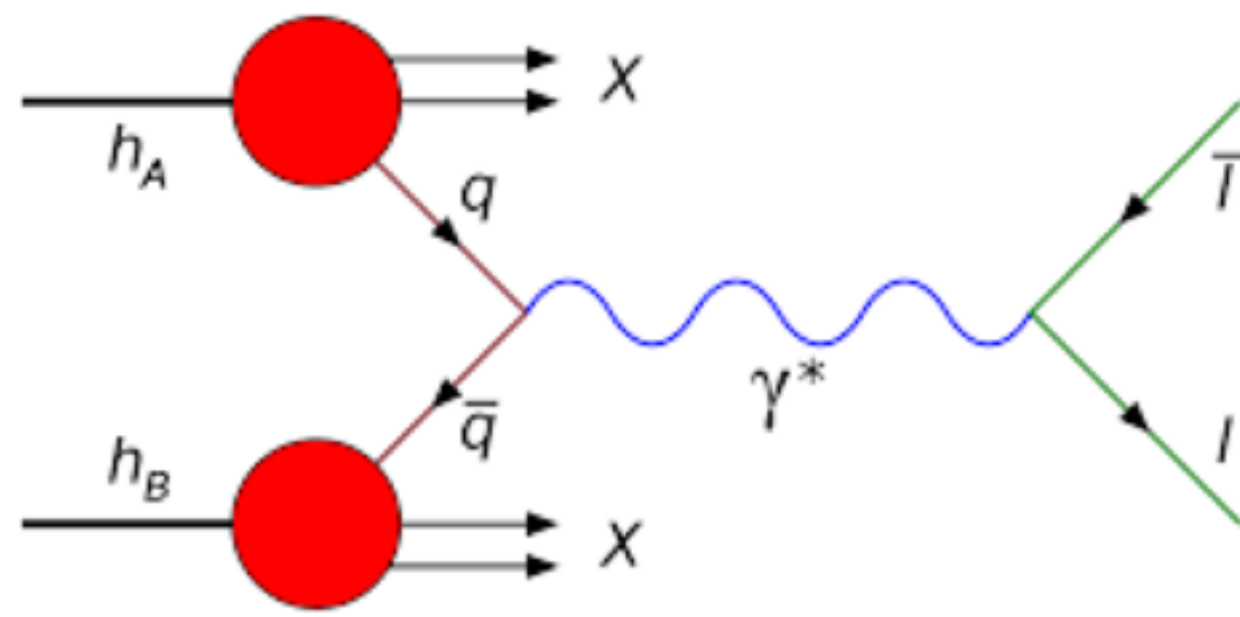
Predictions for di- J/ψ production at LHCb



Upcoming

A000BER

Apparatus for Meson and Baryon
Experimental Research

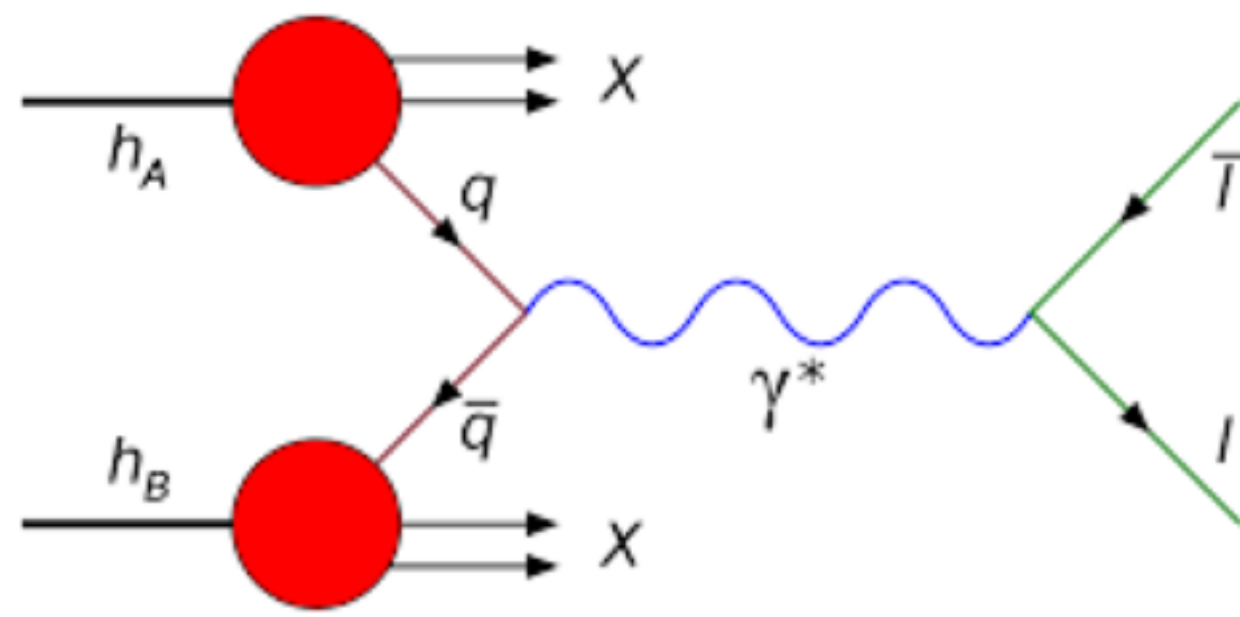


Meson structure

Upcoming

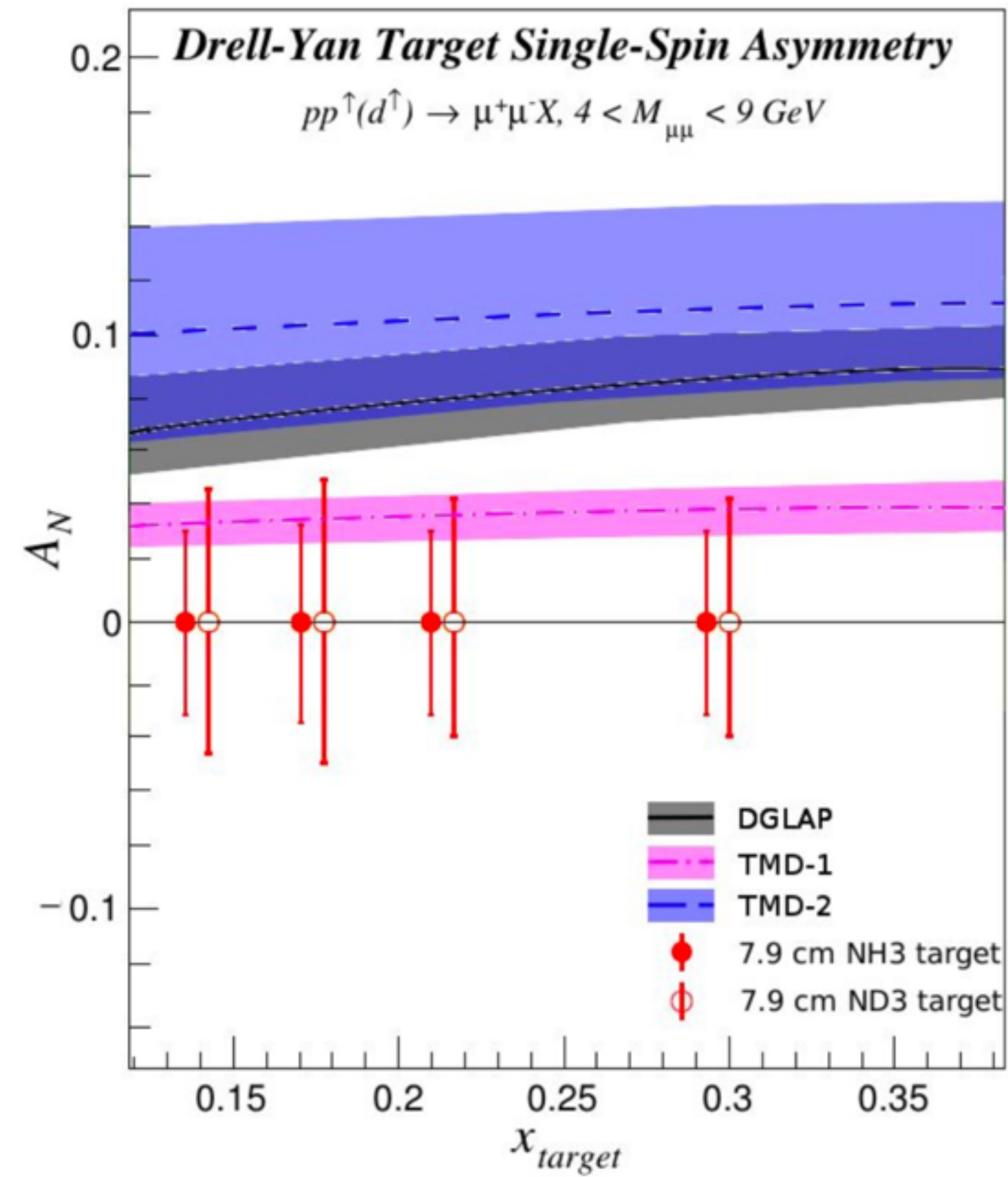
A000BER

Apparatus for Meson and Baryon
Experimental Research



Meson structure

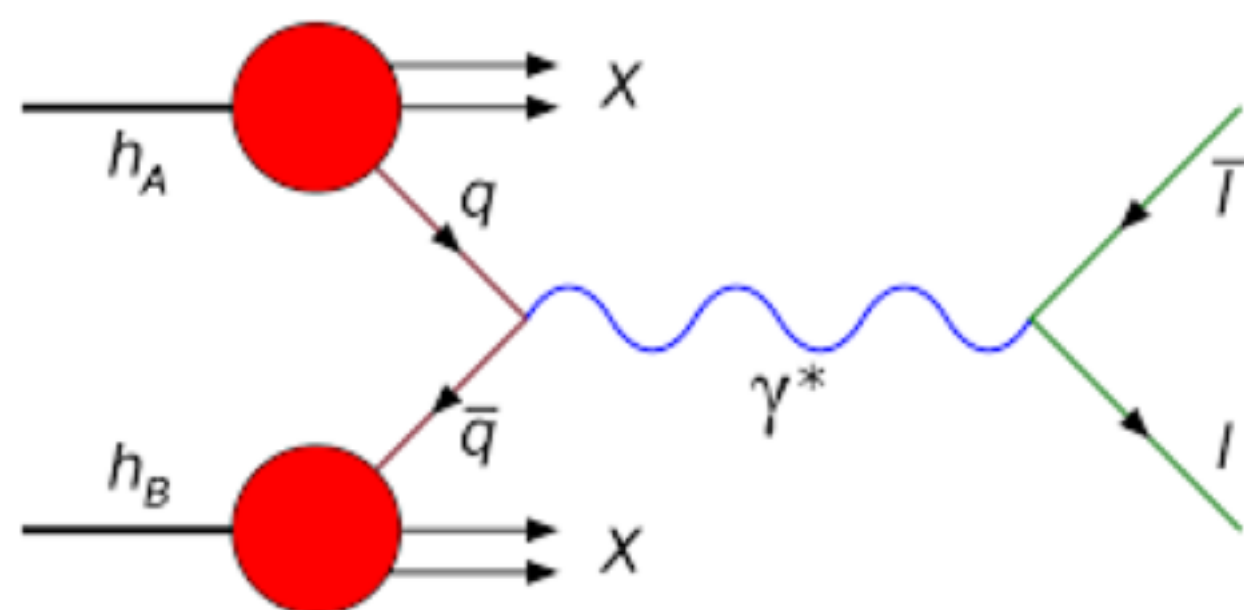
SpinQuest \longrightarrow Siviers function



Upcoming

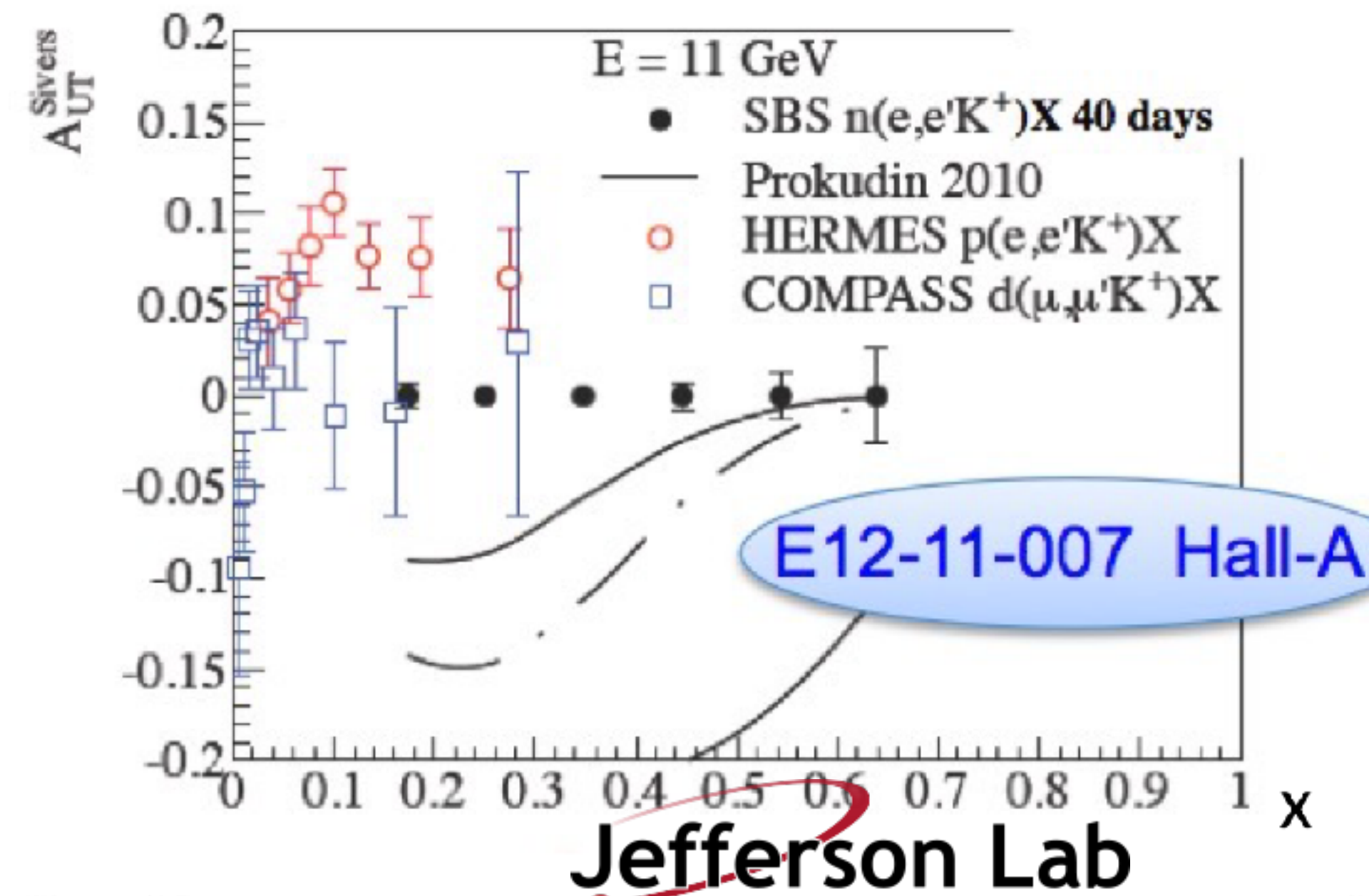
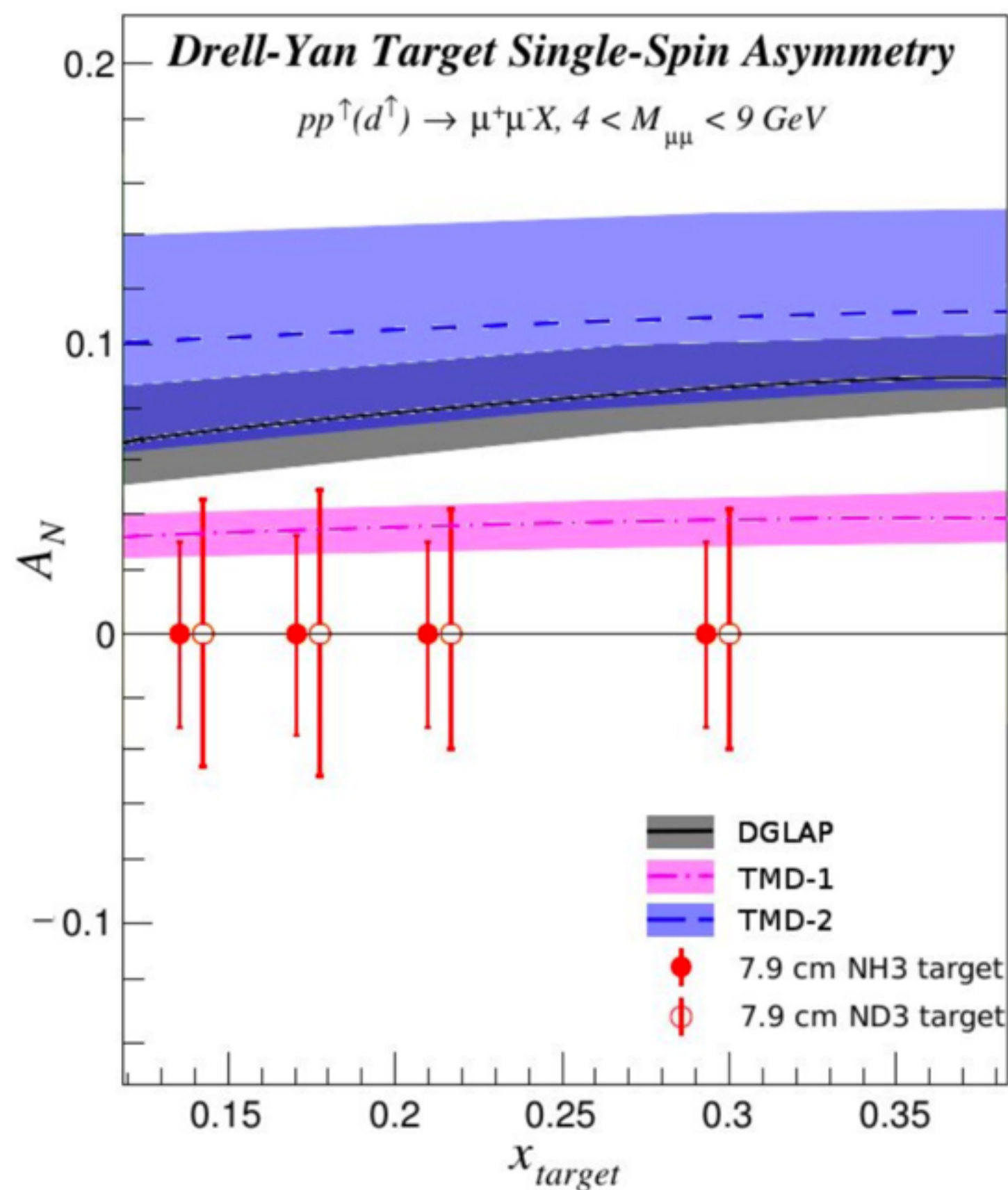
A000BER

Apparatus for Meson and Baryon
Experimental Research

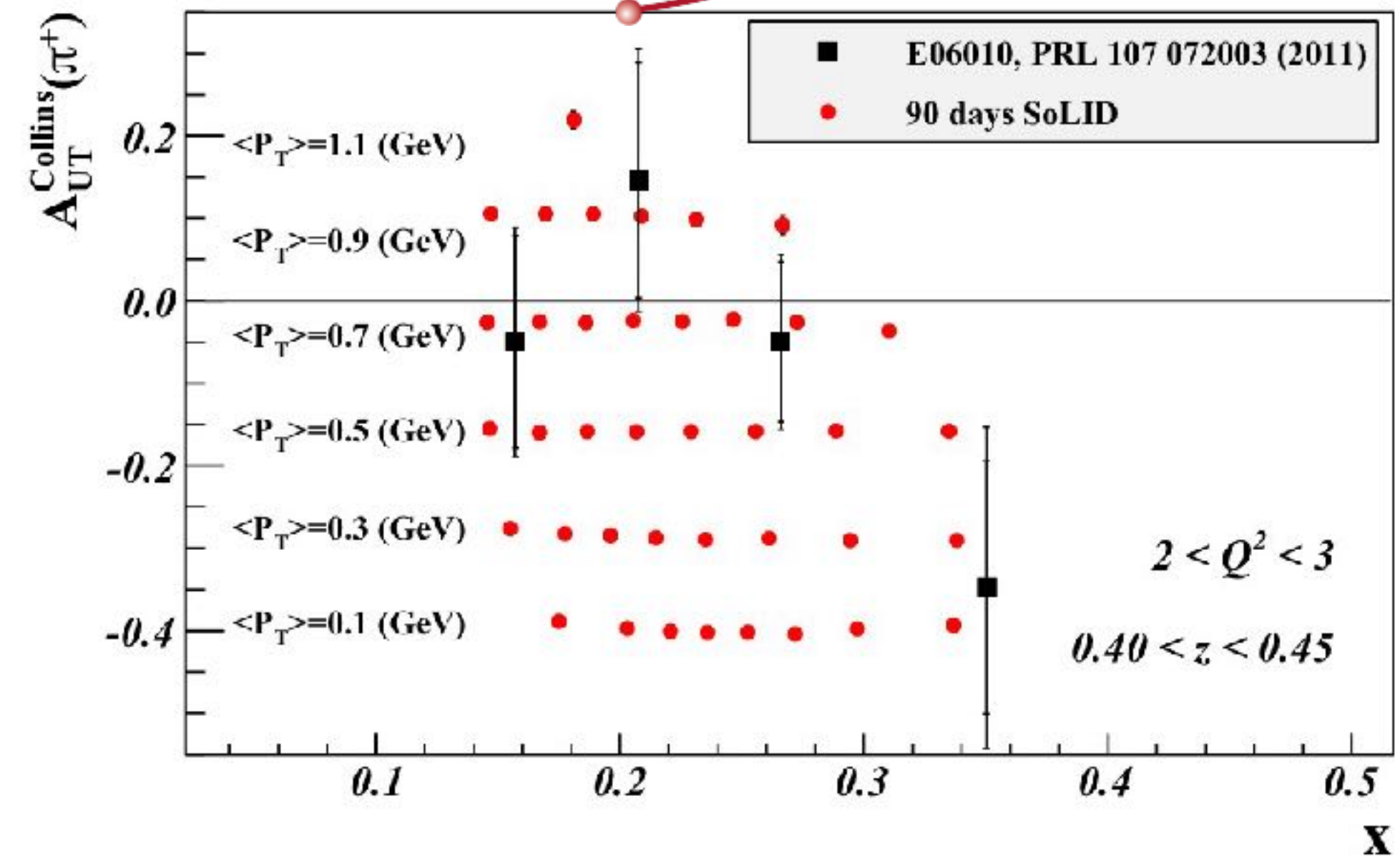


Meson structure

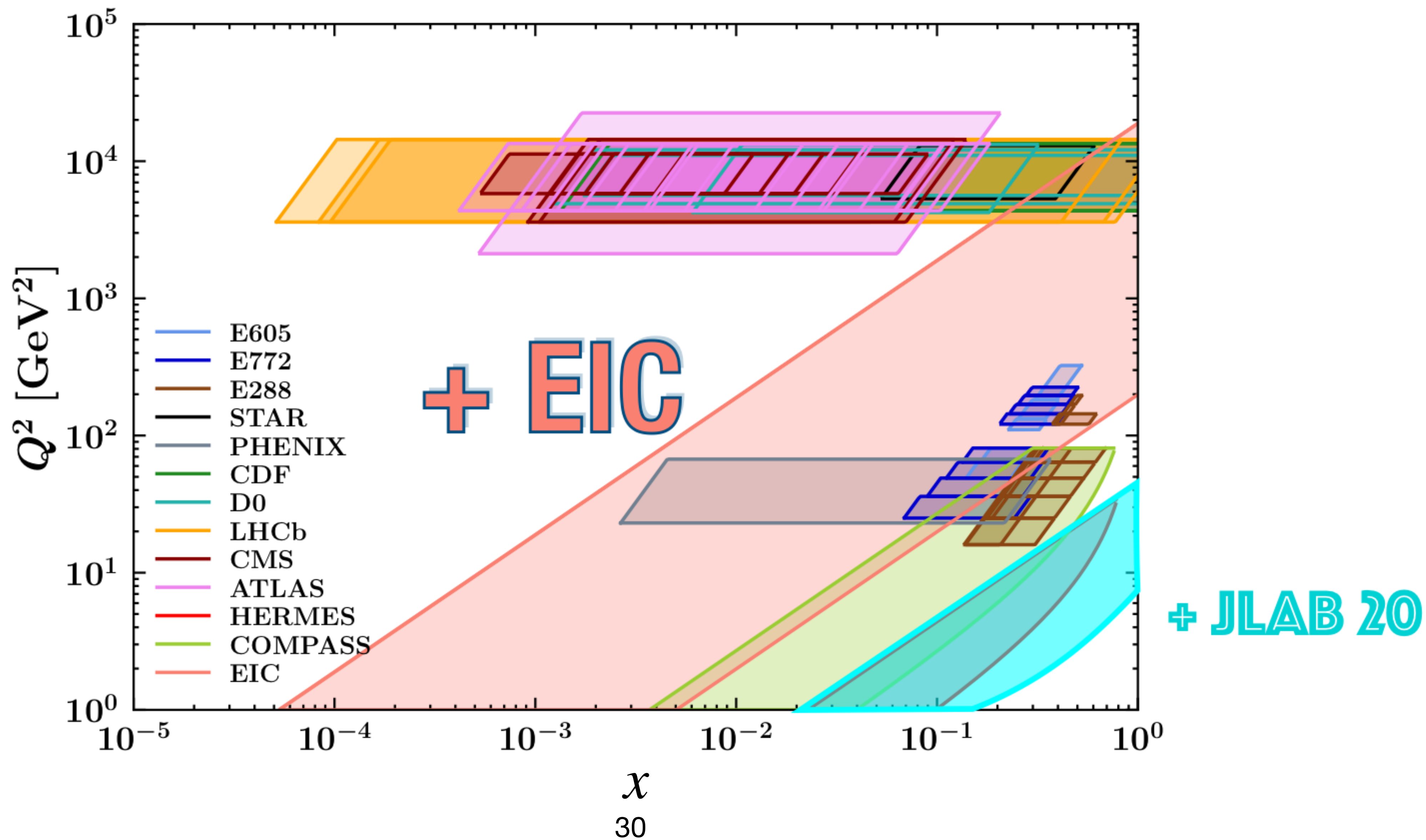
SpinQuest \longrightarrow Sivvers function



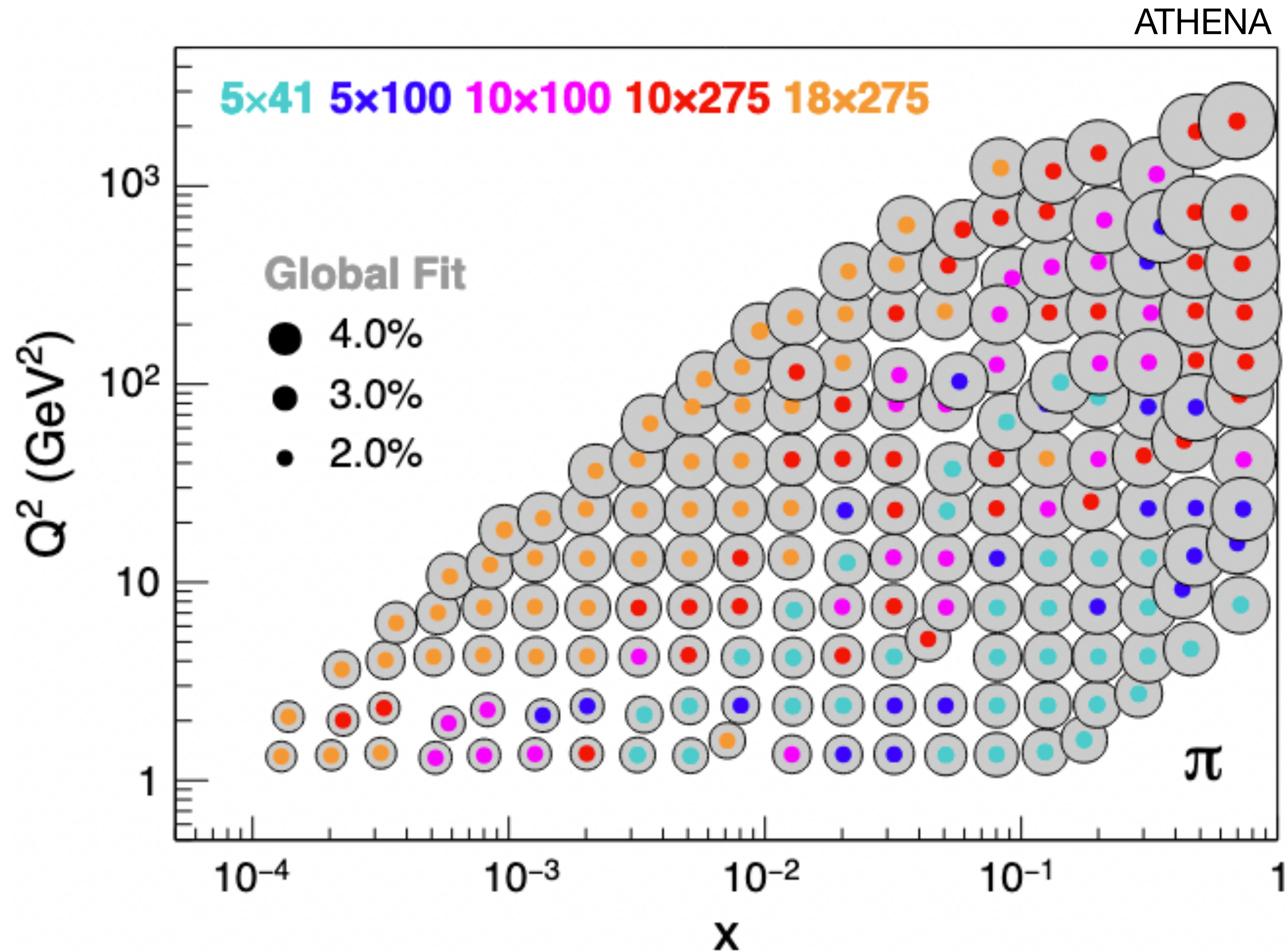
Jefferson Lab



Future



Spin-independent TMD PDFs at EIC



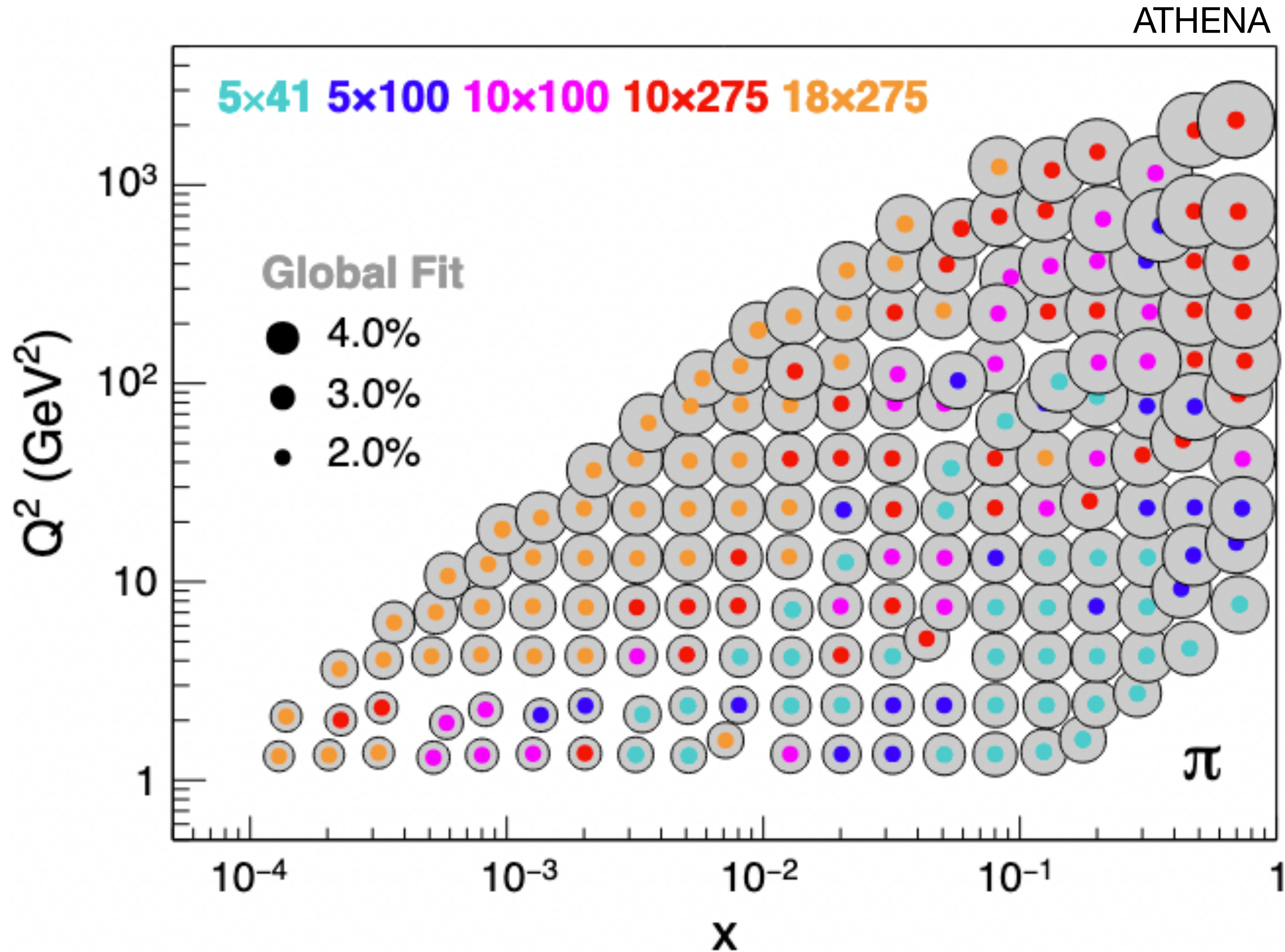
Fit:
 A. Bacchetta et al.,
 JHEP 06 (2017) 081,
 JHEP 06 (2019) 051 (erratum)

EIC uncertainties dominated
 by assumed
 3% point-to-point uncorrelated uncertainty
 3% scale uncertainty

Theory uncertainties dominated by
 TMD evolution.

Spin-independent TMD PDFs at EIC

Large lever-arm in Q^2 over large x range
 → Q^2 evolution of TMD PDF

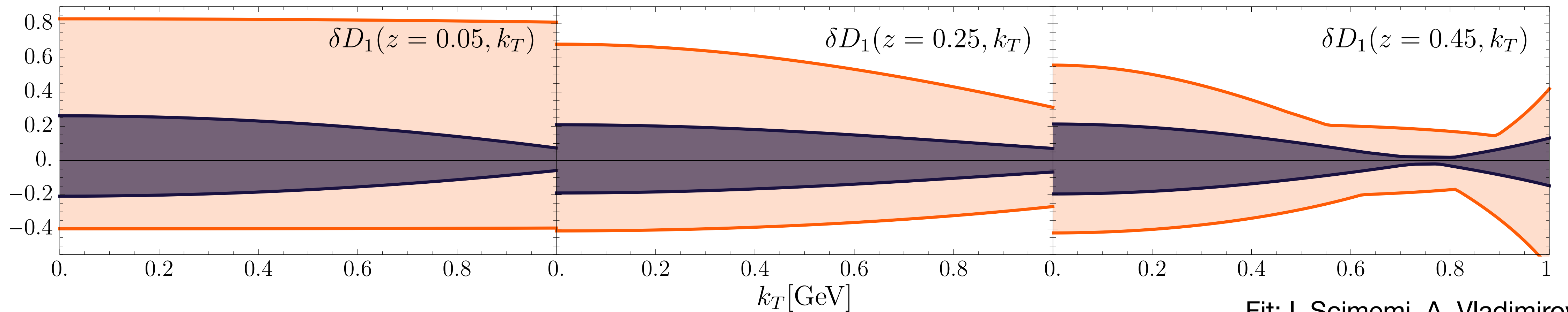
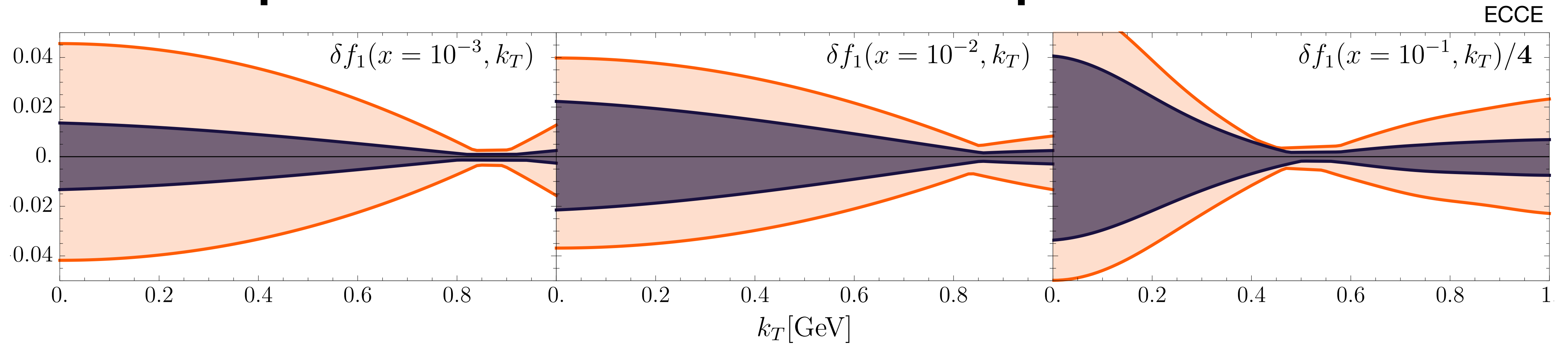


Fit:
 A. Bacchetta et al.,
 JHEP 06 (2017) 081,
 JHEP 06 (2019) 051 (erratum)

EIC uncertainties dominated
 by assumed
 3% point-to-point uncorrelated uncertainty
 3% scale uncertainty

Theory uncertainties dominated by
 TMD evolution.

Spin-independent TMD PDF: impact of EIC



DIS variables via scattered lepton

$Q^2 > 1 \text{ GeV}^2$
 $0.01 < y < 0.95$
 $W^2 > 10 \text{ GeV}^2$

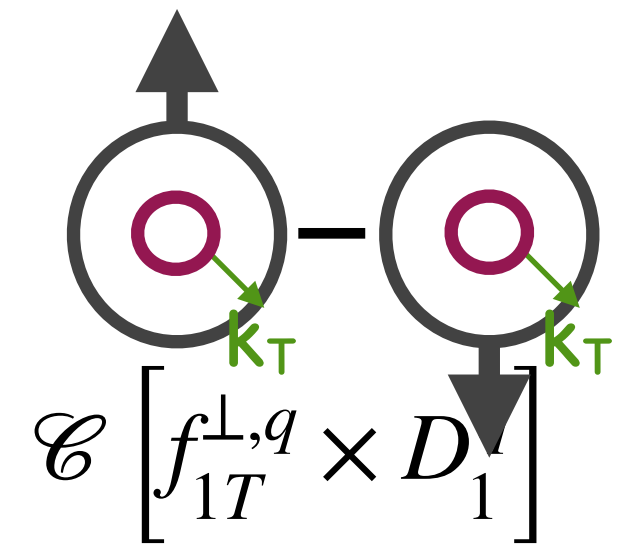
$5 \times 41 \text{ GeV}^2$
 $10 \times 100 \text{ GeV}^2$
 $18 \times 100 \text{ GeV}^2$
 $18 \times 275 \text{ GeV}^2$

$\mathcal{L} = 10 \text{ fb}^{-1}$ for each collision energy

systematic uncertainty = |generated - reconstructed|

Fit: I. Scimemi, A. Vladimirov
 JHEP, 06:137, 2020

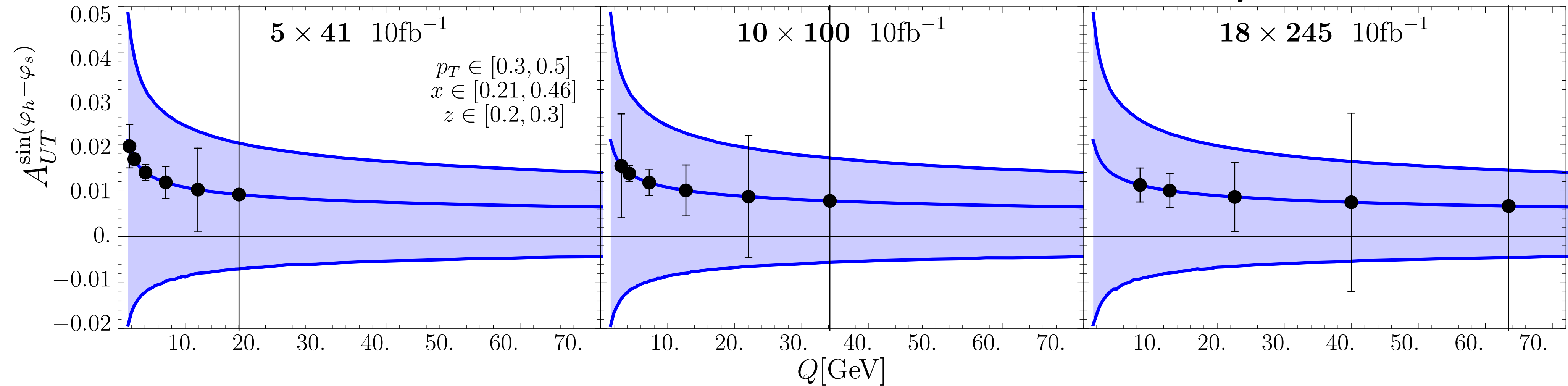
Sivers TMD PDF: TMD evolution



Sivers asymmetry

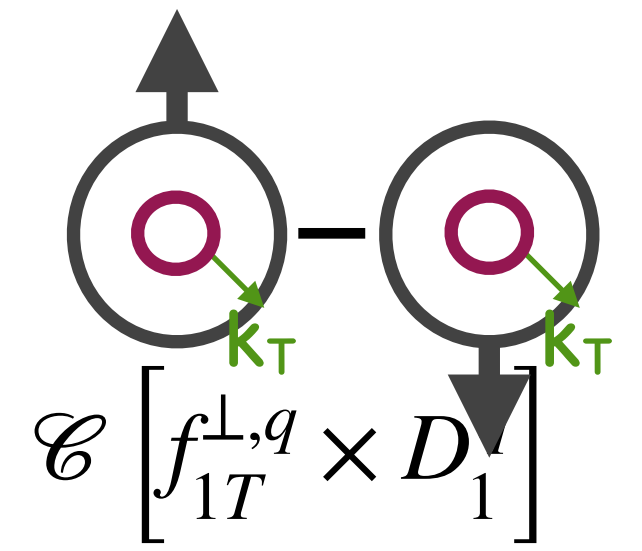
ECCE

Parametrisation: M. Bury et al., JHEP, 05:151, 2021

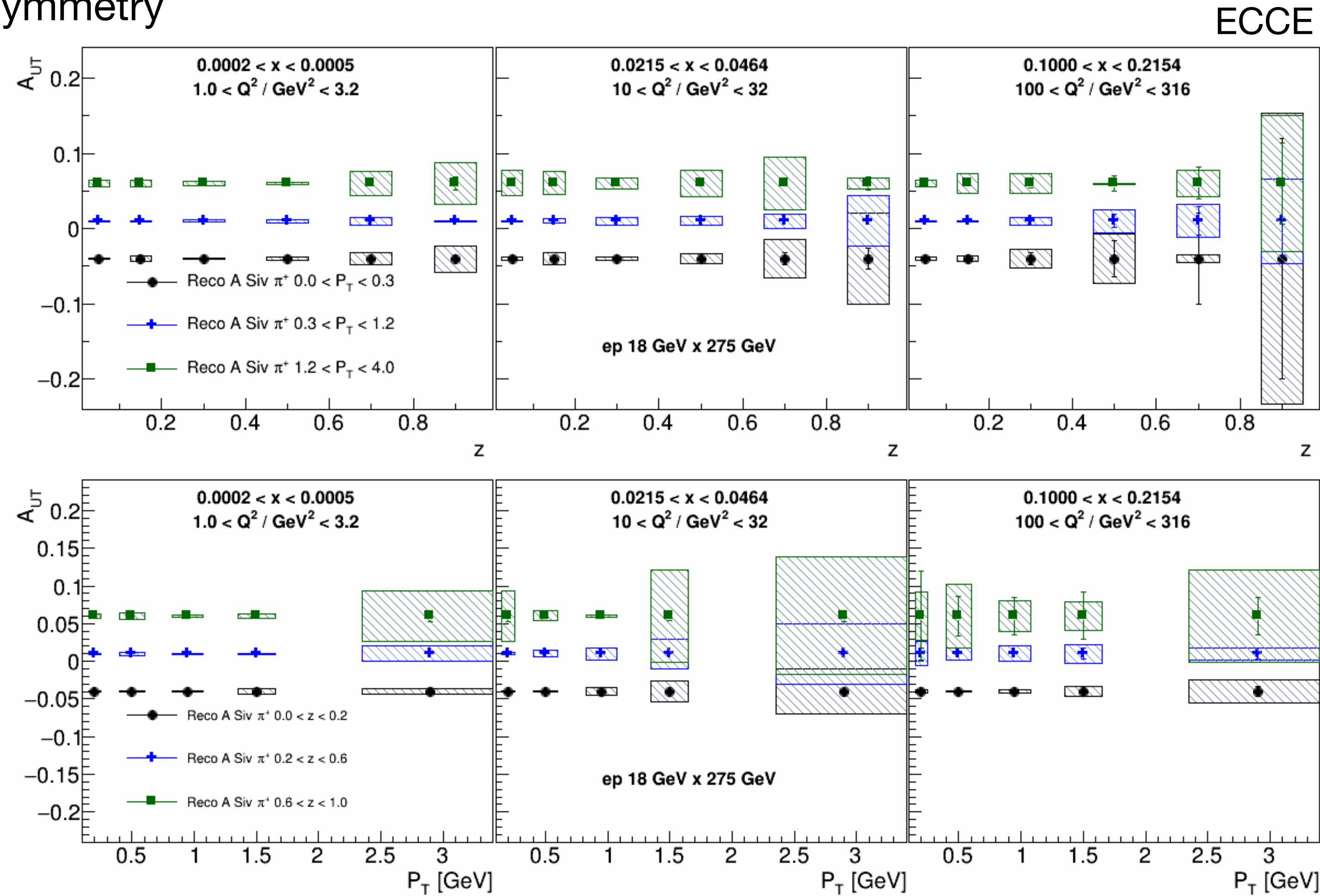


Decrease of asymmetry with increasing $Q^2 \rightarrow$ need high precision ($<1\%$) to measure asymmetry at high Q^2

Uncertainties Sivers asymmetry at EIC



Sivers asymmetry



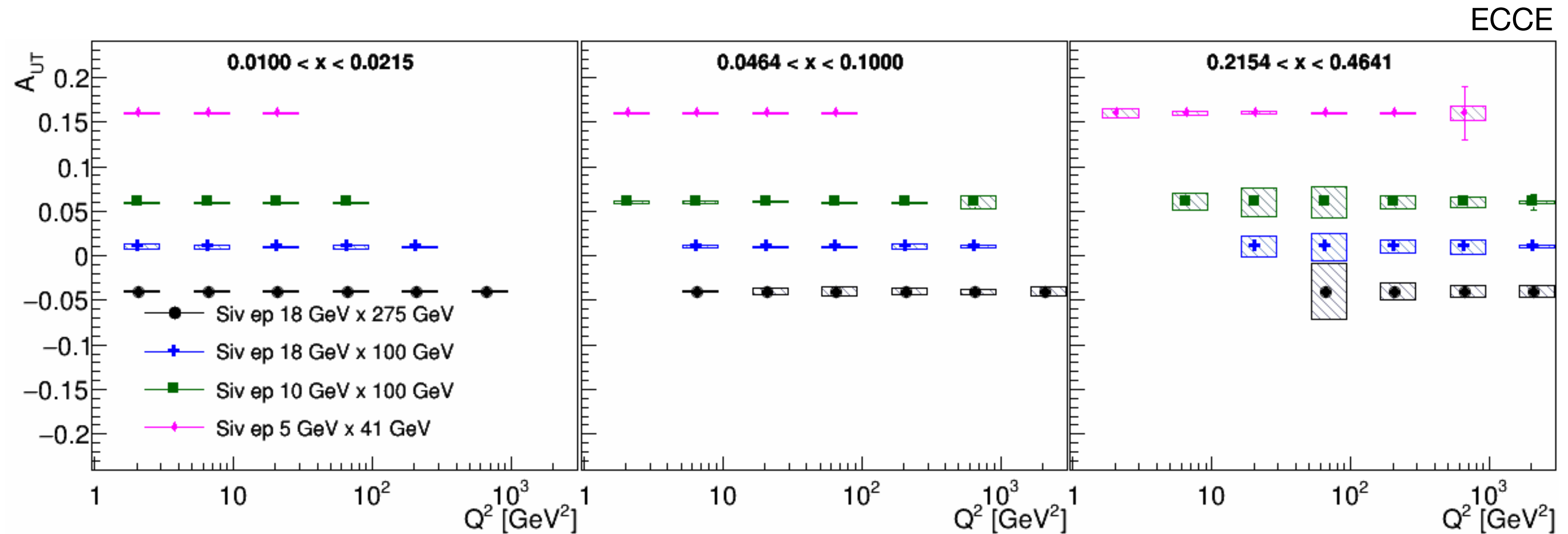
Beam polarisations assumed to be 70%.

systematic uncertainty = |generated - reconstructed|

Additionally: 3% scale uncertainty

- Low x and Q^2 : small statistical uncertainty. High precision is needed since asymmetry at low x and Q^2 well below 1%.
- For not too large z and P_T , statistical uncertainty well below 1%.
- Systematic uncertainties increase with z and P_T : likely because of higher smearing effects.

Q^2 dependence of the Sivers asymmetry at EIC

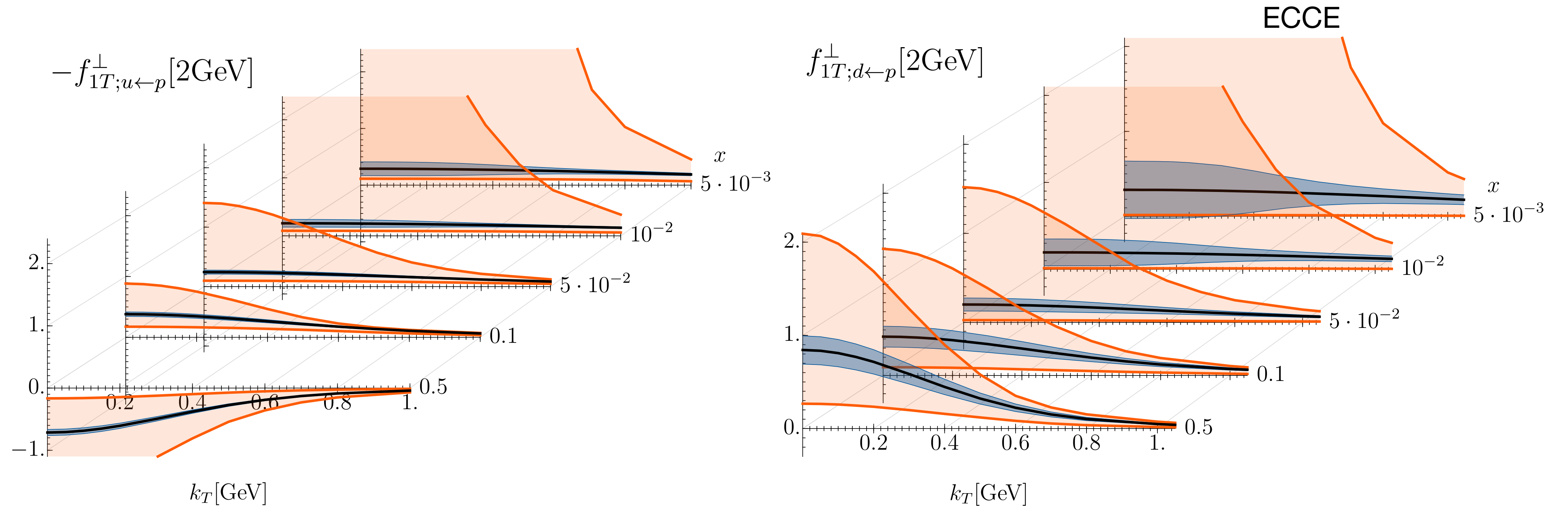


Intermediate and high x : good coverage in Q^2 ,
with complementarity in coverage at different COM energies.

Sivers TMD PDF: impact of EIC

Parametrisation from
M. Bury et al., JHEP, 05:151, 2021

$Q=2$ GeV



DIS variables via scattered lepton

$$\begin{array}{lll}
 Q^2 > 1 \text{ GeV}^2 & 5 \times 41 \text{ GeV}^2 & \\
 0.01 < y < 0.95 & 10 \times 100 \text{ GeV}^2 & \mathcal{L} = 10 \text{ fb}^{-1} \text{ for each collision energy} \\
 W^2 > 10 \text{ GeV}^2 & 18 \times 100 \text{ GeV}^2 & \\
 & 18 \times 275 \text{ GeV}^2 &
 \end{array}$$

Summary

- Transverse momentum dependent hadron structure and hadron formation: rich field of physics, with sensitivity to correlations between quark and hadron spin and transverse momentum.
- Pioneering fixed-target experiments at HERMES, COMPASS, JLab 6 GeV: quark distributions
- Entering era of precision measurements:
 - JLab 12 GeV: unique precision in the valence region
 - EIC: extending down to $x=10^{-4}$
 - LHC measurements can provide additional, invaluable high energy input
 - need to extend measurements with sensitivity to gluons